Tropical rainforests getting their fix: The ecological drivers and consequences of nitrogen-fixing trees in regenerating Costa Rican rainforests

Benton Taylor

Submitted in partial fulfillment of the
requirements for the degree of
Doctor of Philosophy
in the Graduate School of Arts and Sciences

COLUMBIA UNIVERSITY

2018

ABSTRACT

Tropical rainforests getting their fix: The ecological drivers and consequences of nitrogen-fixing trees in regenerating Costa Rican rainforests

Benton Taylor

Tropical rainforests have an unparalleled capacity to sequester carbon, harbor biodiversity, and cycle water and nutrients due to their high rates of primary production. The large biomass stocks and rapid regeneration rates of these forests are often attributed to ample soil nitrogen and quick recovery of the nitrogen cycle in tropical soils following disturbance. Symbiotic nitrogen-fixing trees, which are relatively abundant at tropical latitudes, have the greatest capacity to provide tropical rainforests with new nitrogen, yet the ecological drivers of tropical symbiotic nitrogen fixers and their effects on the forests they inhabit are not well understood. This dissertation consists of four chapters that examine the patterns, environmental controls, and ecological consequences of symbiotic nitrogen-fixing trees in regenerating and intact rainforests in the Caribbean lowlands of Costa Rica. In chapter 1, I use field sampling in a chronosequence of rainforest plots to show that symbiotic nitrogen fixation declines through succession despite increases in the basal area of nitrogen-fixing trees. Chapters 2 and 3 describe results from a controlled shadehouse experiment assessing the effects of light, soil nitrogen, and plant competition on nitrogen fixation rates and the growth and biomass allocation of nitrogen fixers and non-fixers. In chapter 2, I demonstrate that light regulates nitrogen fixation more strongly than soil nitrogen availability. This is a departure from the historical focus on soil nitrogen as the primary regulator of nitrogen fixation and has the potential to resolve longstanding paradoxes of tropical nitrogen cycling. In chapter 3, I show that nitrogen fixation provides some resistance to competitive effects from neighboring plants in nitrogen-limited conditions, and that nitrogen

fixers in these conditions downregulate their fixation rates in the presence of a competitor. This chapter also demonstrates that nitrogen fixation does not represent a significant structural cost to the plant, as reduced root biomass of nitrogen fixers more than compensates for allocation to nodule production. Finally, in Chapter 4, I demonstrate that nitrogen-fixing trees in our chronosequence plots do not promote forest growth, as expected given their capacity to fertilize their neighbors, but rather inhibit forest growth because they are strong competitors. These chapters describe several unexpected findings – i.e. that light primarily drives nitrogen fixation and that nitrogen fixers slow forest growth – which provide new and important insight into the role that nitrogen-fixing trees play in the growth of Costa Rican rainforests.

TABLE OF CONTENTS

LIST OF FIGURES AND TABLES

ACKNOWLEDGEMENTS

The work that this dissertation represents has been one of the most challenging and rewarding experiences of my life, and surely would have failed without the help of many colleagues, friends, and loved ones. First, I must thank my advisor, Duncan Menge, for his unending support and guidance—celebrating my successes and being a Virgil during the inevitable dark periods of graduate school. I cannot thank him enough for taking a chance on me as a student when he himself was entering the unknown of a new faculty position. Duncan has taught me so much about how nature works, and, just as importantly, how to go about figuring out the aspects of nature we still do not understand. As I move on to the next stages of my life I look forward to having him as a close friend and colleague.

Fortunately for Duncan, he had plenty of help molding me into a scientist from my four additional committee members, Robin Chazdon, Kevin Griffin, Shahid Naeem, and Maria Uriarte. Without the support and connections that Robin has provided me at La Selva, very little of my field work would have been successful. She has also been an incredible resource for understanding how forests change as they grow older. Kevin has taught me how to think like a plant, how to get people excited about my work, and that being happy and being scientifically productive are not mutually exclusive. Shahid has taught me to think big. His ability to connect seemingly disparate ideas in ecology has been a wonderful example for me. If Kevin has taught me how to think like a plant, Maria has taught me how to think like a forest. She has challenged me not to settle for partial answers and helped me understand my data in the broader context of the forest's daily operations.

The small-but-mighty community in E3B has been an incredible environment in which to grow as a scientist. Post-docs and senior graduate students like Jesse Lasky, Carla Staver, Bob

Muscarella, Bene Bachelot, Case Prager, Brian Weeks, and Naomi Schwartz immediately took me in, put up with my coding questions, and gave me the gift of lasting friendship. Amrita Neelakantan and Lais Coelho have been wonderful cohort-mates as we've grown together, faced challenges, and won victories in both our personal and scientific lives. The Menge, Griffin, and Uriarte lab groups have also provided much support and feedback. In particular, Amy Wolf, Andrew Quebbeman, Tom Bytnerowicz, Alex Huddell, Anika Petach, Sian Kou-Giesbrecht, Palani Akana, and Wenying Liao have been wonderful friends with which to share life, love of nitrogen, and fear of dry-erase markers.

I am also deeply indebted to many people at La Selva Biological Station for an immense amount of help with my field work. The staff at La Selva, including Carlos de la Rosa, Orlando Vargas, Bernal Matarrita, and Danilo Brenes provided critical logistical support for my work. The members of the Bosques Project staff, Janette Paniagua, Bernal Paniagua, and Enrique Salicetti, gave so much of their time to teaching me tree species, helping me collect samples, and teasing me about my Spanish. I also had the pleasure of working with three wonderful undergraduate assistants in the field—Richard Li, Ben Scott, and especially Megan Wilcots were critical to the success of my field work and will all make wonderful future scientists.

Lastly, I thank my family. My in-laws, Steven and Nancy, who let me set up a biogeochemistry lab in their spare bedroom. My hometown friends, who, like brothers, have kept me grounded by refusing to believe I'd study something as boring as tree roots. My wife, Sarah, has kept me focused, grounded, happy, and loved in the happiest and hardest times of both our lives. Her unwavering support has meant everything to me. My dad, Tom, set me on my path as an ecologist at an early age – from teaching me about nature at the cabin to helping me learn concepts of fire ecology for science fair projects. My mom, Nan, has always shown me what a

true love for the natural world looks like. She will always be my reference for plant identification and my inspiration for loving the places I study. Finally, my brother, Robert, has guided me through graduate school just as he has done our entire lives. Our long-distance talks about science have largely shaped how I think about my work and communicate it to others.

I believe we are each a mosaic of different pieces of the many people in our lives. As such, this dissertation is a communal accomplishment resulting from the work, support, patience, advice, and influence of those listed here and many others, and for that I am extremely grateful.

To my wife, Sarah, for the many sacrifices she has made supporting my love for studying nature

INTRODUCTION

Despite comprising only 15% of Earth's land surface, tropical forests account for two-thirds of global carbon (C) storage (Pan et al. 2011, 2013), one-third of global net primary productivity (Sabine et al. 2004, Pan et al. 2013), and large fractions of global evaporative cooling (Bonan 2008) and nutrient cycling (Vitousek and Sanford 1986, Chapin III et al. 2011). The important functions that tropical forests serve to the biosphere are the result of high rates of gross primary productivity (Pan et al. 2013), which is typically attributed to favorable climate and soils that are notably rich in nitrogen (N) (Vitousek and Sanford 1986, Hedin et al. 2009, Brookshire et al. 2012). Indeed, a widely-cited study estimated that mature tropical forests offset 14% of global annual anthropogenic C emissions (Pan et al. 2011). The future of this sink, however, is uncertain, and depends directly on human land use in tropical regions and how tropical forests respond to this human land use.

Tropical forests are noteworthy both in their potential to mitigate human impacts on the biosphere and in their vulnerability to human activities. Over the past two decades, forests within the tropics have received more land use change than any other region (FAO 2010, Taubert et al. 2018), and regenerating tropical forests now represent the largest potential terrestrial C sink on Earth (Pan et al. 2011). As the majority of forested area in the tropics is currently recovering from some type of human land use (FAO 2010), there is increasing interest in the conservation, biogeochemical, ecological, and economic value of these forests (Brown and Lugo 1990, Chazdon 2008, Chazdon et al. 2009). Unfortunately, tropical forests represent one of the least-well understood parts of terrestrial C models, with the factors determining future C dynamics in these forests largely unknown (Wårlind et al. 2014, Cavaleri et al. 2015). Thus, understanding

what will control future tropical forest primary production, especially in regenerating tropical forests, is of growing importance.

The ecological function of tropical secondary forests is closely tied to their regeneration rates. Because biomass, soil nutrients, and species richness tend to accumulate during forest succession (Vitousek and Reiners 1975, Chazdon et al. 2007), rates of recovery from disturbance largely determine the ability of tropical secondary forests to capture C, stabilize nutrient cycling, and harbor biodiversity. Recent work has demonstrated that Neotropical forests experience rapid recovery rates, with secondary forests capturing 11 times more C than primary forests during the first 20 years of growth and recovering 90% of their biomass by 66 years following disturbance (Poorter et al. 2016). These rapid regeneration rates highlight the potential impact that tropical secondary forests can have on the global biosphere, but the environmental factors that dictate regeneration rates remain largely unresolved. Factors such as land-use history (Chazdon 2003), neighboring forest type and proximity (Guariguata and Ostertag 2001, Chazdon 2003, Chazdon et al. 2007), and climate (Chazdon et al. 2005, Poorter et al. 2016) have all been shown to influence rates of tropical forest regeneration. In addition to these factors, soil nutrient availability may play an important role in tropical forest recovery.

Soil nutrients are key potential limiting resources to the primary production of tropical rainforests. While N is the most commonly limiting nutrient in terrestrial systems (LeBauer and Treseder 2008), the historical paradigm for tropical nutrient limitation poses that phosphorus (P), not N, limits tropical forest production (Walker and Syers 1976, Vitousek 1984). Supporting evidence for this view can be seen in some tropical fertilization experiments (Tanner et al. 1998, Elser et al. 2007) and high losses of inorganic N in many tropical streams (suggesting that N supply exceeds plant demand) (Brookshire et al. 2012). However, this view has been challenged

in recent decades (Elser et al. 2007, LeBauer and Treseder 2008, Townsend et al. 2008, 2011). Current evidence now suggests that N also plays an important role in limiting the production of tropical forests – especially those regenerating from disturbance (Davidson et al. 2004, 2007, LeBauer and Treseder 2008, Batterman et al. 2013a). Given the increasing proportion of tropical forests that are currently in some phase of regeneration, much of the focus of future tropical forest limitation now centers on N availability (Wårlind et al. 2014).

The source of new N into ecosystems represents a biogeochemical oddity. Unlike other major plant nutrients, which are derived from weathering of parent material, N is brought into most ecosystems primarily through the biological fixation of atmospheric di-nitrogen gas into bioavailable forms (Chapin III et al. 2011, Schlesinger and Bernhardt 2013). The largest potential natural source of N fixation comes from symbioses between N-fixing bacteria housed in the roots of higher plants, primarily in the family *Fabaceae* (Binkley et al. 1994, Binkley and Giardina 1997, Sprent 2009). In this way, the abundances and fixation rates of these N-fixing plant symbioses (hereafter "N fixers") largely determine N availability in an ecosystem.

Neotropical forests are notable in their high relative abundances of N fixers (Cleveland et al. 1999, Hedin et al. 2009), housing more than 10-fold the number of N fixers as their temperate counterparts (ter Steege et al. 2006, Menge et al. 2010, 2014, 2017a). Moreover, symbiotic N fixation (SNF) has recently been identified as a key N input that fuels biomass accumulation in regenerating tropical forests (Batterman et al. 2013a). Despite recognizing the potential importance of SNF to the process of tropical forest regeneration, our understanding of the patterns, controls, and effects of SNF on forest regeneration rates remains poor. **The goal of this dissertation is to investigate the patterns of SNF during tropical forest regeneration, which**

environmental factors drive rates of SNF, and the effect of N fixers on forest regeneration rates.

To understand the influence of SNF on tropical forest regeneration rates, we must first understand the patterns of SNF during the regeneration process. Ecosystem theory suggests that SNF should be progressively downregulated during secondary forest succession as canopy density increases and soil N accumulates in an ecosystem (Rastetter et al. 2001). These theoretical predictions are often confirmed empirically in tropical forests, with many studies finding relatively high rates of SNF in early successional forests compared to relatively small inputs from SNF later in succession (Pearson and Vitousek 2001, Gehring et al. 2005, Batterman et al. 2013a, Sullivan et al. 2014, but see Winbourne et al. 2018). However, evidence may point to a slight increase in SNF from older secondary forests to mature old-growth forests (Batterman et al. 2013a, Sullivan et al. 2014) potentially caused by gap dynamics creating hotspots of N fixation in mature tropical forests (Barron et al. 2011). In general, our current understanding of the successional dynamics of SNF indicate relatively high N inputs from SNF soon after disturbance that may help fuel the rapid recovery of biomass (Batterman et al. 2013a) and N cycling (Davidson et al. 2004, 2007, Winbourne et al. 2018) in regenerating tropical forests. These successional patterns in SNF are likely the result of complex environmental changes that take place during forest succession. However, no clear consensus currently exists on how N fixers and SNF respond to various environmental conditions.

Understanding which environmental factors most strongly regulate SNF is critical to making mechanistic predictions of the dynamics of SNF and how SNF influences tropical secondary forests. Because of this, environmental regulators of SNF have received ample attention in the literature over the past several decades. The vast majority of this work has

focused on how soil nutrient availability influences SNF rates. Because SNF represents a direct alternative to soil N uptake, rates of SNF should be negatively correlated with soil N availability, and a number of studies have shown either complete or incomplete downregulation of SNF with increasing soil N (Barron et al. 2011, Batterman et al. 2013b, Menge et al. 2015). Other soil resources, such as P and water have also been shown to regulate SNF rates, with proposed mechanisms relating to increased soil P mining and increased water use efficiency of N fixers, respectively (Crews 1993, Houlton et al. 2008, Batterman et al. 2013b, Wurzburger and Miniat 2014). Based on the temperature sensitivity of the nitrogenase enzyme that conducts N fixation, SNF has also been shown to fluctuate with ambient temperature (Houlton et al. 2008). One additional environmental regulator that has received relatively little empirical attention is light availability. Light energy fuels the fixation process, and both theory and limited experimental data suggest it may be a strong driver of SNF (Sprent 1973, Gutschick 1981, Rastetter et al. 2001, Myster 2006), but the relative importance of light for determining SNF rates is poorly understood. While each of these factors may control SNF rates in some conditions, knowing which factors *most strongly* drive SNF rates is key to our mechanistic understanding of SNF. This mechanistic understanding will help us predict the dynamics and the effects of SNF in regenerating tropical forests.

If we are to fully understand the effect of SNF on tropical forest regeneration, the ultimate question is: how do N fixers and their N inputs from SNF influence growth rates of regenerating tropical forests? The prevailing assumption in the field posits that N fixers should have a net positive effect on the growth of N-limited forests due to their ability to fertilize the surrounding ecosystem as fixed N eventually enters the soil N pool via biomass turnover (Vitousek and Howarth 1991). While this view conforms to our understanding of the flow of N

through the process of SNF (from atmosphere to N fixer to the surrounding ecosystem), the idea that an N fixer would expend energy on a process that provides a net benefit to neighboring competitors is potentially at odds with our basic understanding of natural selection (Darwin 1859). Some N fixers do provide N to the surrounding ecosystem, but they also compete with neighboring plants for N, light, and other resources, and the ability to fix N may make these plants particularly good competitors for other resources (i.e. N fixation may allow for high growth rates aiding in the competition for light). Currently, however, the net effect N-fixer facilitation vs. competition on forest growth is unknown. Empirical data on the net growth effects of N fixers and their fixation rates in regenerating tropical forests is critical to understanding and predicting how SNF will influence the function of the > 50% of global tropical forests that are currently recovering from disturbance (FAO 2010).

This dissertation pairs field sampling and manipulative shadehouse experiments in the humid tropical lowland forests in and around La Selva Biological Station, Costa Rica to investigate the patterns, controls, and effects of N fixers and SNF in regenerating tropical forests. The four studies presented here address localized mechanisms that influence N-fixer success and SNF rates as well as broad-scale patterns of how SNF influences tropical forest ecosystems. Together, these studies present a robust assessment of SNF in these forests and provide an improved understanding of how SNF influences C capture and biomass regeneration in regenerating Neotropical forests.

CHAPTER 1: SUCCESSIONAL DYNAMICS OF NITROGEN FIXATION, NITROGEN AVAILABILITY, AND FOREST GROWTH IN REGENERATING COSTA RICAN RAINFORESTS

Benton N. Taylor, Robin L. Chazdon, and Duncan N.L. Menge

Abstract

Regenerating tropical forests have an immense capacity to capture carbon and harbor biodiversity. The recuperation of the nitrogen cycle following disturbance can fuel biomass regeneration, but few studies have evaluated the successional dynamics of nitrogen and nitrogen inputs in tropical forests. We assessed soil inorganic nitrogen pools, nitrogen inputs from asymbiotic and symbiotic nitrogen fixation, and tree growth in a series of 5 tropical forest plots ranging from 19 years in age to old-growth forests. Tree growth was highest in our youngest plots and declined through succession. Soil nitrogen availability was high in all plots and declined slightly as forests aged. Inputs from symbiotic nitrogen fixation declined, while asymbiotic nitrogen fixation increased through succession. This resulted in a successional switch from symbiotic fixation to asymbiotic fixation as the dominant nitrogen input measured. Interestingly, symbiotic nitrogen fixation rates were not correlated with basal area of nitrogen-fixing trees across our study plots, highlighting the danger in using nitrogen-fixing trees as a proxy for rates of symbiotic nitrogen fixation. Our results demonstrate that the nitrogen cycle has largely recuperated by 19 years following disturbance, allowing for rapid biomass regeneration at our site. This work provides important insight into the sources and dynamics of nitrogen cycling that support rapid growth and carbon capture in regenerating neotropical forests.

Introduction

Increases in human land-use change in the tropics over the last half century have dramatically increased the global extent of regenerating tropical secondary forests (Houghton 1994, Taubert et al. 2018), such that these secondary forests now make up more than half of the world's tropical forests (FAO 2010). Secondary tropical forests are increasingly being recognized for their critical role in capturing carbon (Pan et al. 2011, 2013, Poorter et al. 2016), cycling water and nutrients (Powers and Marín-Spiotta 2017), harboring biodiversity (Finegan 1996, Chazdon et al. 2009, Dent et al. 2013), and supporting local economies (Brown and Lugo 1990). The ability of tropical secondary forests to serve these roles is largely dependent on their regeneration rates, but the controls over tropical forest regeneration are not well understood.

In addition to the effects of previous land use (Powers and Marín-Spiotta 2017) and landscape context (Chazdon et al. 2007), tropical forest regeneration is often limited by the availability of soil nutrients, especially nitrogen (N) (Erickson et al. 2001, Davidson et al. 2004, 2007, Davidson and Martinelli 2009, Batterman et al. 2013a). Although primary tropical forests are typically thought to be relatively N rich (Hedin et al. 2009, Brookshire et al. 2012), substantial losses of N during vegetation clearing and land use (Kauffman et al. 1995, McGrath et al. 2001, Davidson et al. 2007, Davidson and Martinelli 2009) can result in low N availability early in tropical secondary succession. Despite the recognition that N dynamics are an important potential control over tropical forest regeneration rates, characterizing these N dynamics has been hampered by the large biogeochemical heterogeneity across secondary tropical forests (Vitousek and Sanford 1986, Townsend et al. 2008) and the limited (but growing (Powers and Marín-Spiotta 2017)) number of studies on the subject.

One of the main ways N is brought back into regenerating tropical forests is via biological N fixation – the conversion of N_2 gas into bioavailable forms either asymbiotically by free-living bacteria or symbiotically by certain legumes and their endosymbiotic bacteria. Symbiotic N fixation (SNF) has an exceptionally large potential to bring new N into tropical forests, with measured rates of SNF exceeding 100 kg N ha^{-1} yr^{-1} (Binkley and Giardina 1997). By contrast, asymbiotic N fixation (ANF) rates typically have lower maxima, but are less variable across the landscape (Cleveland et al. 2010, Reed et al. 2011). Despite the large discrepancy in potential N inputs via these two N-fixation pathways, the relative importance of ANF vs. SNF for actual N inputs into tropical secondary forests is not well understood. While SNF plays a key role in meeting the external N demands of some regenerating tropical forests (Batterman et al. 2013a), the absence of N-fixing trees in some tropical forests (Vitousek 2004) and the downregulation of SNF by many tropical N-fixing trees mean that ANF can be the dominant N input into many tropical forests (Reed et al. 2011, Sullivan et al. 2014).

Ecosystem theory may help form predictions about the relative importance of N inputs from ANF and SNF during tropical forest succession. Many theoretical models of successional N-fixation dynamics focus on changes in the cost/benefit ratio of SNF vs. soil N uptake in plants as forests age (Pastor and Binkley 1998, Vitousek and Field 1999, Rastetter et al. 2001, Wang et al. 2007). These models generally show that SNF is cost-effective in young forests, but becomes increasingly cost-ineffective as soil N accumulates through succession (Vitousek and Field 1999, Rastetter et al. 2001). This produces predictions of peak SNF rates early in succession that decline to near 0 in older forests. ANF is rarely incorporated into these models explicitly and may not experience the same successional cost/benefit dynamics. Compared to symbiotic N-fixers, free-living N-fixers access a more localized soil N pool, which might be more

idiosyncratic through succession, and they also require litter or soil C, which might increase through succession. Therefore, ANF might increase in importance relative to SNF in later successional stages as SNF is progressively downregulated.

These models strongly suggest that total fixation N inputs and the relative importance of ANF vs. SNF during tropical succession depend largely on the environmental factors that regulate each N-fixation pathway and how those environmental factors change as forests regrow. ANF rates can be controlled by such environmental factors as temperature (Houlton et al. 2008), moisture (Reed et al. 2007), N availability (Barron et al. 2009), phosphorus availability (Reed et al. 2007, Wurzburger et al. 2012), molybdenum (Barron et al. 2009, Wurzburger et al. 2012) or other micronutrient (Crews et al. 2000, 2001) availability, patterns of canopy litterfall (Reed et al. 2008), and asymbiotic N-fixing bacteria taxonomy (Reed et al. 2010). While all of these factors likely change during succession, the only two studies (to our knowledge) that explicitly measured the dynamics of ANF during secondary succession in tropical forests found either decreases in ANF from secondary to primary forests (Sullivan et al. 2014) or no successional changes in ANF (Winbourne et al. 2018).

SNF is typically considered to be more variable across secondary forests than ANF (Reed et al. 2011, Sullivan et al. 2014), with a variety of environmental factors believed to regulate this variability. Tropical SNF can be regulated by resources such as soil N (Barron et al. 2011, Batterman et al. 2013b), phosphorus (Crews 1993, Pearson and Vitousek 2001, Houlton et al. 2008, Batterman et al. 2013b, Nasto et al. 2014), and light (Taylor and Menge n.d., McHargue 1999, Myster 2006). However, similar to ANF, few studies have been conducted on the dynamics of SNF during tropical forest succession. Of the studies that have assessed SNF, directly or indirectly, during tropical forest succession, all but one show that SNF rates decline

through succession (Pearson and Vitousek 2001, Gehring et al. 2005, Batterman et al. 2013a, Sullivan et al. 2014, Bauters et al. 2016). Winbourne et al. (2018) found no significant successional change in SNF rates in regenerating Brazilian Atlantic forests, which they suggest may be due to an N cycle that fully recovered prior to the age range they assessed. Some evidence suggests that SNF rates increase slightly from older secondary forests to primary forests (Batterman et al. 2013a) as gap dynamics become more prominent (Barron et al. 2011), but few data explicitly test this.

Despite the evidence suggesting that tropical forest regeneration is often N limited, and that biological N fixation is often the dominant source of N into regenerating forests, only a handful of studies have empirically assessed the dynamics of N availability, ANF, SNF, and biomass growth during tropical forest recovery, and only one (Sullivan et al. 2014) has assessed all four factors simultaneously. This paucity of data limits our understanding of the controls of tropical forest regeneration rates and hinders our ability to predict the function of these forests in the global biosphere. To improve this understanding, we measured soil inorganic N, ANF, SNF, and tree biomass in a chronosequence of humid tropical forest plots, asking: 1) How do soil N, ANF, and SNF change through forest succession relative to tree biomass and tree growth? 2) What is the relative contribution of ANF vs. SNF to ecosystem N inputs at each stage of succession? and 3) How are changes in N-fixing tree abundance through succession related to changes in SNF? Based on available theory and limited data, we predicted that tree biomass and soil N would accumulate through succession, that SNF would decline as soil N accumulates and shading from neighboring trees intensifies during succession, but that ANF rates would remain relatively constant across our age gradient. These predicted N fixation dynamics led us to further predict that SNF would be a much larger source of N than ANF early in succession, but that

these two fixation pathways would be relatively similar in primary forests as has been demonstrated empirically (Sullivan et al. 2014). Finally, because tropical N-fixing trees have high potential SNF rates, we predicted that the prevalence of N-fixing trees would be positively correlated with SNF at our study sites.

Methods

Study Site and Plot Design – Our study took place in humid tropical rainforests in the Caribbean lowlands of northeastern Costa Rica, in and around La Selva Biological Station (10.4233 °N, 84.022 °W). These forests receive approximately 4,500 mm yr^{-1} of rainfall, with a pronounced dry season from January to April, and a second, less-pronounced dry season in September and October. Mean annual temperature at La Selva is 25°C, and is relatively constant throughout the year (McDade and Hartshorn 1994). Soils at these sites are primarily composed of weathered ultisols (Sollins et al. 1994).

We measured tree growth, soil N concentrations, and symbiotic and asymbiotic N fixation in five 1-ha (50 m x 200 m) plots. Four of the plots span a gradient of forest ages from 19 to 37 years since agricultural abandonment, and one is in primary, old-growth forest that has no history of disturbance for at least 200 years. Putative N-fixing species comprise between 24% and 33% of total tree basal area in these plots (Table S1, Menge and Chazdon 2016, Taylor et al. 2017). All plots are within 15 km of each other, are similar in elevation (5 to 220 m), have similar topography and soil type, and experience similar climatic conditions. Each plot is subdivided into 100 10 x 10 m subplots. These plots are a subset of an 8-plot chronosequence that has been described in detail elsewhere (Chazdon et al. 2005, Lasky et al. 2014), including

studies on the demographics of and neighborhood interactions between N-fixing and non-fixing trees (Menge and Chazdon 2016, Taylor et al. 2017).

Sampling for tree growth, soil N concentrations, and N fixation – Within each plot, all adult trees ≥ 5 cm diameter at breast height (DBH) were tagged, identified to species, measured for DBH, and mapped onto a plot-level X,Y coordinate system using the subplot corners as reference points. Our analyses use data from censuses in 2013 and 2014 to calculate tree basal area and basal area increment (the change in basal area from one census to the next, which accounts for growth, recruitment, and mortality). Based on species identification, each tree was categorized as a putative N fixer if it was listed or was a congener (fixation is thought to be primarily conserved at the genus level (Sprent et al. 2017)) of a species listed as an N fixer in Sprent (2009). We also checked for actinorhizal N fixers in our data using the list in Werner et al. (2014), but none were present in our plots. We calculated basal area and basal area increment for all trees, N fixers only, and non-fixers only for each plot (Table S1).

We sampled soil N concentrations using both plot- and tree-based approaches. Plot-based samples were taken in 10 locations in each plot spread evenly across the subplot grid in July, 2015 (Appendix 1 - Fig. S1). Tree-based samples were taken around 20 randomly selected N fixers in each plot in July 2017. Three individual samples were taken at each sampling location resulting in 90 individual samples at 30 sampling locations in each of the five plots. Samples were taken in a triangular configuration with individual samples 1 m apart for plot-based sampling and 2.8 m apart for tree-based sampling (to allow sufficient distance from the tree base). For each sample, soil was extracted using an 8-cm diameter soil core to a depth of 15 cm, homogenized in a plastic bag, and approximately 5 g of soil was massed and immediately placed in 30 ml of 2M KCl extractant. Following incubation and filtering, we analyzed KCl extractions

for inorganic N (NH_4^+ and NO_3^-) concentrations on a Smartchem 170 Discrete Analyzer (Westco Scientific Instruments, CT, USA) at Columbia University.

We measured N inputs via asymbiotic N fixation in the leaf litter at 8 sampling locations distributed evenly across each plot (Appendix 1 - Fig. S1). At each sample location, we removed all leaf litter and fine woody debris from a 50 cm^2 area of the forest floor, placed it in an air-tight glass container, and incubated the sample for 24 hrs in an atmosphere where 49% of the natural N_2 was replaced with isotopically labeled $^{15}N_2$. Samples were incubated *in situ* to approximate ambient environmental conditions as well as possible. We then calculated asymbiotic N fixation rates using the deviation of each sample's isotopic signature (% of atoms that were ^{15}N as opposed to ^{14}N) from the natural isotopic signature in the environment (Appendix 1 - Supplementary Methods).

We estimated symbiotic N fixation inputs by pairing nodule biomass sampling with per-nodule-biomass N fixation rates. To measure nodule biomass, we used both a plot- and tree-based sampling approach similar to that used for soil N sampling (Appendix 1 - Fig. S1). Plot-based nodule sampling took place at 20 evenly distributed locations in each plot using an 8-cm diameter soil core sampled to a depth of 15 cm. Nodulation around specific N-fixers (tree-based approach) was measured on the same samples taken for tree-based soil N measurements. This resulted in 80 individual samples (20 plot-based, 60 tree-based) taken at 50 sampling locations per plot (Appendix 1 - Fig S1). Each soil sample was hand-searched for nodules on the same day as collection, and all nodules were dissected to verify N-fixation activity based on the characteristic pink color of actively fixing nodule tissue. All nodules in an individual sample were then dried at 60°C for at least 3 days and massed.

Per-nodule-biomass fixation rates were measured using $^{15}N_2$ incubations similar to those described above for asymbiotic N fixation. To minimize destructive sampling within the plots, we sampled nodules from 11 *Pentaclethra macroloba* (which comprise 69% of the N fixers in these plots, (Menge and Chazdon 2016)) trees surrounding and adjacent to each plot. For each tree, nodules were removed from the soil by hand and separated from the tree leaving approximately 5 cm of proximate root tissue attached. Nodules were then placed in an air-tight chamber containing an atmosphere of 20 atom % ^{15}N and incubated for 30 minutes. N fixation rates were calculated using the deviation from natural N isotope ratios in a similar manner to asymbiotic N fixation calculations (Appendix 1 - Supplementary Methods). For both ANF and SNF, our use of $^{15}N_2$ incubations obviates the need for the acetylene reduction method, which is cheaper but a source of much uncertainty (Anderson et al. 2004). Therefore, although our nodule incubation sample size is lower than some studies that use ARA, our approach yields more robust results.

Scaling soil nodule biomass and N fixation rates – Each sample for asymbiotic N fixation incorporated all leaf litter in a given area of the forest floor, allowing us to directly scale these rates up to the plot level. Asymbiotic N fixation for each sample was calculated as the mass of N that had been fixed during the incubation period (24 hrs), yielding units of g N fixed·cm^{-2} sample·day^{-1}. This number was then scaled to plot level and annual units (kg N fixed·ha^{-1}·yr^{-1}) assuming that our sampling was representative of the entire plot and year. Scaling ANF measurements from a single time point to annual fluxes should be approached with caution (Reed et al. 2011), but we based our assumption on the fact that our sites experience relatively constant temperature, light, and precipitation (factors thought to control seasonal ANF variability

(Reed et al. 2011)) throughout the year compared to many of the sites where annual variability has been reported.

Because our tree-based sampling locations were chosen specifically to be within 2 m of an N fixer, we had to account for the possibility that these samples would be more likely to contain nodules than our plot-based sampling, which was not oriented regarding N-fixer proximity. To compare these two sampling techniques we normalized our samples using an N-fixer crowding index (NCI), which incorporated the number, size, and proximity of all N fixers within 10 m, as a metric for N-fixer density around each core sample (following methods in Taylor et al. (2017)). We found no relationship between N-fixer crowding around a core location and the biomass of nodules in that sample ($P = 0.88$ for a linear model comparing nodule biomass to N-fixer crowding; see Results section), which agrees with theoretical predictions for sites with high N-fixer abundances such as ours (Menge and Levin 2017) and allowed us to combine plot- and tree-based sampling data when scaling SNF rates. Nodule biomass per sample (g dry nodule biomass$\cdot$ha^{-1}) was then multiplied by per-nodule-biomass fixation rates (g N fixed$\cdot$g^{-1} dry nodule biomass$\cdot$hr^{-1}) to calculate SNF rates in units of kg N fixed$\cdot$ha$^{-1}\cdot$hr^{-1}, then scaled up to yearly rates assuming constant fixation rates throughout the year. A lack of seasonal variation in SNF in a tropical forest in Panama with a stronger dry season than our site (Barron et al. 2011) supports the assumption of constant annual SNF rates.

Statistical Analyses – While our analyses all involved regression-style tests, we implemented slightly different model approaches based on the underlying structure of different datasets. To address successional dynamics of soil N, ANF, SNF, and tree growth using individual core-, focal tree-, or subplot-scale data, we used a maximum-likelihood framework to compare null (no change), linear (or exponential if the response variable was log-transformed), and gaussian fits

between the response variable and stand age. In some cases, additional models were also fit (Appendix 1 - Table S2). Data for soil N and ANF inputs were natural-log transformed for statistical analyses to meet parametric assumptions. Because data for SNF (both SNF inputs and nodule biomass) were zero-inflated lognormally distributed, we used a two-part model that accounted for both the probability of a non-zero value and the distribution of non-zero values separately following methods in Tian & Wu (2006) (see Appendix 1 - Supplemental Methods). This model structure allowed us to separately test for successional changes in the probability of finding nodules and the biomass of nodules (or SNF rates) when they occurred. In all figures where SNF data are presented, we plot the measured and predicted geometric means (median of the lognormal distribution) accounting for zero inflation (Appendix 1 - Supplemental Methods).

Although our old-growth forest plot has no recorded history of disturbance, for regression purposes we used a conservative age assumption of 100 yrs. For each response variable, models were compared using differences in the corrected Akaike Information Criterion (ΔAIC_c) (Anderson 2008). We interpreted models with ΔAIC_c's < 2 to be similar fits. We report results for the model with the lowest AIC_c along with ΔAIC_c for the next best-fit model. All models and ΔAIC_c values can be seen in Appendix 1, Tables S2 – S4. For plot-scale analyses that used plot means as individual data points, we used ordinary least squares regression models with $\alpha = 0.05$. All analyses were done in the base and `bbmle` packages of R statistical software version 3.4.3 (Bolker and R Development Core Team 2017, R Core Team 2017).

Results

How do soil N, ANF, and SNF change through forest succession relative to tree biomass and tree growth?

Our data showed a hump-shaped trend of total soil N through succession, with a peak in our 29-yr-old forests (Fig. 1a; $\Delta AIC_c = 85.3$; Table S2). Ammonium (NH_4^+) made up the vast majority (90-96% for plot-level means; Fig. S2) of soil inorganic N at these sites. Due to the large contribution of ammonium to total soil inorganic N, the successional pattern of ammonium largely mirrored that of total soil N – a hump-shaped trend through succession ($\Delta AIC_c = 219.2$; Table S3). Soil nitrate (NO_3^-), also followed a hump-shaped relationship through succession ($\Delta AIC_c = 82.0$; Table S3). Due to general decreases in ammonium and increases in nitrate with forest age, we found the percent contribution of nitrate to total soil inorganic N was higher in our older plots than in our youngest plots and peaked in our 37-yr plot. ($\Delta AIC_c = 40.38$; Table S3; Fig S2b).

ANF also changed through succession in a hump-shaped fashion ($\Delta AIC_c = 21.5$; Table S2; Fig. 1b), peaking in the 37-yr-old plot, where N inputs from ANF were ~3.9 times greater than our 19-yr plots. This variation in ANF came primarily from variation in asymbiotic fixation rates per gram of leaf litter rather than variation in the amount of leaf litter per ground area (Fig. S3). Our best-fit model for asymbiotic fixation rates per-gram of litter was a hump-shaped trend through succession, similar to the dynamics of total ANF ($\Delta AIC_c = 22.2$, Table S3, Fig S3), whereas our best-fit model for the amount of leaf litter mass per ground area showed no successional change ($\Delta AIC_c = 2.1$, Table S3, Fig. S3).

SNF decreased in an exponential fashion through succession in our sites (Fig. 1c). The geometric mean of SNF was over 4 times greater in our 19-yr plots than in our old-growth plot. Our best-fit model indicated no successional change in the probability of SNF occurring within a core (probability of finding active nodules), but an exponential decrease in SNF through succession for cores that contained nodules ($\Delta AIC_c = 1.46$; Table S2). The two primary sources

of variation in SNF are variation in nodule biomass and in fixation rates per gram of nodule biomass. Variation in nodule biomass was the primary driver of the successional dynamics in total SNF in our plots (Fig. S4). Nodule biomass declined in an exponential fashion through succession (ΔAIC_c = 1.46; Table S3), such that geometric mean nodule biomass was ~6.8 times greater in 19-yr plots than at our old-growth forest site. Conversely, our best-fit model for fixation rates per gram of nodule biomass was a quadratic relationship where per-nodule fixation rates were intermediate in our youngest plots, declined in mid-successional forests, and were greatest in our old-growth forest plot (ΔAIC_c = 38.01; Table S3; Fig. S4). We found significantly positive but noisy relationships between SNF and total inorganic N (ΔAIC_c = 2.03; Table S3; R^2 = 0.09) and between SNF and soil ammonium (ΔAIC_c = 2.05; Table S3; R^2 = 0.095), but no relationship (non-significant negative trend) between SNF and soil nitrate (ΔAIC_c =1.8; Table S3; R^2 = 0.01) (Fig. S6).

Plot-level tree growth declined significantly through succession (ΔAIC_c = 8.65; Table S1, S2; Fig. 1d, S7), as has been previously reported for these plots (Chazdon et al. 2007, Menge and Chazdon 2016, Taylor et al. 2017). Despite our data showing declines in both SNF and tree growth through succession, we found no significant relationship between SNF and tree growth at either the individual-tree scale or the plot scale (Fig S8). At the individual-tree level, our best-fit model showed that SNF in the cores taken around a focal N-fixer did not correlate to the growth of that N fixer (ΔAIC_c = 2.18; Table S4). At the subplot-scale, we also found that our best-fit models described no relationship between total basal area change or basal area change of N fixers and SNF inputs in the subplot (ΔAIC_c = 2.33 and ΔAIC_c = 1.85 for total basal area change and N-fixer basal area change, respectively; Table S4). This was also true at the plot-scale where we found no significant relationships between total basal area change or N-fixer basal area

change and SNF inputs (P = 0.541 and P = 0.116, respectively). We also found no significant relationship between total plot-level tree growth and the combined N inputs from ANF and SNF (P = 0.324; Fig. 2a) although the trend in this relationship was positive.

What is the relative contribution of ANF vs. SNF at each stage of succession?

Overall, N inputs from ANF and SNF were roughly equivalent when combining all plots across our chronosequence, with ANF averaging 3.9 kg N ha^{-1} yr^{-1} and the geometric mean of SNF being 3.5 kg N ha^{-1} yr^{-1}. However, the dominant N input from fixation changed from early- to late-successional forests (Fig. 3). In our 19 yr-old forests, N inputs from SNF were 1.7 times that of ANF. SNF also dominated N inputs in our 29-yr plot, where SNF was 2.2 times greater than ANF. However, ANF was 8.9 times greater than SNF in our 37-yr plot and 5.1 times greater than SNF in our old-growth plot.

How are changes in N-fixing tree abundance through succession related to changes in SNF?

To better understand both localized and stand-level patterns in the relationship between N-fixer abundance and SNF, we assessed this relationship at the core-, tree-, and plot-level. At the individual core level, we did not find a significant relationship between SNF rates and the crowding of N-fixers around the location of the core sample (ΔAIC_c = 3.38; Table S4). We also found no relationship between the crowding of other N fixers around a focal N-fixing tree and SNF estimates for that tree (ΔAIC_c = 2.79; Table S4; Fig. 4a). At the plot level, we found no significant relationship between the basal area of N fixers in a plot and geometric mean SNF inputs in that plot (P = 0.23; Fig. 4b), although the trend in this relationship was negative. There was also no correlation between geometric mean SNF inputs and the stem density of N fixers (P = 0.345) or the ratio of N-fixer to non-fixer stems (P = 0.227) at the plot level.

Discussion

Combining measurements of soil N availability, ANF, SNF, and tree growth, our study provides a rare and robust assessment of the recuperation of N cycling and how N dynamics relate to tree growth in regenerating tropical forests. We found neither systematic increases nor decreases in inorganic soil N availability or ANF inputs across the successional range we studied, but we did find significant declines in SNF and tree growth from our youngest (19-yr) plots to our old-growth forest site. These findings support our hypotheses of declining SNF rates, accumulating tree biomass, and ANF rates that do not vary systematically with forest age. However, our data contradict our hypothesis that soil N would accumulate across the successional gradient we measured. Declines in SNF through succession led to a successional switch in the dominant N-fixation input that we measured. As hypothesized, SNF dominated inputs in our youngest forest sites, but contrary to our predictions, ANF was a much larger N input than SNF in our later successional plots. We also found that SNF rates were not related to N-fixing tree abundances (and the trend was negative, not positive), directly contradicting our hypothesis. Together, these results indicate that N-fixer abundance is a poor predictor of SNF rates, that ANF makes an important (and sometimes dominant) contribution to N inputs from fixation, and that N cycling has largely recovered in these forests by 19 years following disturbance.

The recovery rate of the N cycle represents a critical, but poorly understood, aspect of tropical forest succession. Our results indicate that the N cycle has largely recovered at our site prior to 19 years post-disturbance (Fig 1a) and that our site exhibits high inorganic soil N availability compared to many other Neotropical forest sites (Vitousek and Denslow 1986, Matson et al. 1987, Piccolo et al. 1994, Silver et al. 2001, Davidson et al. 2007, Sullivan et al.

2014). This suggests that either N losses during disturbance were low at these sites or that large N inputs in the early years of secondary succession drove rapid recuperation of the N cycle in these forests. Given that these sites have land-use histories that are thought to create large N losses (Kauffman et al. 1995, McGrath et al. 2001, Davidson et al. 2007, Davidson and Martinelli 2009), it seems more likely that N inputs have driven the rapid recuperation of N cycling at our sites.

Recently, Winbourne et al. (2018) reported rapid recovery of N cycling in Brazilian Atlantic Forests, similar to the rates found at our study site. These rapid rates of N-cycle recovery contrast with estimates from Panama (Batterman et al. 2013a) and the Brazilian Amazon (Davidson et al. 2007) that it takes 30-70 years for the N cycle to recover following disturbance. While many differences exist between these study sites, one potentially important difference may be N-fixer abundances. Both fast-recovery sites (ours and Winbourne et al. 2018) exhibit high N-fixer abundances (~30% of forest basal area), whereas N fixers only comprise ~6% of the basal area at the Panama site that exhibited slower N-cycle recovery. N-fixer abundances in the Brazilian Amazon site were not reported, but typically range from 6-14% regionally (ter Steege et al. 2006). Although N-fixer abundance is not a good predictor of realized SNF rates at any individual place or successional time period (Fig 4a, b), N-fixer abundances do indicate the maximum potential SNF rates for a forest. Thus, sites with high N-fixer abundances may experience especially high SNF rates in the earliest years of forest regrowth, allowing the N cycle to recover more rapidly than in forests with lower N-fixer abundances. Studies explicitly comparing SNF rates in early successional stages of forests that vary in N-fixer abundances, and investigating the environmental regulators of SNF rates in these

forests, are important future steps in understanding the speed of N-cycle recovery in regenerating tropical forests.

Because of the large potential for SNF to bring new N into regenerating tropical forests, the environmental factors that regulate SNF rates are important for both N cycling and biomass recovery dynamics. Much of the ecosystem theory on forest succession predicts that SNF is downregulated as it becomes energetically unfavorable relative to soil N uptake as succession proceeds (Rastetter et al. 2001, Menge et al. 2008). Our data do show a successional trend in SNF inputs (Fig 1c), but this trend was not negatively related to soil N availability (Fig S6b, d, f), suggesting that other resources might play a stronger role. Although we did not measure light availability in this study, recent shadehouse and field data for the most common N fixer in our plots, *P. macroloba*, demonstrates that light availability can be a strong driver of SNF rates (Taylor and Menge n.d.). Light availability to the understory and horizontal light exposure to canopy trees decrease with canopy closure during succession (Denslow et al. 2000, Guariguata and Ostertag 2001), and a pattern of progressively reduced light availability leading to lower SNF rates matches the successional SNF pattern found in our study. Other environmental factors not measured in this study, such as soil phosphorus, moisture, and pH, may also influence successional SNF dynamics.

We found no evidence that the abundance of N-fixing trees determined SNF rates in our plots, contrary to our predictions. The lack of a relationship between N-fixer abundances and SNF in our plots has at least two important implications. First, as ours and other recent studies have shown (Batterman et al. 2013a, Sullivan et al. 2014), SNF rates in mature tropical forests are often low even in forests that have many N fixers. Many early estimates of tropical SNF were based on the assumption that high abundances of putative N fixers in tropical forests lead to high

inputs from SNF (Cleveland et al. 1999, reviewed in Sullivan et al. 2014). Our data add to a growing body of evidence suggesting these early calculations overestimate tropical SNF inputs (Vitousek et al. 2013), especially in intact old-growth tropical forests (Gehring et al. 2005, Batterman et al. 2013a, Sullivan et al. 2014, Bauters et al. 2016). The second implication of our data goes beyond the concept that "N fixers do not always indicate SNF" to show that, in our plots, the relative abundance of N fixers shows a negative trend with SNF (Fig. 4b). Although not a significant relationship, the plots in our study with the highest N-fixer relative abundance (by basal area) were the plots with the lowest SNF inputs while those with the lowest N-fixer relative abundance had among the highest inputs from SNF.

The lack of a positive correlation between N-fixer abundance and SNF rates shown here highlights the potential danger of using N-fixer abundances as a proxy for SNF inputs when estimating N cycling in tropical forests. Some of our earliest estimates of the role of SNF in tropical secondary succession were largely based on the dynamics of N-fixer abundances (Gehring et al. 2005). However, the results presented here add to a growing number of studies showing that N-fixer prevalence is a poor predictor of SNF rates in neotropical forests (Sullivan et al. 2014, Winbourne et al. 2018). As we continue to improve our estimates of N-fixer abundances over large areas of the tropics (e.g. ter Steege et al. 2006, Menge et al. 2017b), it may be tempting to assume that areas with many N fixers experience high SNF rates that could fuel rapid forest growth. Our data indicate that this assumption is not valid and could mislead our understanding of how N and C cycles are coupled in regenerating tropical forests.

In addition to N inputs from SNF, our data suggest that ANF plays an important role providing N for forest regeneration at our study site. Recent studies on N inputs into regenerating tropical forests have drawn different conclusions about the relative importance of SNF to total

forest N fixation inputs. Batterman et al. (2013a) demonstrated that SNF plays a key role in meeting the N demands of regenerating tropical forests, while Sullivan et al. (2014) found that SNF made up < 50% of N inputs in both secondary and primary tropical forests. In our youngest (19-yr and 29-yr) plots, inputs from SNF were greater than those from leaf-litter ANF, lending qualitative support to the findings of Batterman et al. (2013a). However, in our older (37-yr and old-growth) plots, ANF represented the dominant N input from fixation, supporting the assertion of Sullivan et al. (2014) and others (Reed et al. 2011) that ANF is the largest N input via fixation in many, especially mature, tropical forests. Ours is, to our knowledge, the first report of a successional switch from SNF as the dominant N input in early successional tropical forests to ANF as the dominant N input in older forests. It is important to note that Batterman et al. (2013a) did not estimate ANF in their study and reported relatively low SNF rates in late-successional forests, allowing for the possibility that ANF may also be the dominant N input in later stages of succession at their site in Panama and other sites throughout the tropics.

Given the important contribution that ANF can have to total N inputs, understanding the drivers of variation in ANF can provide important insight into successional N dynamics in regenerating tropical forests. The two previous studies assessing the dynamics of ANF in secondary successional tropical forests reported either a reduction in leaf-litter ANF from secondary to primary forests (Sullivan et al. 2014) or no successional trend in ANF (Winbourne et al. 2018). This paucity of data inhibits any broad empirical consensus about the successional trajectory of ANF in tropical forests. However, our results do provide important insight that per-litter-biomass fixation rates (rather than litter mass itself) are the primary driver of variation in leaf-litter ANF. Current evidence suggests that tropical ANF rates increase with the availability of litter phosphorus (Thompson and Vitousek 1997, Crews et al. 2000, Benner et al. 2007, Reed

et al. 2008, 2010, Cusack et al. 2009), molybdenum (Barron et al. 2009), moisture (Reed et al. 2007, Cusack et al. 2009), and C quality (Thompson and Vitousek 1997, Vitousek and Hobbie 2000), but decline with litter N concentrations (Thompson and Vitousek 1997, Cusack et al. 2009). Although many of these environmental factors change through succession, their effects on ANF may interact and counteract one another, currently inhibiting our ability to make general predictions of how ANF rates change during tropical forest succession.

The successional dynamics of soil N, SNF, and ANF reported in this study can also provide important context to our broader understanding of N richness in tropical forests. A fundamental question in tropical ecosystem ecology asks why many lowland, humid tropical forests often export large amounts of inorganic N (Brookshire et al. 2012) given that the largest potential N input in these forests, SNF, should cease once N limitation has been relieved (Rastetter et al. 2001, Menge et al. 2015). Hedin et al. (2009) describe this question in detail and provide a potential resolution, proposing that SNF rapidly replenishes the soil N cycle but shuts off under N saturated conditions, and that other sources of N fixation that are not tied to ecosystem N richness (such as N deposition and leaf litter and canopy ANF) sustain the high N exports by continuing to bring N into N-saturated tropical forests. Our findings show that SNF does downregulate through tropical forest succession, but that ANF continues to bring significant N into mature tropical forests regardless of high soil N availability, lending support to Hedin et al.'s assertion that total biological N fixation represents a "leaky nitrostat" in mature tropical forests. Other Neotropical forest sites indicate similar patterns of downregulation of SNF through succession (Batterman et al. 2013a, Sullivan et al. 2014, but see Winbourne et al. 2018) and sustained inputs from ANF in N-saturated primary tropical forest sites (Sullivan et al. 2014, Winbourne et al. 2018). In light of these studies and the results presented in our current work, we

deem Hedin et al.'s "leaky nitrostat" model a likely contributor to the observed N richness of tropical forests but cannot rule out the importance of incomplete downregulation of SNF, which the authors also note could be important at many sites.

Conclusions

Taken together, our data provide confirmation for several long-standing paradigms in tropical forests, add support to some emerging patterns, and demonstrate some previously unreported N dynamics during tropical forest regeneration. Our soil N data indicate high inorganic soil N availability, which has long been suggested as the norm in humid tropical forests (Vitousek and Sanford 1986, Vitousek and Matson 1988, Martinelli et al. 1999). This high soil N availability and the absence of a relationship between N inputs and tree growth suggest that N pools have largely recuperated prior to 19 yrs post agricultural abandonment at our site, similar to the rapid recuperation of N pools seen in other sites with high N-fixer abundances (Winbourne et al. 2018). Our data also show a successional decrease in SNF and relatively low SNF inputs in mature forests, which has been commonly reported for tropical forests (Gehring et al. 2005, Barron et al. 2011, Batterman et al. 2013a, Sullivan et al. 2014, Bauters et al. 2016). In our late successional plots, ANF was the dominant N input that we measured, similar to the findings of Sullivan et al (2014). However, we also report the novel result that the dominant N input in our plots switches from SNF to ANF as tropical forests age, which we hope will guide future research on tropical N cycling at various successional stages.

Understanding the successional N dynamics of regenerating tropical forests is critical for well-informed modeling efforts and management practices. The rapid recuperation of N cycling and corresponding accumulation of biomass in these forests suggest that the biomass resilience seen in many tropical secondary forests (Poorter et al. 2016) may be at least partially attributable

to successional N dynamics. That both N and C pools in our plots recovered from disturbance within 20-40 years without human intervention qualitatively supports recent studies showing that natural forest regeneration is at least as effective as active restoration in tropical forests (Crouzeilles et al. 2017, Meli et al. 2017). Together, these data suggest that the dynamics of N cycling are critical to the C-capturing potential of secondary tropical forests, and that current and future studies on these N dynamics will prove useful for global models that predict how tropical forests will respond to future environmental and land-use changes.

Acknowledgements:

The authors would like to thank J. Paniagua, B. Paniagua, E. Salicetti, B. Scott, B. Matarrita, and D. Brenes for assistance with data collection and laboratory analyses. R. L. C. received funding for plot establishment and censuses from the Andrew W. Mellon Foundation, NSF DEB-0424767, NSF DEB-0639393, NSF DEB-1147429, NASA Terrestrial Ecology Program, and the University of Connecticut Research Foundation. B. N. T. received funding for this work from the Garden Club of America, Columbia University's Institute for Latin American Studies, and Columbia University's Ecology, Evolution, and Environmental Biology Department.

Figures and Tables

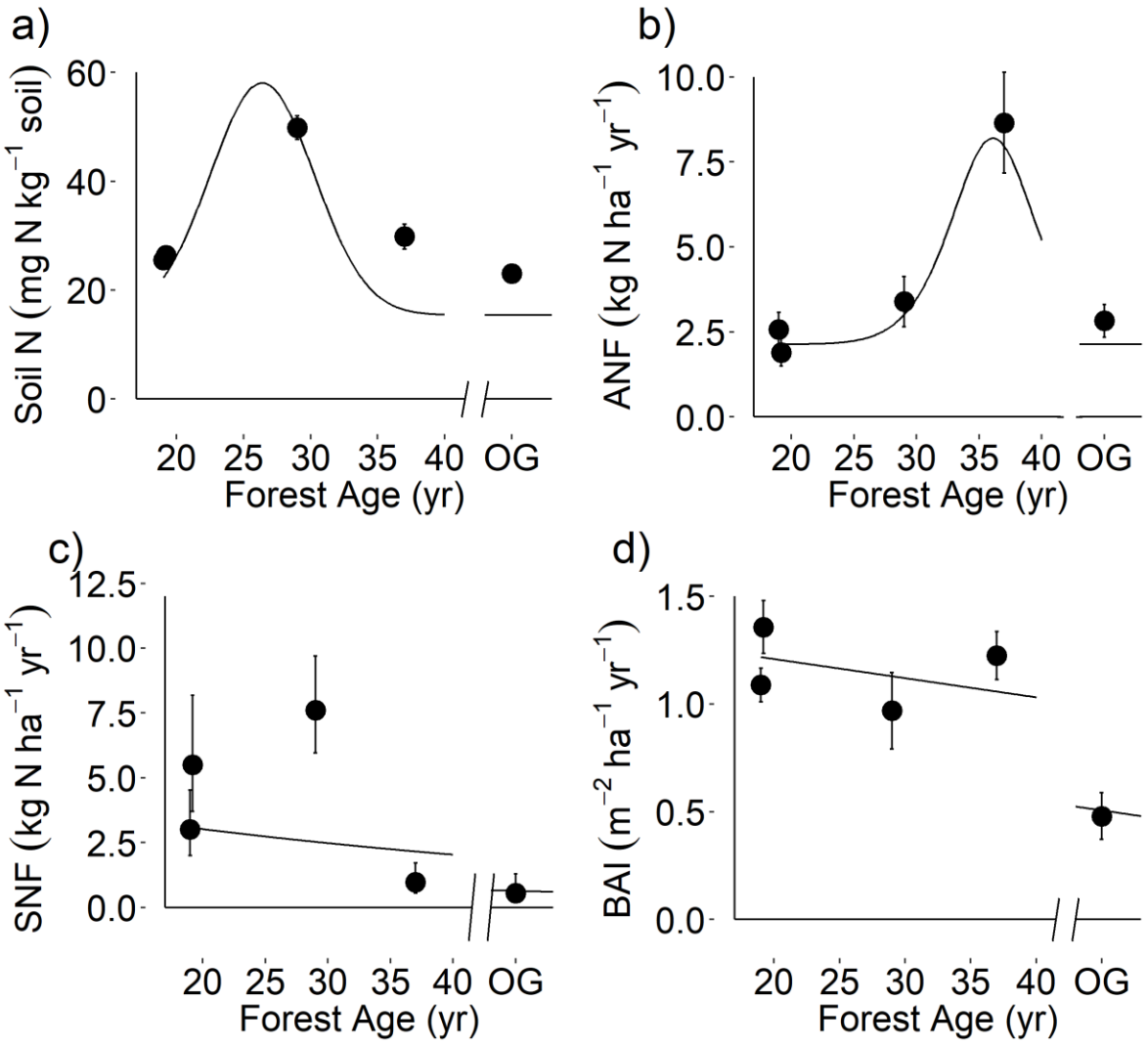

Figure 1: Successional dynamics of N cycling and tree growth.

Dynamics of **a)** soil inorganic N, **b)** asymbiotic N fixation, **c)** symbiotic N fixation, and **d)** tree growth (basal area increment) across forest succession in our 5 study plots. Each point represents the plot-level mean (geometric mean in **c**) with error bars representing ±1 S.E. Curves represent the best-fit models for each variable across forest age. Both left-hand points represent 19-yr forests but are jittered for viewing purposes. OG indicates our old-growth plot that has no recorded history of disturbance.

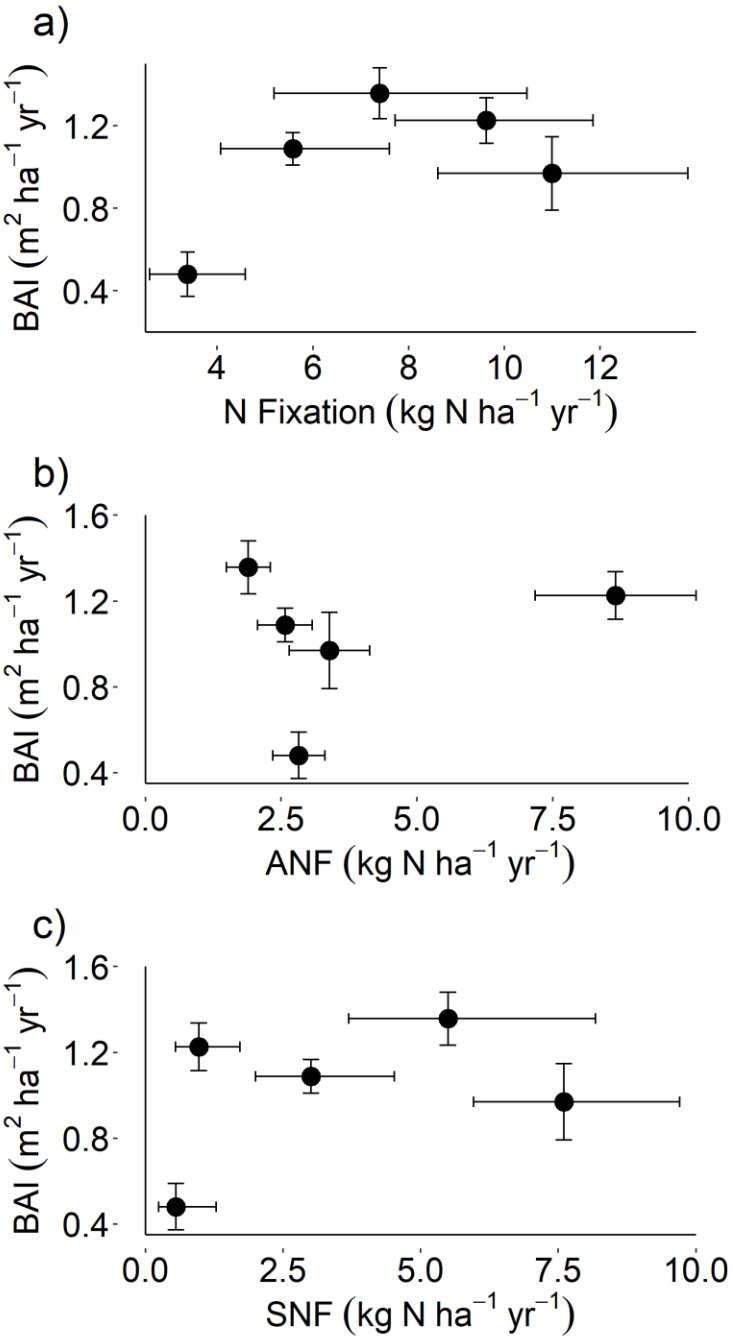

Figure 2: Basal Area Increment vs. N fixation.

Plot-level tree growth (basal area increment) is not significantly related to **a)** total N inputs from fixation (SNF + ANF) **b)** inputs from ANF, or **c)** inputs from SNF in our plots. Points represent each of our five 1-ha study plots. BAI is the mean (±1 S.E.) of BAI in each of 100 10 x 10 m subplots scaled to 1-ha area.

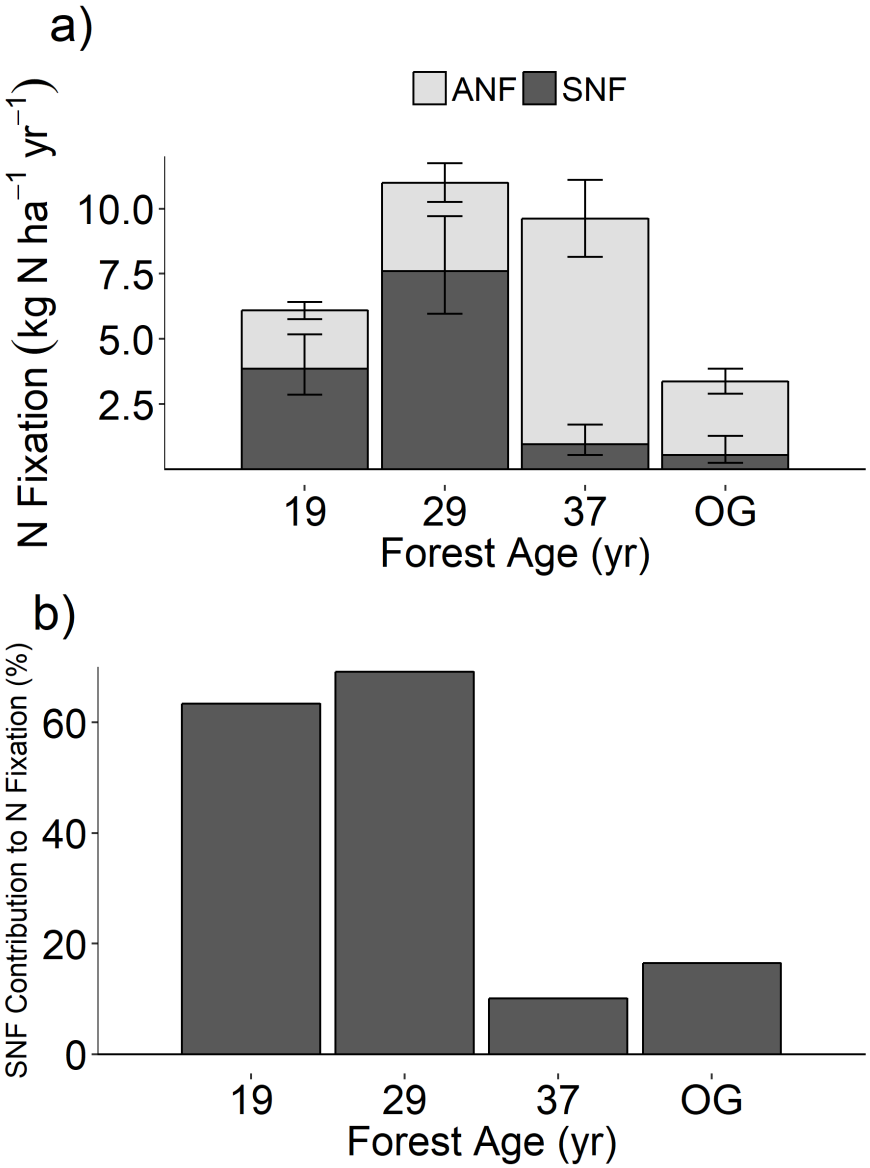

Figure 3: Components of N fixation

The **a)** relative contributions of asymbiotic N fixation (ANF) and symbiotic N fixation (SNF) and **b)** percent contribution of SNF to total N fixation inputs measured in forests from 19 yrs old to old-growth (OG). The bar for 19-yr forests represents the mean rates of our two 19-yr forest plots. Bars for ANF and SNF represent arithmetic and geometric means, respectively (see Appendix 1). Error bars represent ±1 S.E. The dominant N input measured switched from SNF in young plots to ANF in older forests.

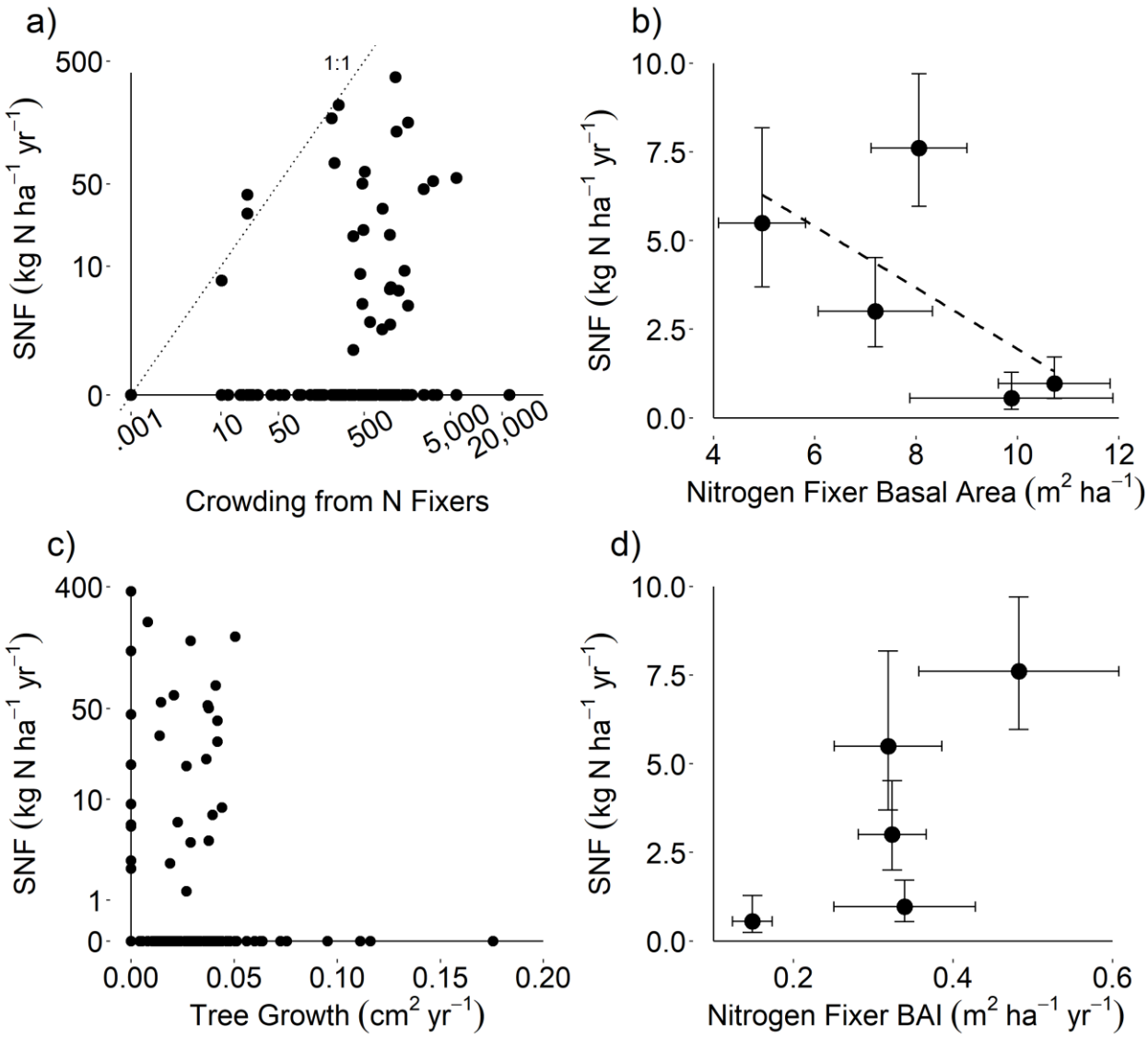

Figure 4: SNF vs. N-Fixer Abundance

The relationship between symbiotic N fixation (SNF) and N-fixer prevalence at the **a)** individual tree, **b)** N-fixer basal area at the plot scale, **c)** N-fixer tree growth at the individual tree scale, and **d)** N-fixer basal area increment at the plot scale. The vertical values of points in **a)** and **c)** represent SNF rates sampled from 3 cores each for 100 N-fixing trees. The horizontal values in **a)**, "crowding from N fixers," were measured as the neighborhood crowding index (NCI, which is unitless) from neighboring N fixers for each focal tree. Points in **b)** and **d)** represent plot-level

geometric means for SNF and arithmetic means (±1 S.E) for N-fixer basal area and N-fixer BAI, respectively. The dashed line in **b)** represents a non-significant linear regression for the relationship between SNF and N-fixer basal area. Both axes in **a)** and the vertical axis in **b)** are presented on log scales with linear (untransformed) values. Panels **a)** and **c)** plotted with linear axes are presented in Appendix 1, Fig. S8. We found no relationship between SNF and crowding from N fixers at the tree scale.

CHAPTER 2: LIGHT REGULATES SYMBIOTIC NITROGEN FIXATION MORE STRONGLY THAN SOIL NITROGEN AVAILABILITY

Benton N. Taylor, Duncan N. L. Menge

Abstract

Nitrogen (N) limits primary production in almost every major biome on Earth (Elser et al. 2007, LeBauer and Treseder 2008). Symbiotic N fixation (SNF), conducted by certain angiosperms and their endosymbiotic bacteria, is the largest potential natural source of new N into the biosphere (Chapin III et al. 2011), influencing global primary production, carbon sequestration, and element cycling. Because SNF represents an alternative to soil N uptake, much of the work on SNF regulation has focused on soil N availability (Vitousek and Howarth 1991, Barron et al. 2011, Batterman et al. 2013a, 2013b, Menge et al. 2015). However, because SNF is an energetically expensive process (Gutschick 1981), light availability to the plant may also regulate SNF rates (Vitousek and Field 1999, Rastetter et al. 2001). Despite the importance of SNF to biosphere functioning, the environmental factors that most strongly regulate this process remain unresolved. Here we show that light regulates SNF more strongly than does soil N, and that light mediates the response of SNF to soil N availability. In shadehouse experiments, low light levels (comparable to forest understories) completely shut down SNF, whereas soil N levels that far exceeded plant demand did not fully down-regulate SNF at high light. For *in-situ* forest seedlings, light was the only significant predictor of SNF activity. Light as a primary regulator of SNF is a departure from decades of focus on soil N availability. This shift in our understanding of SNF regulation can resolve long-standing biogeochemical paradoxes (Hedin et al. 2009), and will improve our ability to predict how SNF will fuel the global forest carbon sink and respond to human alteration of the global N cycle.

Introduction

One of the largest uncertainties in current climate-change predictions is the extent to which symbiotic N-fixing plants will fuel increased forest growth under future CO_2 conditions (Gerber et al. 2010, Wårlind et al. 2014). These symbiotic "N fixers" have the potential to relieve N limitation by converting atmospheric N_2 gas into bio-available forms—potentially increasing the terrestrial carbon sink, but whether they do so depends on how much N they fix. Many N fixers can regulate how much N they fix per unit biomass (Crews 1993, Barron et al. 2011, Batterman et al. 2013a, Menge et al. 2015), but which environmental factors govern this regulation remain largely unresolved.

The availability of soil nutrients (Vitousek and Howarth 1991, Crews 1993, Barron et al. 2011, Batterman et al. 2013b), light (Vitousek and Field 1999, Rastetter et al. 2001), water (Wurzburger and Miniat 2014), and temperature (Houlton et al. 2008) have all been suggested to play a role in regulating SNF. Of these, soil resources – especially soil N availability – have received the most attention. Because SNF represents a direct alternative to soil N uptake, the availability of soil N represents a logical regulator of SNF. However, because SNF is energetically expensive (Gutschick 1981), an N fixer's access to light may also determine how much N the plant fixes. Although existing theory suggests that light could strongly regulate SNF (Vitousek and Howarth 1991, Vitousek and Field 1999, Rastetter et al. 2001) and light has been shown to regulate SNF in some agricultural N fixers (e.g. MacDowall 1982, Murphy 1986), little empirical work has directly tested this mechanism in natural systems (Sprent 1973, McHargue 1999, Myster 2006).

Methods

We paired a shadehouse experiment with natural field sampling under varying conditions of light and soil N availability to ask: Does light or soil N availability have a stronger influence on the regulation of SNF? Our shadehouse experiment grew individuals of a common Neotropical N fixer, *Pentaclethra macroloba*, under a full-factorial design of 3 soil N treatments and 3 light treatments. While our light treatments (8%, 16%, and 40% full sunlight) represented a subset of possible natural conditions a plant could experience, the high end of our N treatments (0.51, 20, and 40 g N m^{-2} yr^{-1} added to a sand/soil mix) far exceeded natural N conditions. *P. macroloba* individuals were raised from seed for 6 months in an open-air shadehouse in Costa Rica, after which the plants were harvested to measure biomass growth, allocation to root nodules (the symbiotic structures where SNF occurs), and rates of SNF (see Appendix 2). Our field sampling involved assessing light availability using hemispherical photographs and soil inorganic N availability using KCl extracts for 100 *P. macroloba* seedlings/saplings growing naturally in forest understories. We then harvested each of these plants and assessed nodulation as a proxy for SNF activity (see Appendix 2).

Results

Light limited the biomass growth of *P. macroloba* in the low- and medium-light treatments (Figure 5a-c) similar to field observations for this species (Chou et al. 2017). Low N levels limited plant growth in the high-light treatments only (Figure 5c). Nodule biomass responded most strongly to light availability: within low-N treatments, N fixers allocated over 230-fold more of their belowground biomass to nodules in high- vs. low-light (Figure 5d-f). The addition of soil N also influenced nodule biomass, but to a much smaller degree. In the high-light treatments, N fixers allocated 7.7-fold more of their belowground biomass to nodules in low- vs. high-N fertilization.

Using an isotopic soil ^{15}N tracer to track the various sources of plant N, we calculated the percent of each plant's N it derived from SNF ($\%N_{dfa}$). $\%N_{dfa}$ varied across treatments in a similar pattern to nodulation (Figure 5g-i). In the high-light treatments, plants fixed 34% and 20% of their N in low- and high-N treatments, respectively, whereas plants fixed 0% of their N in the medium- and low-light treatments, regardless of N conditions. We also found that total N fixed by each plant ($\%N_{dfa}$ multiplied by total N in each plant) was much more strongly influenced by light than by N (Figure 6).

Interestingly, light availability at 8% of full sunlight (more than most forest understories (Chazdon and Pearcy 1991)) completely inhibited N fixation, as did 16% sunlight (though we did find some nodules in the lowest N treatment). However, soil N availability that demonstrably relieved N limitation (medium and high N treatments) did not fully inhibit SNF at 40% full sunlight. The response of fixation to light suggests that below some threshold of light availability, *P. macroloba* down-regulates SNF completely because it is not N limited, because it lacks sufficient energy resources to fix N, or both. By contrast, the incomplete downregulation of SNF in response to N fertilization at high light demonstrates that, given sufficient light, *P. macroloba* continues to engage in SNF even when it is not N limited.

Because plants reared in shadehouse conditions are only a limited reflection of nature, we sought to verify our experimental findings with forest seedlings *in situ*. We measured the % of belowground biomass allocated to nodules (to control for variation in plant size) on 100 *P. macroloba* seedlings growing across a spectrum of light and soil N conditions in rainforest understories. We found that nodulation was significantly positively correlated with light availability ($\Delta AIC_c > 1.63$, Figure 7a) but was not correlated with soil N ($\Delta AIC_c > 1.62$, Figure 7b). Our models indicated that the positive effect of light on nodulation was driven by an

increase in the probability that a plant nodulated with increasing light availability. Due to differences in other potential SNF regulators (e.g. non-N soil resources, plant competition, or herbivory) between our shadehouse and field studies, we suggest approaching direct comparisons of our environmental gradients between these two studies with caution. Still, these *in-situ* data lend support to our shadehouse results that light is a stronger driver of SNF than soil N availability.

Discussion

Three prior studies assessing the effects of light on nodulation found complete or near-complete downregulation of allocation to nodules in low-light conditions, just as we did (Sprent 1973, McHargue 1999, Myster 2006). Although these prior studies did not directly measure SNF rates, our current understanding of SNF suggests that complete downregulation of nodulation fully inhibits SNF activity. Evidence for how strongly soil N regulates SNF is more mixed. Several studies found incomplete downregulation of SNF in response to N fertilizer (McHargue 1999, Myster 2006, Pons et al. 2007, Batterman et al. 2013b), similar to our high-light treatment, while others report that N additions completely downregulated SNF (McHargue 1999, Myster 2006, Menge et al. 2015), similar to our medium- and low-light treatments. Our data suggest that one possible explanation for the discrepancy between these studies may be differences in light availability under different experimental conditions. The ability of light to mediate SNF responses to soil N (and potentially other factors such as phosphorus) may help us develop our emerging understanding of why and how some species match SNF closely with N demand while others are either over-regulators or under-regulators (Menge et al. 2015).

Our results can also help refine SNF regulation theory. Current theory (Menge et al. 2015) envisions that different plant species vary in how they regulate SNF in response to

limitation by N and another resource (e.g. light (Rastetter et al. 2001), soil phosphorus (Houlton et al. 2008, Menge et al. 2015), or an undefined density-dependent resource (Menge et al. 2009, 2017a)). Perfectly facultative N fixers decrease from relatively high SNF under conditions of N limitation to zero SNF under conditions of limitation by the other resource. Obligate N fixers maintain similar SNF rates per unit biomass regardless of which resource limits them, and incomplete down-regulators are in between (Menge et al. 2015). Our data demonstrate that species' SNF strategies, rather than simply being traits intrinsic to the taxa, vary as functions of light availability. *Pentaclethra macroloba* is perfectly facultative at low light, but an incomplete down-regulator at high light (Figures 5g-i, 8). Incorporating light regulation of SNF strategies may inform aspects of SNF theory ranging from the ability of individual plants to regulate SNF (Menge et al. 2015) to the effects that SNF regulation has on global patterns of N cycling (Houlton et al. 2008, Menge et al. 2017a).

In particular, SNF has for almost a decade been the focus of an apparent paradox in the biogeochemistry literature – that of tropical forest N richness. Many tropical forests export large amounts of bio-available N, which budgets suggest come largely from overactive SNF (Brookshire et al. 2012). Yet intuition, theory, and field observations (Barron et al. 2011, Batterman et al. 2013a, Sullivan et al. 2014) have suggested that N fixers in tropical forests downregulate SNF in a perfectly facultative manner (black line, Fig. 8), which should minimize exports of bio-available N (Brookshire et al. 2012, Menge et al. 2015). Large N exports from tropical forests are only paradoxical if SNF shuts off completely when N limitation has been overcome (Menge et al. 2015). In our shadehouse experiment, plants that were demonstrably N saturated continued to fix N at ~80% the rate of N-limited plants when given ample light availability (Fig. 6c). Even small amounts of SNF that continue after N limitation has been

relieved (pink area in Fig. 8) can lead to large bio-available N export (Menge et al. 2015), and our results suggest that SNF may be substantial in N-saturated environments when there is sufficient light. Given that tropical forests receive ample solar energy (Liang et al. 2014), light-driven SNF rates well exceeding plant demand could be common, which would lead to large exports of bio-available N (Menge et al. 2015) and would, therefore, resolve the paradox. This paradox is just one important example of how a stronger consideration of light as the primary regulator of SNF can improve our understanding of N inputs into the biosphere.

Here, we provide clear evidence that light can be a strong and absolute (has the capacity to completely inhibit) driver of SNF, and can mediate the responses of SNF to soil N. While our study focused on a single N-fixing tree species, the limited number of studies that assess light effects on SNF cover a broad spectrum of woody and herbaceous N-fixing taxa from multiple legume subfamilies, and all show strong effects of light on SNF regulation (Sprent 1973, MacDowall 1982, Murphy 1986, McHargue 1999, Myster 2006). This suggests that SNF research should shift from past decades' focus on soil N to looking at other factors, such as light, as the dominant regulators of N inputs into the biosphere. The taxonomic diversity and geographic extent of symbiotic N fixers imply that a variety of environmental factors may play a role in regulating SNF, but our results suggest that the strongest regulator in some ecosystems is not soil N. Given the magnitude of the responses seen in this study, we suggest that regulation by light be a primary consideration as we continue to improve our understanding of the role that SNF plays in global N and C cycling.

Acknowledgments

The authors would like to thank E. Salicetti, M. Wilcots, R. Li, B. Scott, E. Utset, B. Matarrita, D. Madrigal, and O. Vargas for help conducting the experiment, collecting, and

processing samples. This work was supported by the Garden Club of America's Award in Tropical Botany, Columbia University's Earth Institute, and the Institute for Latin American Studies.

Figures and Tables

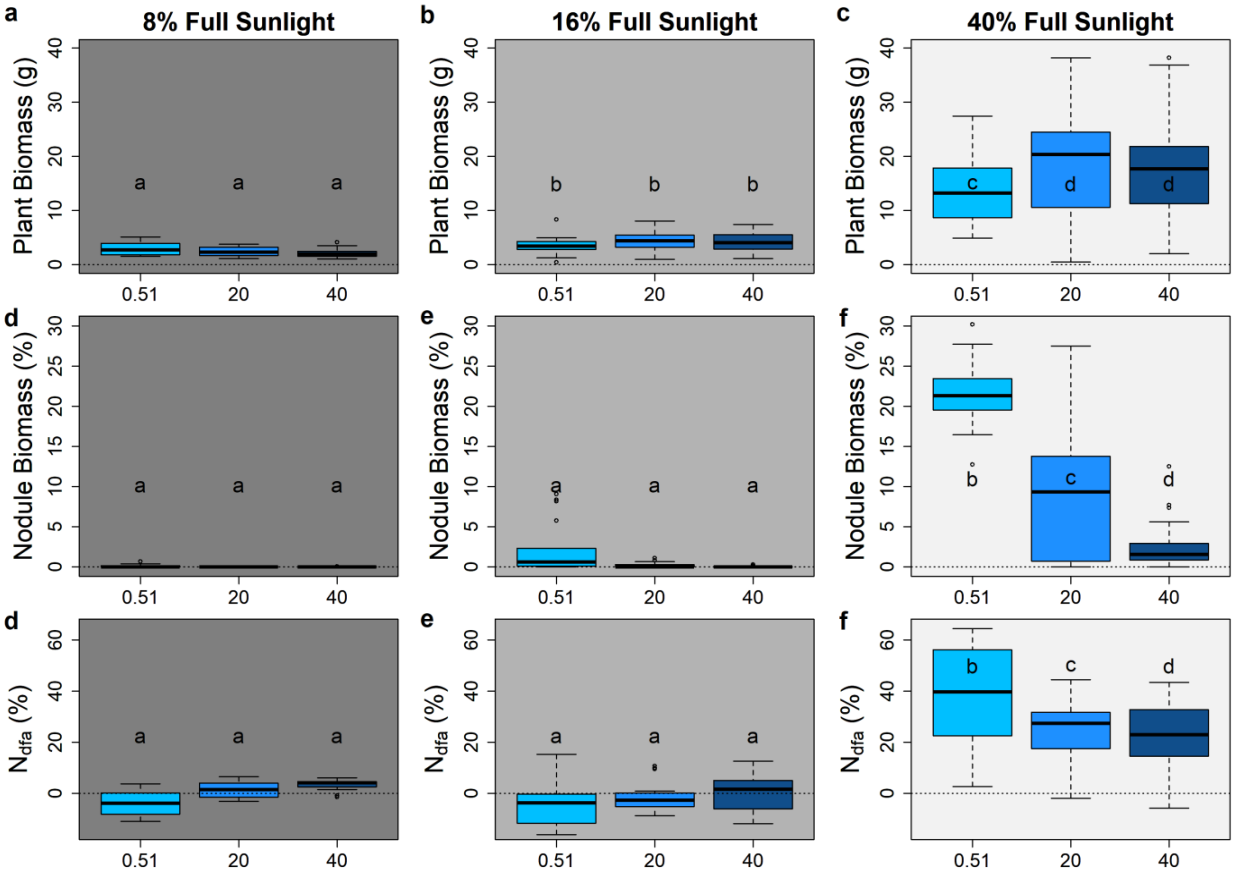

Figure 5: Light is a stronger driver than soil N for biomass and N fixation.

a-c, Plant biomass, **d-f**, allocation to nodules (% of belowground biomass), and **g-i,** percent of plant N derived from fixation (%N_{dfa}) all varied more strongly across light treatments than across N treatments. Light treatments are shown as the left, middle, and right-hand columns. Nitrogen treatments are represented by the three bars within each panel. Error bars represent ± 1 S.E. from the mean, with mixing-model end-member variation incorporated into error bars for **g-i**. Within each row, bars with different letters are statistically different.

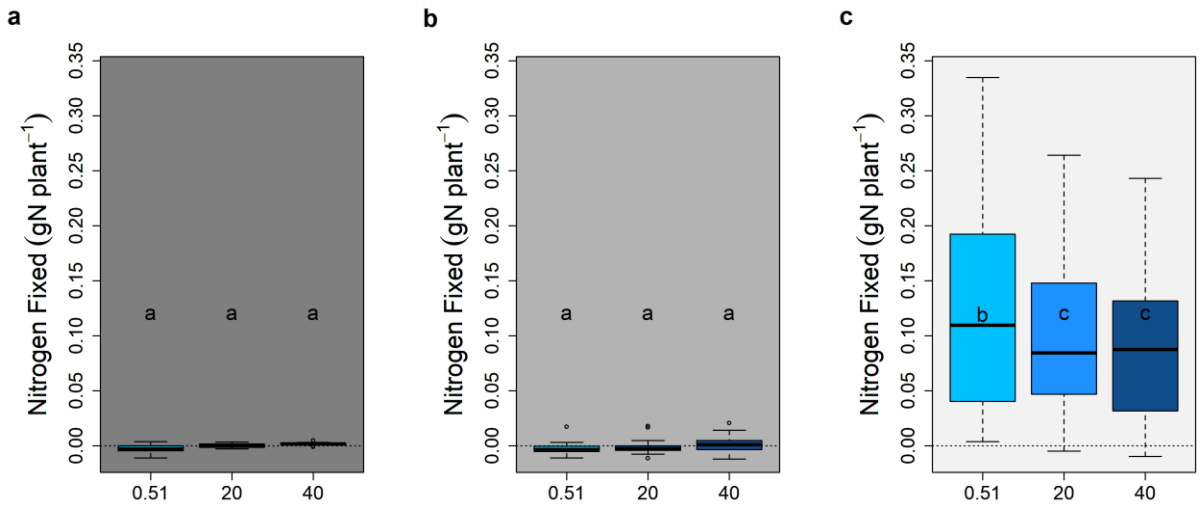

Figure 6: Light drives total fixed N in plants more strongly than soil N

The total amount of N fixed per plant for shadehouse plants grown in **a,** low-, **b,** medium-, and **c**, high-light treatments. Low-, medium-, and high-nitrogen treatments are represented by the three bars in each panel. Error bars represent ± 1 S.E. from the mean, and bars with different letters are statistically different.

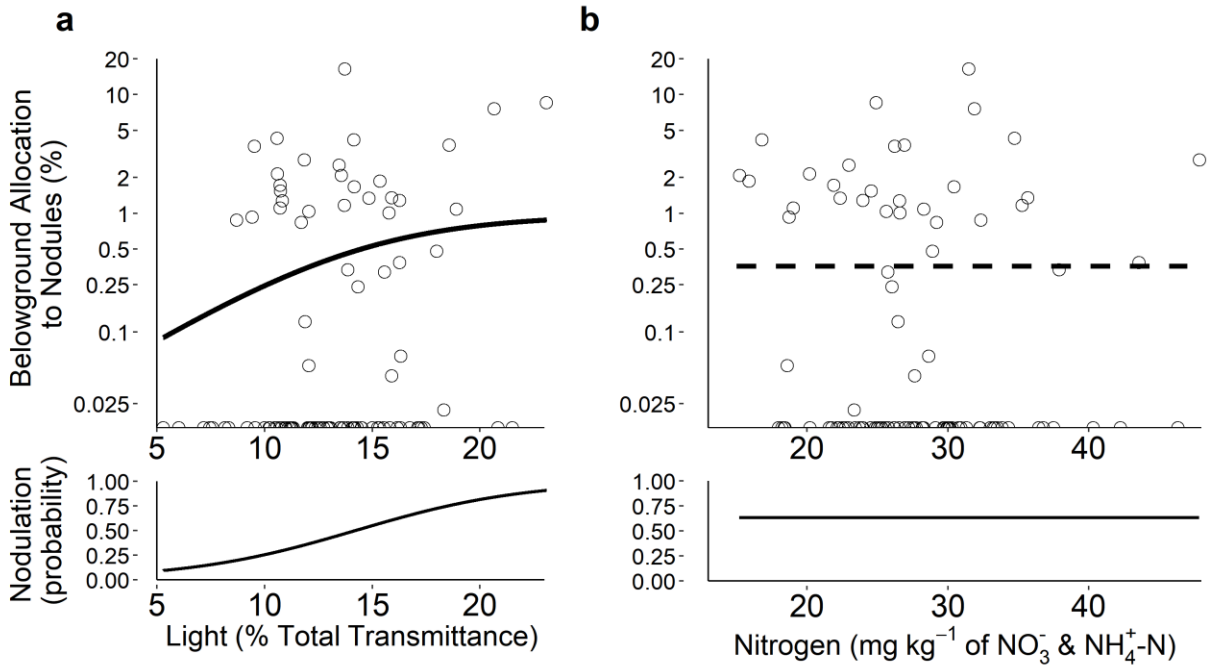

Figure 7: *In-situ* field nodulation varies with light, but not soil N

a, Nodule biomass (on a log scale) and the probability of a plant nodulating increased significantly with seedling light availability in 100 seedlings growing in the rainforest understory. **b,** However, nodule biomass and the probability of a plant nodulating did not vary significantly with soil N availability in field-sampled seedlings. Points along the x-axis represent individuals with 0% allocation to nodules. Versions of these figures with linear-scale y-axes are available in Extended Data Figure 1.

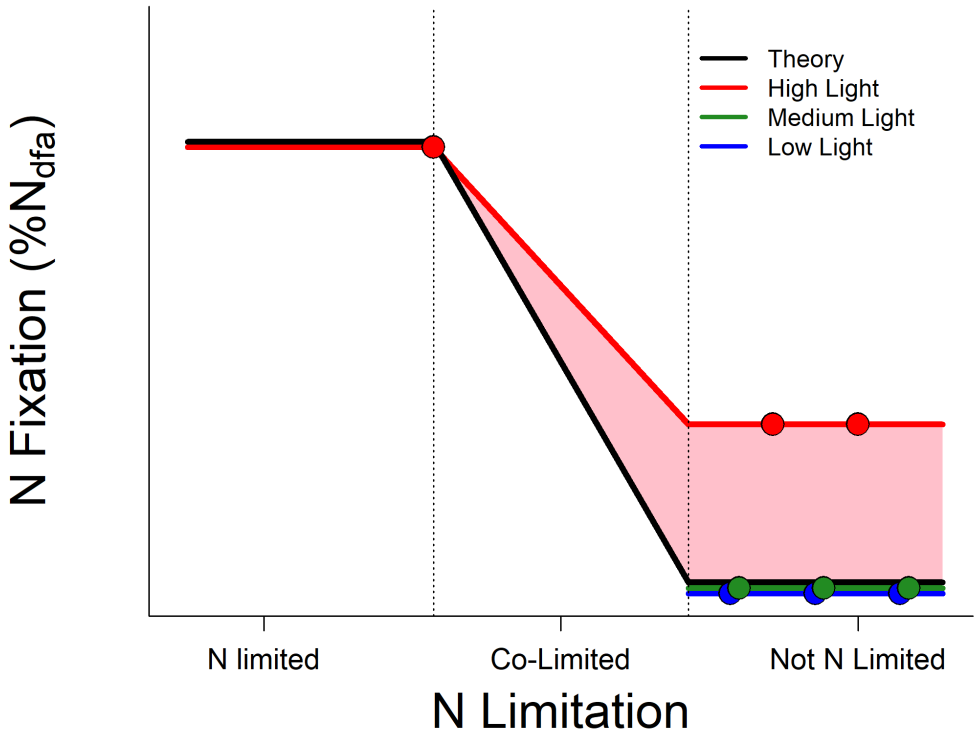

Figure 8: Results in the context of SNF theory

Theory (black) predicts that SNF will respond to limitation by N and another resource in equal but opposite directions. By contrast, our data suggest that SNF responds to N limitation differently depending on light availability. In high-light (red), our plants continued to fix even when N limitation was relieved, but in low- (blue) and medium-light (green) they did not fix N despite low soil N levels. Points represent results from our 9 shadehouse treatments. The pink-shaded region shows conditions where theory under-predicts SNF relative to our results.

CHAPTER 3: TROPICAL NITROGEN-FIXING TREES RESPOND TO COMPETITION AND ENVIRONMENTAL CONDITIONS DIFFERENTLY DEPENDING ON THEIR ABILITY TO FIX NITROGEN

Benton N. Taylor and Duncan N.L. Menge

Abstract

Symbiotic nitrogen (N) fixers are unique among plants in their dual ability to take up N from the soil and access the vast atmospheric N pool through fixation, but taking advantage of N fixation is energetically expensive. The ability to fix N may confer a competitive advantage or disadvantage to the plant depending on the relative availability of soil N and energy to fuel the fixation process. Understanding the competitive effects of the ability to fix N is critical to our theoretical predictions of ecosystem dynamics, but empirical data on the growth effects of the ability to fix N are exceedingly rare. We grew active N-fixing and inactive N-fixing plants (N-fixing plant species without their symbiotic bacteria) in isolation and in direct competition with non-fixing plants under gradients of light and soil N availability to assess how the ability to fix N affects growth, biomass allocation, and competitive success. The ability to fix N did not convey a growth advantage to active N fixers in any environmental treatment, even when N demonstrably limited growth. However, active N fixers were more resistant to competition effects on plant height than inactive N fixers in N-limited conditions. Active N fixers in N-limited conditions fixed less N in the presence of a competitor, likely increasing their competitive influence on neighbors when soil N is scarce. Moreover, N fixation did not represent a net structural cost to the plant, even in cases where N fixation more than exceeded plant N demand. These results suggest that the ability to fix N may be a key competitive strategy to avoiding competition when

soil N is limiting in tropical forests, and that luxury N fixation may not represent a large cost to tropical N fixers under high-light conditions.

Introduction

Due to their ability to convert atmospheric nitrogen (N) gas into bioavailable forms, symbiotic N-fixing plants can have important impacts on the ecosystems they inhabit. N inputs from these "N fixers" have the potential to be a dominant source of new N into terrestrial ecosystems (Chapin III et al. 2011, Vitousek et al. 2013), but whether this potential is realized depends on both the relative abundance of N fixers and their individual N fixation rates. The ecological factors that control these abundance and fixation-rate patterns, however, are not well understood.

In tropical forests, many N fixers regulate N fixation rates in response to the environment (Chapter 2, Barron et al. 2011, Batterman et al. 2013a). This creates an important distinction between the ability to fix N (being a plant species that can form a symbiosis with N-fixing bacteria) and actual N fixation (the process of converting N_2 gas into bioavailable forms). Hereafter, we will use the terms "ability to fix N" and "N fixation" to refer to N fixers with access to their symbionts and the process of N fixation separately. Following convention, we also use the term "N fixer" to describe any plant that can form N-fixing symbioses, regardless of whether or how much it is fixing. While the ability to fix N is largely a static trait (a plant either is or is not a putative N fixer (Sprent 2009)), N fixation can vary within an individual plant depending on the environmental conditions and the access to symbiotic bacteria.

Just as the ability to fix N and the process of N fixation are distinct, the environmental regulation of the ability to fix N and environmental regulation of the N fixation process are related, but distinct, ecological processes that take place at different spatial and temporal scales. Environmental regulation of N fixation itself takes place within an individual N fixer. Theory suggests that a plant should regulate N fixation to maximize the fitness benefits and minimize the

costs of N fixation, both of which are influenced by environmental conditions. N fixation can benefit the plant by providing an alternate source of N when soil N is scarce (Vitousek and Howarth 1991) or by supplementing N to allow the plant to create N-rich compounds for mining phosphorus (Houlton et al. 2008, Batterman et al. 2013b, Nasto et al. 2014) or deterring herbivores (Mattson 1980, Coley and Barone 1996). Alternatively, N fixation represents a large potential carbon (C) cost to the N fixer. N fixation is an energetically expensive process, requiring 2 to 4 times more energy than soil N uptake, and the root nodules where N fixation occurs represent an additional potential structural cost to the plant (Gutschick 1981). This means that acquiring N from fixation should cost the plant more C than acquiring N from soil N uptake under all but the most N-limited conditions. Together, this suggests that the net cost or benefit of N fixation to the N fixer may be largely determined by some combination of light (energy) and soil N availability, in addition to other environmental factors.

Because the ability to fix N is static in an individual plant, the environmental regulation of the ability to fix N is inherently a community-level process determined by the demographic rates of N fixers compared to competing non-fixers. For N fixers, the unique ability to access the vast atmospheric N pool might make them relatively insensitive to belowground competition and thus have relatively high survival rates when soil N is the primary limiting resource (Vitousek and Field 1999, Rastetter et al. 2001). However, the costs of fixation suggest that N fixers might be relatively sensitive to competition for other resources, such as light (Vitousek and Field 1999, Rastetter et al. 2001, Menge et al. 2008). Additionally, intuition tells us that there must be some cost to or constraint on the ability to fix N itself, otherwise all plants would be N fixers that perfectly regulate fixation in response to N demand (Vitousek and Howarth 1991).

Temporal variation in N availability could also create a net advantage or disadvantage for N fixers. The ability to fix N could create a net benefit if it allows N fixers to survive periods of N scarcity. Alternatively, if the ability to fix N represents a large structural cost (maintenance of nodule tissue, for example) during periods of N richness when N fixation is downregulated, it could create a net competitive disadvantage to N fixers (Menge et al. 2009, 2015). Thus, both the ability to fix N and N fixation can create either a net advantage or a net disadvantage when N fixers and non-fixers compete depending on environmental conditions and the costs and benefits of fixation.

In addition to growth and competitive success, the ability to fix N and N fixation may have important effects on the allocation of biomass within an individual N fixer. The functional equilibrium theory of biomass allocation poses that plants allocate more resources to acquiring the most limiting resource (Canham et al. 1996, Poorter and Nagel 2000). In non-fixers, this means that plants should increase allocation to light-capturing stuctures (leaves) when soil resources are abundant but allocate biomass to root tissue when soil resources are scarce. N fixers should follow similar patterns in response to non-N soil resources. However, under N-limited conditions, N fixers may allocate biomass either to roots and nodules for enhanced N acquisition or to leaves for enhanced photosynthesis to fuel the N fixation process. Together, these theoretical predictions suggest that the ability to fix N and N fixation should have important effects on the growth and biomass allocation of N fixers, but these predictions have rarely been empirically tested and the costs and benefits of fixation remain poorly quantified.

In tropical forests, dense tree communities (Pan et al. 2013), relatively high N-fixer abundances (ter Steege et al. 2006, Menge et al. 2017a), and heterogeneous environmental conditions (Townsend et al. 2008) mean that the competitive success of N fixers vs. non-fixers

may be especially important in shaping local tree communities and nutrient pools. The limited evidence from studies on the competitive dynamics of tropical N fixers and non-fixers is mixed. In a shadehouse competition experiment, Nasto et al. (2017) found either no effect or positive effects of competition on the growth of two tropical N-fixing species, but negative growth responses to competition for non-fixers. Alternatively, Taylor et al. (2017) found that the growth of N fixers *in situ* in regenerating tropical forests was reduced by competition equally or more-so than that of non-fixers depending on forest age. These varying responses highlight our poor understanding of how environmental conditions affect the growth, biomass allocation, and competitive success of N fixers and non-fixers in tropical forests.

To better understand how the ability to fix N and N fixation influence growth, resource allocation, and response to competition under different environmental conditions, we conducted a controlled shadehouse experiment with active N-fixing plants, inactive N-fixing plants, and non-fixing plants across gradients of light- and soil N-availability asking: 1) *Under what conditions does the ability to fix N convey a growth advantage or disadvantage to N fixers?* 2) *Does the ability to fix N change how plants allocate aboveground and belowground resources under different environmental conditions?* 3) *Under what environmental conditions does nodule production for N fixation represent a structural cost vs. benefit to the plant?* Based on the above theoretical and empirical evidence, we hypothesized that N fixers would experience a growth advantage over non-fixers in high-light, low-N conditions, but a growth disadvantage under low-light, high-N conditions. We also hypothesized that under N-limited conditions (high-light, low-N), N fixers would allocate more biomass aboveground to acquire light resources to fuel fixation, whereas non-fixers would allocate more biomass belowground to forage for scarce soil N.

Finally, we predicted that N fixation would represent a structural cost under high-N conditions, but a structural benefit under N-limited conditions.

Methods

Study Site and Species – Our study was conducted in an open-air shadehouse at La Selva Biological Station in the Caribbean lowlands of northeastern Costa Rica (10.4233 °N, 84.022 °W). This site receives approximately 4,500 mm yr^{-1} of rainfall, with a pronounced dry season from January to April, and a second, less-pronounced dry season in September and October. Mean annual temperature at La Selva is 25°C, and is constant throughout the year (McDade and Hartshorn 1994). The shadehouse where we conducted our experiment was located in an open field receiving direct sun for the majority of daylight hours. All sides and the ceiling of our shadehouse were lined with shade cloth to manipulate light (see below) and to deter vertebrate and invertebrate herbivores. Above the shade-cloth ceiling was a clear plastic roof, which allowed us to control water availability to plants. All plants in our study experienced ambient fluctuations in temperature and relative humidity.

We studied growth and resource allocation of active and inactive N fixers under varying levels of light, soil N, and competition with non-fixers using seedlings of the most common N-fixing tree at our site, *Pentaclethra macroloba*, and a common non-fixing tree at our site, *Virola koschnyi*. These species were chosen because they are both common canopy trees that occur in forests of all successional ages in our study region, and so are common competitors in natural settings. Both species have relatively large seeds (arithmetic means: *P. macroloba* = 6.3 g, *V. koschnyi* = 3.0 g) that germinate in a similar timeframe (*P. macroloba* = 8-10 days, *V. koschnyi* = 11-14 days) and have high germination rates (~90% for both species) (Flores 2002a, 2002b).

The primary objective of this study was to determine the growth and competition effects of the ability to fix N and N fixation itself, separate from any confounding species effects. This required us to compare plants that differ in the ability to fix N but are otherwise identical. To achieve this, we created inactive N fixers by growing *P. macroloba* in autoclave-sterilized growing medium without access to their symbiotic N-fixing bacteria, making them identical to active N fixers except for the ability to fix N.

Experimental Design – Seedlings of *P. macroloba* and *V. koschnyi* were grown from seed in 7-liter pots under varying conditions of light, soil N availability, and plant competition. We created three light treatments using varying thicknesses of shade cloth such that high-, medium-, and low-light treatments corresponded to 40%, 16%, and 8% full irradiance, respectively, which we measured by comparing PAR sensors in each light treatment paired with a sensor set in the adjacent open field exposed to full sunlight.

Within each light treatment, plants were assigned to one of three soil N availability treatments. Growing medium for all plants was a 1:1 mixture of forest soil and locally-sourced sand to reduce the available soil N in the lowest N treatment. To this sand/soil mixture we added the equivalent of 0.51, 20, and 40 g N m^{-2} yr^{-1} as ammonium-nitrate (NH_4-NO_3) fertilizer to create low-, medium-, and high-N treatments, respectively. Fertilizer was split into two doses—one at the time of seed sowing and one at the midpoint of the experimental growth period. Pots in the three soil N treatments were arranged in each light treatment in a randomized fashion.

Our third experimental manipulation involved exposing active and inactive N fixers to competition with neighboring non-fixers. Within each of the nine environmental (light and soil N) treatments, we grew 5 “reference” plants of each N fixer type, which were grown individually in pots without the presence of a competitor. Active and inactive N fixers could not be grown in

direct competition in a single pot because the bacteria would transfer to the inactive N fixer. So, to assess the competitive effects of the ability to fix N and N fixation, we simulated these comparisons using pairwise competition between each *P. macroloba* fixer type and our non-fixing species, *V. koschnyi*. We grew 5 plants of each fixer type in pots with a neighboring non-fixer competitor. Competition pairs were randomly arranged within soil N and light treatments.

Growth Period, Biomass Harvesting, Leaf Area, and Root Length – Seeds of *P. macroloba* and *V. koschnyi* were obtained from a local plant nursery, massed (to account for initial seed size in biomass data), and sowed according to each species' specifications in Flores (2002a, 2002b). After 2 weeks, any seeds that had not germinated were replaced. Plants were grown under each experimental treatment for 6 months, from July 2015 to January 2016. During the growth period, plants were given ample water via individual watering pans beneath each pot.

Following the 6-month growth period, all plants were harvested by washing the growing medium away from the plant's roots and dissecting the plant into leaf, stem, root, and nodule (where applicable) tissue pools. At the time of harvesting, all leaf and root tissues were photographed on a white background with a scale bar for analyses of leaf area and root length, respectively. Leaf area for each leaf photo was analyzed using the program Easy Leaf Area (University of California Department of Plant Sciences, California, USA). Root length for each root photo was analyzed using WinRhizo™ root analysis software (Regent Instruments, Québec, Canada). When multiple images were needed for leaves or roots of an individual plant, leaf area or root length, respectively, was summed for all photos for that plant. All plant tissue was then dried at 60°C for at least 3 days to constant mass. Once dried, each tissue pool for each plant was massed separately to assess biomass allocation. Specific leaf area (SLA) was calculated by dividing the total leaf area for a plant by the dry mass of that plant's leaf tissue. Specific root

length (SRL) was calculated by dividing the total root length for a plant by the dry mass of that plant's root tissue.

We used an isotopically enriched ^{15}N tracer added to the potting mixture of active N-fixer pots to calculate the percent N derived from N fixation ($\%N_{dfa}$) for each active N fixer. This tracer changed the isotopic ^{15}N:^{14}N ratio of the soil N such that it was measurably different than the ^{15}N:^{14}N ratio of atmospheric N. This allowed us to differentiate plant N that was derived from soil N uptake vs. N fixation. Equivalent trace amounts of non-isotopically enriched N were also added to the pots of inactive N fixers to create equivalent N treatments between N-fixer types. Leaf tissue for active N fixers was isotopically analyzed using a PDZ Europa ANCA-GSL elemental analyzer interfaced to a PDZ Europa 20-20 isotope ratio mass spectrometer (Sercon Ltd., Cheshire, UK) at the University of California Stable Isotope Laboratory, and a three end-member mixing model was used to calculate the percent of the plant's $\%N_{dfa}$. A detailed description of these calculations is available in Appendix 2.

Statistics – We tested for differences in biomass, height, tissue allocation, and $\%N_{dfa}$ between plants in different environment and competition treatments using a maximum likelihood framework. Although our experimental design allows for a classic ANOVA framework, given the large number of possible comparisons in our study (9 environmental treatments x 2 competition treatments x 3 fixer types), we chose to use a maximum likelihood approach, which allowed us to focus on only the comparisons that were reasonable or of particular interest (Burnham et al. 2011). We pooled both competition and reference plants for comparisons between environmental treatments (the number of plants in competition vs. reference pots was similar in each environmental treatment). To test for competition effects within an environmental treatment, we did not test for winners and losers between plants competing in the same pot with

each other but rather, we tested for differences between plants in competition pots vs. plants in reference pots of the same fixer type and environmental treatment.

Comparisons between environmental treatments were made using a series of maximum likelihood models that fit means to different combinations of treatments. For all tests, a null model was first fit that applied a single mean to all treatment groups, as well as a full model that fit a different mean for each of the 9 environmental treatments (or two competition types in each environmental treatment for competition analyses). We then built additional models based on the question of interest and tested all biologically reasonable comparisons. We compared models by assessing differences in the corrected Akaike Information Criterion between models (ΔAIC_c). We report results from our best-fit model and note the ΔAIC_c of our next-best model. We interpreted a model as being significantly better than other models when $\Delta AIC_c > 2$ (Anderson 2008). Descriptions of all models and their corresponding ΔAIC_c's are presented in Appendix 3 Tables S2-S15. Data for leaf area, root length, and SRL were log-transformed to meet assumptions of normality, but back-transformed for figure presentation. All analyses were done in the base and `bbmle` packages of R statistical software (Bolker and R Development Core Team 2017, R Core Team 2017).

Our non-fixing species *V. koschnyi*, was significantly smaller than either our active or inactive N fixers (both *P. macroloba*) regardless of environmental treatment ($\Delta AIC_c = 65.65$ and $\Delta AIC_c = 166.77$ for biomass and height comparisons, respectively), which we attribute to intrinsic differences in seed size and growth patterns between these species rather than an effect of the ability to fix N. The primary focus of our study was on the effects of the ability to fix N, not on species-level differences in growth. Under our experimental design, non-fixing *V. koschnyi* primarily served as a common competitor for both active and inactive N fixers. Thus,

we focus our results in the main text on comparisons between active and inactive N fixers only and provide results for non-fixing *V. koschnyi* in Supplementary Figures and Tables in Appendix 3.

Results

To be able to compare patterns of biomass allocation to resource needs for active and inactive N fixers, we first assessed under which conditions each fixer type was limited by light, N, or both. Total biomass for active N fixers (*P. macroloba* with access to symbiotic bacteria) was light limited in our low- and medium- light treatments, and N addition had no effect on biomass in either of these light groups. Under high light, active N fixers were N-limited in our low N treatment, but N limitation was relieved in our medium- and high-N treatments (ΔAIC_c = 2.14) (Fig. 9a-c). For inactive fixers (*P. macroloba* without access to symbiotic bacteria), our best model indicated similar limitation patterns as for active N fixers (ΔAIC_c = 0.76) (Fig 9d-f).

Does the ability to fix N convey a growth advantage?

To evaluate how the ability to fix N influences plant growth at the broadest level, we first assessed differences in total plant biomass between active and inactive N fixers pooling all environmental and competition treatments. Our best-fit model indicated no differences in total plant biomass (ΔAIC_c = 2.43) or plant height (ΔAIC_c = 1.01) between active and inactive N fixers. (Appendix 3 - Fig. S1). Because we might expect the ability to fix to have the greatest effect on growth under conditions where fixation occurs, we compared the growth of active and inactive N fixers in our high-light treatment, where active fixers fix most (Chapter 2). Our best model indicated no significant differences between active and inactive N fixers in any of the

three N treatments within our high light group for either biomass ($\Delta AIC_c = 2.42$) (Fig. 10a) or plant height ($\Delta AIC_c = 0.56$) (Appendix 3 - Fig. S2).

Next, we tested for the possibility that the ability to fix N conveys a unique advantage to N fixers in response to direct competition from neighboring plants. We found no significant effects of competition on biomass (plants grown in competition pots had similar biomass to reference plants grown in isolation) for either active ($\Delta AIC_c = 1.50$) or inactive ($\Delta AIC_c = 0.95$) N fixers in any of our high-light treatments (Appendix 3 - Fig. S3). We also found no significant effects of competition on the height of active N fixers in high-light conditions ($\Delta AIC_c = 1.50$, Fig. 10b, Appendix 3 – Fig. S4). Competition did, however, make inactive N fixers significantly shorter in our N limited (high-light, low-N) treatment ($\Delta AIC_c = 2.57$) (Fig. 10c, Appendix 3 – Fig. S4)

Does the ability to fix N change how plants allocate aboveground and belowground biomass?

Our first assessment of biomass allocation was to test for differences in the ratio of aboveground biomass to belowground biomass (AGB:BGB) between active and inactive N fixers with all environmental and competition treatments pooled. Our best-fit model showed that active and inactive N fixers exhibited similar AGB:BGB ($\Delta AIC_c = 2.19$) (Appendix 3 - Fig. S5). When assessing changes in AGB:BGB across environmental treatments, we found that active N fixers tended to allocate less biomass aboveground in medium- and high-light conditions. In medium- and high-light groups, active N fixers allocated more biomass belowground in low-N treatments, but in low-light conditions they allocated more biomass aboveground in the low-N treatment ($\Delta AIC_c = 0.92$) (Fig. 11a-c). For inactive N fixers, plants allocated more biomass belowground with increasing light availability, and within each light group plants allocated more biomass belowground in low-N treatments than medium- and high-N treatments, although the N

treatment effect was not significant between low- and high-N in high-light ($\Delta AIC_c = 0.87$) (Fig. 11d-f).

Because AGB:BGB provides an incomplete assessment of allocation to various resource acquisition strategies (Poorter and Nagel 2000), we also assessd biomass allocation to specific tissue pools that specialize in acquiring different resources. For aboveground plant tissue, we were interested in the amount and efficiency of allocation to light-capturing tissue (leaf area and specific leaf area, respectively) for each fixer type in each environmental treatment. Both active and inactive N fixers produced more total leaf area with increasing light availability but did not change total leaf area in response to N availability ($\Delta AIC_c = 1.12$ and $\Delta AIC_c = 1.95$ for active and inactive N fixers, respectively) (Appendix 3 - Fig. S6a-f).

To control for differences in total biomass across environmental treatments, we also assessed the percent of a plant's biomass allocated to leaf tissue as well as SLA. The percent of biomass allocated to leaves tended to be higher in higher N treatments for all fixer types and light groups except one: active N fixers in high-light, where medium- and high-N significantly decreased the percent of total biomass in leaves ($\Delta AIC_c = 1.46$) (Appendix 3 - Table S1, Fig. S7). For inactive N fixers, our model with the lowest AIC showed the highest percent allocation to leaves in medium-light, the lowest in high-light, and increases in percent allocation to leaves from low- to medium- and high-N within each light group except high-light, where low- and high-N treatments were similar ($\Delta AIC_c = 2.30$) (Appendix 3 - Fig. S7). For both active and inactive N fixers, specific leaf area (SLA) was lower in our high-light treatments but did not vary with N availability within our light treatments ($\Delta AIC_c = 1.70$ and $\Delta AIC_c = 1.98$ for active and inactive N fixers, respectively) (Fig. 12).

Belowground, we investigated the ability and efficiency of plants to obtain soil resources by assessing total root length and specific root length (SRL). Total root length for both active and inactive N fixers increased with increasing light availability across our three light treatments but was not affected by N treatment ($\Delta AIC_c = 2.81$ and $\Delta AIC_c = 2.47$ for active and inactive N fixers, respectively) (Appendix 3 - Fig S8a-f). Similar to total root length, the SRL of active N fixers increased with each increasing light availability but was not affected by N treatment ($\Delta AIC_c = 1.65$) (Fig 13a-c). For inactive N fixers, however, SRL was unaffected by light treatment but was higher in low-N treatments than either medium- or high-N ($\Delta AIC_c = 2.09$) (Fig. 13d-f).

Does N fixation represent a structural cost or benefit under different environmental conditions?

Because nodule production has the potential to be offset by reduced root production, we assessed the structural cost/benefit of N fixation by comparing root biomass, total belowground biomass, and the proportion of biomass each plant allocated to root and all belowground tissue between active and inactive N fixers. When all environmental and competition treatments were pooled, we found no differences in root biomass ($\Delta AIC_c = 2.04$) or total belowground biomass ($\Delta AIC_c = 2.31$) between active and inactive N fixers. Similarly, we found no differences in the percent of total biomass allocated to roots ($\Delta AIC_c = 0.05$) or all belowground biomass ($\Delta AIC_c = 2.08$) (Appendix 3 – Table S1, Fig S9).

Because we might expect the ability to fix N to have the greatest influence on belowground allocation in N-limited conditions, we specifically assessed differences in belowground allocation between active and inactive N fixers in our high-light, low-N treatment where we demonstrated these plants are N-limited and where active N-fixing plants fix significant amounts of N (Chapter 2). We found that active N fixers in these conditions allocated

a smaller percent of their total biomass to root tissue (ΔAIC_c = 10.9) and to all belowground tissue (ΔAIC_c = 2.09) than inactive N fixers (Fig. 14a, Appendix 3 - Table S1).

Finally, we were interested in whether direct competition with a neighboring plant influenced N fixation for active N fixers. When comparing active N fixers in competition vs. reference pots in our high-light group (where active N fixers produced nodules), we found no effect of competition on the percent of biomass allocated to nodules in any N treatment (ΔAIC_c = 1.91) (Fig. 14b). However, we found that active N fixers fixed less N (lower $\%N_{dfa}$) when a competitor was present under N-limited conditions (high-light, low-N) (ΔAIC_c = 0.02; Fig. 14c).

Discussion

Current theory on the controls of N-fixer abundances, N fixation, and by extension, N limitation, is based on predictions of the costs and benefits of the ability to fix N and the act of doing so under various environmental conditions and how those costs and benefits influence the competitive success of N fixers. These predictions make sense but are based on limited empirical data. Direct assessments of the growth, resource allocation, and competitive responses of N fixers are critical to refining our expectations of how environmental factors drive the abundance of N fixers and their N inputs from fixation.

Growth effects of N fixation

Our growth analyses did not provide support for our hypothesis that the ability to fix N conveys a growth advantage to the plant, as we found no differences between active and inactive N fixers for either biomass or plant height in any environmental treatment. We did, however, find some evidence for an advantage conveyed by the ability to fix N when we assessed responses to competition with neighboring plants. Our active N fixers in high-light conditions

showed no response to the presence of competition, while our inactive N fixers were significantly shorter in the presence of a competitor in our N-limited treatment. These results support findings by Nasto et al. (2017) and indicate that the ability to fix N may be particularly important for young N fixers to gain height quickly and overtop neighboring competitors when soil N is limiting.

Recent work in nearby forests where *P. macroloba* is the most common N fixer has shown that N fixers have strong competitive effects on neighboring plants (Taylor et al. 2017). The results of our study suggest that the ability to grow tall and shade neighbors even in the presence of competition is one potential mechanism for the strong competitive effects of N fixers documented *in situ*. Here, we also demonstrate that active N fixers decrease their N fixation rates in the presence of a competitor in N-limited conditions. This suggests that N fixers decrease their potential to fertilize the surrounding forest in the presence of competition, which supports the *in-situ* finding that the negative competitive effects of N fixers outweighs their fertilization effect in nearby forests (Taylor et al. 2017). Overall, these data suggest that *P. macroloba* is a strong competitor, at least in part because of it's ability to fix N and to downregulate N fixation in the presence of competitors.

The lack of any growth advantage to active N fixers in N saturated conditions (our high-light, high- and medium-N treatments) raises an interesting question. Why do N fixers in N saturated conditions continue to incur the energetic expense of N fixation (Chapter 2) when they could allocate those C resources to growth? Incomplete downregulation of N fixation may be a bet-hedging strategy for times of N scarcity (Menge et al. 2009). However, another intriguing possibility exists involving the plant's endosymbiotic bacteria. Given that inoculation with endosymbiotic bacteria can create physiological changes in N fixers regardless of how much N

the bacteria are fixing (Wolf et al. 2017), it seems plausible that under conditions of high energy availability, the bacteria can induce the plant to continue engaging in N fixation even at the expense of potential plant growth. Although some data suggest that plants can penalize bacterial symbionts that do not fix N for the host (Kiers et al. 2003, but see: Marco et al. 2009, Gubry-Rangin et al. 2010), it is unknown whether plants can also penalize their endosymbionts for continuing to fix under N-saturated conditions. Clearly our understanding of how the regulation of N fixation influences the growth and competitive success of N fixers remains incomplete.

Biomass allocation effects of N fixation

Independent of any effects on total growth, the ability to fix N may have important impacts on the allocation of biomass to different tissue pools within a plant, altering above- and belowground resource acquisition strategies. Our analysis of AGB:BGB showed that both active and inactive N fixers tended to allocate biomass toward capturing the scarcest resource—plants allocated more biomass aboveground in low-light conditions, but more biomass belowground in low-N conditions—which agrees with current theory on plant biomass allocation (Poorter and Nagel 2000). In general, however, our data indicate that the ability to fix N does not create large differences in whether plants allocate biomass above- or belowground.

Further exploring the allocation to aboveground tissue pools, however, did show an interesting difference in response to the ability to fix N. Allocation to leaves increased from low- to medium- and high-N treatments for all fixer types and light groups except active N fixers in high light, where plants were actively engaging in N fixation. Instead of allocating biomass to leaves, these high-light, medium- and high-N active N fixers tended to allocate more biomass to stem production (Appendix 3 - Table S1), which may be an alternative light-capturing strategy for these plants that were "over fixing" based on our theoretical expectations (Chapter 2).

One of the more interesting allocation patterns that our data showed was that of SRL. Inactive N fixers exhibited high SRL (more efficient root foraging per unit root biomass) in low N conditions. Active N fixers, however, showed no response of SRL to N treatments, but increased SRL with increasing light availability. One possible explanation for this discrepancy is that inactive N fixers increase root foraging efficiency to capture the most limiting soil resource, but that active N fixers (that can supplement their N demands with fixation) adjust fine root foraging when high light availability creates demand for other soil resources such as water or phosphorus. Although SRL doesn't provide direct information on the biomass costs/benefits of fixation, these patterns suggest some tradeoff between N fixation and root foraging.

The structural cost/benefit of N fixation

Although we found no direct evidence that N fixation conveyed a growth advantage to active N fixers, we also found no evidence that the ability to fix N or N fixation represent a net structural cost to the plant. Much of the ecosystem theory on N fixation assumes some cost of being an N fixer (Vitousek and Field 1999, Rastetter et al. 2001, Menge et al. 2008, 2009, 2015), largely based on the intuition that if there were no cost of the ability to fix N, N fixers would dominate N-limited ecosystems, which they do not (Menge et al. 2008, 2009, 2017a). However, these costs are often not specified in models, and rarely quantified empirically.

One obvious potential cost of N fixation is the structural cost of nodule production. Our data show that although active N fixers in high-light conditions allocated up to 9.5% of their total biomass to nodule production, any investment in nodules was offset by reductions in root biomass. In N-limited conditions (high-light, low-N), active N fixers allocated significantly less tissue belowground than inactive N fixers, suggesting that nodule production represents a net

belowground structural benefit to the plant (nodule production is more than offset by reduced root production).

Because nodule tissue only helps the plant acquire N, while root tissue can acquire a diverse suite of soil resources, the structural cost/benefit of nodule production is likely dependent on the primary limiting soil resource (Gutschick 1981). However, our data suggest that costs of labile C fed directly to endosymbionts (Gutschick 1981), tradeoffs such as reduced N-use efficiency (Menge et al. 2008, Wolf et al. 2017), or increased herbivory (Mattson 1980, Ritchie and Tilman 1995, Knops et al. 2000, Vitousek et al. 2002) may be more important costs of N fixation than nodule production.

Conclusions

Taken together, our data indicate that the ability to fix N does not convey a growth advantage to *P. macroloba* but may make N fixers more resistant to competition from neighboring plants in N-limited conditions. Active N fixers allocated less biomass belowground in N-limited conditions and decreased fixation in the presence of a competitor, which may increase their competitive influence on neighboring plants. Interestingly, we also found that when *P. macroloba* fixed N even in N-saturated conditions, this luxury N fixation did not create a growth disadvantage to the plant. The relationships between the ability to fix N, growth, and competitive success have important implications for N-fixer abundance distributions, N fixation rates, and our ability to predict them both through ecosystem theory. This makes data such as these critical for our understanding of how N-fixing plants influence tropical forest ecosystems.

Acknowledgements

The authors would like to thank E. Salicetti, M. Wilcots, R. Li, B. Scott, E. Utset, B. Matarrita, D. Madrigal, and O. Vargas for help conducting the experiment, collecting, and processing samples. This work was supported by the Garden Club of America's Award in Tropical Botany, Columbia University's Earth Institute, and the Institute for Latin American Studies.

Figures and Tables

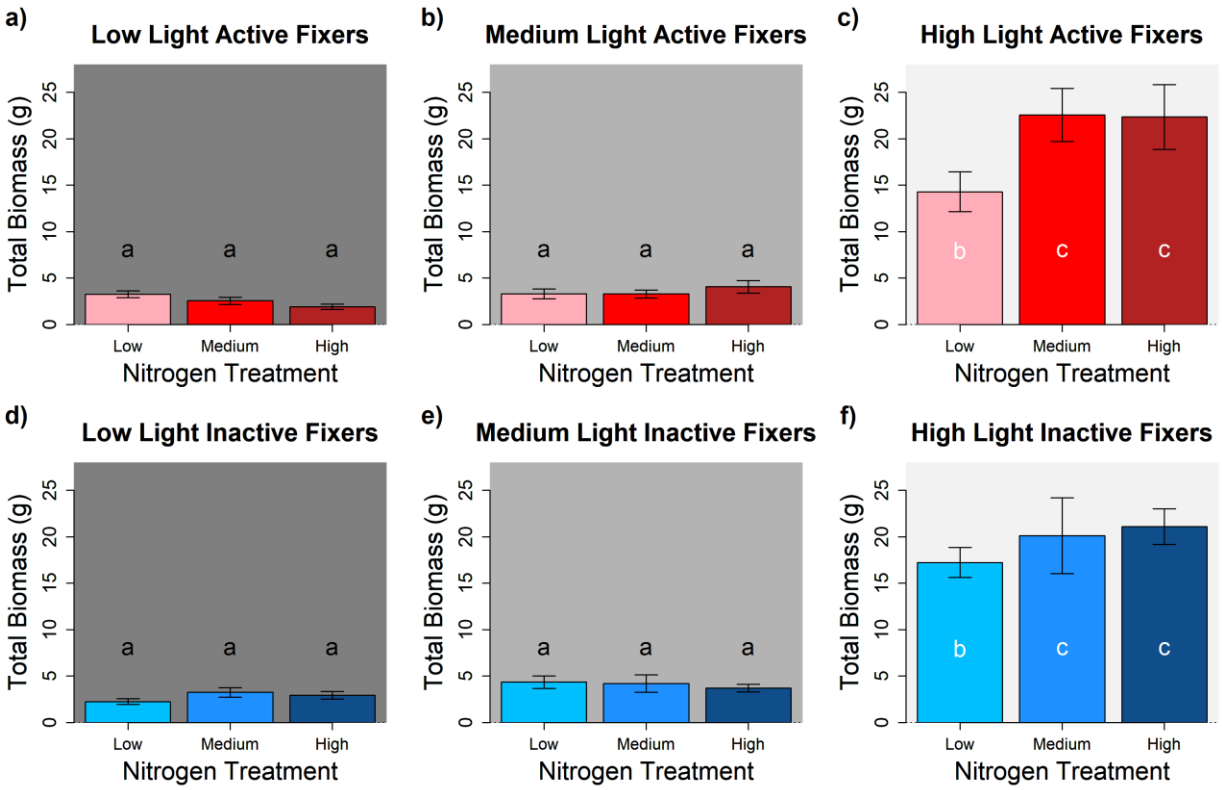

Figure 9: Biomass of active and inactive N fixers

Effects of light and nitrogen treatments on biomass for each plant fixer type. Total plant biomass for active N fixers (inoculated *Pentaclethra macroloba*; red, **a-c**) and inactive N fixers (uninoculated *P. macroloba*; blue, **d-f**) are shown for low- (**a, d**), medium- (**b, e**), and high-light (**c, f**) groups. Bars within each panel represent the 3 N addition treatments within each light group. Across each row, different letters represent significant differences with increasing letters corresponding to increasing mean values. Error bars represent ± 1 S.E. For both plant types, low and medium light levels strongly limit plant growth at all N levels, and low N levels limit plant growth at high light.

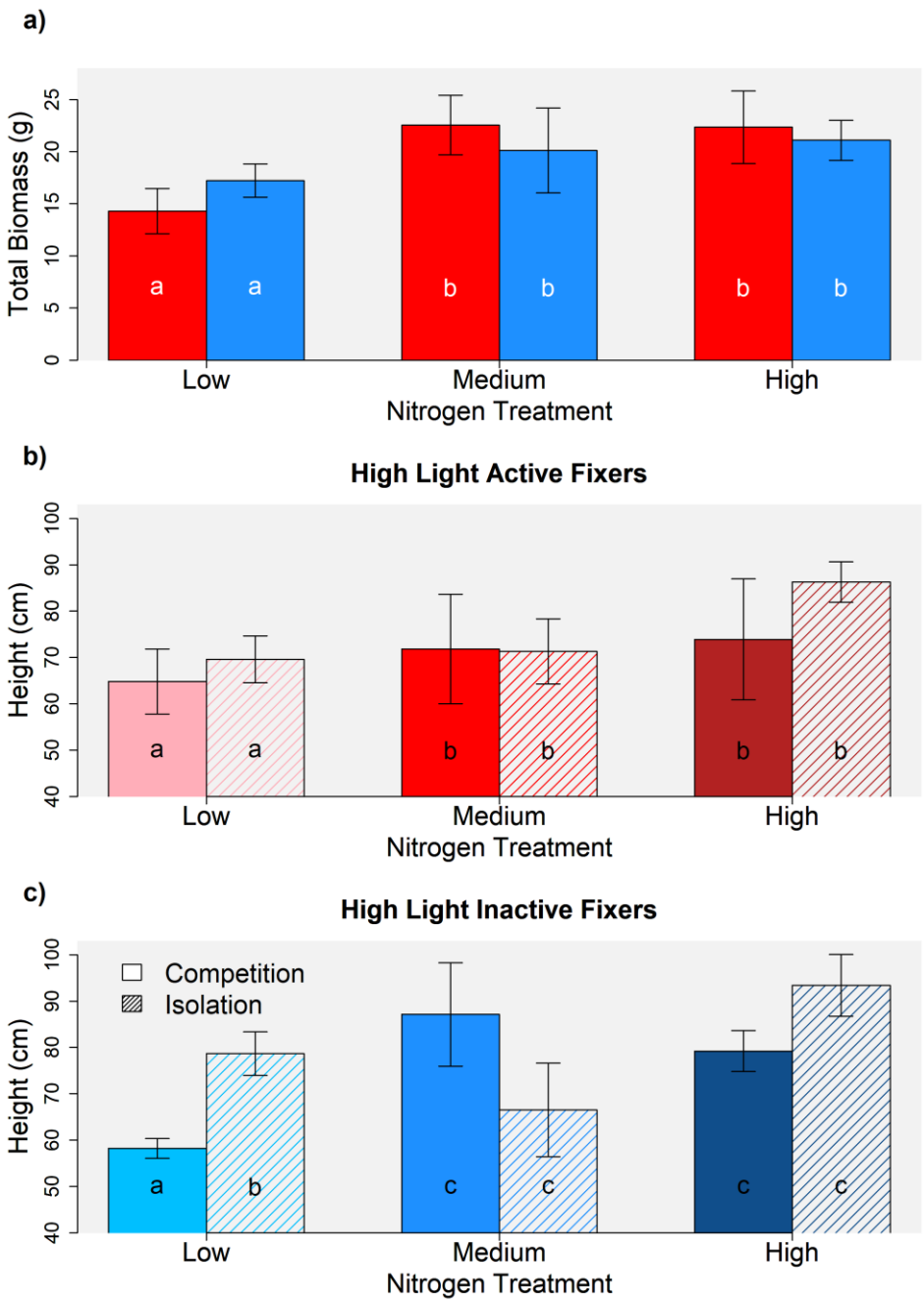

Figure 10: Competition effects for high-light N fixers

N fixation compensates for N limitation when plants are grown in competition but not when they are grown alone. **a)** Total plant biomass for active (red) and inactive (blue) N fixers in our high-light group with all competition treatments pooled. The effect of direct plant competition on our high-light plants is shown for height of active N fixers (**b**) and inactive N fixers (**c**). For each N

treatment in **b** and **c**, solid bars represent plants grown with a competing plant in the same pot and hatched bars represent plants grown in isolation. Null models for b and c fit a mean for reference plants in low-N and a different mean for reference plants in medium-and high-N based on biomass analyses (Figure 9). Alternate models tested for differences in the biomass of plants grown in competition within each N treatment. Letters and error bars are as in Figure 9.

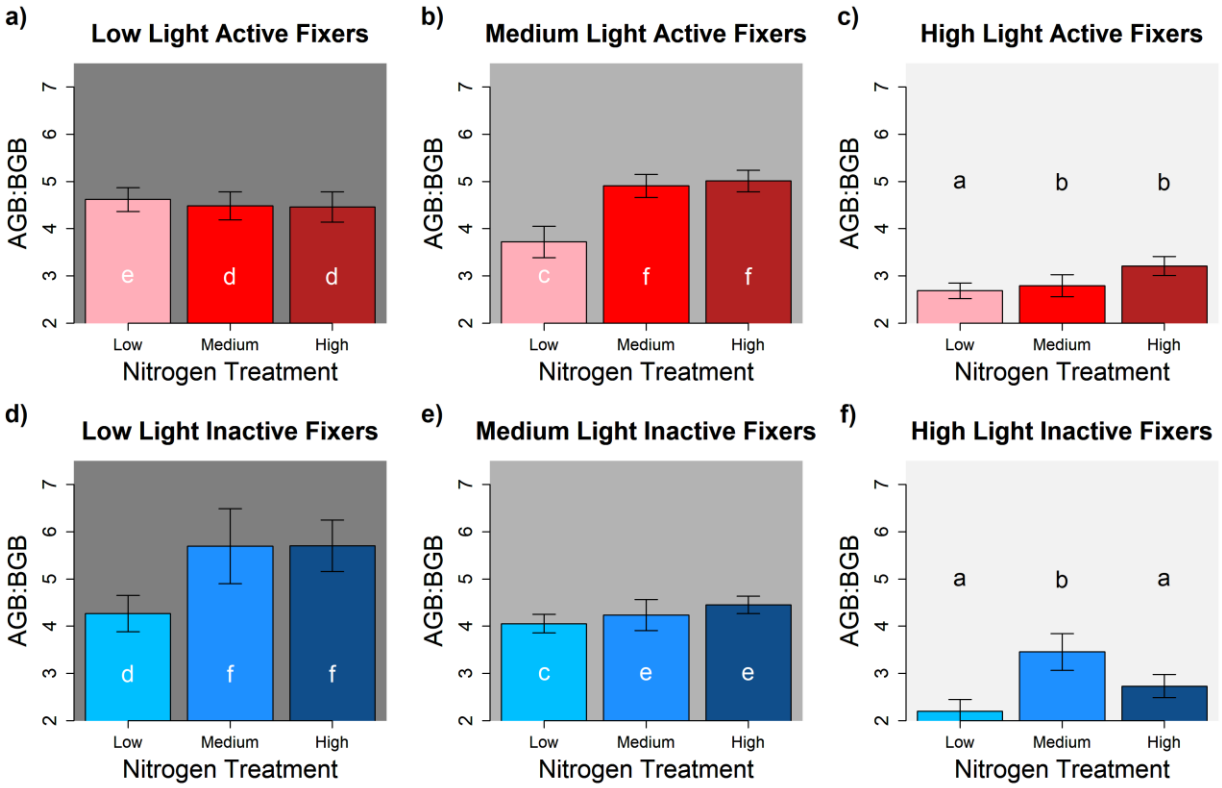

Figure 11: AGB:BGB for active and inactive N fixers

Effects of light and N availability on aboveground-belowground biomass ratio (AGB:BGB) for each plant fixer type. All colors, bars, letters, and error bars are as in Figure 9. In general, more light makes plants rootier (lower AGB:BGB) and more nitrogen makes plants shootier (higher AGB:BGB).

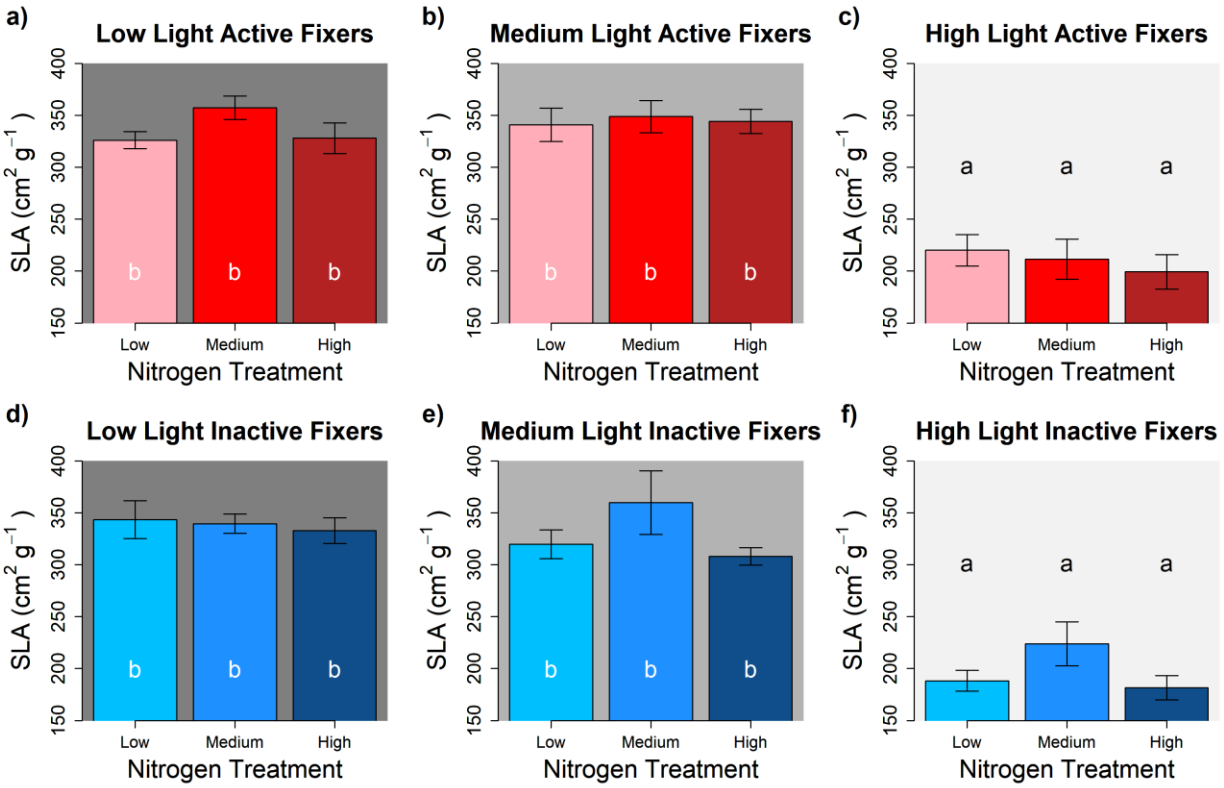

Figure 12: SLA for active and inactive N fixers

Effects of light and N availability on specific leaf area (SLA) for each plant fixer type. All colors, bars, letters, and error bars are as in Figure 9. High light makes leaves thicker for all plant types but N treatment has no effect on leaf thickness.

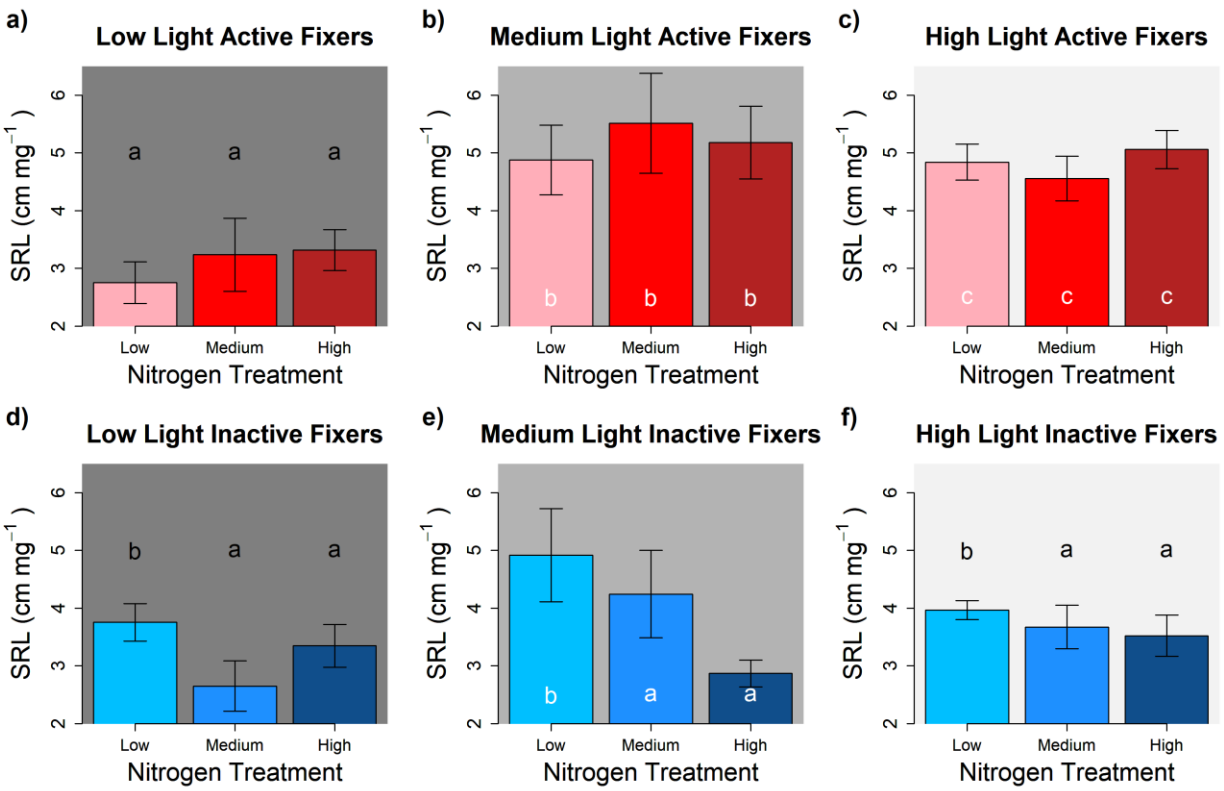

Figure 13: SRL for active and inactive N fixers

Effects of light and N availability on specific root length (SRL) for each plant fixer type. All colors, bars, letters, and error bars are as in Figure 9. Active N fixer roots are thinner at high light, but do not respond to N. Inactive N fixer roots do not respond to light, but become thinner at low N.

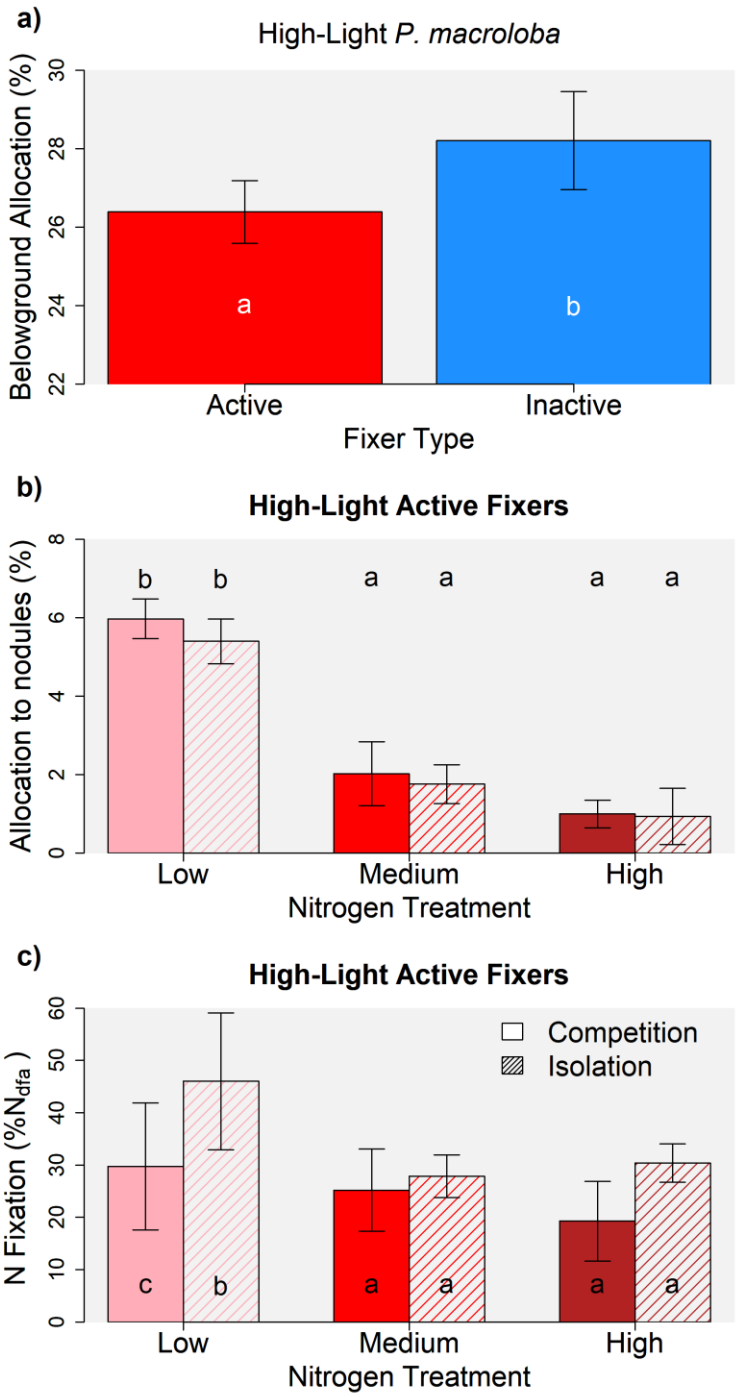

Figure 14: Belowground biomass allocation and %N_{dfa} for high-light N fixers

The effect of N fixation, soil N, and competition on belowground structural costs. **a)** The percent of total plant biomass allocated belowground for active (red) and inactive (blue) N fixers in our high-light group with all N treatments pooled. **b**) The percent of total plant biomass allocated to

nodules for high-light active N fixers in each N treatment. **c**) The percent of plant N derived from fixation ($\%N_{dfa}$) for high-light active N fixers in each N treatment. In **b** and **c**, solid bars represent plants grown with a competing plant in the same pot and hatched bars represent plants grown in isolation. Letters and error bars are as in Figure 9. There were virtually no nodules in low and medium light treatments, which are not plotted. Competition has no effect on allocation to nodules, but active N fixers decrease $\%N_{dfa}$ in response to competition under N-limited conditions.

CHAPTER 4: NITROGEN-FIXING TREES INHIBIT GROWTH OF REGENERATING COSTA RICAN RAINFORESTS

Benton N. Taylor, Robin L. Chazdon, Benedicte Bachelot, and Duncan N.L. Menge

Abstract

More than half of the world's tropical forests are currently recovering from human land use, and this regenerating biomass now represents the largest carbon (C)-capturing potential on Earth. How quickly these forests regenerate is now a central concern for both conservation and global climate-modeling efforts. Symbiotic nitrogen-fixing trees are thought to provide much of the nitrogen (N) required to fuel tropical secondary regrowth, and therefore to drive the rate of forest regeneration, yet we have a poor understanding of how these N fixers influence the trees around them. Do they promote forest growth, as expected if the new N they fix facilitates neighboring trees? Or do they suppress growth, as expected if competitive inhibition of their neighbors is strong? Using 17 consecutive years of data from tropical rainforest plots in Costa Rica that range from 10 years since abandonment to old-growth forest, we assessed how N fixers influenced the growth of forest stands and the demographic rates of neighboring trees. Surprisingly, we found no evidence that N fixers facilitate biomass regeneration in these forests. At the hectare scale, plots with more N-fixing trees grew slower. At the individual scale, N fixers inhibited their neighbors even more strongly than did non-fixing trees. These results provide strong evidence that N-fixing trees do not always serve the facilitative role to neighboring trees during tropical forest regeneration that is expected given their N inputs into these systems.

Introduction

The past two decades have seen a dramatic increase in the appreciation for the role that tropical secondary forests play in local economies (Brown and Lugo 1990), species conservation (Chazdon et al. 2009), and climate change mitigation (Pan et al. 2011). As this interest has spurred new research into the dynamics of tropical forest regeneration, we are beginning to recognize the wide range of regeneration rates and trajectories that tropical secondary forests can exhibit (Poorter et al. 2016). In addition to climatic drivers (Poorter et al. 2016), soil N availability can regulate tropical forest regrowth (Davidson et al. 2004, 2007) and dictate how these forests respond to changing climatic conditions (Hungate et al. 2003, Gerber et al. 2010, 2013, Wårlind et al. 2014). The largest potential source of new N into tropical secondary forests is from symbiotic N-fixing plants (Binkley and Giardina 1997, Gehring et al. 2005), which form specialized root nodules to house symbiotic bacteria that convert atmospheric N_2 gas into plant-available forms of N. These "N fixers" can fix up to 150 kg N ha^{-1} yr^{-1} (Binkley and Giardina 1997), which becomes available to the surrounding ecosystem as N-fixer tissues return to the soil and the N in those tissues is mineralized. These N inputs from N fixers are thought to meet most of the external N demands of rapidly regenerating forests (Batterman et al. 2013a). However, the effect that these N fixers have on tropical forest regrowth depends on both their N inputs and how they influence the demographic rates of the neighboring trees around them.

The unique potential for N fixers to bring newly fixed N into the surrounding ecosystem (Chapin III et al. 1994) means that they might fertilize neighboring trees, but N fixers also compete with their neighbors for light and other resources. N fixers have, on average, higher tissue N content in their foliage than non-fixers (Townsend et al. 2007, Fyllas et al. 2009, Nasto et al. 2014, Adams et al. 2016). Litterfall and decomposition of this N-rich leaf tissue is the

primary means by which N fixers fertilize the surrounding ecosystem. However, high N content can also fuel rapid growth of the N fixer itself (Gehring et al. 2005, Batterman et al. 2013a, Menge and Chazdon 2016), potentially increasing the N fixer's competitive influence on its surrounding neighbors. If the fertilization effect is strong, N fixers might facilitate neighbors, or at least inhibit neighbors less than non-fixers (hereafter, "weak inhibition"; Fig. 15a, b). Alternatively, if their competitive effect outweighs their fertilization effect, N fixers might inhibit neighbors more than non-fixers do ("strong inhibition"; Fig. 15c, d) (Boyden et al. 2005).

How N fixers affect neighboring trees is especially important in Neotropical secondary forests, which have great capacity for carbon storage (Pan et al. 2011, Poorter et al. 2016), are often thought to be N limited (Davidson et al. 2004, 2007), and have high relative abundances of N fixers. In Neotropical forests, N fixers typically comprise ~10% of all trees (compared to < 1% at higher latitudes in North America) (ter Steege et al. 2006, Menge et al. 2014, 2017b), and commonly make up 30-55% of the forest basal area at some sites (Sullivan et al. 2014, Menge and Chazdon 2016) (Table 1, Fig. 16), making their impact on neighboring trees critical to the growth of these forests.

Do N fixers promote or inhibit growth in regenerating tropical forests? We addressed this question at multiple spatial scales using 10-17 years of census data from eight 1-ha moist tropical rainforest plots in Northeastern Costa Rica—six regenerating forests ranging in stand age from 10 to 42 years old and two old-growth forests (Chazdon et al. 2007, Lasky et al. 2014, Menge and Chazdon 2016) (Table 1). First, we asked whether the abundance of N fixers affects forest growth at the 1-ha forest plot and 10 x 10 m subplot levels. Next, we analyzed the effects of N fixers on their neighbors at the individual scale—the scale where competition and facilitation interactions likely occur. Specifically, we asked how the makeup of a tree's neighborhood—the

percent of its crowding that comes from neighboring N fixers rather than from non-fixers—affects its growth, recruitment, and survival.

Methods

Plot and Census Data Description

We studied eight 1-ha plots in a humid tropical rainforest in the Caribbean lowlands of northeastern Costa Rica, in and around La Selva Biological Station (10.4233 °N, 84.022 °W). All plots were within 15 km of each other, were similar in elevation (5 to 220 m), have similar topography and soil type, and experience similar climatic conditions. Similar sets of species dominate all of the plots, but species relative abundances change with stand age throughout succession in our plots (Chazdon et al. 2007). *Pentaclethra macroloba*, an N fixer, was the most common species across all plots, and *Inga cocleensis* and *Inga pezizifera* were the second and third most abundant N fixers in our dataset (Appendix 4 - Table S4). The three most common non-fixing species across all of our plots were *Miconia affinis*, *Casearia arborea*, and the palm *Socratea exorrhiza*. Detailed descriptions of plot design and census methods are available elsewhere (Chazdon et al. 2005, Lasky et al. 2014, Menge and Chazdon 2016).

Each plot is 50 m x 200 m for a total area of 1 ha. Plots are broken up into 100 square subplots with 10 m sides. Six plots are located in naturally regenerating secondary forests that ranged in age from 10 to 25 years at the time of establishment. The remaining two plots are located in primary, old-growth forest that have remained undisturbed for at least 200 years. Within each plot, all adult trees ≥ 5 cm DBH were tagged, identified to species, measured for diameter at breast height (1.3 m above ground level), and mapped onto a plot-level X,Y coordinate system using the subplot corners as reference points. Based on species identification, each tree was categorized as a putative N fixer or non-fixer based on methods in (Menge and

Chazdon 2016). This designation followed a three-tiered approach in which species identifications were first checked for reports of nodulation in (Sprent 2009) and the US Forest Service's GRIN database. After these two N-fixer lists were exhausted, we assigned species as N fixers if they were in a genus with ≥ 60% congeners that were confirmed N fixers, as fixation is thought to be a trait primarily conserved at the genus level.

Plot-scale Effects of N Fixers

To determine the effect of N fixers on plot- and subplot-level growth, we calculated the percent change in tree basal area (ΔBA) as the change in tree basal area divided by the total tree basal area for each plot or subplot over each census period and multiplied by 100. Changes in non-fixer basal area were scaled by total non-fixer basal area in the same fashion. We used generalized mixed linear regression to model changes in total basal area and non-fixer basal area in response to the proportion of a plot or subplot comprised of N fixers accounting for variation in total basal area and including a random plot effect.

Individual-scale Effects of N Fixers

At the individual scale, we calculated absolute growth rate and survival of each tree over each annual census period. For recruitment, we calculated the frequency of recruits into each 10 x 10 m subplot over each annual census period. NCI was calculated as the squared DBH of each neighbor divided by the squared distance of that neighbor to the focal individual, summed for all neighbors within 10 m. We modeled the response of individual growth and survival, and subplot recruitment, to the NCI and proportion of NCI comprised of N fixers that each individual or subplot experienced using a hierarchical Bayesian approach. Each demographic process (growth, recruitment, and survival) was individually modeled as a response to the effects of NCI, the

proportion of NCI made up of N-fixers, DBH (for growth and survival), and the interactions between these variables, as well as the plant's fixer type (N fixer or non-fixer) and plot. 95% credible intervals that did not overlap 0 were interpreted as statistically significant.

For each tree in each census year, we indicated whether that individual had recruited into the adult dataset or suffered a mortality event. We calculated growth since the previous census for each tree that was present in consecutive census years. Recruitment and mortality were treated as binary variables for each individual in each census year. Growth rate was calculated as $G_{i,c} = \frac{(DBH_{\mathrm{i,c}} - DBH_{i,c-1})}{t}$ where $G_{i,c}$ is the growth rate of tree *i* in census *c*, DBH is the diameter at breast height of tree *i* in census *c*, and *t* is the time interval between censuses. Because census intervals varied slightly from year to year, *t* was calculated as the time between measurements of an individual tree in days. The neighborhood crowding index (NCI) of each tree was calculated to represent the crowding that each individual experienced within a set radius around the individual's stem. We calculated NCI as $NCI_i = \sum_{j=1, j\neq i}^{n} \frac{DBH_j^2}{d_{j,i}^2}$ where NCI of individual *i* is the sum of the squared DBH of all neighbors *j* divided by the squared distance of each neighbor *j* to individual *i* of which there are *n* number of neighbors within a set radius of 10 m. Using a radius of 10 m meant that all trees ≤ 10 m from the plot edge were excluded as focal trees from neighborhood-scale analyses as NCI could not be accurately calculated along the plot edge.

Model Description

We used a set of three Bayesian models to determine how tree size, fixation status, and neighborhood crowding influence the growth and survival of an individual tree, and the recruitment of individuals into 10 x 10 m subplots, in a given census year. Data for DBH and NCI were natural log-transformed and data for the proportion of NCI comprised of N fixers were

arcsine-square root transformed prior to analysis. Each demographic model estimated the effect of each covariate [ln(DBH), ln(NCI), the proportion of NCI comprised of N fixers [arcsin($\sqrt{Neigh\_Fix}$)], (ln(DBH) x ln(NCI), ln(NCI)^2, and (ln(NCI) x [arcsin($\sqrt{Neigh\_Fix}$)])] on the demographic response variable (growth, recruitment, or survival). Random intercepts were included in the growth and survival models for each species, individual, and plot, and in the recruitment model for each plot and stem. To allow for comparison between variables in different units, data for growth, DBH, NCI, and Neigh_Fix were z-transformed by subtracting the mean value for that variable and dividing by the standard deviation. Within the model, each of these parameter estimates could vary based on whether the individual was an N fixer or non-fixer. We modeled each parameter estimate as a normal distribution with uninformative priors (mean and standard deviation of 0 and 100, respectively), and all error terms associated with random effects (plot, species, and individual random effects) were modeled as gamma distributions with uninformative priors (shape and scale of 100 and 100, respectively). All models were run in the stan package of R version 3.2.2 (R Core Team 2017).

Standardized absolute growth rate data (change in the DBH of a tree over the census period; $G_{i,c}$ in cm day^{-1}) were modeled as a function of each of the six transformed covariates listed above along with random intercept effects for individual tree ID, species ID, and plot. Each parameter estimate could vary based on the N fixation status of the individual tree. The structure of the growth model was as follows:

$$G_{i,j,p,f} \sim Normal(E(G_{i,j,p,f}), \sigma^2)$$

$$E(G_{i,j,p,f}) = \mu_{j,f} + (\sigma_i) + (\sigma_p) + (Plot_p) + (\beta_{1,f} * DBH_i) + (\beta_{2,f} * NCI_i) + (\beta_{3,f} * Neigh\_Fix_i) + (\beta_{4,f} * NCI_i^2) + (\beta_{5,f} * (DBH_i * NCI_i)) + (\beta_{6,f} * (NCI_i * Neigh\_Fix_i))$$

where *G* and *E(G)* are the standardized growth rate of individual *i* of species *j* in plot *p* with fixation status *f* and its expected value, respectively. The intercept ($\mu_{j,f}$) is species-specific and fixation-specific, and the error terms represent the random effects of individual stem (σ_i) and plot (σ_p) to account for repeated measurements. Parameter estimates $\beta_1 - \beta_6$ were modeled for each covariate (described above) and allowed to vary based on the fixation status (*f*) of the individual.

Survival was modeled as a binary variable using a logit link, which could vary as a function of the six covariates used in the growth model with random species-specific and fixation-species intercepts ($\mu_{j,f}$), and random effects for individual *i* and plot *p* (σ_i, σ_p). Again, each parameter estimate could vary based on the fixation status of the individual. The structure of the survival model was:

$$S_{i,j,p,f} \sim Bernouli(s_{i,j,p,f})$$

$$s_{i,j,p,f} \sim logit^{-1}\left[\mu_{j,f} + (\sigma_i) + (\sigma_p) + (\beta_{1,f} * DBH_i) + (\beta_{2,f} * NCI_i) + (\beta_{3,f} * Neigh\_Fix_i) + (\beta_{4,f} * NCI_i^2) + (\beta_{5,f} * (DBH_i * NCI_i)) + (\beta_{6,f} * (NCI_i * Neigh\_Fix_i))\right]^t$$

where *S* and *s* represents the survival and the probability of survival, respectively, of an individual (*i*) in a given time interval (*t*) with all subscripts the same as the growth and model above.

Recruitment was modeled as the frequency of individual trees recruiting into each 10 x 10 m subplot, that varied as a function of the standardized, transformed covariates: average NCI of trees in that subplot [ln(NCI)], the average proportion of NCI comprised of N fixers for all

trees in the subplot [arcsin($\sqrt{Neigh\_Fix}$)], ln(NCI)^2, and ln(NCI) x the proportion of NCI comprised of N fixers [arcsin($\sqrt{Neigh\_Fix}$)], with random intercepts for plot and subplot. For our recruitment model, we did not include any covariates corresponding to the DBH of recruiting trees as all recruits had DBH's at or very close to the minimum size classified in the data set (5 cm). As with the growth model above, each parameter estimate could vary based on the fixation status of the individual. Because recruitment into a subplot within a year was often 0, we used an adjusting model structure, which employed both Bernoulli and Poisson distributions to model the 0-inflated subplot recruitment data as follows:

$$Rec_{i,j,p,f} \sim \begin{cases} Bernouli\left(logit^{-1}(r_{i,j,p,f})^t\right) & with\ probability\ \alpha \\ Poisson\left(r_{i,j,p,f}\right) & with\ probability\ 1-\alpha \end{cases}$$

$$r_{i,j,p,f} \sim \mu_{j,f} + (\sigma_i) + \left(\sigma_{sp}\right) + (\beta_{1,f} * NCI_i) + (\beta_{2,f} * Neigh\_Fix_i) + (\beta_{3,f} * {NCI_i}^2) + (\beta_{4,f} * (NCI_i * Neigh\_Fix_i))$$

where *Rec* is the recruitment of an individual in a given census year with all subscripts the same as in the growth and survival equations above except for σ_{sp} which represents the random effect of subplot.

Results

If N fixers promote forest growth at the 1-ha plot level, we would expect a positive relationship between the abundance of N fixers and the annual increase in tree basal area of a plot. However, we found that plots with more N fixers had lower overall growth ($P < 0.0001$; Fig. 16a) and lower non-fixer growth ($P < 0.0001$; Fig. 16c), even after accounting for variation in total plot basal area. A change in N-fixer prevalence from 10% to 35% of the plot's basal area corresponded to a reduction of total annual growth from 2.2% to 0.6%, and reduced non-fixer

growth from 2.0% to 0.06%. To overcome potential confounding correlations between plot age, N-fixer abundance, and growth, we also assessed growth at the 10 x 10 m subplot scale within each plot. We found a non-significant negative trend between total growth and N-fixer prevalence ($P = 0.12$; Fig. 16b), and a significant negative correlation between non-fixer growth and N-fixer prevalence ($P < 0.0001$; Fig. 16d). These results suggest that N fixers are inhibiting, not facilitating, overall growth and growth of local non-fixers in our study region.

To gain a more mechanistic understanding of how individual N fixers drive plot-level growth patterns, we assessed how N fixers affect individual neighboring trees. This requires spatially explicit data on the demographic rates of individual trees over relatively long timescales. We estimated the degree of neighbor crowding that each individual experienced using a Neighborhood Crowding Index (NCI). A larger NCI (more crowding) could come from any combination of more neighbors, bigger neighbors, and closer neighbors. To estimate crowding from N fixers, we calculated the percent of each tree's NCI coming from neighboring N fixers—a continuous scale from 0% (all of an individual's neighbors are non-fixers) to 100% (all of an individual's neighbors are N fixers). We then used hierarchical Bayesian models to examine how crowding from N fixers affected the growth, survival, and recruitment of each tree (both N fixers and non-fixers), after accounting for overall crowding and tree size (Canham et al. 2004). Based on established changes in tree demographic rates at this site (Menge and Chazdon 2016), we ran our models independently for forest stands ≤ 25 years old ("young forests") and > 25 years old ("old forests").

If N fixers facilitate or weakly inhibit their neighbors, we would expect tree demographic rates to increase with crowding from N fixers (Fig. 15a, b). Our results showed the opposite trend. N fixers strongly inhibited their neighbors – exhibiting greater negative effects on their

neighbors than non-fixers did (Figs. 17, 18, Appendix 4 - Figs. S2-S4, resembling Fig. 15c, d). In young forests, crowding from N fixers strongly inhibited all demographic rates of neighboring non-fixers, and strongly inhibited the growth rates of neighboring N fixers (Fig. 17). In old forests, N fixers strongly inhibited both the growth and survival of neighboring N fixers (Fig. 18). This N-fixer inhibition effect was stronger on the growth of neighboring N fixers than neighboring non-fixers regardless of forest age (Fig. 17b, 18b), and on the survival of neighboring N fixers in old forests (Fig. 18f). However, N-fixers more strongly inhibited the recruitment of neighboring non-fixers than neighboring N fixers in young forests (Fig. 17d).

Discussion

Together, our individual-scale results and our 1-ha plot-scale findings show that N fixers in these forests inhibit their neighbors more than do non-fixers. It is important to note that the strong inhibition of N fixers we report is independent of the overall level of crowding and tree size. For example, an average-sized non-fixing tree (DBH ~ 13 cm) with an average amount of crowding (NCI ~1,900) in a young forest stand would have a 43% lower expected growth rate if its neighbors were all N fixers than if its neighbors were all non-fixers. If this "average tree" is an N fixer itself, a neighborhood with all N fixers reduces its expected growth rate by over 60% compared to a neighborhood with all non-fixers.

The negative influence that N fixers have on their neighboring trees in our study region is likely due to two factors. First, high growth and survival rates of N fixers in these plots (Menge and Chazdon 2016), and the high nutrient demand of N fixers (McKey 1994, Fyllas et al. 2009, Nasto et al. 2014, Adams et al. 2016), mean that N fixers likely cast more shade and take up more soil nutrients and water than do non-fixers. Second, the presumed facilitation of N fixation might not occur because non-fixers are not limited by N availability. It is also possible that

facilitation might not occur because N fixers are not fixing much N, but we find this possibility less likely. The lower cost of acquiring N from the soil than from fixation (Gutschick 1981) suggests that N fixers down-regulate fixation when soil N is available, and a number of recent studies are consistent with this idea (Barron et al. 2011, Batterman et al. 2013a, Sullivan et al. 2014). However, our observations from preliminary soil cores indicate that the N fixers in our plots commonly have active nodules, and theory suggests that even small amounts of N fixation can enhance the growth of neighboring non-fixers if they are N limited (Menge et al. 2015). This suggests that the N fixers in our study are not merely operating ecologically as non-fixers—they are bringing new N into these ecosystems—but rather that non-fixers in our study do not respond to this greater N availability.

Our results come from a single region with high annual rainfall, so they may not be ubiquitous across tropical forests. However, because ours is the first study to assess the effect of N fixers on the growth of neighboring trees, statistical sampling suggests that our results are likely not rare. Beyond this sampling argument, several lines of evidence indicate that our findings might be common in moist tropical forests. First, the climate and soil type of our study area are commonly found in other moist tropical forest sites (McDade and Hartshorn 1994). Second, although we do not have rigorous soil N data from our plots, litterfall N and N transformation rates in our broad study area (La Selva Biological Station) are similar to those in many rainforests in the African, Asian, American, and Australian tropics (Vitousek and Matson 1988, Brookshire et al. 2012), indicating that N cycling at our site is representative of many moist tropical forests worldwide. Finally, the most likely mechanism for the strong competitive effects of N fixers that we found is high N-fixer growth rates, which are also common at other

moist tropical forest sites (Pearson and Vitousek 2001, Gehring et al. 2005, Batterman et al. 2013a).

Despite the similarities between our study site and many moist tropical forests, the heterogeneity in this biome (Townsend et al. 2008) means that differences in local features, such as soil nutrient availability, may drive N fixers to have different effects on their neighbors in some sites. Although no other studies have assessed the effects of N fixers on the demographic rates of their neighbors in regenerating tropical forests, two previous studies have investigated how N fixers influence ecosystem-scale biomass accumulation in other regenerating moist tropical forests in Brazil and Panama (Gehring et al. 2005, Batterman et al. 2013a). Contrary to our 1-ha plot-scale findings, both of those studies showed that N fixers were correlated with total biomass accumulation, primarily due to N fixers' own high growth rates. Although N fixers also grow faster than non-fixers at our study sites (Menge and Chazdon 2016), we found that N-fixing trees inhibit biomass accumulation at the plot scale (Fig. 2a) because their inhibition of neighbors outweighs their own rapid growth.

Why might N-fixers inhibit their neighbors more in our sites than in sites in Brazil (Gehring et al. 2005) and Panama (Batterman et al. 2013a)? The three studies differ in the primary N-fixing taxa (*Pentaclethra macroloba* here vs. *Inga* spp. in Batterman et al. (2013a) and a diverse group of legumes in Gehring et al. (2005)) and the age range of succession studied (our youngest sites are 10 yr vs. 5 yr in Batterman et al. (2013a) and 2 yr in Gehring et al. (2005)). One of our study plots, TIR, was dominated by *Inga* rather than *P. macroloba* N fixers, yet still demonstrated the same patterns as our other plots—N fixers inhibited neighbors more than did non-fixers (Appendix 4 - Fig. S7)—suggesting that species identity is not the primary driver of our results. Could the age range explain the discrepancy? In a site near ours, Gilman et

al. experimentally planted a diverse set of N fixers in fallow cattle pasture and found no positive influence of these N fixers on the recruitment and growth of neighboring trees during the first 5 years of succession (Gilman et al. 2016). Their study suggests that N fixers do not facilitate their neighbors at earlier ages in these forests, but given the substantial differences between studies (e.g., naturally regenerating forest in ours vs. experimental planting in theirs), we cannot rule out the possibility that N fixers might have facilitated or weakly inhibited neighbors in earlier years in our plots. More likely, however, other site-specific factors like soil water, nitrogen, phosphorus, and molybdenum availability explain the discrepancy between inhibitory versus facilitative effects of N fixers in our region versus other sites. More broadly, N fixers may play different roles in the dynamics of dry forests (Ferreira da Silva et al. 2017), which cover 523 million hectares of the world's tropics (Bastin et al. 2017).

Current modeling efforts allow for high C-capturing potential in tropical secondary forests, but only if N-fixing trees relieve N limitation (Gerber et al. 2013, Wårlind et al. 2014). Based on the N inputs of N fixers into these systems, modelers may be tempted to use high N-fixer abundances in forests as an indicator of high growth and C-capturing potential, especially given that advances in remote sensing of tropical N fixers (Asner et al. 2008) may soon make abundance data much more readily available than direct data on N inputs. Our findings suggest that these modeling results might be misleading for some or even many moist tropical forest sites, and that a more critical evaluation of N fixers' effect on forest growth is needed to accurately predict the regeneration dynamics and future C sink of the world's secondary tropical forests.

Conclusions

The influence that N fixers have on the surrounding forest is a balance between their negative competitive interactions with neighboring plants and the facilitative effects of their N inputs into the surrounding ecosystem. Because their ability to bring N into ecosystems is both important and rare within the plant kingdom, it is easy to focus on the potential facilitative effects of N fixers. However, our results demonstrate that the competitive effects of N fixers on their neighbors can be sufficiently strong that N fixers inhibit tropical forest growth. Many Earth System models now incorporate dynamic N cycles (including N fixation) into estimates of future tropical forest carbon capture. As we refine how N fixers are incorporated into these models, our results highlight that we must consider that N fixers may have a negative influence on tropical forests' ability to capture and store C in some sites. Given the large potential for C capture in regenerating tropical forests, improving our understanding of how N fixers influence this C-capturing potential is vital to our ability to predict future climate scenarios.

Acknowledgements

The authors thank J. Paniagua, B. Paniagua, and E. Salicetti for their work collecting field data, and M. Uriarte, N. Schwartz, and A. Quebbeman for statistical advice. This work was supported by grants to R. Chazdon from the National Science Foundation (DEB-0424767, DEB-0639393, DEB-1147429), the Andrew W. Mellon Foundation, the NASA Terrestrial Ecology Program, and the University of Connecticut Research Foundation.

Figures and Tables

Table 1: Characteristics of Bosques plots

Characteristics of 8 tropical forest study plots in the Bosques project. Each plot name corresponds to an acronym used in Figure 2. For each plot, the range of stand ages (years since agricultural abandonment) during the study period, mean total basal area, mean proportion of basal area comprised of N fixers, mean proportion of stems comprised of N fixers, and the mean annual change in basal area are presented along with standard errors.

Plot	Age Range (yrs)	Basal Area (±SE) [m^2/ha]	Fixer Proportion of Basal Area (±SE)	Fixer Proportion of Stems (±SE)	Δ Basal Area (±SE) [m^2/ha/yr]
Bejuco (BEJ)	10-20	24.36 (±0.61)	0.23 (±0.007)	0.26 (±0.012)	0.60 (±0.069)
Juan Enrique (JE)	10-20	17.10 (±0.71)	0.21 (±0.007)	0.17 (±0.004)	0.74 (±0.100)
Lindero Sur (LSUR)	12-29	23.82 (±0.70)	0.25 (±0.008)	0.21 (±0.007)	0.42 (±0.211)
Tirimbina (TIR)	15-32	22.54 (±0.47)	0.10 (±0.001)	0.13 (±0.001)	0.31 (±0.133)
Lindero El Peje Secondary (LEPS)	20-37	29.48 (±0.42)	0.33 (±0.003)	0.19 (±0.004)	0.31 (±0.095)
Cuatro Rios (CR)	25-42	33.25 (±0.28)	0.22 (±0.002)	0.14 (±0.002)	0.12 (±0.136)
Lindero El Peje Primary (LEPP)	300+	30.40 (±0.17)	0.31 (±0.002)	0.11 (±0.001)	0.15 (±0.050)
Selva Verde (SV)	300+	33.26 (±0.12)	0.26 (±0.001)	0.09 (±0.001)	0.10 (±0.097)

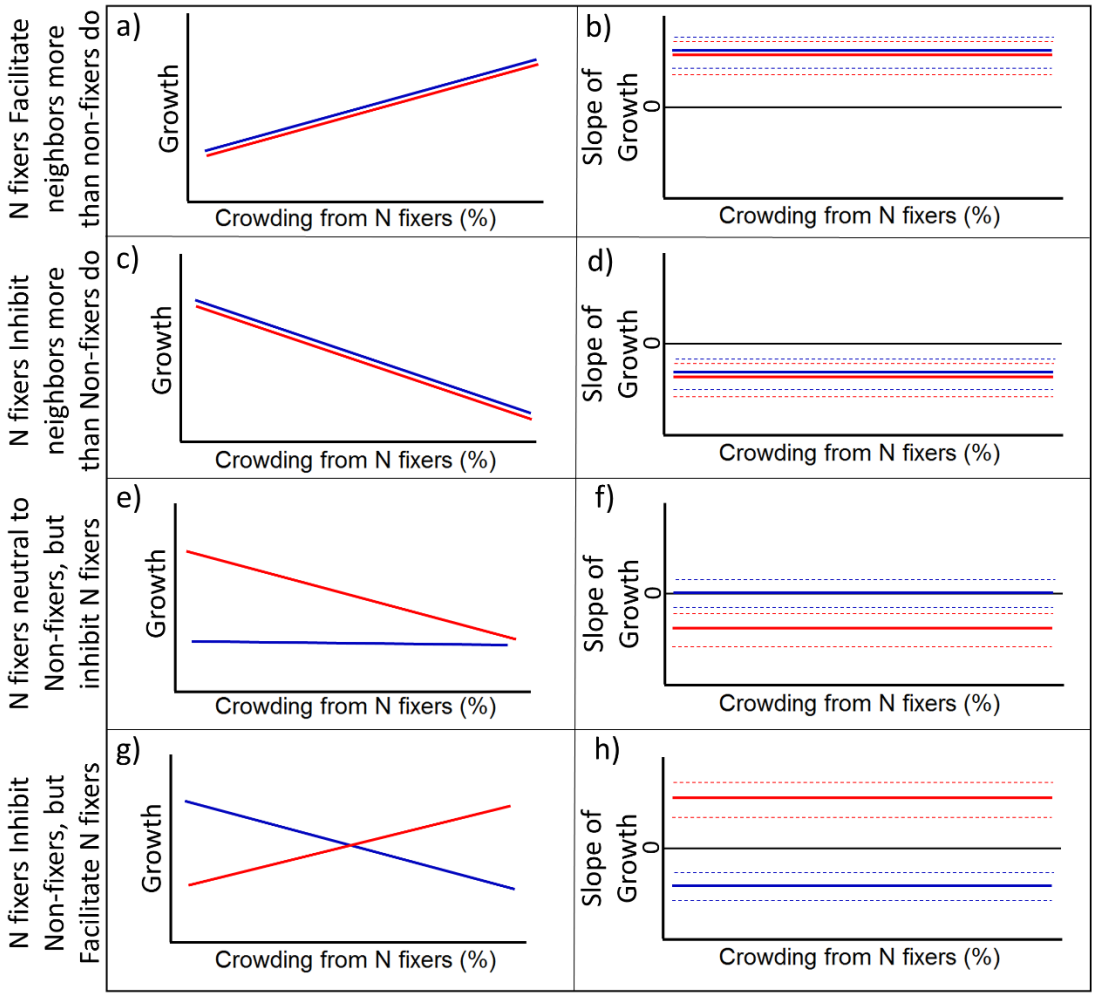

Figure 15: Potential effects of N fixers on neighboring trees

Potential effects of N fixers on neighbor growth (also applies to recruitment or survival) are shown (a, c, e) along with the slopes of these relationships (b, d, f). Red and blue lines indicate the response of neighboring N fixers and neighboring non-fixers, respectively. A positive slope (a, b) indicates that N fixers either facilitate or weakly inhibit their neighbors. A negative slope (c, d) indicates that N fixers strongly inhibit their neighbors. A zero slope (blue line in e, f) indicates that N fixers and non-fixers affect their neighbors equally.

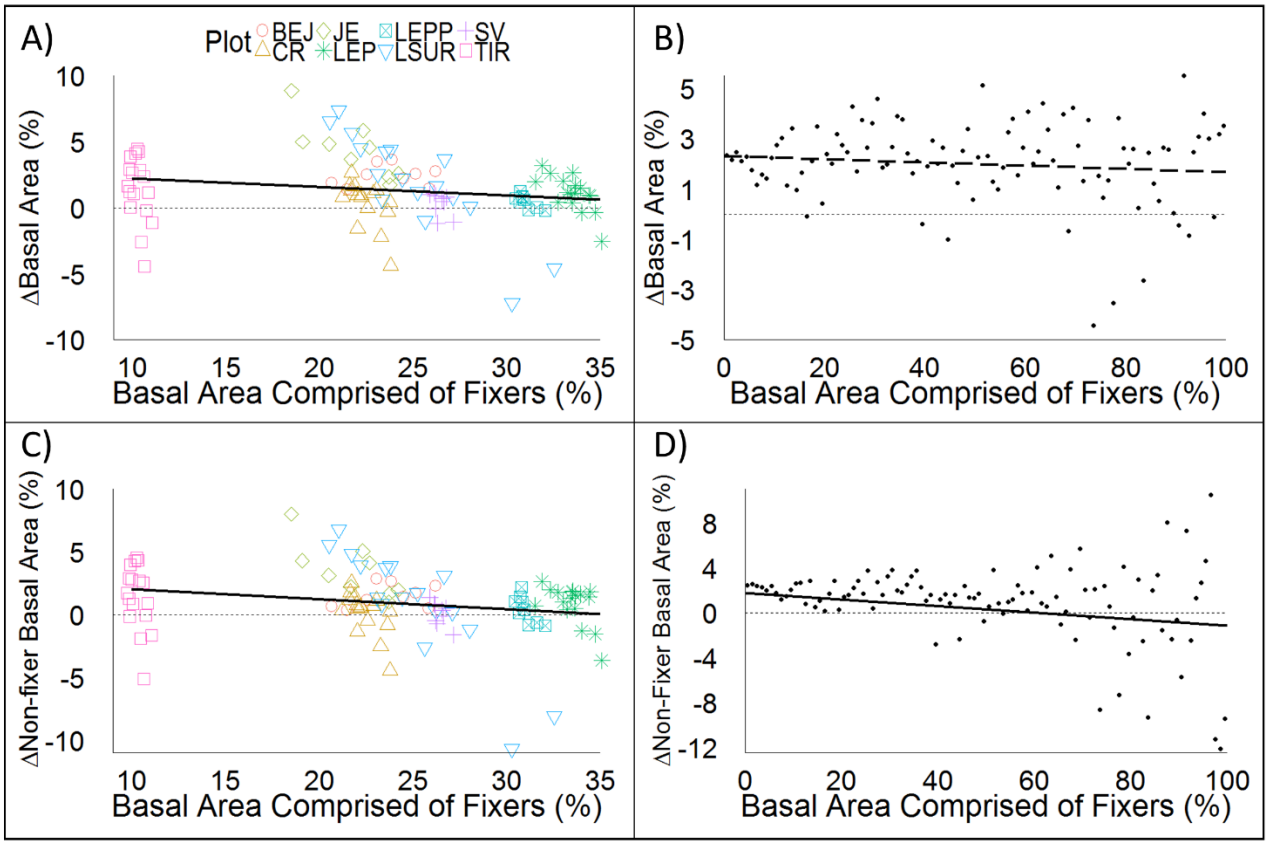

Figure 16: Effects of N fixers on plot- and subplot-level BAI

At the plot level, changes in a) total and c) non-fixer basal area were negatively correlated with the proportion of the plot's basal area comprised of N fixers. Each point represents an individual plot over a single census period. At the subplot level, changes in b) total and d) non-fixer basal area were also negatively related to N-fixer prevalence, but this relationship was not significant for total basal area change (b). Points represent means of basal area change for all subplots within 1% bins of N-fixer prevalence. (a) and (c) represent 104 individual data points (plots in individual census years), and (b) and (d) represent 7,030 individual data points (subplots in individual census years).

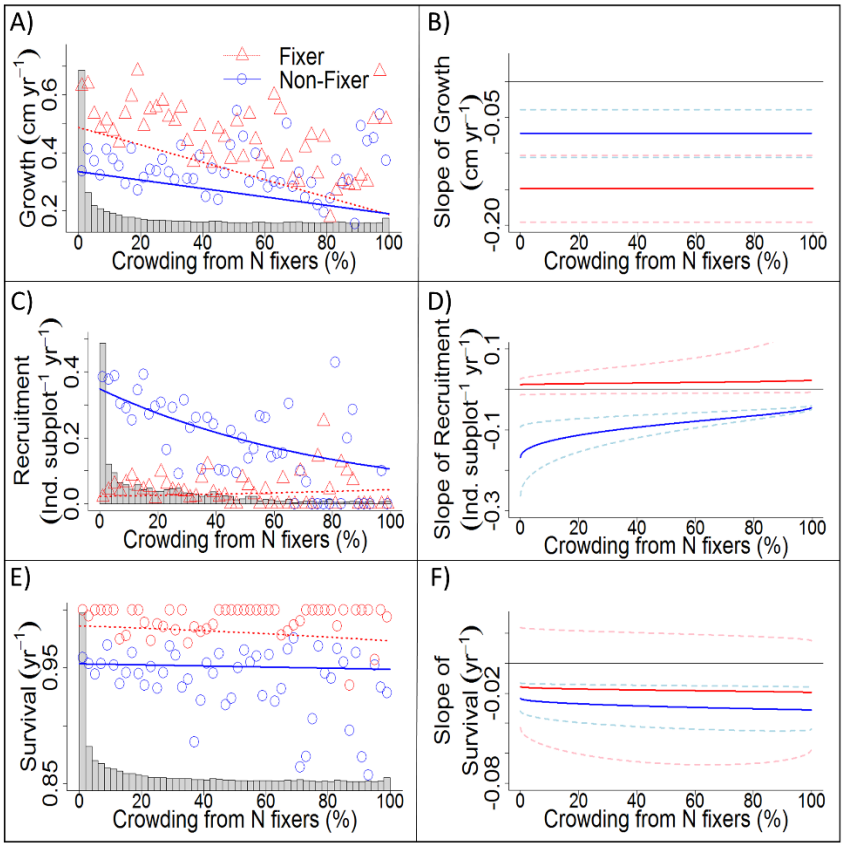

Figure 17: Effects of N-fixer crowding on neighbors in young forests

Growth (a), recruitment (c), and survival (e) of N fixers (red) and non-fixers (blue) are plotted as a function of the proportion of a tree's crowding coming from N fixers. Each symbol represents a binned average of trees. Gray histograms represent the relative data density in each proportion bin. Median slopes (solid curves) and their 95% credible intervals (CIs; dashed curves) are shown for growth (b), recruitment (d), and survival (f). Non-overlapping 95% CI's indicate significant differences. These plots show the effects of N fixers on neighboring trees, independent of overall tree crowding and tree size. Growth and survival models (a, b, e, and f) represent 20,586 data points (individual trees), and recruitment models (c and d) represent 2,770 individual data points (subplots).

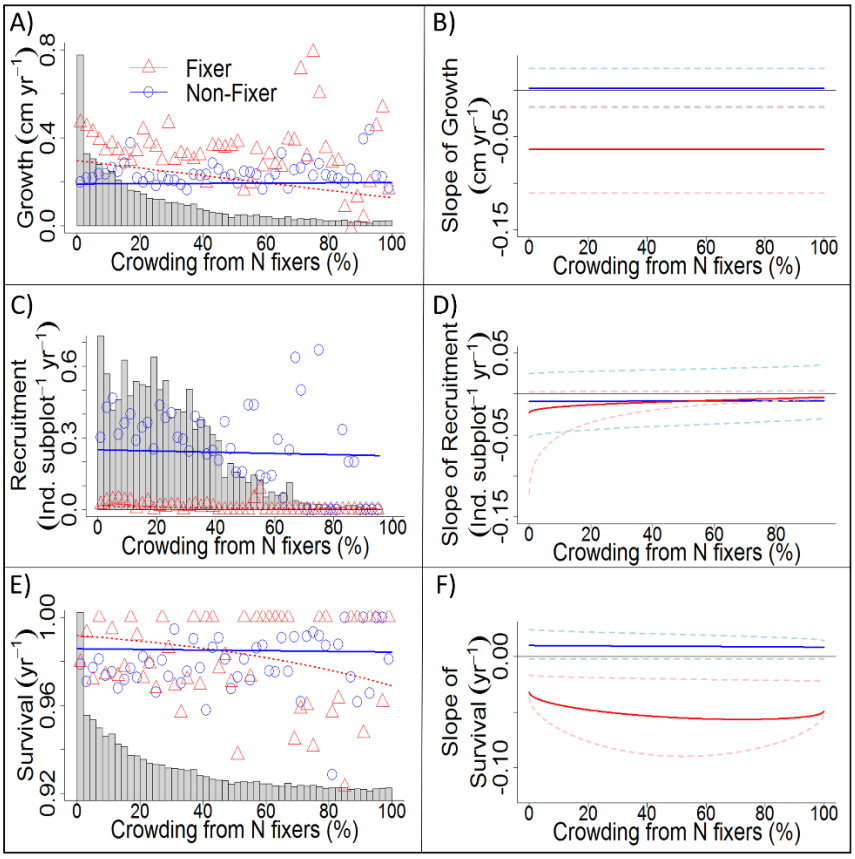

Figure 18: Effects of N-fixer crowding on neighbors in old forests

Growth (a), recruitment (c), and survival (e) as well as the slopes of growth (b), recruitment (d), and survival (f) are plotted as a function of the proportion of a tree's crowding coming from N fixers. All colors and symbols are as in Figure 3. Growth and survival models (a, b, e, and f) represent 27,065 data points (individual trees), and recruitment models (c and d) represent 3,259 individual data points (subplots).

CONCLUSION

Regenerating tropical forests have an immense potential to capture carbon and harbor biodiversity (Brown and Lugo 1990, Chazdon et al. 2009, Pan et al. 2011, 2013), but whether this capacity is realized is partially dependent on the role of symbiotic N fixation (SNF) in promoting or inhibiting forest regeneration rates. Unfortunately, our understanding of the patterns, controls, and effects of SNF is sufficiently poor to hinder our ability to predict the regeneration dynamics of these secondary tropical forests (Gerber et al. 2013, Wårlind et al. 2014). This dissertation examined the dynamics of SNF, ANF, soil N, and tree growth through succession, the relative effects of light and soil N on the growth, biomass allocation, and SNF rates of N fixers, and the influence that N fixers have on regeneration rates in tropical secondary forests. I have focused on linking manipulative experiments that provide a detailed mechanistic understanding of the ecology of N fixers with *in-situ* field work that seeks to verify experimental results in natural settings.

Given that only a handful of studies have measured SNF in regenerating tropical forests, the information that this dissertation provides on the successional dynamics of SNF is an important addition to our growing knowledge of the processes that control tropical forest regeneration. In Chapter 1, I show that SNF declines through successional time through late-successional secondary forests and that ANF dominates N inputs from fixation in old-growth forests. Results from Chapter 2's investigation of the relative effects of light and soil N on SNF suggest that the successional declines in SNF seen in Chapter 1 are likely primarily due to the reduction in light availability as canopy density increases through succession. The positive (although non-significant) relationship between tree growth and N inputs from fixation (both

SNF and ANF) also indicate that N fixation plays an important role in fueling biomass recovery in these forests.

The plot-level analyses presented in Chapter 1 also tell a cautionary tale. In these forests, N-fixer abundance is (non-significantly) negatively correlated with total SNF rates - a surprising result given that SNF is dependent on the presence of N fixers. Measuring N-fixer abundances in tropical forests (identifying trees and measuring their DBH) is relatively easy compared to the intense sampling, soil sorting, and gas incubation work required to directly measure SNF rates. The difficulty of directly estimating SNF makes N-fixer abundance data a tempting proxy. Indeed, early studies on N fixation dynamics in tropical forests were based largely on N-fixer abundances (Gehring et al. 2005). The results of Chapter 1 warn that this is not a valid assumption. Rather, these results suggest that if biogeochemists and global modelers utilize regional N-fixer abundance data (e.g. ter Steege et al. 2006) to estimate SNF in tropical forests, our understanding of SNF dynamics and their influence on forest growth may be greatly misled.

One unique aspect of this dissertation is its ability to link observational patterns of tropical forest succession and the dynamics of SNF inputs with experimental data identifying the likely mechanisms driving these patterns in nature. The shadehouse experiment described in Chapters 2 and 3 provides important new information about the ecological drivers of N-fixer success and N fixation rates. For N fixation rates, results from Chapter 2 provide both mechanistic explanations for the successional patterns seen in Chapter 1 and call for a shift in the focus of future research on the environmental drivers of SNF. High SNF rates early in forest succession could be due low N availability, high light availability, or both in these young forest stands. Results from Chapter 2 suggest the answer is “both,” but that these patterns of SNF are much more strongly driven by the dynamics of light availability than soil N dynamics. Results

from Chapter 2 also showed plants fixing substantial amounts of N even when growing in N-saturated conditions as long as the plants had ample light available to them. If light can drive N fixers to engage in SNF even under N-saturated conditions where theory predicts SNF should be downregulated, over time this could create an N surplus in tropical forests and explain the large N exports measured in many tropical streams (Brookshire et al. 2012).

From a growth perspective, Chapter 3 shows that N fixers don't seem to gain a large growth advantage from the ability to fix N, but fixation also doesn't represent a major structural cost the plant (nodule production is offset by reduced root growth). The ability to fix N does, however, make the height of N fixers less susceptible to competition from neighboring plants under N-limited conditions, and N fixers tend to downregulate N fixation rates under N-limited conditions when in the presence of a competing plant. This suggests that N fixers can continue to grow tall, presumably to overtop and shade out their neighbors under N-limited conditions, while at the same time downregulating the N fixation that has the potential to provide a facilitative effect to their neighbors. This supports observational data presented in Chapter 4 showing that N fixers in early successional forests (presumably where N limitation is most likely to occur) exert particularly strong competitive effects on neighboring plants.

While understanding the patterns and controls of SNF in regenerating tropical forests is important for predicting SNF at other tropical forest sites, this information does not tell us what effect N fixers and their fixation rates have on the regeneration rates of tropical secondary forests. Results from Chapter 4 show that N fixers inhibit growth of the surrounding forest at both the plot- and individual-tree scales. Yes, N fixers do have the potential to fertilize the surrounding forest through their fixation activity, but they also exert competitive pressure on neighboring trees. At our study sites, these competitive forces outweigh any fertilization effect to

create a net inhibitory effect of N fixers on forest growth. These results tell yet another cautionary tale to modelers. Intuition could easily lead modelers to assume that high N-fixer abundances indicate high SNF rates which lead to rapid forest growth. Results from Chapter 1 already indicate that N-fixer abundance is not positively related to SNF rates, breaking the first link in this logic chain. Results from Chapter 4 indicate that N fixers can actually inhibit regeneration rates, breaking the second. Clearly additional studies on the direct effects of N fixers on forest growth are needed before we can make broad predictions of how N fixers and their fixation rates influence tropical forest regeneration.

Together, the results from these four chapters demonstrate that SNF is an important component of the process of tropical forest regeneration, but that N fixers may not have the positive effect on forest growth rates or be positively correlated with SNF rates, as is often assumed. Some of the most exciting parts of conducting this dissertation were the surprising findings in several chapters, which often contradicted prevailing paradigms in the tropical biogeochemistry literature. For example, the lack of a positive relationship between N-fixer abundance and SNF rates, the strong regulation of SNF by light even under N saturated conditions, and the inhibitory effects of N fixers on forest growth all contradict assumptions commonly held by practicing ecologists in the field. The frequency of these surprising results is maybe the strongest evidence that we still have a relatively poor understanding of the ecology of SNF and how it influences tropical forest regeneration. I hope that the work contained in this dissertation furthers our understanding of the important and complex process of SNF, and helps researchers and modelers improve predictions of how SNF will influence future growth and C capture in regenerating tropical forests.

REFERENCES CITED

Adams, M. A., T. L. Turnbull, J. I. Sprent, and N. Buchmannc. 2016. Legumes are different: Leaf nitrogen, photosynthesis, and water use efficiency. Proceedings of the National Academy of Sciences 113:4098–4113.

Anderson, D. R. 2008. Model based inference in the life sciences: A primer on evidence. Springer New York, New York, USA.

Anderson, M. D., R. W. Ruess, D. D. Uliassi, and J. S. Mitchell. 2004. Estimating N_2 fixation in two species of *Alnus* in interior Alaska using acetylene reduction and $^{15}N_2$ uptake. Écoscience 11:102–112.

Asner, G. P., M. O. Jones, R. E. Martin, D. E. Knapp, and R. F. Hughes. 2008. Remote sensing of native and invasive species in Hawaiian forests. Remote Sensing of the Environment 112:1912–1926.

Barron, A. R., D. W. Purves, and L. O. Hedin. 2011. Facultative nitrogen fixation by canopy legumes in a lowland tropical forest. Oecologia 165:511–20.

Barron, A. R., N. Wurzburger, J. P. Bellenger, S. J. Wright, A. M. L. Kraepiel, and L. O. Hedin. 2009. Molybdenum limitation of asymbiotic nitrogen fixation in tropical forest soils. Nature Geoscience 2:42–45.

Bastin, J.-F., N. Berrahmouni, A. Grainger, D. Maniatis, D. Mollicone, R. Moore, C. Patriarca, N. Picard, B. Sparrow, E. M. Abraham, K. Aloui, A. Atesoglu, F. Attore, Ç. Bassüllü, A. Bey, M. Garzuglia, L. G. García-Montero, N. Groot, G. Guerin, L. Laestadius, A. J. Lowe, B. Mamane, G. Marchi, P. Patterson, M. Rezende, S. Ricci, I. Salcedo, A. S.-P. Diaz, F. Stolle, V. Surappaeva, and R. Castro. 2017. The extent of forest in dryland biomes. Science 356:635–638.

Batterman, S. A., L. O. Hedin, M. van Breugel, J. Ransijn, D. J. Craven, and J. S. Hall. 2013a. Key role of symbiotic dinitrogen fixation in tropical forest secondary succession. Nature 502:224–7.

Batterman, S. A., N. Wurzburger, and L. O. Hedin. 2013b. Nitrogen and phosphorus interact to control tropical symbiotic N_2 fixation: A test in *Inga punctata*. Journal of Ecology 101:1400–1408.

Bauters, M., N. Mapenzi, E. Kearsley, B. Vanlauwe, and P. Boeckx. 2016. Facultative nitrogen fixation by legumes in the Central Congo Basin is downregulated during late successional stages. Biotropica 48:281–284.

Benner, J. W., S. Conroy, C. K. Lunch, N. Toyoda, and P. M. Vitousek. 2007. Phosphorus fertilization increses the abundance and nitrogenase activity of the cyanolichen *Pseudocypellaria crocata* in Hawaiian montane forests. Biotropica 36:400–405.

Binkley, D., K. Cromack, and D. D. Backer. 1994. Nitrogen fixation by red alder: Biology, rates, and controls. Pages 57–72 *in* D. Hibbs, R. Tarrant, and D. DeBell, editors. The Biology and Managment of Red Alder. Oregon State University Press, Corvalis, OR.

Binkley, D., and C. Giardina. 1997. Nitrogen fixation in tropical forest plantations. ACIAR Monograph Series 43:297–337.

Bolker, B. M. 2008. Ecological models and data in R. Princeton University Press, Princeton, NJ.

Bolker, B. M., and R Development Core Team. 2017. bbmle: Tools for General Maximum Likelihood Estimation.

Bonan, G. 2008. Forests and climate change: Forcings, feedbacks, and the climate benefits of forests. Science 320:1444–1450.

Boyden, S., D. Binkley, and R. Senock. 2005. Competition and facilitation between *Eucalyptus* and nitrogen-fixing *Falcataria* in relation to soil fertility. Ecology 86:992–1001.

Brookshire, E. N. J., S. Gerber, D. N. L. Menge, and L. O. Hedin. 2012. Large losses of inorganic nitrogen from tropical rainforests suggest a lack of nitrogen limitation. Ecology Letters 15:9–16.

Brown, S., and A. E. Lugo. 1990. Tropical secondary forests. Journal of Tropical Ecology 6:1–32.

Burnham, K. P., D. R. Anderson, and K. P. Huyvaert. 2011. AIC model selection and multimodel inference in behavioral ecology: Some background, observations, and comparisons. Behavioral Ecology and Sociobiology 65:23–35.

Canham, C. D., A. R. Berkowitz, V. R. Kelly, G. M. Lovett, S. V Ollinger, and J. Schnurr. 1996. Biomass allocation and multiple resource limitation in tree seedlings. Canadian Journal of Forest Research 26:1521–1530.

Canham, C. D., P. T. LePage, and K. D. Coates. 2004. A neighborhood analysis of canopy tree competition: Effects of shading versus crowding. Canadian Journal of Forest Research 34:778–787.

Cavaleri, M., S. Reed, W. Smith, and T. Wood. 2015. Urgent need for warming experiments in tropical forests. Global Change Biology 21:2111–2121.

Chalk, P. M. 1985. Estimation of N_2 fixation by isotope dilution: An appraisal of techniques involving ^{15}N enrichment and their application. Soil Biology and Biochemistry 17:389–410.

Chapin III, F., P. Matson, and P. Vitousek. 2011. Principles of terrestrial ecosystem ecology. Springer, New York.

Chapin III, F. S., L. Walker, C. Fastie, and L. Sharman. 1994. Mechanisms of primary succession following deglaciation at Glacier Bay, Alaska. Ecological Monographs 64:149–175.

Chazdon, R., A. R. Brenes, and B. V. Alvarado. 2005. Effects of climate and stand age on annual tree dynamics in tropical second-growth rain forests. Ecology 86:1808–1815.

Chazdon, R. L. 2003. Tropical forest recovery: Legacies of human impact and natural disturbances. Perspectives in Plant Ecology, Evolution and Systematics 6:51–71.

Chazdon, R. L. 2008. Beyond deforestation: Restoring forests and ecosystem services on

degraded lands. Science 320:1458–60.

Chazdon, R. L., S. G. Letcher, M. van Breugel, M. Martínez-Ramos, F. Bongers, and B. Finegan. 2007. Rates of change in tree communities of secondary Neotropical forests following major disturbances. Philosophical Transactions of the Royal Society of London. Series B, Biological sciences 362:273–289.

Chazdon, R. L., and R. W. Pearcy. 1991. The importance of sunflecks for forest understory plants. BioScience 41:760–766.

Chazdon, R. L., C. A. Peres, D. Dent, D. Sheil, A. E. Lugo, D. Lamb, N. E. Stork, and S. E. Miller. 2009. The potential for species conservation in tropical secondary forests. Conservation Biology 23:1406–17.

Chou, C. B., L. O. Hedin, and S. W. Pacala. 2017. Functional groups, species and light interact with nutrient limitation during tropical rainforest sapling bottleneck. Journal of Ecology:1–11.

Cleveland, C. C., B. Z. Houlton, C. Neill, S. C. Reed, A. R. Townsend, and Y. Wang. 2010. Using indirect methods to constrain symbiotic nitrogen fixation rates: A case study from an Amazonian rain forest. Biogeochemistry 99:1–13.

Cleveland, C. C., A. Townsend, D. Schimel, H. Fisher, R. Howarth, L. Hedin, S. Perakis, E. Latty, J. Von Fischer, A. Elseroad, and M. Wasson. 1999. Global patterns of terrestrial biological nitrogen (N_2) fixation in natural ecosystems. Global Biogeochemical Cycles 13:623–645.

Coley, P. D., and J. A. Barone. 1996. Herbivory and plant defenses in tropical forests. Annual Review of Ecology and Systematics 27:305–335.

Crews, T. E. 1993. Phosphorus regulation of nitrogen fixation in a traditional Mexican agroecosystem. Biogeochemistry 21:141–166.

Crews, T. E., H. Farrington, and P. M. Vitousek. 2000. Changes in asymbiotic, heterotrophic nitrogen fixation on leaf litter of *Metrosideros polymorpha* with long-term ecosystem development in Hawaii. Ecosystems 3:386–395.

Crews, T. E., L. M. Kurina, and P. M. Vitousek. 2001. Organic matter and nitrogen accumulation and nitrogen fixation during early ecosystem development. Biogeochemistry 52:259–279.

Crouzeilles, R., M. S. Ferreira, R. L. Chazdon, D. B. Lindenmayer, J. B. B. Sansevero, L. Monteiro, A. Iribarrem, A. E. Latawiec, and B. B. N. Strassburg. 2017. Ecological restoration success is higher for natural regeneration than for active restoration in tropical forests. Science Advances 3:e1701345.

Cusack, D. F., W. Silver, and W. H. McDowell. 2009. Biological nitrogen fixation in two tropical forests: Ecosystem-level patterns and effects of nitrogen fertilization. Ecosystems 12:1299–1315.

Darwin, C. 1859. On the origin of species by means of natural selection, or preservation of favoured races in the struggle for life. John Murray, London.

Davidson, E. A., C. J. R. de Carvalho, A. M. Figueira, F. Y. Ishida, J. P. H. B. Ometto, G. B. Nardoto, R. T. Sabá, S. N. Hayashi, E. C. Leal, I. C. G. Vieira, and L. A. Martinelli. 2007. Recuperation of nitrogen cycling in Amazonian forests following agricultural abandonment. Nature 447:995–8.

Davidson, E. A., J. R. C. Claudio, I. C. G. Vieira, R. O. Figueiredo, F. Y. Ishida, M. T. P. Santos, J. B. Guerrero, K. Kalif, and R. T. Saba. 2004. Nitrogen and phosphorus limitation of biomass growth in a tropical secondary forest. Ecological Applications 14:150–163.

Davidson, E. A., and L. A. Martinelli. 2009. Nutrient limitations to secondary forest regrowth. Pages 299–309 *in* M. Keller, M. Bustamante, J. Gash, and P. S. Dias, editors. Amazonia and global change. American Geophysical Union, Washington DC.

Denslow, J. S., S. Guzman G, S. Julie, and G. Guzman. 2000. Variation in stand structure, light and seedling abundance across a tropical moist forest chronosequence, Panama. Journal of Vegetation Science 11:201–212.

Dent, D. H., S. J. Dewalt, and J. S. Denslow. 2013. Secondary forests of central Panama increase in similarity to old-growth forest over time in shade tolerance but not species composition. Journal of Vegetation Science 24:530–542.

Elser, J. J., M. E. S. Bracken, E. E. Cleland, D. S. Gruner, W. S. Harpole, H. Hillebrand, J. T. Ngai, E. W. Seabloom, J. B. Shurin, and J. E. Smith. 2007. Global analysis of nitrogen and phosphorus limitation of primary producers in freshwater, marine and terrestrial ecosystems. Ecology Letters 10:1135–42.

Erickson, H., M. Keller, and E. A. Davidson. 2001. Nitrogen oxide fluxes and nitrogen cycling during postagricultural succession and forest fertilization in the humid tropics. Ecosystems 4:67–84.

FAO. 2010. Global forest resources assessment. Rome.

Ferreira da Silva, A., A. D. Santiago de Freitas, T. L. Costa, P. I. Fernandes-Junior, L. M. V. Martins, C. E. de Rosalia e Silva Santos, K. A. S. Menezes, and E. V. de Sa Barretto Sampaio. 2017. Biological nitrogen fixation in tropical dry forests with different legume diversity and abundance. Nutrient Cycling in Agroecosystems 107:321–334.

Finegan, B. 1996. Pattern and process in neotropoical secondary rain forests: The first 100 years of succession. Trends in Ecology and Evolution 11:119–124.

Flores, E. M. 2002a. *Pentaclethra macroloba* (Willd .) Kuntze. Pages 601–604. Tropical tree seed manual: Agricultural handbook. Academia Nacional de Ciencias de Costa Rica, San Jose, Costa Rica.

Flores, E. M. 2002b. *Virola koschnyi* Warb. Pages 772–774. Tropical tree seed manual: Agricultural handbook. Academia Nacional de Ciencias de Costa Rica, San Jose, Costa Rica.

Fyllas, N. M., S. Patiño, T. R. Baker, G. B. Nardoto, L. A. Martinelli, C. A. Quesada, R. Paiva, M. Schwarz, V. Horna, L. M. Mercado, A. Santos, L. Arroyo, E. M. Jimenez, F. J. Luizao, D. A. Neill, N. Silva, A. Prieto, A. Rudas, M. Silviera, I. C. G. Vieira, G. Lopez-Gonzalez, Y. Malhi, O. L. Phillips, and J. Lloyd. 2009. Basin-wide variations in foliar properties of

Amazonian forest: Phylogeny, soils and climate. Biogeosciences 6:2677–2708.

Gehring, C., P. L. G. Vlek, L. A. G. de Souza, and M. Denich. 2005. Biological nitrogen fixation in secondary regrowth and mature rainforest of central Amazonia. Agriculture, Ecosystems & Environment 111:237–252.

Gerber, S., L. O. Hedin, S. G. Keel, S. W. Pacala, and E. Shevliakova. 2013. Land use change and nitrogen feedbacks constrain the trajectory of the land carbon sink. Geophysical Research Letters 40:5218–5222.

Gerber, S., L. O. Hedin, M. Oppenheimer, S. W. Pacala, and E. Shevliakova. 2010. Nitrogen cycling and feedbacks in a global dynamic land model. Global Biogeochemical Cycles 24:1–15.

Gilman, A., S. G. Letcher, R. M. Fincher, A. I. Perez, T. W. Madell, A. L. Finkelstein, and F. Corrales-Araya. 2016. Recovery of floristic diversity and basal area in natural forest regeneration and planted plots in a Costa Rican wet forest. Biotropica 48:798–808.

Guariguata, M. R., and R. Ostertag. 2001. Neotropical secondary forest succession: Changes in structural and functional characteristics. Forest Ecology and Management 148:185–206.

Gubry-Rangin, C., M. Garcia, and G. Bena. 2010. Partner choice in *Medicago truncatula*-Sinorhizobium symbiosis. Proceedings of the Royal Society B: Biological Sciences 277:1947–1951.

Gutschick, V. 1981. Evolved strategies in nitrogen acquisition by plants. American Naturalist 118:607–637.

Hedin, L. O., E. N. J. Brookshire, D. N. L. Menge, and A. R. Barron. 2009. The nitrogen paradox in tropical forest ecosystems. Annual Review of Ecology, Evolution, and Systematics 40:613–635.

Houghton, R. 1994. The worldwide extent of land use change. BioScience 44:305–313.

Houlton, B. Z., Y.-P. Wang, P. M. Vitousek, and C. B. Field. 2008. A unifying framework for dinitrogen fixation in the terrestrial biosphere. Nature 454:327–30.

Hungate, B. A., J. S. Dukes, M. R. Shaw, Y. Luo, and C. B. Field. 2003. Nitrogen and climate change. Science 302:1512–3.

Joker, D., and R. Salazar. 2000. *Pentaclethra macroloba*. Seed Leaflet 35:1–3.

Kauffman, J. B., D. L. Cummings, D. E. Ward, and R. Babbitt. 1995. Fire in the Brazilian Amazon: 1. Biomass, nutrient pools, and losses in slashed primary forest. Oecologia 104:397–408.

Kiers, E. T., R. A. Rousseau, S. A. West, and R. F. Denison. 2003. Host sanctions and the legume-rhizobium mutualism. Nature 425:78–81.

Knops, J. M. H., M. E. Ritchie, and D. Tilman. 2000. Selective herbivory on a nitrogen fixing legume (*Lathyrus venosus*) influences productivity and ecosystem nitrogen pools in an oak savanna. Ecoscience 7:166–174.

Lasky, J. R., M. Uriarte, V. K. Boukili, and R. L. Chazdon. 2014. Trait-mediated assembly processes predict successional changes in community diversity of tropical forests. Proceedings of the National Academy of Sciences 111:5616–21.

LeBauer, D., and K. Treseder. 2008. Nitrogen limitation of net primary productivity in terrestrial ecosystems is globally distributed. Ecology 89:371–379.

Liang, S., X. Zhang, Z. Xiao, J. Cheng, Q. Liu, and X. Zhao. 2014. Incident photosynthetically active radiation. Pages 143–159. Global LAnd Surface Satellite (GLASS) Products. Springer, New York.

Lieberman, D., and M. Lieberman. 1987. Forest tree growth and dynamics at La Selva, Costa Rica (1969-1982). Journal of Tropical Ecology 3:347.

MacDowall, F. D. H. 1982. Effects of light intensity and CO_2 concentration on the kinetics of 1st month growth and nitrogen fixation of alfalfa. Canadian Journal of Botany 61:731–740.

Marco, D. E., J. P. Carbajal, S. Cannas, R. Pérez-Arnedo, Á. Hidalgo-Perea, J. Olivares, J. E. Ruiz-Sainz, and J. Sanjuán. 2009. An experimental and modelling exploration of the host-sanction hypothesis in legume-rhizobia mutualism. Journal of Theoretical Biology 259:423–433.

Martinelli, L. A., M. C. Piccolo, A. R. Townsend, P. M. Vitousek, E. Cuevas, W. McDowell, G. P. Robertson, O. C. Santos, and K. Treseder. 1999. Nitrogen stable isotopic composition of leaves and soil: Tropical versus temperate forests. Biogeochemistry 46:45–65.

Matson, P. A., P. M. Vitousek, J. J. Ewel, M. J. Mazzarino, and G. P. Roberston. 1987. Nitrogen transformations following tropical forest felling and burning on a volcanic soil. Ecology 68:491–502.

Mattson, W. 1980. Herbivory in relation to plant nitrogen content. Annual Review of Ecology and Systematics 11:119–161.

McDade, L., and G. Hartshorn. 1994. La Selva: Ecology and natural history of a Neotropical rain forest. University of Chicago Press, Chicago.

McGrath, D. A., C. K. Smith, H. L. Gholz, and F. D. A. Oliveira. 2001. Effects of land-use change on soil nutrient dynamics in Amazonia. Ecosystems 4:625–645.

McHargue, L. A. 1999. Factors affecting the nodulation and growth of tropical woody legume seedlings. Florida International University.

McKey, D. 1994. Legumes and nitrogen: The evolutionary ecology of a nitrogen-demanding lifestyle. Pages 211–228 *in* J. Sprent and D. McKey, editors. Advances in legume systematics 5: The nitrogen factor. Royal Botanic Gardens, Kew.

Meli, P., K. D. Holl, J. M. R. Benayas, H. P. Jones, P. C. Jones, D. Montoya, and D. M. Mateos. 2017. A global review of past land use, climate, and active vs. passive restoration effects on forest recovery. PLoS ONE 12:1–17.

Menge, D., J. Lichstein, and G. Angeles-Perez. 2014. Nitrogen fixation strategies can explain the latitudinal shift in nitrogen-fixing tree abundance. Ecology 95:2236–2245.

Menge, D. N. L., S. A. Batterman, L. O. Hedin, W. Liao, S. W. Pacala, and B. N. Taylor. 2017a. Why are nitrogen-fixing trees rare at higher compared to lower latitudes? Ecology 98:3127–3140.

Menge, D. N. L., S. A. Batterman, W. Liao, B. N. Taylor, J. W. Lichstein, and G. Ángeles-Pérez. 2017b. Nitrogen-fixing tree abundance in higher-latitude North America is not constrained by diversity. Ecology Letters 20:842–851.

Menge, D. N. L., and R. L. Chazdon. 2016. Higher survival drives the success of nitrogen-fixing trees through succession in Costa Rican rainforests. New Phytologist 209:965–977.

Menge, D. N. L., J. L. DeNoyer, and J. W. Lichstein. 2010. Phylogenetic constraints do not explain the rarity of nitrogen-fixing trees in late-successional temperate forests. PLoS ONE 5:e12056.

Menge, D. N. L., and S. A. Levin. 2017. Spatial heterogeneity can resolve the nitrogen paradox of tropical forests. Ecology 98:1049–1061.

Menge, D. N. L., S. A. Levin, and L. O. Hedin. 2008. Evolutionary tradeoffs can select against nitrogen fixation and thereby maintain nitrogen limitation. Proceedings of the National Academy of Sciences of the United States of America 105:1573–8.

Menge, D. N. L., S. A. Levin, and L. O. Hedin. 2009. Facultative versus obligate nitrogen fixation strategies and their ecosystem consequences. The American Naturalist 174:465–77.

Menge, D. N. L., A. A. Wolf, and J. L. Funk. 2015. Diversity of nitrogen fixation strategies in Mediterranean legumes. Nature Plants 1:15064.

Murphy, P. M. 1986. Effect of light and atmospheric carbon dioxide concentration on nitrogen fixation by herbage legumes. Plant and Soil 95:399–409.

Myster, R. W. 2006. Light and nutrient effects on growth and allocation of *Inga vera* (Leguminosae), a successional tree of Puerto Rico. Canadian Journal of Forest Research 36:1121–1128.

Nasto, M. K., S. Alvarez-Clare, Y. Lekberg, B. W. Sullivan, A. R. Townsend, and C. C. Cleveland. 2014. Interactions among nitrogen fixation and soil phosphorus acquisition strategies in lowland tropical rain forests. Ecology Letters 17:1282–9.

Nasto, M. K., B. B. Osborne, Y. Lekberg, G. P. Asner, C. S. Balzotti, S. Porder, P. G. Taylor, A. R. Townsend, and C. C. Cleveland. 2017. Nutrient acquisition, soil phosphorus partitioning and competition among trees in a lowland tropical rain forest. New Phytologist 214:1506–1517.

Oberbauer, S. F., and B. R. Strain. 1985. Effects of light regime on the growth and physiology of *Pentaclethra macroloba* (Mimosaceae) in Costa Rica. Journal of Tropical Ecology 1:303.

Pan, Y., R. A. Birdsey, J. Fang, R. Houghton, P. E. Kauppi, W. A. Kurz, O. L. Phillips, A. Shvidenko, S. L. Lewis, J. G. Canadell, P. Ciais, R. B. Jackson, S. W. Pacala, A. D. McGuire, S. Piao, A. Rautiainen, S. Sitch, and D. Hayes. 2011. A large and persistent carbon sink in the world's forests. Science 333:988–93.

Pan, Y., R. A. Birdsey, O. L. Phillips, and R. B. Jackson. 2013. The structure, distribution, and biomass of the world's forests. Annual Review of Ecology, Evolution, and Systematics 44:593–622.

Pastor, J., and D. Binkley. 1998. Nitrogen fixation and the mass balances of carbon and nitrogen in ecosystems. Biogeochemistry 43:63–78.

Pearson, H., and P. Vitousek. 2001. Stand dynamics, nitrogen accumulation, and symbiotic nitrogen fixation in regenerating stands of *Acacia koa*. Ecological Applications 11:1381–1394.

Piccolo, M. C., C. Neill, and C. C. Cerri. 1994. Net nitrogen mineralization and net nitrification along a tropical forest-to-pasture chronosequence. Plant and Soil 162:61–70.

Pons, T. L., K. Perreijn, C. van Kessel, and M. J. A. Werger. 2007. Symbiotic nitrogen fixation in a tropical rainforest: ^{15}N natural abundance measurements supported by experimental isotopic enrichment. New Phytologist 173:154–67.

Poorter, H., and O. Nagel. 2000. The role of biomass allocation in the growth reponse of plants to different levels of light, CO_2, nutrients and water: A quantitative review. Australian Journal of Plant Physiology 27:595–607.

Poorter, L., F. Bongers, T. M. Aide, A. M. Almeyda Zambrano, P. Balvanera, J. M. Becknell, V. Boukili, P. H. S. Brancalion, E. N. Broadbent, R. L. Chazdon, D. Craven, J. S. de Almeida-Cortez, G. A. L. Cabral, B. H. J. de Jong, J. S. Denslow, D. H. Dent, S. J. DeWalt, J. M. Dupuy, S. M. Durán, M. M. Espírito-Santo, M. C. Fandino, R. G. César, J. S. Hall, J. L. Hernandez-Stefanoni, C. C. Jakovac, A. B. Junqueira, D. Kennard, S. G. Letcher, J.-C. Licona, M. Lohbeck, E. Marín-Spiotta, M. Martínez-Ramos, P. Massoca, J. A. Meave, R. Mesquita, F. Mora, R. Muñoz, R. Muscarella, Y. R. F. Nunes, S. Ochoa-Gaona, A. A. de Oliveira, E. Orihuela-Belmonte, M. Peña-Claros, E. A. Pérez-García, D. Piotto, J. S. Powers, J. Rodríguez-Velázquez, I. E. Romero-Pérez, J. Ruíz, J. G. Saldarriaga, A. Sanchez-Azofeifa, N. B. Schwartz, M. K. Steininger, N. G. Swenson, M. Toledo, M. Uriarte, M. van Breugel, H. van der Wal, M. D. M. Veloso, H. F. M. Vester, A. Vicentini, I. C. G. Vieira, T. V. Bentos, G. B. Williamson, and D. M. A. Rozendaal. 2016. Biomass resilience of Neotropical secondary forests. Nature 530:211–214.

Powers, J. S., and E. Marín-Spiotta. 2017. Ecosystem processes and biogeochemical cycles during secondary tropical forest succession. Annual Review of Ecology, Evolution, and Systematics 48:497–519.

R Core Team. 2017. R: A language and environment for statistical computing. R Foundation for Statistical Computing, Vienna, Austria.

Rastetter, E., P. Vitousek, and C. Field. 2001. Resource optimization and symbiotic nitrogen fixation. Ecosystems 4:369–388.

Reed, S. C., C. C. Cleveland, and A. R. Townsend. 2007. Controls over leaf litter and soil nitrogen fixation in two lowland tropical rain forests. Biotropica 39:585–592.

Reed, S. C., C. C. Cleveland, and A. R. Townsend. 2008. Tree species control rates of free-living nitrogen fixation in a tropical rain forest. Ecology 89:2924–2934.

Reed, S. C., C. C. Cleveland, and A. R. Townsend. 2011. Functional ecology of free-living nitrogen fixation: A contemporary perspective. Annual Review of Ecology, Evolution, and Systematics 42:489–512.

Reed, S. C., A. R. Townsend, C. C. Cleveland, and D. R. Nemergut. 2010. Microbial community shifts influence patterns in tropical forest nitrogen fixation. Oecologia 164:521–531.

Ritchie, M. E., and D. Tilman. 1995. Responses of legumes to herbivores and nutrients during succession on a nitrogen-poor soil. Ecology 76:2648–2655.

Sabine, C. L., M. Heimann, P. Artaxo, D. C. E. Bakker, C.-T. A. Chen, C. B. Field, N. Gruber, C. L. Le Quere, R. G. Prinn, J. E. Richey, P. R. Lankao, J. A. Sathaye, and R. Valentini. 2004. Current status and past trends of the global carbon cycle. Pages 17–44 *in* C. B. Field and M. R. Raupach, editors. The global carbon cycle: Integrating humans, climate, and the natural world. Island Press, Washington DC.

Schlesinger, W., and E. S. Bernhardt. 2013. Biogeochemistry: An analysis of global change. 3rd edition. Elsevier, Oxford.

Silver, W. L., D. J. Herman, and M. K. Firestone. 2001. Dissimilatory nitrate reduction to ammonium in upland tropical forest soils. Ecology 82:2410–2416.

Sollins, P., M. F. Sancho, C. R. Mata, and R. L. Sanford. 1994. Soils and soil process research. Pages 34–54*in* L. McDade, editor. La Selva: Ecology and natural history of a neotropical rain forest. University of Chicago Press, Chicago.

Sprent, J., J. Ardley, and E. K. James. 2017. Biogeography of nodulated legumes and their nitrogen fixing symbionts. New Phytologist 215:40–56.

Sprent, J. I. 1973. Growth and nitrogen fixation in *Lupinus arboreus* as affected by shading and water supply. New Phytologist 72:1005–1022.

Sprent, J. I. 2009. Legume nodulation: A global perspective. Wiley-Blackwell, Oxford.

ter Steege, H., N. C. A. Pitman, O. L. Phillips, J. Chave, D. Sabatier, A. Duque, J.-F. Molino, M.-F. Prévost, R. Spichiger, H. Castellanos, P. von Hildebrand, and R. Vásquez. 2006. Continental-scale patterns of canopy tree composition and function across Amazonia. Nature 443:444–447.

Sullivan, B. W., W. Smith, A. Townsend, M. K. Nasto, S. Reed, R. Chazdon, and C. C. Cleveland. 2014. Spatially robust estimates of biological nitrogen (N) fixation imply substantial human alteration of the tropical N cycle. Proceedings of the National Academy of Sciences 111:8101–8106.

Tanner, E. V. J., P. M. Vitousek, E. Cuevas, and N. Jan. 1998. Experimental investigation of nutrient limitation of forest growth on wet tropical mountains. Ecology 79:10–22.

Taubert, F., R. Fischer, J. Groeneveld, S. Lehmann, M. S. Müller, E. Rödig, T. Wiegand, and A. Huth. 2018. Global patterns of tropical forest fragmentation. Nature:1–4.

Taylor, B. N., R. L. Chazdon, B. Bachelot, and D. N. L. Menge. 2017. Nitrogen-fixing trees inhibit growth of regenerating Costa Rican rainforests. Proceedings of the National

Academy of Sciences 114:8817–8822.

Taylor, B. N., and D. N. L. Menge. Light regulates symbiotic nitrogen fixation more strongly than soil nitrogen availability. Nature Plants (In Review).

Thompson, M. V., and P. M. Vitousek. 1997. Asymbiotic nitrogen fixation and litter decomposition on a long soil-age gradient in Hawaiian montane rain forest. Biotropica 29:134–144.

Tian, L., and J. Wu. 2006. Confidence intervals for the mean of lognormal data with excess zeros. Biometrical Journal 48:149–156.

Townsend, A. R., G. P. Asner, and C. C. Cleveland. 2008. The biogeochemical heterogeneity of tropical forests. Trends in Ecology & Evolution 23:424–31.

Townsend, A. R., C. C. Cleveland, G. P. Asner, and M. M. C. Bustamante. 2007. Controls over foliar N:P ratios in tropical rain forests. Ecology 88:107–118.

Townsend, A. R., C. C. Cleveland, B. Z. Houlton, C. B. Alden, and J. W. White. 2011. Multi-element regulation of the tropical forest carbon cycle. Frontiers in Ecology and the Environment 9:9–17.

Venables, W. N., and B. D. Ripley. 2002. Modern Applied Statistics with S. Fourth edition. Springer, New York, USA.

Vitousek, P., K. Cassman, and C. Cleveland. 2002. Towards an ecological understanding of biological nitrogen fixation. Biogeochemistry 57:1–45.

Vitousek, P., and C. Field. 1999. Ecosystem constraints to symbiotic nitrogen fixers: A simple model and its implications. Biogeochemistry 46:179–202.

Vitousek, P., and R. Howarth. 1991. Nitrogen limitation on land and in the sea: How can it occur? Biogeochemistry 13:87–115.

Vitousek, P. M. 1984. Litterfall, nutrient cycling, and nutrient limitation in tropical forests. Ecology 65:285–298.

Vitousek, P. M. 2004. Nutrient cycling and limitation: Hawaii as a model system. Princeton University Press, Princeton, NJ.

Vitousek, P. M., and J. S. Denslow. 1986. Nitrogen and phosphorus availability in treefall gaps of a lowland tropical rainforest. Journal of Ecology 74:1167–1178.

Vitousek, P. M., and S. Hobbie. 2000. Heterotrophic nitrogen fixation in decomposing litter: Patterns and regulation. Ecology 81:2366–2376.

Vitousek, P. M., and P. A. Matson. 1988. Nitrogen transformations in a range of tropical forest soils. Soil Biology and Biochemistry 20:361–367.

Vitousek, P. M., D. N. L. Menge, S. C. Reed, and C. C. Cleveland. 2013. Biological nitrogen fixation: Rates, patterns and ecological controls in terrestrial ecosystems. Philosophical transactions of the Royal Society of London. Series B, Biological sciences 368:1–9.

Vitousek, P. M., and W. A. Reiners. 1975. Ecosystem succession and nutrient retention: A

hypothesis. BioScience 25:376–381.

Vitousek, P. M., and R. L. Sanford. 1986. Nutrient cycling in moist tropical forests. Annual Review of Ecology and Systematics 17:137–167.

Walker, T. W., and J. K. Syers. 1976. The fate of phosphorus during pedogenesis. Geoderma 15:1–19.

Wang, Y. P., B. Z. Houlton, and C. B. Field. 2007. A model of biogeochemical cycles of carbon, nitrogen, and phosphorus including symbiotic nitrogen fixation and phosphatase production. Global Biogeochemical Cycles 21:1–15.

Wårlind, D., B. Smith, T. Hickler, and A. Arneth. 2014. Nitrogen feedbacks increase future terrestrial ecosystem carbon uptake in an individual-based dynamic vegetation model. Biogeosciences 11:151–185.

Werner, G. D. A., W. K. Cornwell, J. I. Sprent, J. Kattge, and E. T. Kiers. 2014. A single evolutionary innovation drives the deep evolution of symbiotic N_2-fixation in angiosperms. Nature Communications 5:1–9.

Winbourne, J. B., A. Feng, L. Reynolds, D. Piotto, M. G. Hastings, and S. Porder. 2018. Nitrogen cycling during secondary succession in Atlantic Forest of Bahia, Brazil. Scientific Reports 8:1377.

Wolf, A. A., J. L. Funk, and D. N. L. Menge. 2017. The symbionts made me do it: Legumes are not hardwired for high nitrogen concentrations but incorporate more nitrogen when inoculated. New Phytologist 213:690–699.

Wurzburger, N., J. P. Bellenger, A. M. L. Kraepiel, and L. O. Hedin. 2012. Molybdenum and phosphorus interact to constrain asymbiotic nitrogen fixation in tropical forests. PLoS ONE 7:e33710.

Wurzburger, N., and C. F. Miniat. 2014. Drought enhances symbiotic dinitrogen fixation and competitive ability of a temperate forest tree. Oecologia 174:1117–26.

APPENDIX 1: SUPPLEMENTARY INFORMATION FOR CHAPTER 1

Supplementary Methods

Calculating Asymbiotic N Fixation

To estimate total N inputs from ANF we combined data for leaf litter biomass and per-mass litter N fixation rates in each of our study plots. At eight sites oriented in an even grid across each plot we sampled all leaf litter and fine woody debris from a 50.24 cm^2 area of the forest floor. All sampled litter material was placed in a glass jar fitted with an airtight septum. Once sealed, we used a syringe to remove half of the atmospheric head space, which we replaced with an 80:20 mix of 98% atm $^{15}N_2$ and O_2. We then placed the jar on the forest floor glass-up to expose the contents to ambient changes in light and temperature. Samples were incubated in this way for 24 hours, after which they were removed from the $^{15}N_2$-enriched atmosphere and taken to the lab where they were dried and massed. Masses of litter samples were used to calculate average litter mass per m^2 for each study plot. Samples were then analyzed for % N and the ratio of ^{15}N:^{14}N at the Cornell University Stable Isotope Laboratory.

Per-biomass litter fixation rates were calculated using the deviation from the natural ^{15}N:^{14}N ratio that was measured in each sample. The first step in this calculation is to calculate the expected enrichment (E) of $^{15}N_2$ in the atmosphere of the chamber during the incubation using the equation:

$$E = \left(\%^{15}N_{gas}\ x\ f_r\right) + \ (\%^{15}N_{env}\ x\ (1 - f_r)) \quad (1)$$

where E is the expected $^{15}N_2$ enrichment of the jar's headspace, $\%^{15}N_{gas}$ is the percent of ^{15}N atoms in the N_2 gas added to the jar, $\%^{15}N_{env}$ is the percent of ^{15}N atoms in the environment, and f_r is the fraction of the jar's headspace replaced with isotopically enriched gas. For our ANF

sampling, $\%^{15}N_{gas}$ was 98%, $\%^{15}N_{env}$ was .3663%, and f_r was 0.5. We then calculated the percent of N in each sample that was derived from ANF using the equation:

$$\%N_{fix} = \left(\frac{(\%^{15}N_{samp} - \%^{15}N_{env})}{E - \%^{15}N_{env}}\right) x\ 100 \quad (2)$$

where $\%N_{fix}$ is the percent of the sample's N derived from ANF during the incubation period, $\%^{15}N_{samp}$ is the percent of N atoms that were ^{15}N in the sample after incubation, and E and $\%^{15}N_{env}$ are as defined in eq (1). We then calculated ANF rates for each sample using the equation:

$$ANF = \frac{N_{samp}\ x\ \%N_{fix}}{I} \quad (3)$$

where ANF represents asymbiotic N fixation inputs in units of (g N g^{-1} litter incubation^{-1}), N_{samp} is the total amount of N in grams for each litter sample, $\%N_{fix}$ is as defined in eq (2), and I is the incubation period in days, which was 1 for all ANF samples.

Because the ground area for each ANF sample was 0.005024 m^2 (50.24 cm^2) and the incubation period was 1 day, we then multiplied our ANF inputs by 199.0446 and 365 to get ANF inputs in units of g m^{-2} yr^{-1}, which were multiplied by a factor of 10 to convert to units of kg N ha^{-1} yr^{-1} when appropriate.

Calculating Symbiotic N Fixation

We calculated SNF inputs in a similar way to our ANF calculations, with the primary difference being that separate samples were taken for area-based sampling for nodule biomass and per-nodule fixation rates. Sampling for nodule biomass is described in detail in the main text. Per-nodule fixation rates were taken on nodules from 11 *Pentachlethra macroloba* trees adjacent to each plot. Sampled nodules and ~5 cm of attached proximate fine root tissue were placed in an air-tight chamber for enriched $^{15}N_2$ incubations. For nodules, we removed the back

of a 50 ml syringe and placed the nodule and root tissue inside the syringe such that the syringe with a stop-cock fitting served as the air-tight incubation chamber. We then filled 4/5 of the syringe volume with ambient air and 1/5 with an 80:20 mix of 98% atm $^{15}N_2$ and O_2. Thus, our f_r for SNF sampling was 0.2. Nodules were incubated in this enriched atmosphere for 30 minutes, after which they were removed from the syringe and taken to the lab where they were dried and massed. Because per-unit-biomass fixation rates are typically much higher for SNF than ANF, we could achieve measurable deviation in the sample isotopic signature with a smaller f_r and a shorter incubation time. Nodule samples were then analyzed for % N and the ratio of ^{15}N:^{14}N at the Cornell University Stable Isotope Laboratory.

Our calculations for SNF followed eq 1-3 used to calculate ANF rates with the following differences. For SNF, the only change in our application of eq. 1 was an f_r of 0.2 instead of 0.5. We used eq. 2 for SNF calculations in exactly the same way as for ANF calculations. We then used the following equation to calculate SNF rates:

$$SNF = \frac{N_{samp}\ x\ \%N_{fix}}{I} \quad (4)$$

where *SNF* represents rates of symbiotic N fixation in units of (g N g^{-1} nodule incubation^{-1}), N_{samp} was the mass of N in grams in the nodule tissue (after root tissue was removed) for each sample, and all other variables are as in eq 3. For SNF sampling, *I* was 30 min. We then scaled SNF numbers to a per-year basis by multiplying by 17,520 (the number of half-hours in 1 year). Finally, we averaged SNF rates for all samples in a given plot and multiplied this rate by area-based nodule biomass estimates to calculated SNF inputs in units of kg N ha^{-1} yr^{-1}.

Statistical Analyses Symbiotic N Fixation

SNF data are notorious difficult to analyze statistically because they contain many zero values and values that are > 0 are typically log-normally distributed. To account for this data distribution, we adapted the model for zero-inflated log-normal distributions in Tian & Wu (2006) and tested different versions of this model using our Maximum Likelihood framework. This general approach predicts SNF with a dual-process model, simultaneously modeling the probability of encountering a 0 and the mean of the non-zero data. This takes the form of:

$$G(x, \mu, \sigma, \delta) = \begin{cases} \delta & if\ x = 0 \\ \delta + (1 - \delta)\, F(x, \mu, \sigma) & if\ x > 0' \end{cases}$$

where x is the lognormal variable (SNF in kg ha^{-1} yr^{-1}), μ and σ are the mean and standard deviation of SNF in log space, and δ is the probability of encountering a 0 value. $F(x,\mu,\sigma)$ is the lognormal cumulative distribution function of non-zero values. μ could either be a single value (for our null models) or vary in response to an independent variable such as forest age. This allowed us to calculate the predicted population geometric mean, M, as:

$$M = (1 - \delta) * e^{(\mu)}$$

where μ is the mean of the data in log space. For plotting purposes, we calculated a zero-inflated standard error for our SNF data as:

$$SE = (1 - \delta) * e^{(\frac{\sigma}{\sqrt{n}})}$$

where σ is the standard deviation of the data in log space and n is the sample size.

To assess SNF dynamics for each independent variable of interest (forest age, soil N, and individual N-fixer growth), we compared a null model that fit a single geometric mean that did not vary with the independent variable, a model where only δ varied with the independent

variable, a model where only $F(x,\mu,\sigma)$ was a function of the independent variable, and a model where both δ and $F(x,\mu,\sigma)$ were functions of the predictor variable using Maximum Likelihood.

We then calculated confidence intervals for our best-fit model by drawing 1000 random samples from the estimated sampling distribution of our model following methods in (Bolker 2008). This method involved calculating a variance-covariance matrix using the mvrnorm function in the `MASS` package in R (Venables and Ripley 2002) and calculating a mean value for each of the 1000 parameter sets. We then calculated the 95% Confidence Intervals for the 1000 calculated mean values.

Supplementary Tables and Figures

Table S1. Comparison of tree and study plot characteristics. Basal area (BA) and basal area increment (BAI) are shown for trees in each of our five 1-ha plots. Numbers in parentheses represent standard errors calculated from the 10 m x 10 m subplots within each plot.

Plot	Stand Age	BA (m^2 ha^{-1})	N-fixer BA (m^2 ha^{-1})	Non-fixer BA (m^2 ha^{-1})	BAI (m^2 ha^{-1})	N-fixer BAI (m^2 ha^{-1})	Non-fixer BAI (m^2 ha^{-1})
BEJ	19	27.69 (2.30)	7.20 (1.13)	20.50 (2.34)	1.09 (0.08)	0.32 (0.04)	0.76 (0.08)
JE	19	20.42 (1.38)	4.96 (0.86)	15.47 (1.28)	1.36 (0.12)	0.32 (0.07)	1.04 (0.11)
LSUR	29	27.59 (1.73)	8.05 (0.95)	19.54 (1.66)	0.97 (0.18)	0.48 (0.13)	0.49 (0.13)
LEPS	37	32.11 (1.40)	10.73 (1.10)	21.38 (1.27)	1.22 (0.11)	0.34 (0.09)	0.89 (0.06)
LEPP	100	31.60 (2.56)	9.88 (2.01)	21.72 (1.93)	0.48 (0.11)	0.15 (0.02)	0.33 (0.11)

Table S2. Summary table of Maximum Likelihood model comparisons for N dynamics across our chronosequence plots. Model names indicate the shape of the relationship tested between the response (y) and predictor (x) variables. ΔAIC_c values for each model are reported, and the best fit model for each environmental treatment is indicated in bold.

Variables (y vs. x)	Model	ΔAIC_c
Soil N vs. Forest Age	$\log(y) = c$	112.44
	$\log(y) = ax + c$	97.16
	$\log(y) = ax^2 + bx + c$	85.35
	$\boldsymbol{\log(y) = \log\left(c + be^{\left(\frac{-(x-\mu)^2}{2\sigma^2}\right)}\right)}$	**0**
ANF vs. Forest Age	$\log(y) = c$	21.55
	$\log(y) = ax + c$	24.36
	$\boldsymbol{\log(y) = ax^2 + bx + c}$	**0**
	$\log(y) = \log\left(c + be^{\left(\frac{-(x-\mu)^2}{2\sigma^2}\right)}\right)$	106.28
SNF vs. Forest Age	$y = \left(1 - \frac{1}{(1+e^{-\delta})}\right) * e^{\left(\mu + \frac{\sigma^2}{2}\right)}$	3.52
	$y = \left(1 - \frac{1}{1+e^{-(h+j*x)}}\right) * e^{\left(c+bx+\frac{\sigma^2}{2}\right)}$	1.46
	$\boldsymbol{y = \left(1 - \frac{1}{(1+e^{-\delta})}\right) * e^{\left(c+bx+\frac{\sigma^2}{2}\right)}}$	**0**
	$y = \left(1 - \frac{1}{1+e^{-(h+j*x)}}\right) * e^{\left(\mu+\frac{\sigma^2}{2}\right)}$	4.98
	$y = \left(1 - \frac{1}{(1+e^{-\delta})}\right) * e^{\left(c+bx+kx^2+\frac{\sigma^2}{2}\right)}$	1.65
BAI vs. Forest Age	$y = c$	17.14
	$\boldsymbol{y = ax + c}$	**0**
	$y = ax + bx^2 + c$	8.65
	$y = \frac{a}{1 + e^{x-b}} + c$	8.67

Table S3. Summary table of Maximum Likelihood model comparisons for components of N dynamics across our chronosequence plots. Model names indicate the shape of the relationship tested between the response (y) and predictor (x) variables. ΔAIC_c values for each model are reported, and the best fit model for each environmental treatment is indicated in bold.

Variables (y vs. x)	Model	ΔAIC_c
Soil Ammonium vs. Forest Age	$\log(y) = c$	257.57
	$\log(y) = ax + c$	219.22
	$\log(y) = ax^2 + bx + c$	221.86
	$\boldsymbol{\log(y) = \log\left(c + be^{\left(\frac{-(x-\mu)^2}{2\sigma^2}\right)}\right)}$	**0**
Soil Nitrate vs. Forest Age	$\log(y) = c$	21.55
	$\log(y) = ax + c$	24.36
	$\boldsymbol{\log(y) = ax^2 + bx + c}$	**0**
Percent Nitrate vs. Forest Age	$y = c$	41.77
	$y = ax + c$	40.38
	$\boldsymbol{y = ax^2 + bx + c}$	**0**
	$y = \frac{1}{1 + e^{(bx+c)}}$	50.25
Nodule Biomass vs. Forest Age	$y = \left(1 - \frac{1}{(1 + e^{-\delta})}\right) * e^{\left(\mu + \frac{\sigma^2}{2}\right)}$	7.07
	$y = \left(1 - \frac{1}{1 + e^{-(h+j*x)}}\right) * e^{\left(c+bx+\frac{\sigma^2}{2}\right)}$	1.46
	$\boldsymbol{y = \left(1 - \frac{1}{(1 + e^{-\delta})}\right) * e^{\left(c+bx+\frac{\sigma^2}{2}\right)}}$	**0**
	$y = \left(1 - \frac{1}{1 + e^{-(h+j*x)}}\right) * e^{\left(\mu+\frac{\sigma^2}{2}\right)}$	8.52
SNF Rate vs. Forest Age	$y = c$	151.68
	$y = ax + c$	38.01
	$\boldsymbol{y = ax^2 + bx + c}$	**0**
SNF vs. Total Soil N	$y = \left(1 - \frac{1}{(1 + e^{-\delta})}\right) * e^{\left(\mu + \frac{\sigma^2}{2}\right)}$	2.09
	$y = \left(1 - \frac{1}{1 + e^{-(h+j*x)}}\right) * e^{\left(c+bx+\frac{\sigma^2}{2}\right)}$	2.03
	$\boldsymbol{y = \left(1 - \frac{1}{(1 + e^{-\delta})}\right) * e^{\left(c+bx+\frac{\sigma^2}{2}\right)}}$	**0**
	$y = \left(1 - \frac{1}{1 + e^{-(h+j*x)}}\right) * e^{\left(\mu+\frac{\sigma^2}{2}\right)}$	4.11
Litter Biomass vs. Forest Age	$\boldsymbol{\log(y) = c}$	**0**
	$\log(y) = ax + c$	2.10
	$\log(y) = ax^2 + bx + c$	5.22

ANF Rate vs. Forest Age	$y = c$	22.21
	$y = ax + c$	24.67
	$\boldsymbol{y = ax^2 + bx + c}$	**0**

Table S4. Summary table of Maximum Likelihood model comparisons for the relationship between SNF, the crowding of N fixers, and the growth of N fixers and all trees. Model names indicate the shape of the relationship tested between the response (y) and predictor (x) variables. ΔAIC_c values for each model are reported, and the best fit model for each environmental treatment is indicated in bold.

Variables (y vs. x)	Model	ΔAIC_c
SNF vs. N-fixer crowding around the core sample	$\boldsymbol{y = \left(1 - \frac{1}{(1 + e^{-\delta})}\right) * e^{\left(\mu + \frac{\sigma^2}{2}\right)}}$	**0**
	$y = \left(1 - \frac{1}{1 + e^{-(h + j*x)}}\right) * e^{\left(c + bx + \frac{\sigma^2}{2}\right)}$	9.61
	$y = \left(1 - \frac{1}{(1 + e^{-\delta})}\right) * e^{\left(c + bx + \frac{\sigma^2}{2}\right)}$	3.38
	$y = \left(1 - \frac{1}{1 + e^{-(h + j*x)}}\right) * e^{\left(\mu + \frac{\sigma^2}{2}\right)}$	3.91
SNF vs. N-fixer crowding around the sampled tree	$\boldsymbol{y = \left(1 - \frac{1}{(1 + e^{-\delta})}\right) * e^{\left(\mu + \frac{\sigma^2}{2}\right)}}$	**0**
	$y = \left(1 - \frac{1}{1 + e^{-(h + j*x)}}\right) * e^{\left(c + bx + \frac{\sigma^2}{2}\right)}$	21.89
	$y = \left(1 - \frac{1}{(1 + e^{-\delta})}\right) * e^{\left(c + bx + \frac{\sigma^2}{2}\right)}$	2.79
	$y = \left(1 - \frac{1}{1 + e^{-(h + j*x)}}\right) * e^{\left(\mu + \frac{\sigma^2}{2}\right)}$	13.81
Individual N-fixer growth vs. SNF of surrounding cores	$\boldsymbol{y = c}$	**0**
	$y = ax + c$	2.18
	$y = ax^2 + bx + c$	4.83
Growth of all trees in a subplot vs. subplot SNF	$\boldsymbol{y = c}$	**0**
	$y = ax + c$	2.33
	$y = ax^2 + bx + c$	4.37
N-fixer growth in a subplot vs. subplot SNF	$\boldsymbol{y = c}$	**0**
	$y = ax + c$	1.85
	$y = ax^2 + bx + c$	3.69

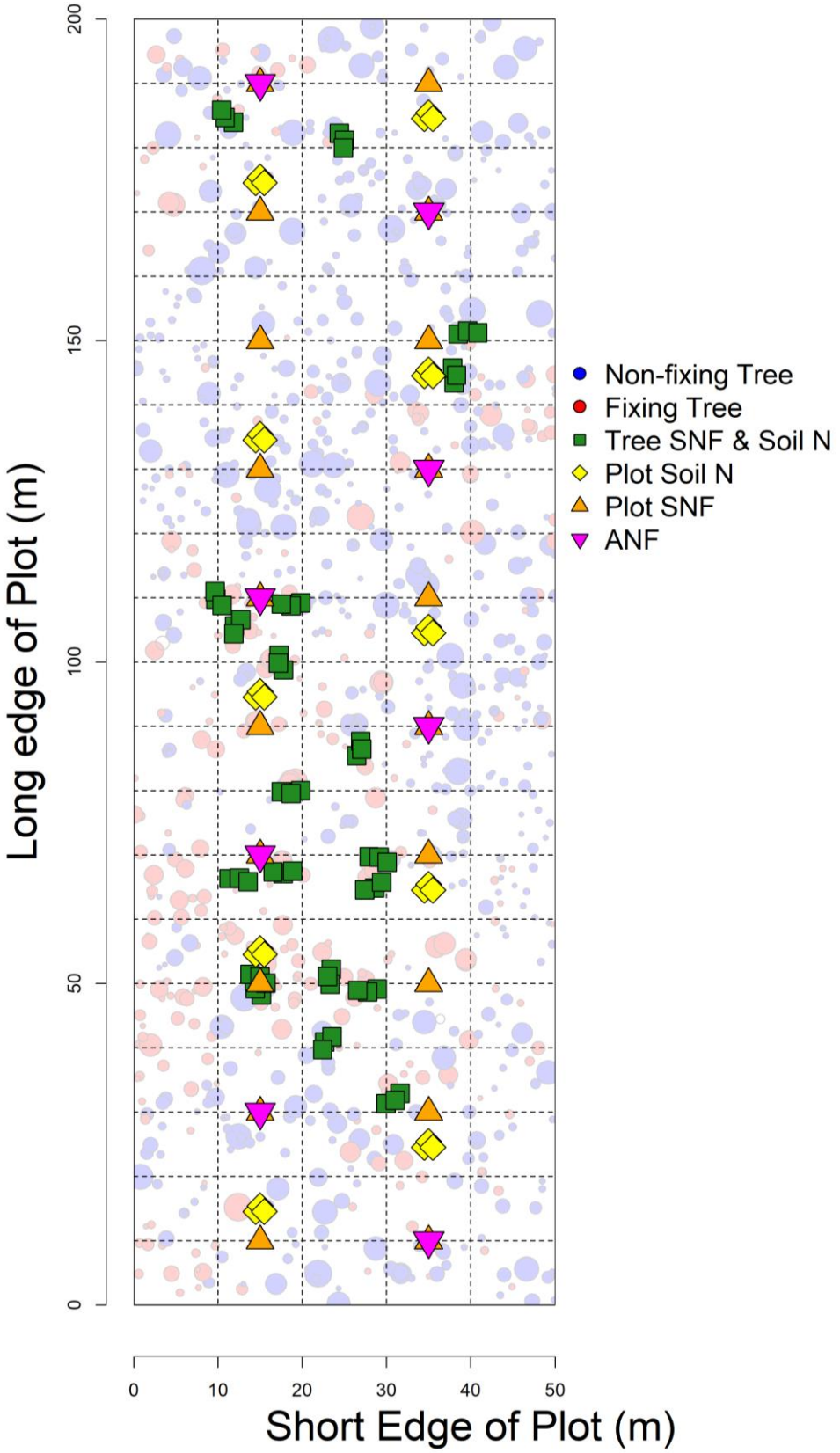
Long edge of Plot (m)
0
50
100
150
200
0
10
20
30
40
50
Short Edge of Plot (m)
Non-fixing Tree
Fixing Tree
Tree SNF & Soil N
Plot Soil N
Plot SNF
ANF

Figure S1. Diagram of sampling effort in an example plot (plot BEJ). Blue and red circles in background represent non-fixing and N-fixing trees, respectively, with relative circle sizes indicating tree DBH. Green squares indicate the approximate position of each core around randomly-selected N-fixing trees for tree-based SNF and soil N sampling conducted in 2017. Yellow diamonds represent plot-based soil N sampling conducted in 2015. Orange triangles represent plot-based SNF sampling conducted in 2016. Magenta triangles represent ANF sampling conducted in 2016.

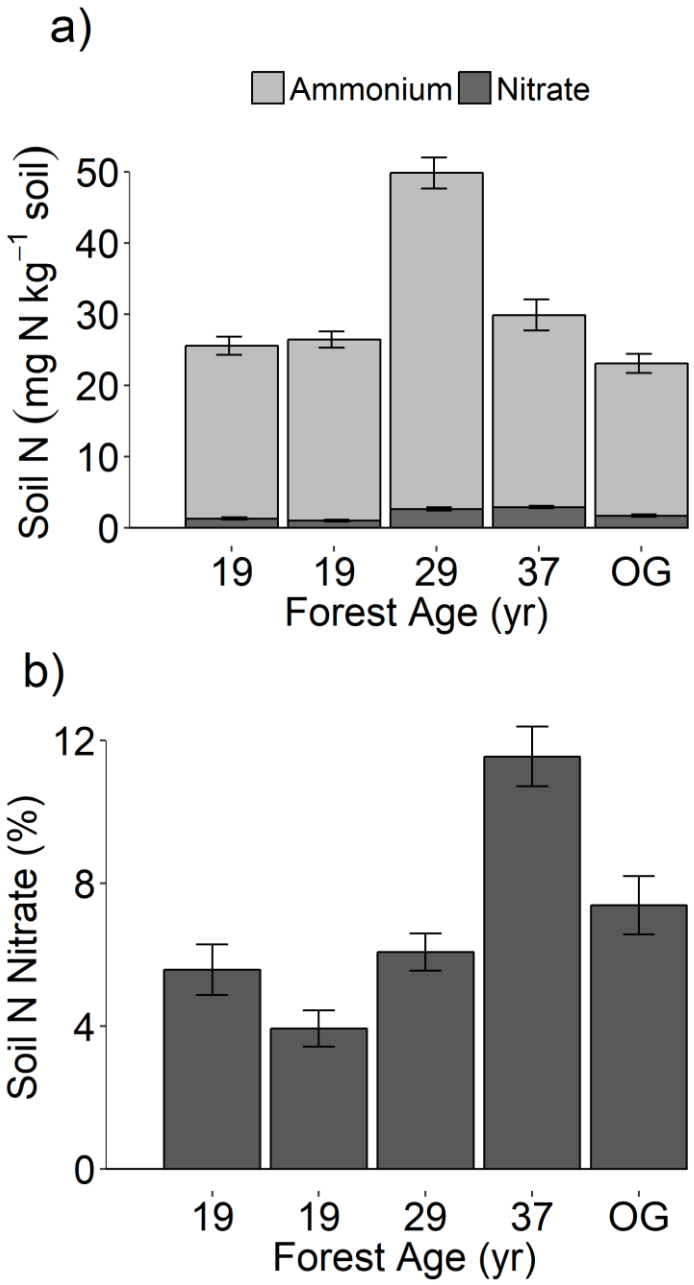

Figure S2. Primary components of the inorganic soil N pool. **a)** The relative contribution of ammonium (gray) and nitrate (black) to total soil inorganic N concentrations (bar height) plotted against forest age for each of our five study plots. **b)** The percent of nitrate to total inorganic soil N for each of our five study plots.

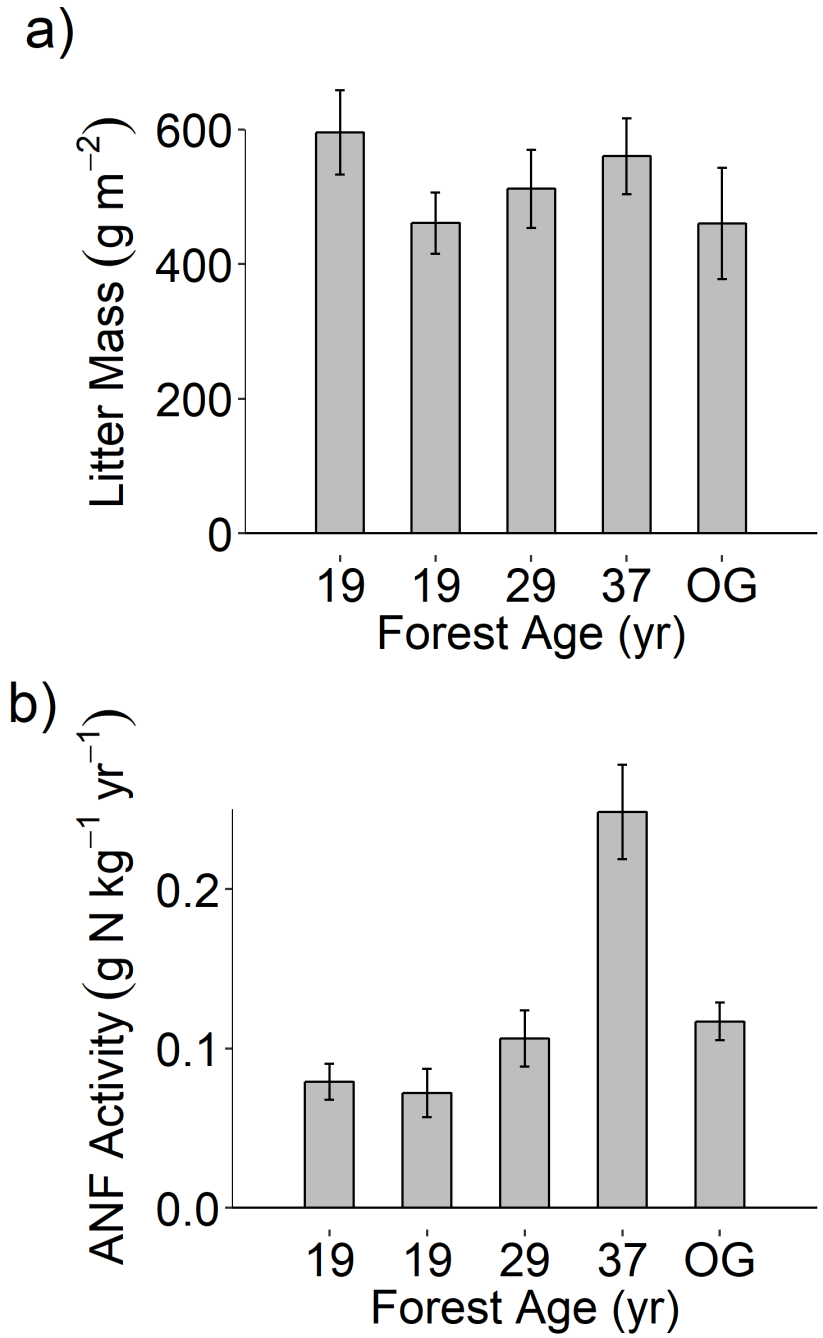

Figure S3. The two primary contributions to variation in N inputs via ANF. **a)** Mean (± 1 S.E.) leaf litter mass plotted against forest age for each of our five study plots. Litter mass included all leaf litter and fine woody debris above the mineral soil layer. **b)** Mean (± 1 S.E.) asymbiotic fixation rates shown as g N fixed per kg of leaf litter per year for each of our five study plots.

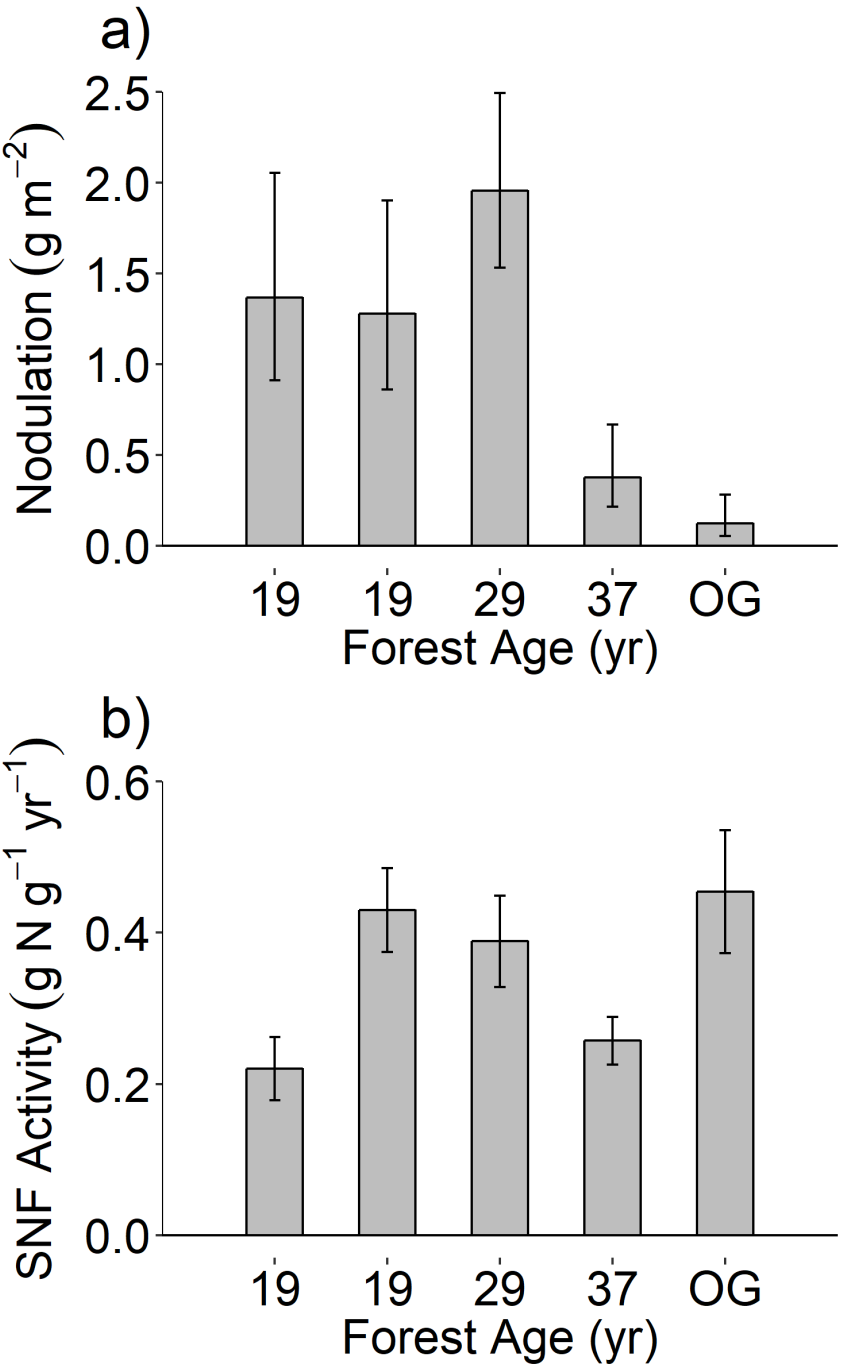

Figure S4. The two primary contributions to variation in N inputs from SNF. **a)** Geometric mean (± 1 S.E.) nodule biomass per m^2 of sampled ground area plotted against forest age for each of our five study plots. **b)** Mean (± 1 S.E.) symbiotic N fixation rates shown as g N fixed per g of nodule biomass per year for each of our five study plots.

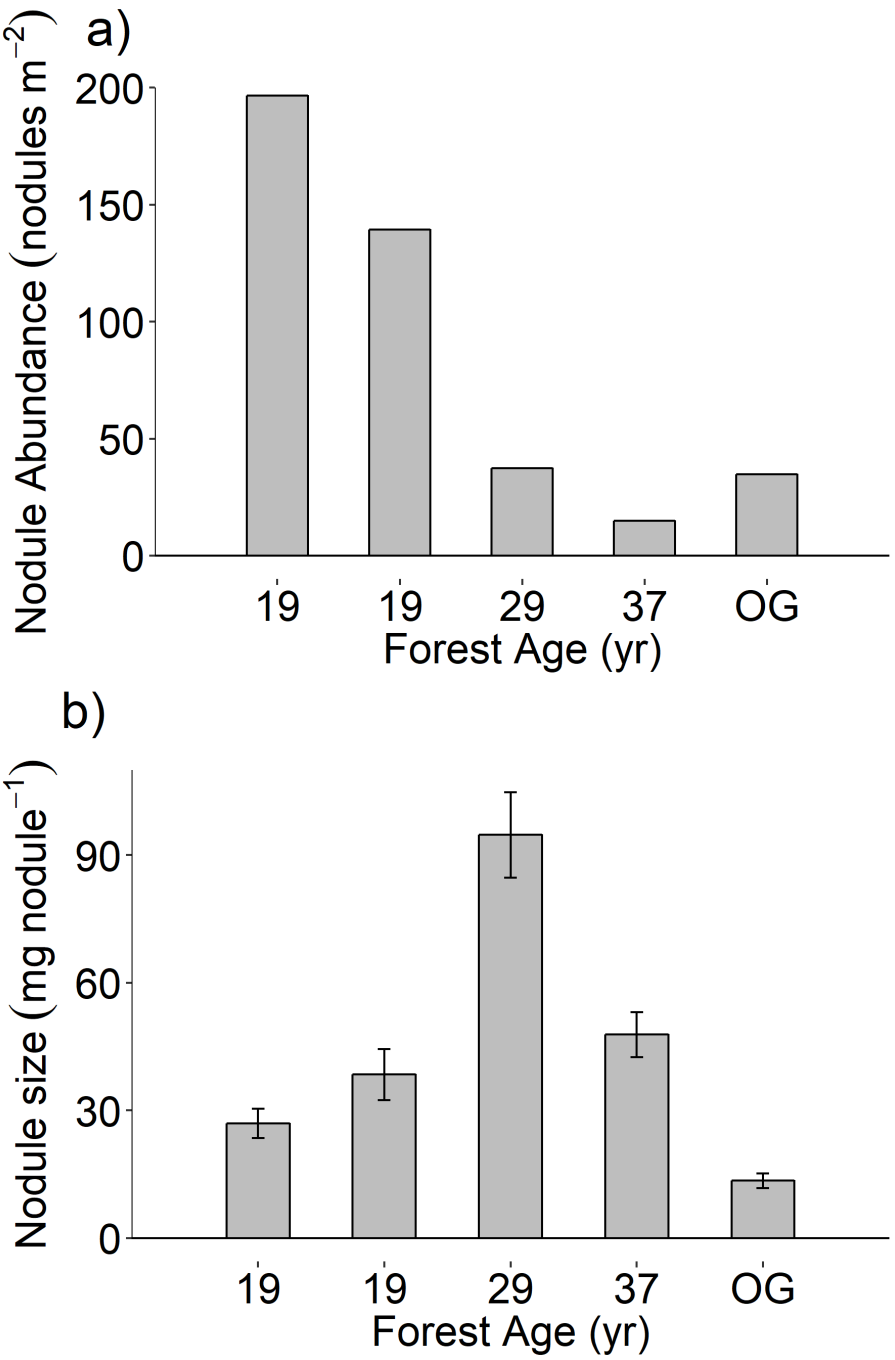

Figure S5. Attributes of nodulation. **a)** The sum of the number of nodules obtained from sampling in each plot presented on a m^{-2} basis plotted against forest age. **b)** Mean (± 1 S.E.) nodule mass for nodules sampled in each of our five study plots.

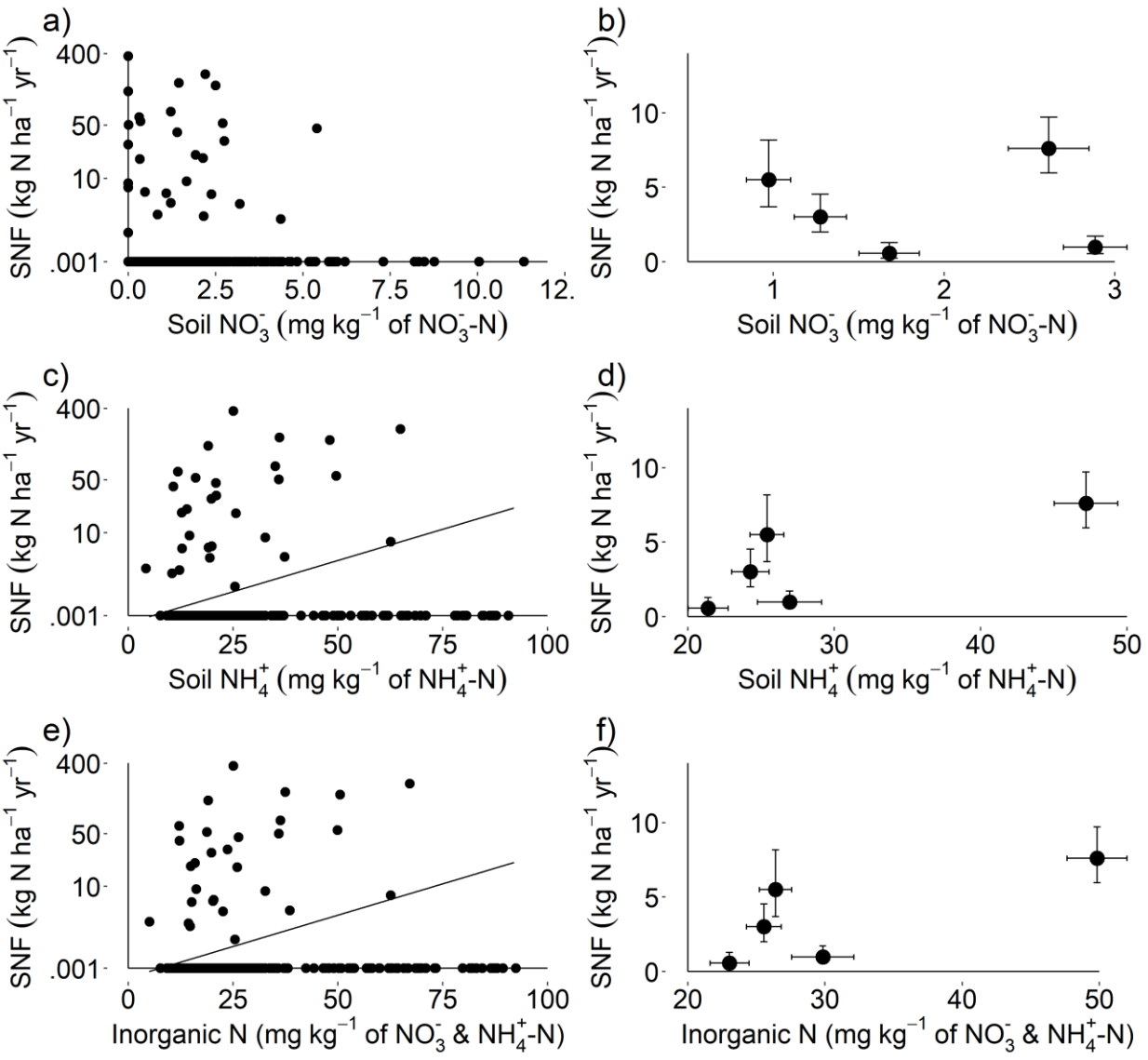

Figure S6. Relationship between SNF and soil inorganic N. SNF was not significantly related to soil nitrate at the **a)** core or **b)** plot scale. SNF was related to soil ammonium at the **c)** core, but not the **d)** plot scale. When soil nitrate and ammonium were summed, SNF was also related to total soil inorganic N at the **e)** core, but not the **f)** plot scale. SNF estimates for individual cores are presented on a log scale with linear (untransformed) units. Error bars in **b)**, **d)**, and **f)** represent ± 1 S.E.

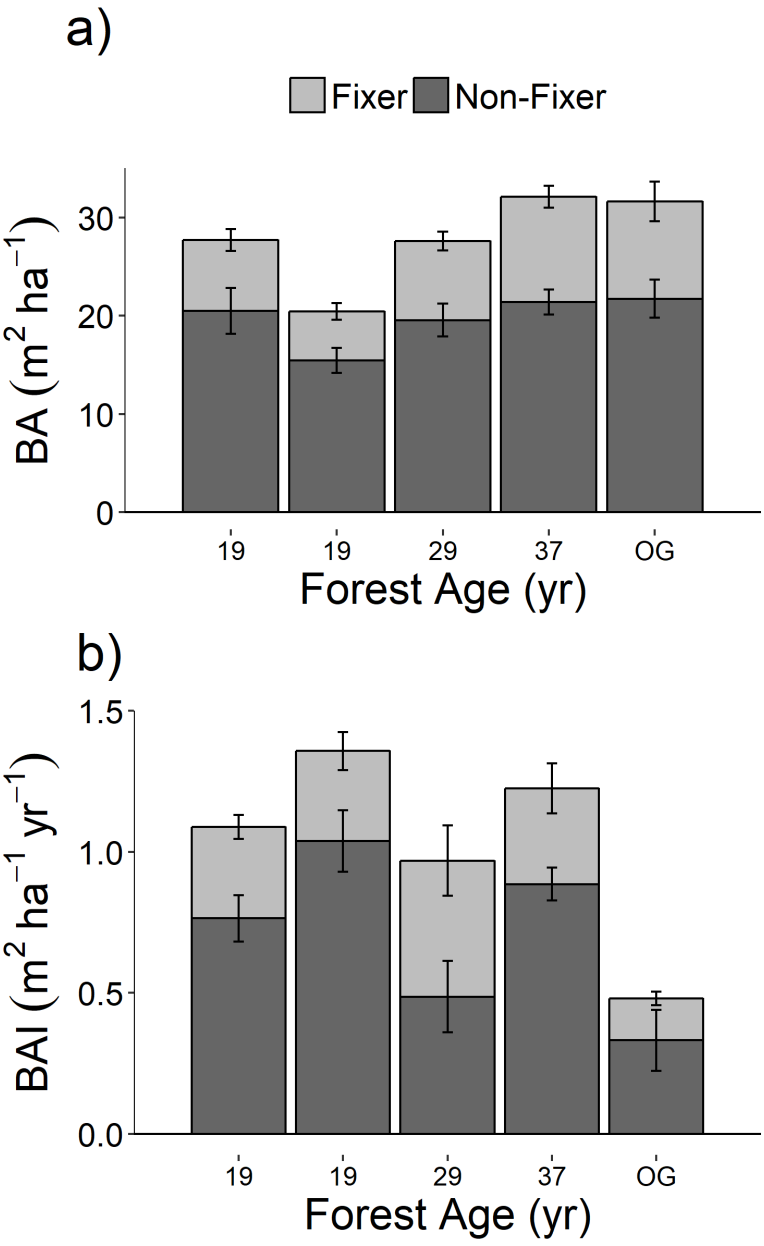

Figure S7. Primary components of the tree community. **a)** The contribution of non-fixing trees (dark gray) and N-fixing trees (light gray) to total summed basal area (bar height) plotted against forest age for each of our five study plots. **b)** The contribution of non-fixing trees (dark gray) and N-fixing trees (light gray) to tree basal area increment (bar height) plotted against forest age for each of our five study plots.

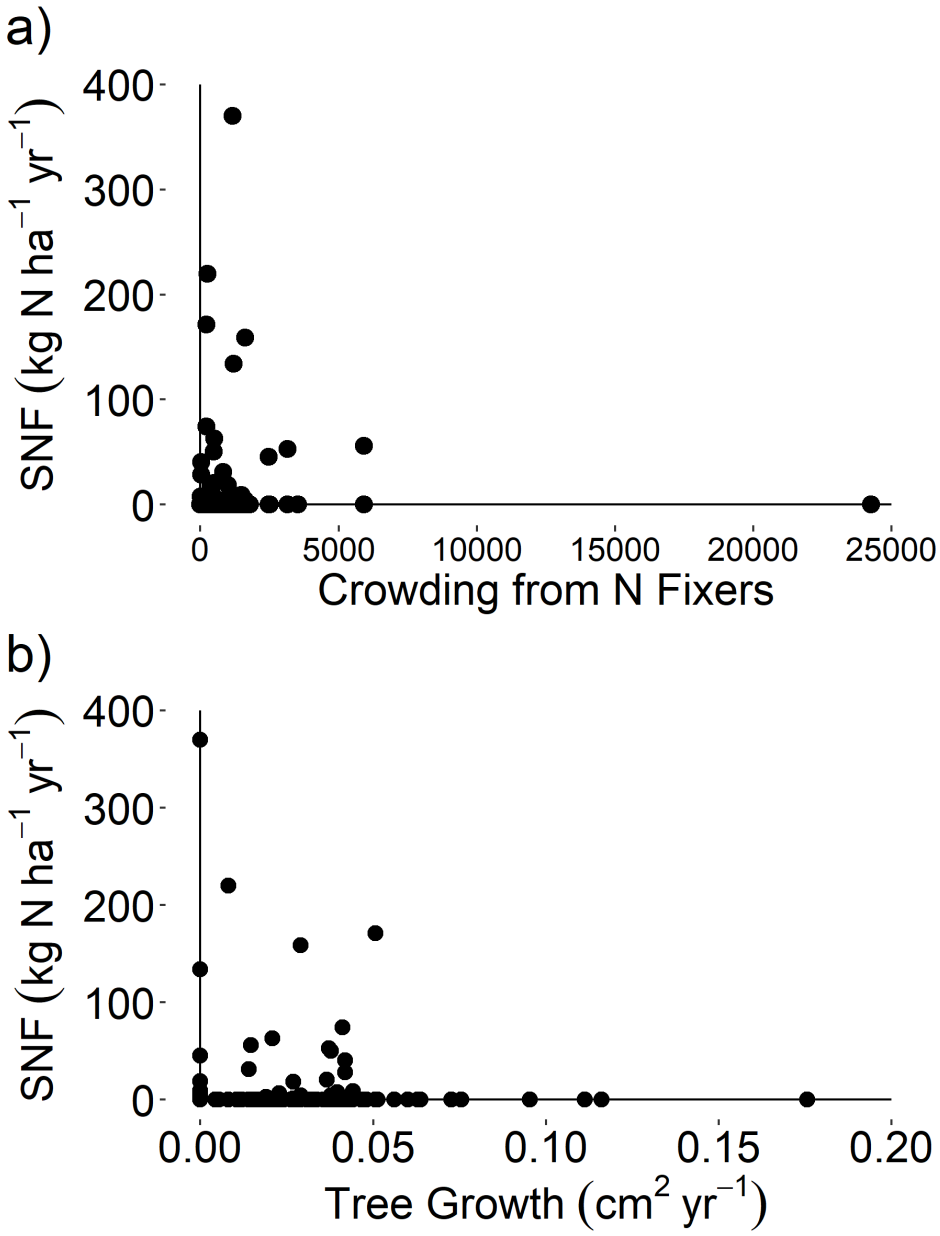

Figure S8. Relationship between SNF and local N-fixer abundance and growth. **a)** Estimates of SNF from each sampled core in our tree-based SNF sampling were not correlated with the crowding of N fixers around the sampled tree. **b)** Estimates of SNF from each sampled core in our tree-based SNF sampling were also not correlated with the growth of the focal N-fixing tree. These figures are presented on log-log axes for **a)** and log-linear axes for **b)** in Figure 4 of the main text.

APPENDIX 2: SUPPLEMENTARY INFORMATION FOR CHAPTER 2

Supplementary Methods

Study Site – We conducted both the open shadehouse experiment and the forest seedling sampling at La Selva Biological Station (10° 25' 53.14" N, 84° 0' 10.51" W) in the premontane wet forests of Heredia province in Costa Rica. This site experiences an average daytime temperature of 25°C, which is relatively constant throughout the year. Annual precipitation at La Selva is approximately 4500 mm yr^{-1} with a pronounced dry season occurring from January through April and a second, less pronounced dry season in September and October. Soils at this site are primarily ultisols derived from weathered basalt (Sollins et al. 1994).

Study Species – To test for the effects of light and soil N on symbiotic N fixation (SNF), we used the native N fixer *Pentaclethra macroloba* (Willd.) Kuntze as a representative species. *Pentaclethra macroloba* is common in lowland forests throughout its range from Nicaragua to the Amazon basin (Flores 2002a), and is the most abundant canopy species at this site(Lieberman and Lieberman 1987). Adults of *P. macroloba* typically reach 30-35 m in height and up to 130 cm in diameter, and produce dry, dehiscent fruits that ballistically disperse 3-8 seeds each weighing approximately 8 g. Seed germination occurs within 8-10 days (Joker and Salazar 2000). Typically considered a shade-tolerant species, *P. macroloba* has been shown to be sensitive to changing light environments (Oberbauer and Strain 1985) and levels of N fixation vary in response to soil N availability(Pons et al. 2007).

Shadehouse Experiment

Experimental Design – We measured the effect of light and soil N availability on *P. macroloba* by comparing the growth of plants in 7-liter pots exposed to varying levels of each

environmental variable between July, 2015 and January, 2016. Seedlings were grown from seed in soil inoculated with *P. macroloba*'s N-fixing rhizobia endosymbionts using 4 ml of slurry containing distilled water and locally collected active *P. macroloba* root nodules. High, medium, and low light treatments were created using varying thicknesses of shade cloth. The light treatments corresponded to 40%, 16%, and 8% full irradiance, respectively, which we determined by comparing paired PAR sensor readings where one sensor was placed above plants in each light treatment and the other sensor was placed in an open field exposed to full sunlight. Within each of these light treatments were three N fertilization treatments. Pots were filled with a mixture of forest soil and locally sourced sand in a 1:1 ratio. Pots were then fertilized using an ammonium-nitrate (NH_4-NO_3) solution applied once at the time of seed sowing and once at the mid-point of the experiment's duration in amounts equivalent to .51, 20, and 40 g N m^{-2} yr^{-1} for low-, medium-, and high-N treatments, respectively. Included in the fertilizer was a 98% isotopically enriched ^{15}N tracer used to determine N fixation (see below). Nitrogen treatments were arranged randomly within each light treatment. This represents a fully replicated factorial design with 9 environmental treatments, each containing 20 plants at the start of the experiment.

Seedling Growth and Data Collection – Plants were grown from locally collected seeds planted in late June 2015. Initial plant (seed) size was determined by weighing seeds prior to planting. Following planting, all visibly dead or inviable seeds were replaced after two weeks. Plants were grown for a period of 6 months during which they were exposed to ambient fluctuations in temperature and relative humidity, but were provided ample water via individual watering pans placed beneath each pot. 94.4% of seeds germinated and survived through the experiment's duration. Sample sizes of surviving plants in each treatment, which were used in all statistical tests for our shadehouse experiment, are available in Table S3.

Following the six-month growing period, plants were harvested by removing them from the potting soil and rinsing excess soil from root surfaces with distilled water. Each plant was then dissected into root, nodule, stem, and leaf fractions. Each tissue component was dried at 60°C to constant mass (approximately 3 days) and massed.

Calculating $\%N_{dfa}$ – We calculated the percent of a plant's N derived from N fixation ($\%N_{dfa}$) for each individual using a three end-member mixing model: one end member for the isotopic signature of soil-derived N, one for the isotopic signature of atmospherically fixed N, and one for the fraction of plant N derived from the seed. Our calculation accounted for variation around each end member. Because we added a highly isotopically enriched ^{15}N tracer to the growing medium, we present ^{15}N data as atom percent, representing the percent of N atoms in a sample that are ^{15}N rather than ^{14}N (as opposed to the per mil notation that is common for natural abundance levels of isotopes).

We calculated the isotopic signature of the soil N end member by estimating N that naturally mineralized in the soil used in our potting mixture, any non-isotopically enriched N fertilizer added to the pot, and the isotopically enriched N fertilizer added. Although the soil N end member is often estimated using a reference plant (Chalk 1985), some of the known problems with the reference plant method (Chalk 1985) made it unviable in our study. Specifically, substantial differences in the root distributions and particularly seed size between our study plants and reference plants, along with relatively well-known amounts and isotopic signatures of N additions to each pot, meant that estimating the isotopic signature of the soil N end member directly gave a better measure than using a reference plant. Mineralized N was estimated for the amount of forest-derived soil added to each pot using the mean and standard deviations of N mineralization rates from (Brookshire et al. 2012) for neotropical forests and

asymbiotic N fixation from (Reed et al. 2011) to randomly generate a series of 10,000 normally distributed N mineralization values for each pot. Sensitivity analyses using ± 50% of these literature values showed no greater than a 2.5 $\%N_{dfa}$ change in any treatment, suggesting our results were insensitive to variation in these values. Each pot then received a total of 0.51 g N m^{-2} yr^{-1} of 98% ^{15}N tracer. The amount of non-isotopically enriched fertilizer varied by N treatment: 0, 20, and 40 g N m^{-2} yr^{-1} for low, medium, and high N, respectively. The isotopic signature of soil N ($\%^{15}N_{soil}$) from each pot was then calculated as follows:

$$\%^{15}N_{soil} = \Big((0.003663 \times f_{min}) + (0.98 \times f_{iso}) + (0.003663 \times f_{fert})\Big) \times 100$$

where f_{min}, f_{iso}, and f_{fert} are the fraction of soil N coming from mineralization, isotopically enriched fertilizer, and non-isotopically enriched fertilizer. This resulted in a distribution of 10,000 values of $\%^{15}N_{soil}$ for each pot to account for uncertainty in soil N mineralization rates.

We used an isotopic signature of 0.3663 atom % for the atmospherically fixed N end member. Variation for this end member is likely to be very small on the scale of enriched isotopes(Menge et al. 2015). Therefore, for each pot we randomly generated 10,000 $\%^{15}N_{fixation}$ values normally distributed with a mean of 0.3663 and a standard deviation of 0.01 (equivalent to 27.5‰ in $\delta^{15}N$ notation). Our results were insensitive to variation in standard deviation values around this end member ranging from 0.005 to 0.05 (13.8‰ to 137.2‰ in $\delta^{15}N$ notation).

Fraction of Plant N Derived from Seed – The large seeds of *P. macroloba* (mean = 6.15 g for plants used in this study) mean that a substantial amount of N within our study plants comes from seed reserves – especially for the plants grown in low- and medium-light conditions where final total plant biomass was often similar to the original seed biomass (explained in detail below). To estimate the proportion of a plant's N derived from the seed (Extended Data Table 1), we used a two-step process. To calculate the original seed dry mass, we used a conversion factor

for wet mass to dry mass of seeds, which we derived from a linear model of wet and dry seed masses of 36 *P. macroloba* seeds collected along with the seeds used for our study plants. However, the entire mass of a seed is not incorporated into a plant, so we then subtracted out the amount of seed mass that wasn't used by the growing seedling. To do this, we collected, dried, and massed the seed material for each plant remaining in the pot at the end of the experiment.

We then subtracted this unused fraction of the seed mass from the total dry seed mass and multiplied this potentially-used seed mass by the N concentration of *P. macroloba* seeds (3.359% obtained by from elemental analysis of 36 seeds collected at the same time as seeds used in our study) to estimate the amount of seed N that was potentially used by each plant. We divided this seed-derived N by the total N contained in each plant to calculate the fraction of seed-derived N in the plant (f_{seed}). For several of our smallest plants, this fraction of potentially seed-derived N exceeded 1, which is impossible (a plant cannot get > 100% of its N from seed). The minimum $\%^{15}N$ value for any plant in our study was 0.383% (well above the natural abundance range; equivalent to $\delta^{15}N = 46‰$) confirming that even our smallest plants did not derive all of their N from seed. For plants with an estimated $f_{seed} > 1$, we assumed that the majority of plant N was, in fact, derived from the seed, and thus we assigned these plants a value of 0.9 for f_{seed}. Sensitivity analyses showed that our results were qualitatively unaffected by varying this assigned value for f_{seed} between .83 and .999. We used 0.3663 atm % for the isotopic signature of seed-derived N ($\%^{15}N_{seed}$) because the seeds were not isotopically labeled.

$\%N_{dfa}$ Calculation – After generating distributions for each of the three end members ($\%^{15}N_{soil}$, $\%^{15}N_{fixation}$, and f_{seed}), we incorporated these end members into a mixing model to calculate the percent of each plant's total N derived from fixation ($\%N_{dfa}$) as follows:

$$\%N_{dfa} = \left(\frac{\%^{15}N_{samp} - (f_{seed} \times \%^{15}N_{seed}) - ((1 - f_{seed}) \times \%^{15}N_{soil})}{(\%^{15}N_{fixation} - \%^{15}N_{soil})}\right) \times 100 \quad (1)$$

where $\%^{15}N_{samp}$ is the isotopic signature of the *P. macroloba* seedling sample, f_{seed} is the fraction of plant N derived from seed, $\%^{15}N_{seed}$ is the isotopic signature of N derived from seed, $\%^{15}N_{soil}$ is the isotopic signature of the N derived from the soil, and $\%^{15}N_{fixation}$ is the isotopic signature of N derived from fixation. This calculation differs slightly from the $\%N_{dfa}$ equation used in (Menge et al. 2015) in that they defined $\%N_{dfa}$ as the percent of a plant's newly acquired N (post germination) whereas here we define $\%N_{dfa}$ as the percent of the plant's total N (including N derived from the seed). Because f_{seed}, $\%^{15}N_{soil}$, and $\%^{15}N_{fixation}$ were distributions of 10,000 values each, this calculation produced 10,000 values of $\%N_{dfa}$ for each plant. Mean and 95% confidence intervals were calculated from this distribution of $\%N_{dfa}$ for each plant to provide our estimate of N derived from fixation and the uncertainty around this estimate.

Statistical Analyses for Shadehouse Experiment – Although our shadehouse experiment was structured as an ANOVA design, it is not possible to incorporate end member variation into a standard ANOVA. We therefore used maximum likelihood models and information theory-based model comparison to achieve the same end as an ANOVA—testing for differences between treatment means—while staying true to the error structure of our data. Specifically, to incorporate error propagation from the 3-end member mixing model calculation of $\%N_{dfa}$ into our maximum likelihood models, we had the maximum likelihood model estimate the mean and standard deviation for $\%N_{dfa}$ in each treatment directly from the $\%^{15}N$ values for each end member of the mixing model (Menge et al. 2015). Furthermore, model comparison allows us to test only the treatment differences that are reasonable, vastly decreasing the number of possible tests and avoiding the need for corrected post-hoc comparisons.

The effects of light and soil N on each response variable were assessed using a series of at least four maximum likelihood models: 1) A null model fitting a single mean to all treatments,

2) a high-light model which fit an single mean for the low- and medium-light treatments and a different mean for high-light treatments, 3) a variation-in-high-light model which fit a single mean to low- and medium-light treatments and an individual mean for each high-light treatment, and 4) an individual-treatment model which fit means for each of the 9 experimental treatments. Additional models were tested based on variation between treatments and specific scientific questions for each response variable (Extended Data Table 2). We determined the best model for our data by comparing ΔAIC values (Anderson 2008).

Code Availability – All statistical code used to calculate and analyze N fixation from isotopic data will be made available upon request to the corresponding author.

Field Sampling

During the summer of 2017 we sampled 100 *P. macroloba* seedlings growing in natural forest understories exposed to varying levels of light and soil N availability. We sampled 20 seedlings from 5 sites each ranging in stand age from 20 yrs since abandonment to old-growth forest – each site adjacent to plots used in the Bosques long-term forest dynamics project (Chazdon et al. 2007), where we have studied the dynamics of adult *P. macroloba* (Menge and Chazdon 2016, Taylor et al. 2017). Seedlings 30–200 cm in height were haphazardly selected to obtain variation in light availability (it was not possible to assess soil N availability prior to sampling).

A hemispherical photograph was taken directly above the tallest leaf of each seedling to assess light availability. Each photograph was analyzed using Gap Light Analyzer software (Cary Institute, NY, USA) for the % Total Light Transmittance. Following photography, each seedling was extracted from the soil taking care to ensure that roots and nodules were not dislocated from the seedling during soil extraction. In cases where we thought it possible that

some roots or nodules were dislocated from the plant, this was noted, but no differences were found between analyses conducted with and without these potentially broken plants in the dataset. To measure soil N availability, we sampled ~5 g of soil directly from the rooting zone of each seedling. Soil samples were extracted in 2M KCl and analyzed for nitrate and ammonium on a Smartchem 170 discrete analyzer (Westco Scientific Instruments, CT, USA) at Columbia University. Following harvesting, we cleaned the root system of each seedling and removed all nodule material using forceps. Root and nodule material were dried and massed separately for each plant to calculate the % of belowground biomass that each plant allocated to nodule biomass.

Statistical Analyses for Field Sampling – Because field nodulation data typically contain many zeros and values > 0 are often lognormally distributed, we analyzed nodulation in field-sampled seedlings using models for zero-inflated lognormal data adapted from Tian & Wu(2006), which were then evaluated using Maximum Likelihood framework. This method predicts nodulation using a dual-process model where the probability of encountering a 0 (nodule presence vs. absence) and the mean of non-zero data (nodule mass when present) are modelled simultaneously. This takes the form of:

$$G(x,\mu,\sigma,\delta) = \begin{cases} \delta & if\ x = 0 \\ \delta + (1-\delta)\,F(x,\mu,\sigma) & if\ x > 0' \end{cases} \quad (2)$$

where x is the lognormal response variable (% belowground allocation to nodules), μ and σ are the mean and standard deviation of the response variable in log space, and δ is the probability of encountering a 0 value. $F(x,\mu,\sigma)$ is the lognormal cumulative distribution function of non-zero values. μ could either be a single value (for our null models) or vary in response to an independent variable such as light or soil N availability. This allowed us to calculate the predicted population geometric mean, M, as:

$$M = (1 - \delta) * e^{(\mu)} \quad (3)$$

where μ is the mean of the non-zero data in log space.

For each predictor variable – percent total light transmittance and soil N availability (ammonium + nitrate concentrations) – separate models were created in which nodulation did not vary with the predictor variable (null model), only the probability of nodulation varied with the predictor variable, only the mean value of non-zero data varied with the predictor variable, and where both the probability of nodulation and the mean of non-zero values varied according to the predictor variable. We tested these four model types for each predictor variable using the `bbmle` package for Maximum Likelihood tests in R statistical software (Bolker and R Development Core Team 2017, R Core Team 2017). We assessed differences between our models using the corrected Akaike Information Criterion (ΔAIC_c) (Anderson 2008) and present the difference in ΔAIC_c between our best and next best-fit models.

Supplementary Tables and Figures

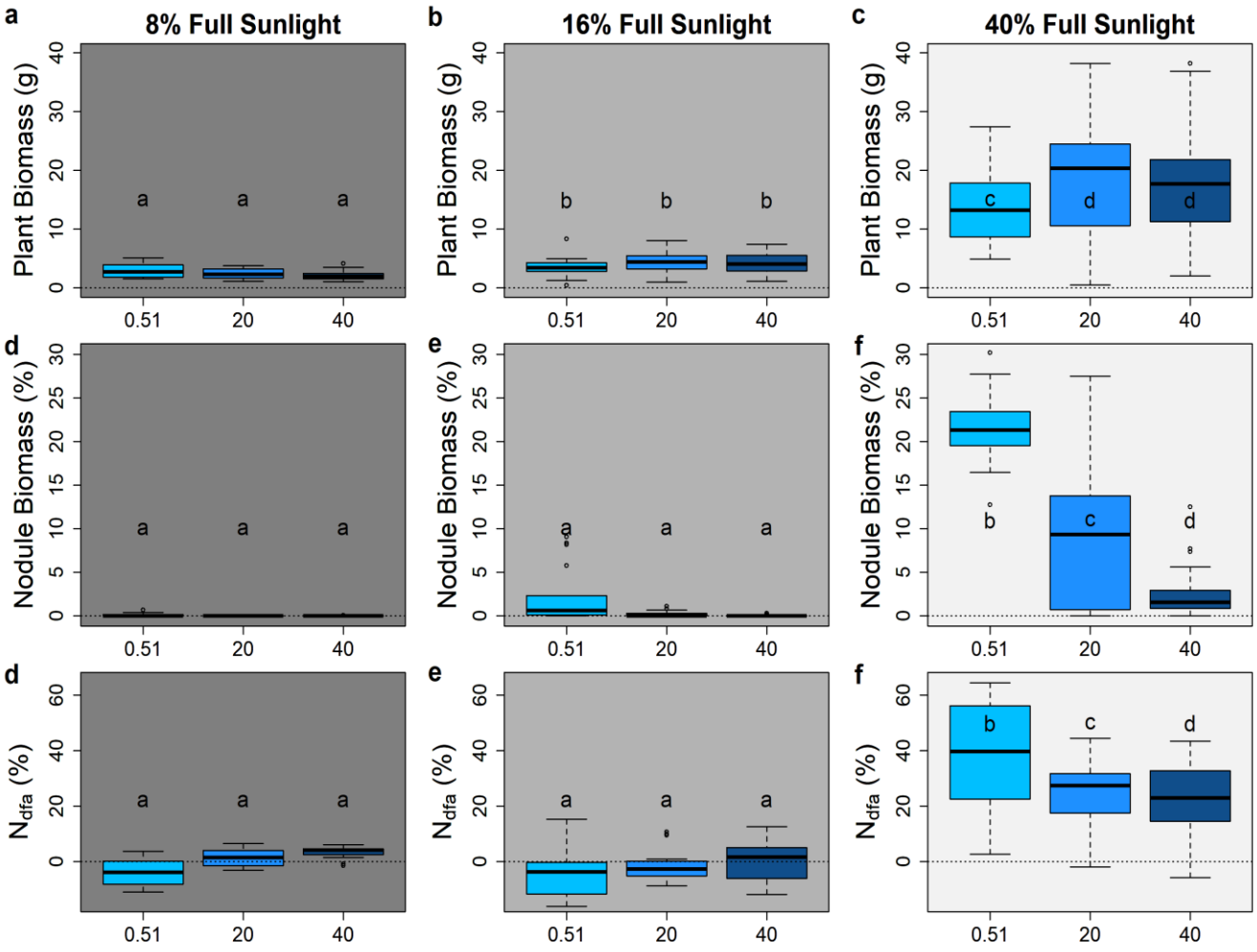

Extended Data Fig 1. **Light is a stronger driver than soil N for plant biomass and N fixation in shadehouse-grown plants**. Panels, response variables, and treatments are arranged as in Fig 1 of the main text. The center line on each bar represents the median of the data, with the first and third quartiles bounding the box. Whiskers extend to the range of the data up to 1.5 times the interquartile range from the edge of the box. Within each row, bars with different letters are statistically different. Corresponding Bar plots are available in Fig 1 of the main text.

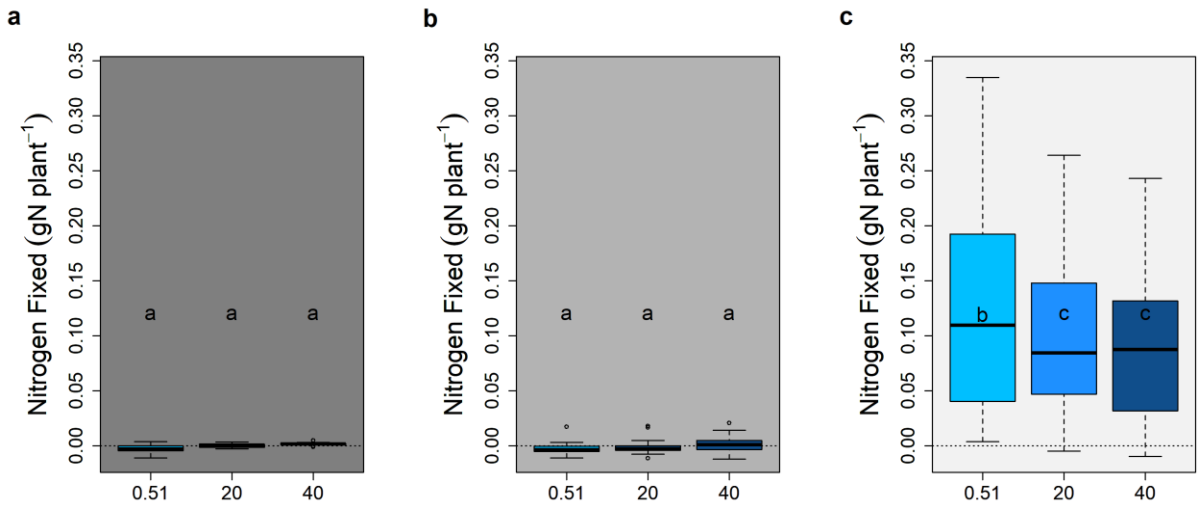

Extended Data Figure 2. Light drives total fixed N in plants more strongly than soil N. Panels, response variables, and treatments are arranged as in Fig 2 of the main text. The center line on each bar represents the median of the data, with the first and third quartiles bounding the box. Whiskers extend to the range of the data up to 1.5 times the interquartile range from the edge of the box. Within each row, bars with different letters are statistically different. Corresponding Bar plots are available in Fig 2 of the main text.

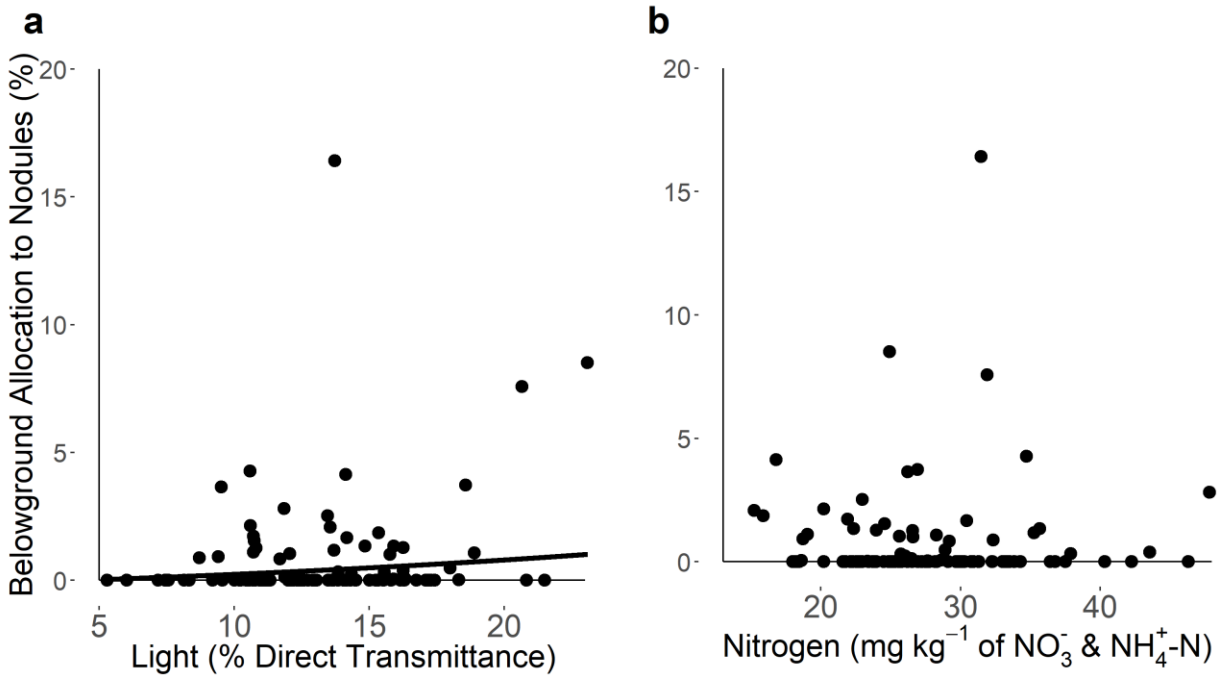

Extended Data Fig. 3. In-situ nodulation varies with light, but not soil N. **a,** Nodule biomass increased significantly with seedling light availability in 100 seedlings growing in the rainforest understory. **b**, However, nodule biomass did not vary significantly with soil N availability in these field sampled seedlings. Versions of these figures with log-scale y-axes are available in Figure 3.

Extended Data Table 1. Mean and Standard Deviation values of the fraction of plant N derived from seed (f_{seed}) for each light treatment.

Light Treatment	Mean	Standard Deviation
High Light	0.506	0.202
Medium Light	0.881	0.065
Low Light	0.900	0.000

Extended Data Table 2. Summary table of Maximum Likelihood model comparison for our shadehouse experiment. Model names indicate the differences in means tested by that model using a letter for each of our 9 environmental treatments from left to right corresponding to Figures 1 and 2. Each model fitted different means for each unique letter in the model. ΔAIC values for each model are reported, and the best fit model for each environmental treatment is indicated in bold.

Response Variable	Model	ΔAIC
Plant Biomass	aaa-aaa-aaa	162.07
	aaa-aaa-bbb	11.25
	aaa-aaa-bcc	0.45
	aaa-aaa-bcd	2.45
	aaa-bbb-ccc	10.98
	aaa-bbb-cdd	**0**
	abc-def-ghi	9.41
Allocation to Nodules	aaa-aaa-aaa	114.71
	aaa-aaa-bbb	37.83
	aaa-aaa-bcc	12.28
	aaa-aaa-bcd	**0**
	aaa-aaa-bca	5.51
	aaa-baa-cdb	3.57
	aaa-baa-cde	1.95
	abc-def-ghi	9.95
$\%N_{dfa}$	aaa-aaa-aaa	123.31
	aaa-aaa-bbb	6.97
	aaa-aaa-bcc	**0**
	aaa-aaa-bcd	1.99
	abc-def-ghi	8.95
N Fixed per Plant	aaa-aaa-aaa	120.43
	aaa-aaa-bbb	3.20
	aaa-aaa-bcc	**0**
	aaa-aaa-bcd	1.01
	abc-def-ghi	10.95

Extended Data Table 3. Sample sizes for each shadehouse experimental treatment. Slight differences in sample sizes between treatments are the result of plant mortality during the experimental growth period. Sample sizes apply to all statistical tests conducted in our shadehouse experiment.

Experimental Treatment	Sample Size (Individuals
Low Light, Low N	18
Low Light, Medium N	17
Low Light, High N	16
Medium Light, Low N	17
Medium Light, Medium N	20
Medium Light, High N	19
High Light, Low N	20
High Light, Medium N	19
High Light, High N	19

APPENDIX 3: SUPPLEMENTARY INFORMATION FOR CHAPTER 3

Table S1. Percent of total biomass allocated to each tissue pool for each plant fixer type in each environmental (Light and Nitrogen) treatment. Mean allocation to each tissue pool is shown as a percent of total plant biomass (± 1 S.E.).

Fixer Type	Light	Nitrogen	Leaf (%)	Stem (%)	Root (%)	Nodule (%)
Active	High	High	34.65 (3.16)	40.29 (2.11)	24.36 (1.36)	0.7 (0.21)
Active	High	Medium	38.03 (1.45)	35.84 (1.56)	23.69 (1.02)	2.44 (0.57)
Active	High	Low	41.13 (1.56)	31.4 (1.19)	21.65 (0.81)	5.81 (0.22)
Active	Medium	High	48.76 (1.25)	34.2 (1)	17.03 (0.59)	0.01 (0)
Active	Medium	Medium	47.61 (0.95)	34.94 (0.91)	17.42 (0.5)	0.03 (0.01)
Active	Medium	Low	41.81 (1.97)	35.89 (1.36)	21.81 (1.2)	0.49 (0.18)
Active	Low	High	46.25 (1.6)	33.89 (1.24)	19.86 (0.92)	0 (0)
Active	Low	Medium	41.41 (1.65)	38.79 (1.52)	19.8 (0.98)	0 (0)
Active	Low	Low	42.61 (1.19)	38.97 (1)	18.4 (0.55)	0.02 (0.01)
Inactive	High	High	33.08 (2.68)	39.1 (2.05)	27.82 (1.74)	0 (0)
Inactive	High	Medium	36.88 (2.83)	39.41 (2.01)	23.7 (1.89)	0.01 (0.01)
Inactive	High	Low	31.17 (2.21)	36.19 (2.16)	30.86 (1.69)	1.78 (0.55)
Inactive	Medium	High	50.35 (1.37)	31.08 (1.19)	18.57 (0.76)	0 (0)
Inactive	Medium	Medium	47.56 (2.61)	32.74 (2.19)	19.7 (1.2)	0 (0)
Inactive	Medium	Low	46.26 (1.35)	33.68 (1.2)	20.04 (0.77)	0.01 (0.01)
Inactive	Low	High	45.19 (0.95)	38.94 (1.23)	15.86 (1.35)	0.01 (0.01)
Inactive	Low	Medium	45.48 (1.71)	38.34 (0.99)	16.18 (1.85)	0 (0)
Inactive	Low	Low	40.41 (1.43)	39.77 (1.7)	19.82 (1.31)	0 (0)
Non-fixer	High	High	43.43 (3.14)	33.65 (1.4)	22.92 (2.04)	0 (0)
Non-fixer	High	Medium	44.84 (2.06)	32.76 (1.1)	22.4 (1.23)	0 (0)
Non-fixer	High	Low	32.23 (2.36)	34.25 (1.09)	33.52 (1.56)	0 (0)
Non-fixer	Medium	High	53.94 (1.31)	28.66 (0.76)	17.4 (0.87)	0 (0)
Non-fixer	Medium	Medium	54.74 (1.24)	28.29 (0.86)	16.97 (0.55)	0 (0)
Non-fixer	Medium	Low	43.91 (1.68)	32.88 (1.08)	23.22 (0.88)	0 (0)
Non-fixer	Low	High	54.29 (1.28)	30.36 (1.16)	15.35 (1.33)	0 (0)
Non-fixer	Low	Medium	52.14 (1.28)	30.6 (0.75)	17.26 (1.23)	0 (0)
Non-fixer	Low	Low	47.17 (1.44)	32.49 (0.79)	20.34 (1.32)	0 (0)

Table S2. Variables, model structures, and ΔAIC_c for all attempted models assessing biomass limitation for active N fixers, inactive N fixers, and non-fixers across our 9 environmental treatments. Model structures have a letter representing the mean in each different environmental treatment. The first, second, and third triplets of letters represent low-, medium-, and high-light groups, respectively. Within each triplet, low-, medium-, and high-N treatments are arranged left-to-right. Thus, letters are arranged in the same orientation from left-to-right as the bars in Figure 9 and similar figures. Different letters within a model indicate different means for those environmental treatments. For each set of variables, the best-fit model (lowest AIC_c) is in bold.

Variables (y vs. x)	Model	ΔAIC_c
Active N fixer Biomass vs. Environmental Treatment	aaa aaa aaa	106.51
	abc def ghi	16.44
	aaa bbb ccc	14.26
	aaa aaa bbb	12.17
	aaa aaa bcc	**0**
	abb abb abb	101.17
	abc abc abc	103.63
	abb cdd eff	7.36
	abb abb cdd	2.53
	aad bbb cdd	2.14
Inactive N fixer Biomass vs. Environmental Treatment	aaa aaa aaa	101.61
	abc def ghi	15.78
	aaa bbb ccc	2.22
	aaa aaa bbb	0.76
	aaa aaa bcc	**0**
	aaa aaa bcd	2.37
	abb abb abb	103.53
	abc abc abc	105.95
	abb cdd eff	6.79
	abb abb cdd	2.52
	aad bbb cdd	1.53
Non- fixer Biomass vs. Environmental Treatment	aaa aaa aaa	104.02
	abc def ghi	**0**
	aaa bbb ccc	5.83

aaa aaa bbb	11.61
aaa aaa bcc	9.03
abb abb abb	103.25
abc abc abc	102.57
abb cdd eff	7.66
abb abb cdd	10.69

Table S3. Variables, model structures, and ΔAIC_c for all attempted models comparing biomass and height between active N fixers, inactive N fixers, and non-fixers across our 9 environmental treatments. Model structures have a letter representing the mean of active N fixers, inactive N fixers, and non-fixers, respectively, from left-to-right. All environmental and competition treatments are pooled. Different letters within a model indicate different means were fit for those fixer types. For each set of variables, the best-fit model (lowest AIC_c) is in bold.

Variables (y vs. x)	Model	ΔAIC_c
Total Biomass vs. Fixer Type	a a a	65.65
	a b c	2.43
	a a b	**0**
Plant Height vs. Fixer Type	a a a	166.77
	a b c	1.01
	a a b	**0**

Table S4. Variables, model structures, and ΔAIC_c for all attempted models comparing biomass and height between active N fixers and inactive N fixers in our N-limited treatment (high-light, low-N). Model structures have a letter representing the mean of active N fixers and inactive N fixers, respectively, from left-to-right. All environmental and competition treatments are pooled. Different letters within a model indicate different means were fit for those fixer types. For each set of variables, the best-fit model (lowest AIC_c) is in bold.

Variables (y vs. x)	Model	ΔAIC_c
Total Biomass vs.	**a a**	**0**
P. Macroloba Fixer Type	a b	1.05
Plant Height vs.	**a a**	**0**
P. Macroloba Fixer Type	a b	2.29

Table S5. Variables, model structures, and ΔAIC_c for all attempted models comparing biomass and height between active N fixers and inactive N fixers in our high-light treatments. Model structures have a letter representing the mean of the response variable in low-, medium-, and high-N treatments in our high-light group, respectively. Letters with a ".a" or ".i" following them indicate different means were fit for active and inactive N fixers in that environmental treatment. For each set of variables, the best-fit model (lowest AIC_c) is in bold.

Variables (y vs. x)	Model	ΔAIC_c
Total Biomass vs. *P. Macroloba* Fixer Type and Environmental Treatment	a a a	3.77
	a b c	2.42
	a a b	**0**
	a.a a.i b.a b.i c.a c.i	9.21
	a.a a.i b c	4.33
	a b.a b.i c.a c.i	7.07
Plant Height vs. *P. Macroloba* Fixer Type and Environmental Treatment	a a a	2.81
	a b c	**0**
	a a b	0.56
	a.a a.i b.a b.i c.a c.i	7.00
	a.a a.i b c	2.51
	a b.a b.i c.a c.i	4.26

Table S6. Variables, model structures, and ΔAIC_c for all attempted models assessing biomass limitation for active N fixers, inactive N fixers, and non-fixers across our 9 environmental treatments. Model structures have a letter representing the mean in each different environmental treatment biomass group assigned by the best-fit models in our non-competition biomass analyses (Table S2). Letters with ".C" or ".R" following them indicate that different means were fit to competition vs. reference plants for that group. For each set of variables, the best-fit model (lowest AIC_c) is in bold.

Variables (y vs. x)	Model	ΔAIC_c
Active N Fixer Biomass vs. Environmental and Competition Treatments	**a b c d**	**0**
	a.C a.R b.C b.R c.C c.R d.C d.R	9.25
	a.C a.R b.C b.R c d	5.36
	a b c.C c.R d.C d.R	3.39
	a b c.C c.R d	1.50
	a b c d.C d.R	1.78
Inactive N Fixer Biomass vs. Environmental and Competition Treatments	**a b c d**	**0**
	a.C a.R b.C b.R c.C c.R d.C d.R	7.47
	a.C a.R b.C b.R c d	4.76
	a b c.C c.R d.C d.R	2.24
	a b c.C c.R d	0.95
	a b c d.C d.R	1.20
Non- Fixer Biomass vs. Environmental and Competition Treatments	**abcdefghi (no competition)**	**0**
	competition in all treatments	11.78
	a.C a.R b c.C c.R d.C d.R e.C e.R f g h.C h.R i	14.78
Active N Fixer Height vs. Environmental and Competition Treatments	**a b c d**	**0**
	a.C a.R b.C b.R c.C c.R d.C d.R	10.05
	a.C a.R b.C b.R c d	5.40
	a b c.C c.R d.C d.R	4.15
	a b c.C c.R d	2.34
	a b c d.C d.R	1.70
	a b c d e.C e.R*	1.32
Inactive N Fixer Biomass vs. Environmental and Competition Treatments	a b c d	2.74
	a.C a.R b.C b.R c.C c.R d.C d.R	5.95
	a.C a.R b.C b.R c d	5.78

	a b c.C c.R d.C d.R	2.57
	a b c.C c.R d	**0**
	a b c d.C d.R	5.21
	a b c d e.C e.R*	2.82
Non-fixer Biomass vs. Environmental and Competition Treatments	**abcdefghi (no competition)**	**0**
	competition in all treatments	25.64
	a.C a.R b c.C c.R d.C d.R e.C e.R f g h.C h.R i	14.20

*upon examining the data, we also fit a model with different means for competition effects only in our high-light, high-N treatment despite a lack of difference in the pooled height means for this treatment and our high-light, medium-N treatment.

Table S7. Variables, model structures, and ΔAIC_c for all attempted models assessing the ratio of aboveground to belowground biomass (AGB:BGB) for active N fixers, inactive N fixers, and non-fixers across our 9 environmental treatments. Models, AIC_c's, and significance are presented as in Table S2.

Variables (y vs. x)	Model	ΔAIC_c
Active N-fixer AGB:BGB vs. Environmental Treatments	aaa aaa aaa	60.34
	abc def ghi	7.37
	aaa bbb ccc	9.01
	aaa aaa bbb	6.62
	aaa aaa bcc	8.06
	abb abb abb	59.67
	abc abc abc	61.74
	abb cdd eff	**0**
	abb abb cdd	4.73
	abb cdd efe	0.92
Inactive N-fixer AGB:BGB vs. Environmental Treatments	aaa aaa aaa	44.77
	abc def ghi	7.74
	aaa bbb ccc	6.55
	aaa aaa bbb	11.61
	aaa aaa bcc	10.85
	abb abb abb	41.47
	abc abc abc	43.87
	abb cdd eff	0.87
	abb abb cdd	7.78
	abb cdd efe	**0**
Non-fixer AGB:BGB vs. Environmental Treatments	aaa aaa aaa	50.09
	abc def ghi	5.46
	aaa bbb ccc	22.52
	aaa aaa bbb	27.87
	aaa aaa bcc	19.75
	abb abb abb	28.64
	abc abc abc	30.04
	abb cdd eff	**0**
	abb abb cdd	4.02

Table S8. Variables, model structures, and ΔAIC_c for all attempted models assessing the total leaf area for active N fixers, inactive N fixers, and non-fixers across our 9 environmental treatments. Models, AIC_c's, and significance are presented as in Table S2.

Variables (y vs. x)	Model	ΔAIC_c
Active N-fixer Leaf Area vs. Environmental Treatments	aaa aaa aaa	57.56
	abc def ghi	9.80
	aaa bbb ccc	**0**
	aaa aaa bbb	1.12
	aaa aaa bcc	2.61
	abb abb abb	59.26
	abc abc abc	61.59
	abb cdd eff	2.43
	abb abb cdd	4.85
Inactive N-fixer Leaf Area vs. Environmental Treatments	aaa aaa aaa	48.92
	abc def ghi	10.65
	aaa bbb ccc	**0**
	aaa aaa bbb	7.83
	abb abb abb	48.59
	abb cdd eff	1.95
	abb abb cdd	8.04
Non-fixer Leaf Area vs. Environmental Treatments	aaa aaa aaa	48.56
	abc def ghi	**0**
	aaa bbb ccc	26.60
	aaa aaa bbb	38.98
	aaa aaa bcc	29.53
	abb abb abb	28.96
	abc abc abc	27.01
	abb cdd eff	13.21
	abb abb cdd	20.44

Table S7. Variables, model structures, and ΔAIC_c for all attempted models assessing the percent of total biomass allocated to leaf tissue for active N fixers, inactive N fixers, and non-fixers across our 9 environmental treatments. Models, AIC_c's, and significance are presented as in Table S2.

Variables (y vs. x)	Model	ΔAIC_c
Active N-fixer Percent Allocation to Leaf Area vs. Environmental Treatments	aaa aaa aaa	8.20
	abc def ghi	10.17
	aaa bbb ccc	7.68
	aaa aaa bbb	6.17
	aaa aaa bcc	6.79
	abb abb abb	8.21
	abc abc abc	9.52
	abb cdd eff	3.53
	abb abb cdd	**0**
	aab cdd eff	1.46
Inactive N-fixer Percent Allocation to Leaf Area vs. Environmental Treatments	aaa aaa aaa	54.33
	abc def ghi	8.32
	aaa bbb ccc	2.14
	aaa aaa bbb	7.05
	abb abb abb	52.68
	abb cdd eff	2.30
	abb abb cdd	4.64
	abb ccd efe	**0**
Non-fixer Percent Allocation to Leaf Area vs. Environmental Treatments	aaa aaa aaa	84.07
	abc def ghi	10.85
	aaa bbb ccc	44.22
	aaa aaa bbb	41.81
	aaa aaa bcc	26.34
	abb abb abb	53.82
	abc abc abc	56.20
	abb cdd eff	2.95
	abb abb cdd	**0**

Table S10. Variables, model structures, and ΔAIC_c for all attempted models assessing specific leaf area (SLA) for active N fixers, inactive N fixers, and non-fixers across our 9 environmental treatments. Models, AIC_c's, and significance are presented as in Table S2.

Variables (y vs. x)	Model	ΔAIC_c
Active N-fixer Specific Leaf Area vs. Environmental Treatments	aaa aaa aaa	90.95
	abc def ghi	14.95
	aaa bbb ccc	1.92
	aaa aaa bbb	**0**
	aaa aaa bcc	1.70
	abb abb abb	93.29
	abc abc abc	95.22
	abb cdd eff	8.15
	abb abb cdd	3.35
Inactive N-fixer Specific Leaf Area vs. Environmental Treatments	aaa aaa aaa	78.03
	abc def ghi	9.42
	aaa bbb ccc	2.02
	aaa aaa bbb	**0**
	aaa aaa bcc	1.98
	abb abb abb	80.25
	abc abc abc	80.63
	abb cdd eff	8.93
	abb abb cdd	4.50
	abb cdd efe	3.43
Non-fixer Specific Leaf Area vs. Environmental Treatments	aaa aaa aaa	122.05
	abc def ghi	8.65
	aaa bbb ccc	**0**
	aaa aaa bbb	2.26
	aaa aaa bcc	3.42
	abb abb abb	123.94
	abc abc abc	124.55
	abb cdd eff	6.10
	abb abb cdd	5.95

Table S11. Variables, model structures, and ΔAIC_c for all attempted models assessing total root length for active N fixers, inactive N fixers, and non-fixers across our 9 environmental treatments. Models, AIC_c's, and significance are presented as in Table S2.

Variables (y vs. x)	Model	ΔAIC_c
Active N-fixer Root Length vs. Environmental Treatments	aaa aaa aaa	122.38
	abc def ghi	11.43
	aaa bbb ccc	**0**
	aaa aaa bbb	17.00
	aaa aaa bcc	15.96
	abb abb abb	124.31
	abc abc abc	126.74
	abb cdd eff	2.81
	abb abb cdd	18.49
Inactive N-fixer Root Length vs. Environmental Treatments	aaa aaa aaa	115.77
	abc def ghi	7.45
	aaa bbb ccc	**0**
	aaa aaa bbb	11.22
	aaa aaa bcc	12.77
	abb abb abb	117.31
	abc abc abc	119.74
	abb cdd eff	2.47
	abb abb cdd	12.86
Non-fixer Root Length vs. Environmental Treatments	aaa aaa aaa	150.80
	abc def ghi	**0**
	aaa bbb ccc	13.51
	aaa aaa bbb	46.19
	aaa aaa bcc	41.63
	abb abb abb	148.09
	abc abc abc	147.46
	abb cdd eff	6.54
	abb abb cdd	40.34

Table S12. Variables, model structures, and ΔAIC_c for all attempted models assessing specific root length (SRL) for active N fixers, inactive N fixers, and non-fixers across our 9 environmental treatments. Models, AIC_c's, and significance are presented as in Table S2.

Variables (y vs. x)	Model	ΔAIC_c
Active N-fixer Specific Root Length vs. Environmental Treatments	aaa aaa aaa	27.32
	abc def ghi	9.05
	aaa bbb ccc	**0**
	aaa aaa bbb	23.64
	aaa aaa bcc	25.63
	abb abb abb	28.02
	abc abc abc	29.62
	abb cdd eff	4.14
	abb abb cdd	25.35
	aaa bbb ccd	1.65
Inactive N-fixer Specific Root Length vs. Environmental Treatments	aaa aaa aaa	4.39
	abc def ghi	9.84
	aaa bbb ccc	6.70
	aaa aaa bbb	5.89
	aaa aaa bcc	7.47
	abb abb abb	**0**
	abc abc abc	2.09
	abb cdd eff	6.52
	abb abb cdd	3.44
Non-fixer Specific Root Length vs. Environmental Treatments	aaa aaa aaa	9.71
	abc def ghi	12.18
	aaa bbb ccc	1.89
	aaa aaa bbb	**0**
	aaa aaa bcc	2.34
	abb abb abb	11.42
	abc abc abc	13.85
	abb cdd eff	7.67
	abb abb cdd	4.38

Table S13. Variables, model structures, and ΔAIC_c for all attempted models assessing root biomass, total belowground biomass, percent allocation to root mass, and percent allocation to belowground biomass between active and inactive N fixers with all environmental and competition treatments pooled. Models, AIC_c's, and significance are presented as in Table S2.

Variables (y vs. x)	**Model**	**ΔAIC_c**
Root Biomass vs.	**a a**	**0**
P. Macroloba Fixer Type	a b	2.04
Belowground Biomass vs.	**a a**	**0**
P. Macroloba Fixer Type	a b	2.31
Percent Allocation to Roots vs.	**a a**	**0**
P. Macroloba Fixer Type	a b	0.047
Percent Allocation Belowground vs.	**a a**	**0**
P. Macroloba Fixer Type	a b	2.08

Table S14. Variables, model structures, and ΔAIC_c for all attempted models assessing percent allocation to root mass and percent allocation to belowground biomass between active and inactive N fixers in our N-limited environmental treatment (high-light, low-N) with competition treatments pooled. Models, AIC_c's, and significance are presented as in Table S2.

Variables (y vs. x)	**Model**	**ΔAIC_c**
Percent Allocation to Roots vs.	a a	10.9
P. Macroloba Fixer Type	**a b**	**0**
Percent Allocation Belowground vs.	a a	2.09
P. Macroloba Fixer Type	**a b**	**0**

Table S15. Variables, model structures, and ΔAIC_c for all attempted models assessing percent allocation to nodule mass and percent N derived from fixation ($\%N_{dfa}$) between competition and reference plants of active N fixers in our high-light treatments. Null models are based on previous results from Chapter 2 (Fig. 9). Models, AIC_c's, and significance are presented as in Table S2.

Variables (y vs. x)	Model	ΔAIC_c
Active N-fixer Percent Allocation to Nodules vs. Competition Treatment	**a b b**	**0**
	a.C a.R b.C b.R	4.35
	a.C a.R b	1.91
Active N-fixer $\%N_{dfa}$ vs. Competition Treatment	a b b	0.02
	a.C a.R b.C b.R	1.95
	a.C a.R b	**0**

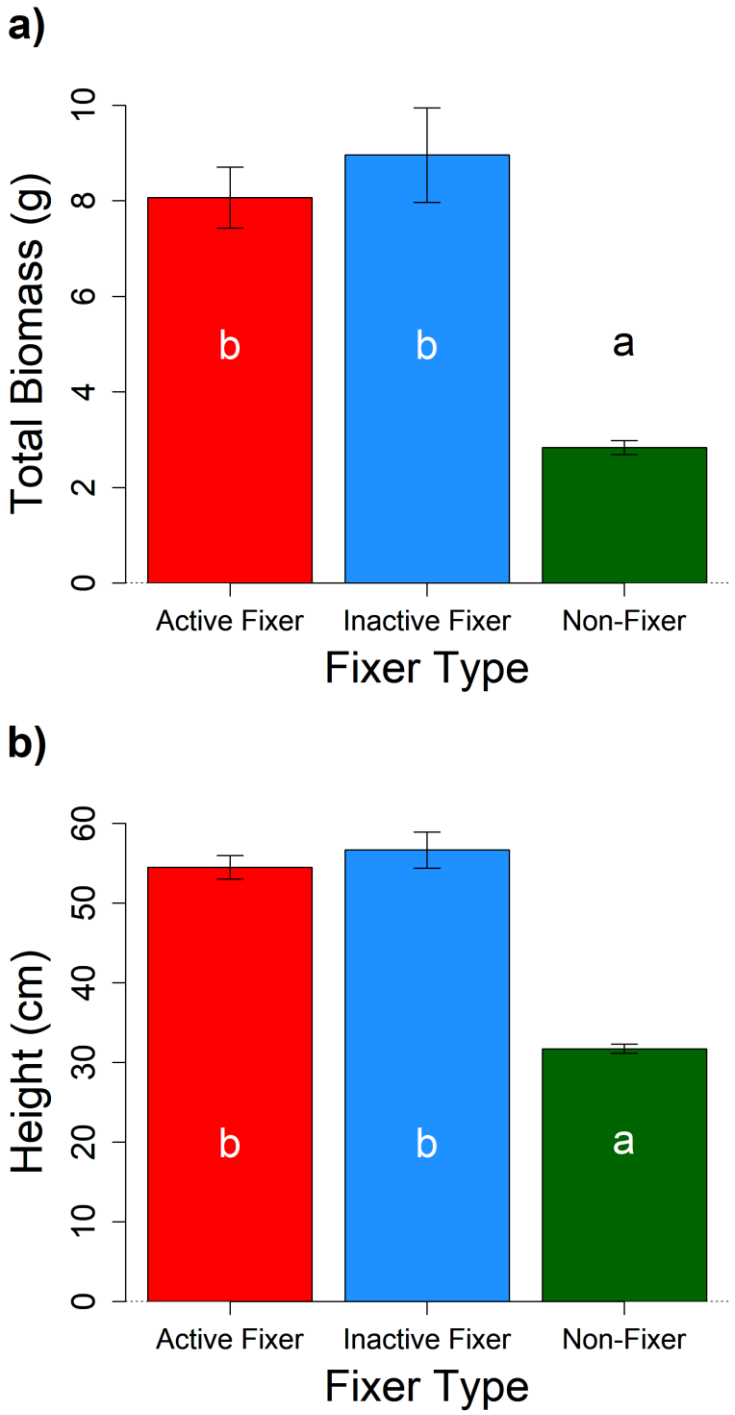

Figure S1. Total plant biomass (**a**) and height (**b**) for active N fixers (red), inactive N fixers (blue) and non-fixers (green). Bars for each fixer type in each panel represent all environmental and competition treatments pooled. Letters and error bars are as in Figure 9 of the main text.

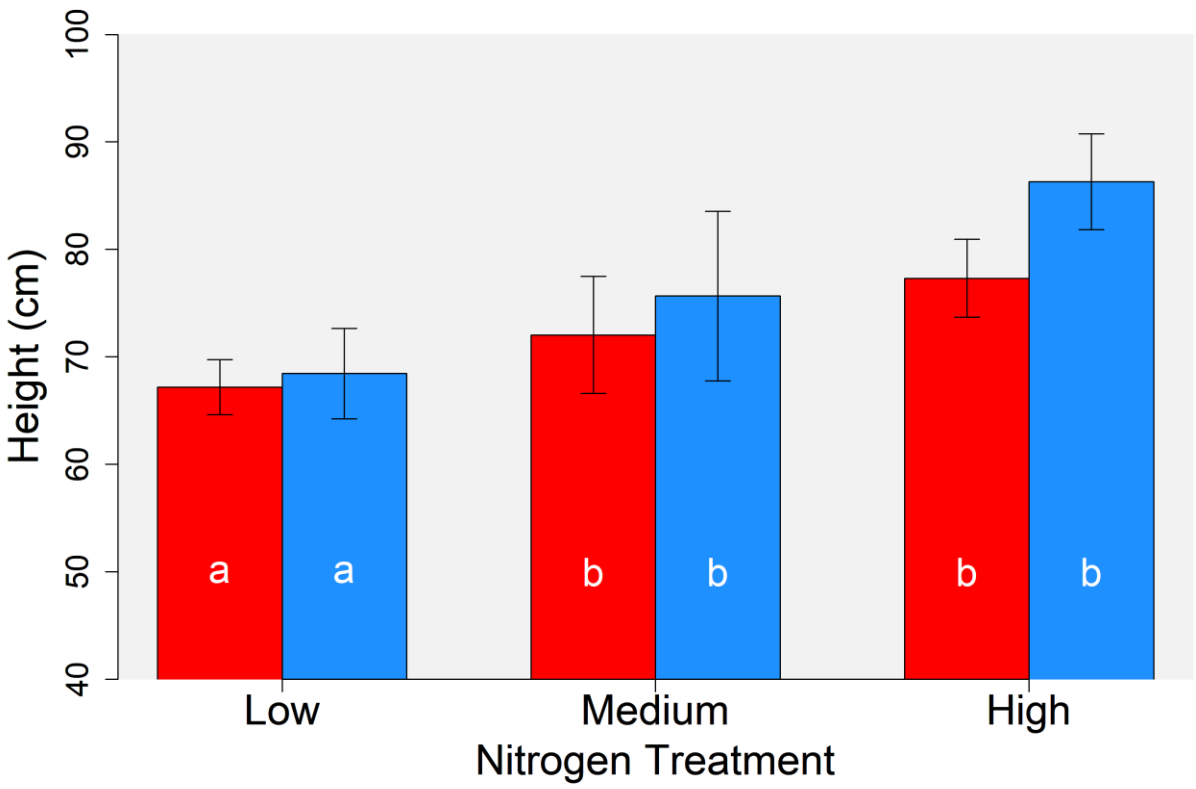

Figure S2. Comparison of height between high-light active (red) and inactive (blue) N fixers. Groups of bars represent each N treatment within our high-light group. Letters and error bars are as in Figure 9 of the main text.

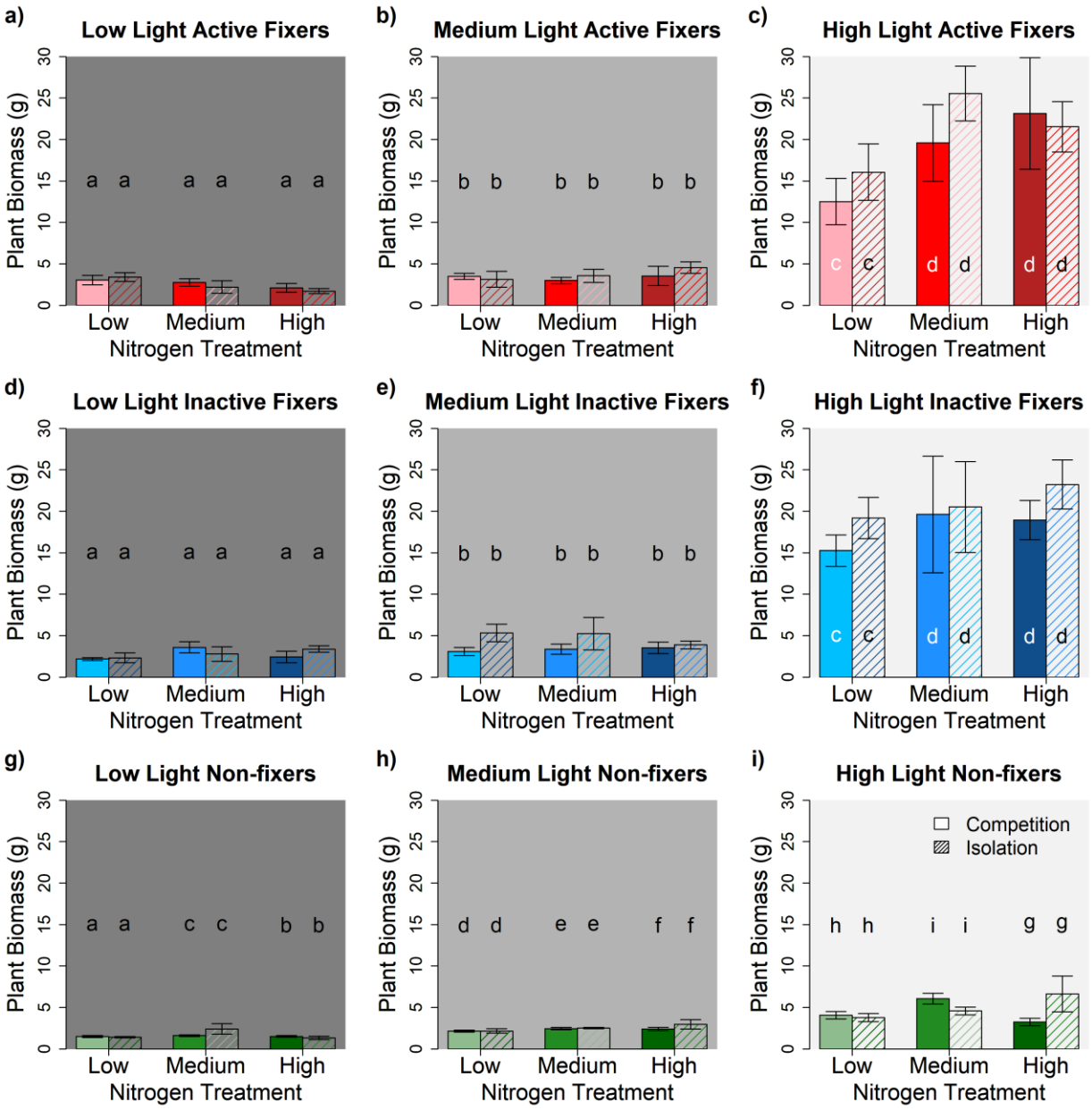

Figure S3. The effect of direct competition on total plant biomass for all fixer types and environmental treatments. Panels, colors, letters, and error bars are arranged as in Figure 9 of the main text. Solid bars represent plants grown with a competing plant in the same pot and hatched bars represent plants grown in isolation.

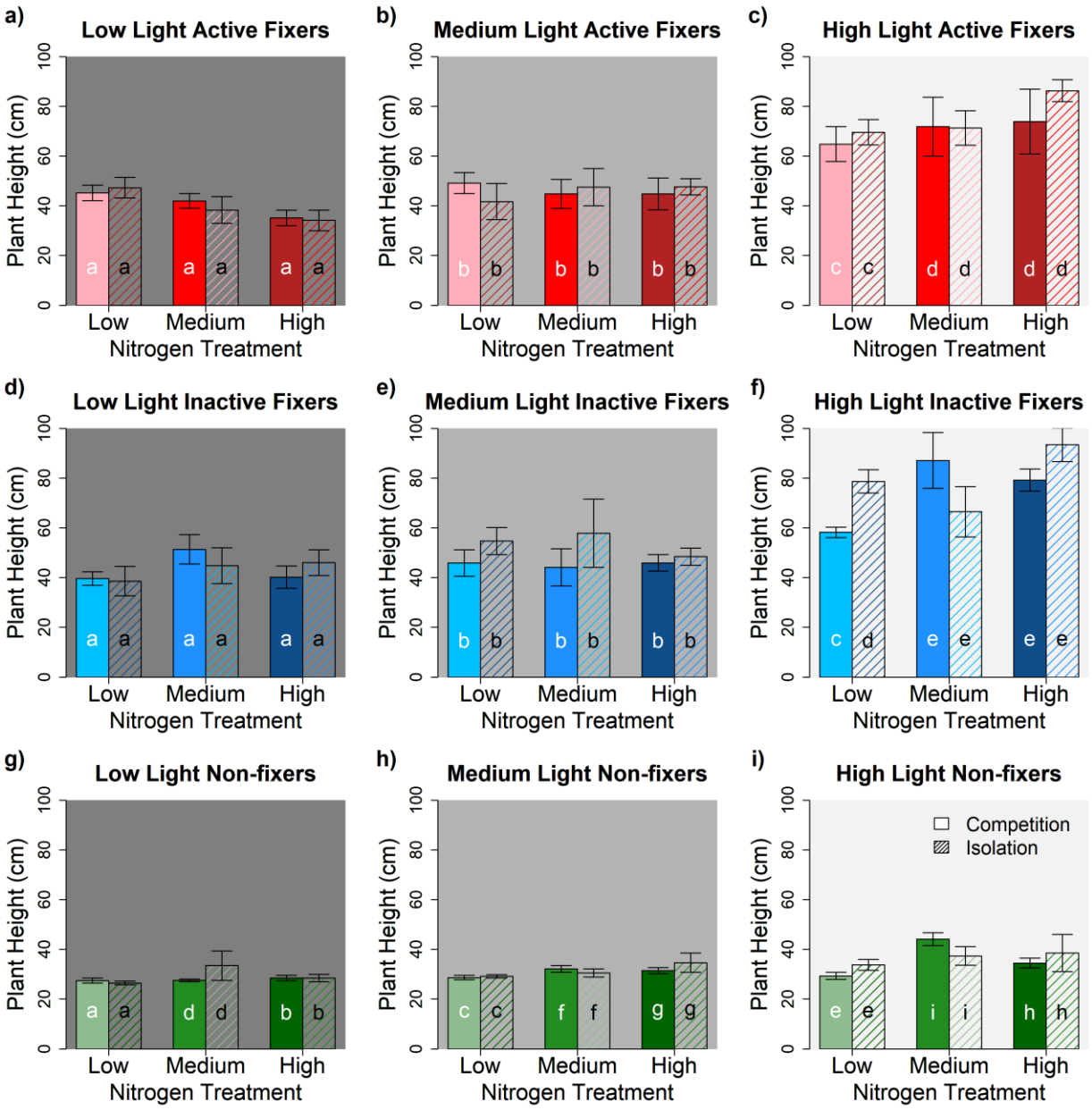

Figure S4. The effect of direct competition on height for all fixer types and environmental treatments. Panels, colors, letters, and error bars are arranged as in Figure 9 of the main text. Solid bars represent plants grown with a competing plant in the same pot and hatched bars represent plants grown in isolation.

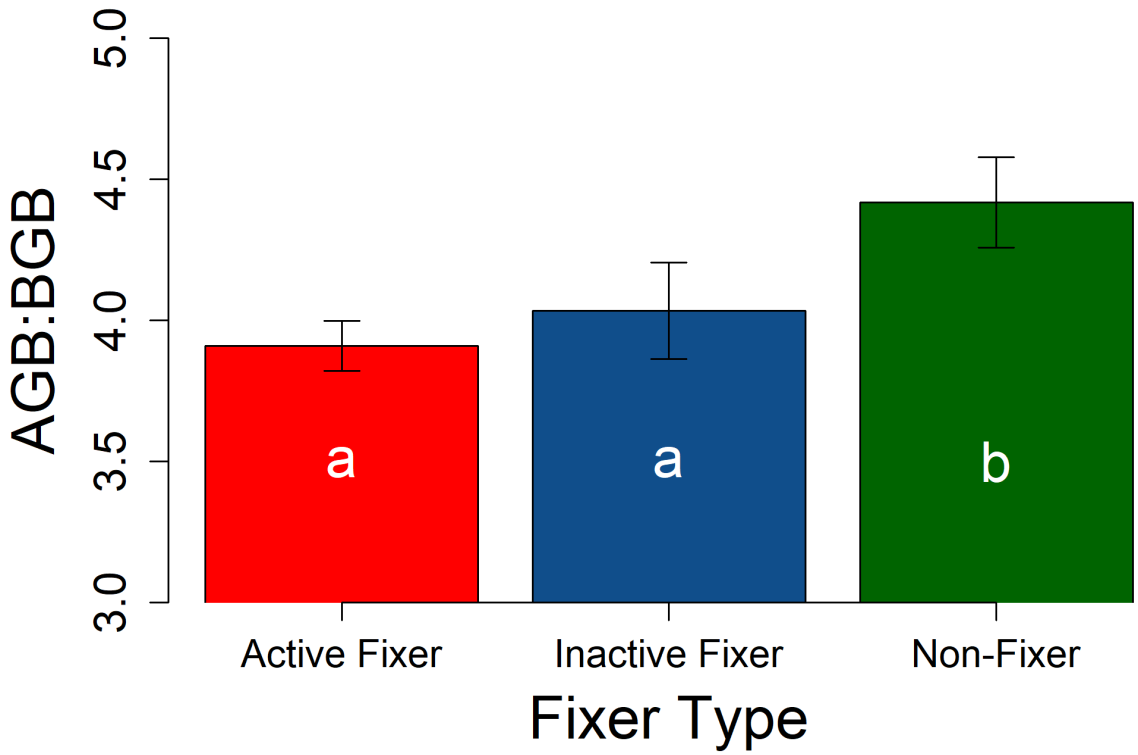

Figure S5. The ratio of aboveground to belowground biomass for each fixer type with all environmental and competition treatments pooled. Colors are as in Figure S1. Letters and error bars are as in Figure 9 of the main text.

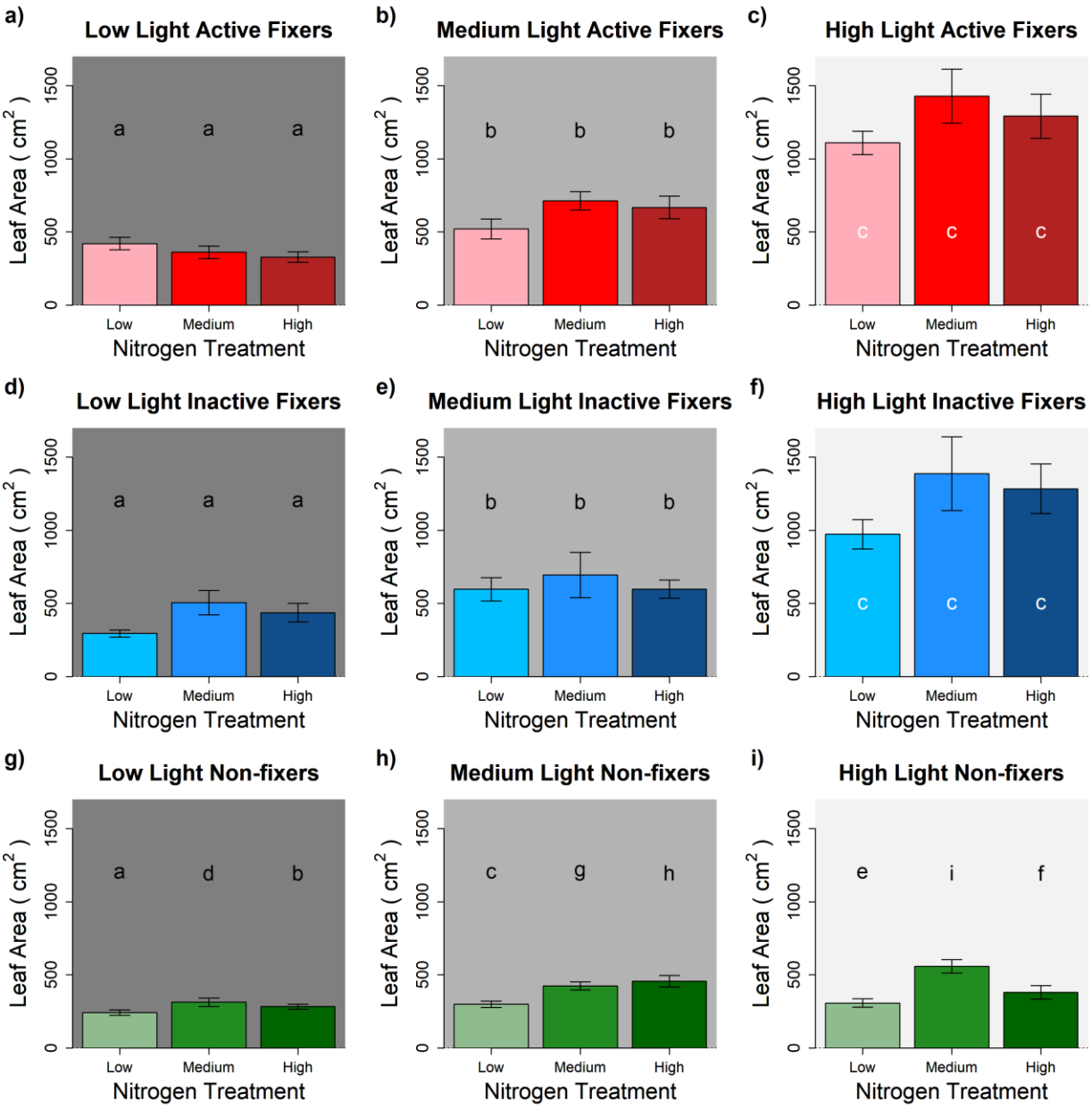

Figure S6. Total leaf area for all fixer types and environmental treatments. Panels, colors, letters and error bars are as in Figure 9 of the main text.

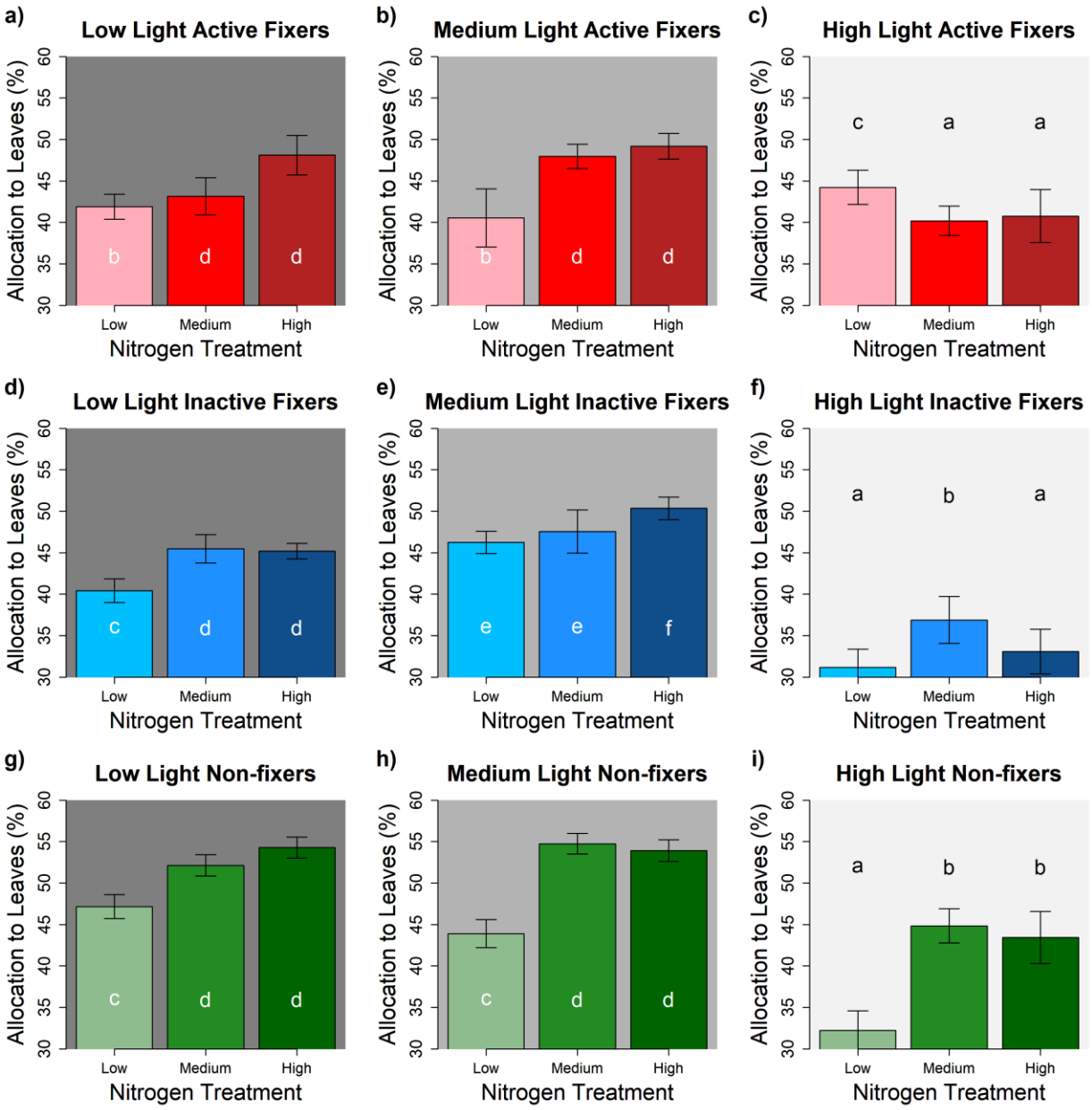

Figure S7. The percent of total biomass allocated to leaf tissue for all fixer types and environmental treatments. Panels, colors, letters and error bars are as in Figure 9 of the main text.

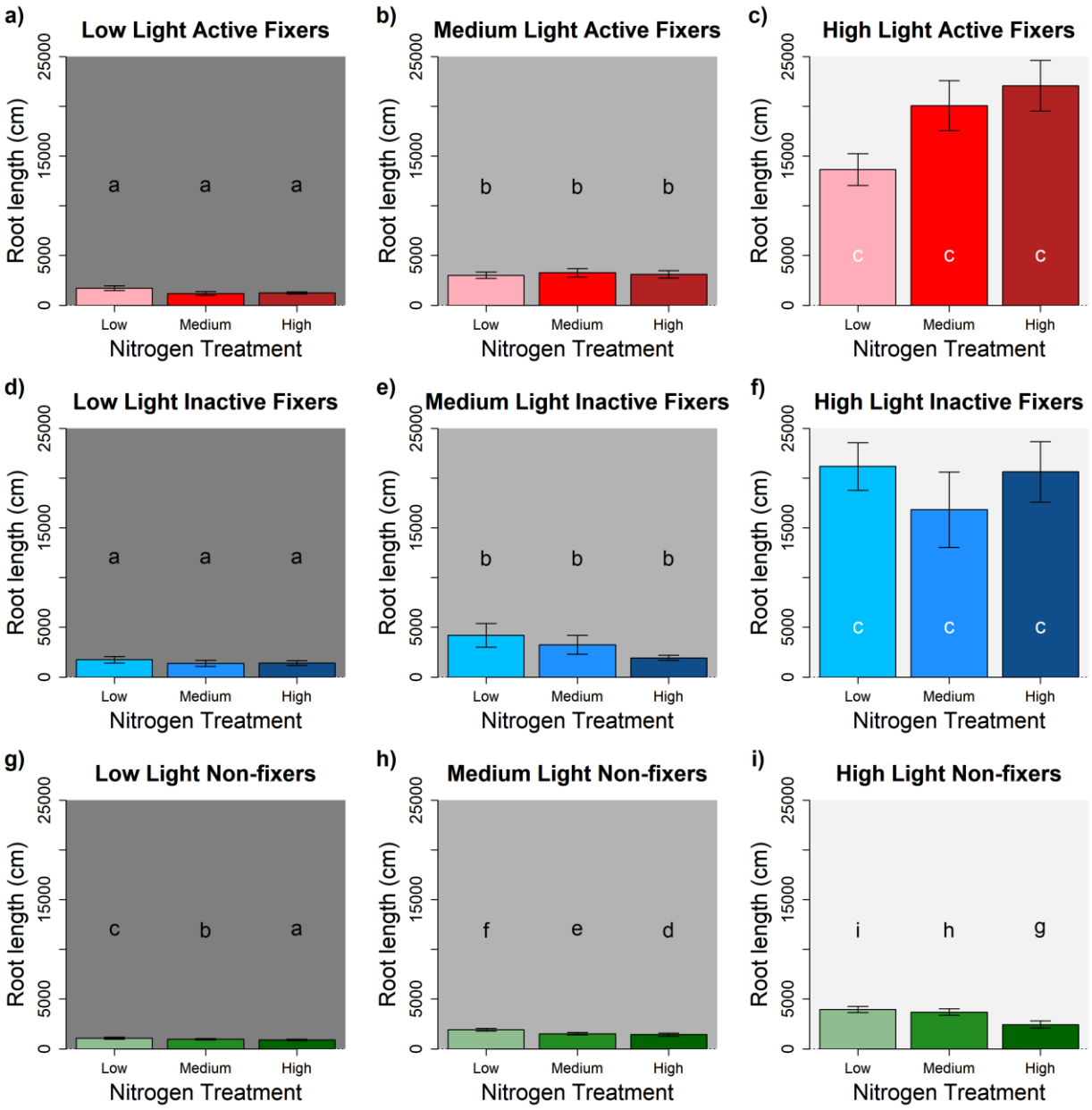

Figure S8. Total root length for all fixer types and environmental treatments. Panels, colors, letters and error bars are as in Figure 9 of the main text.

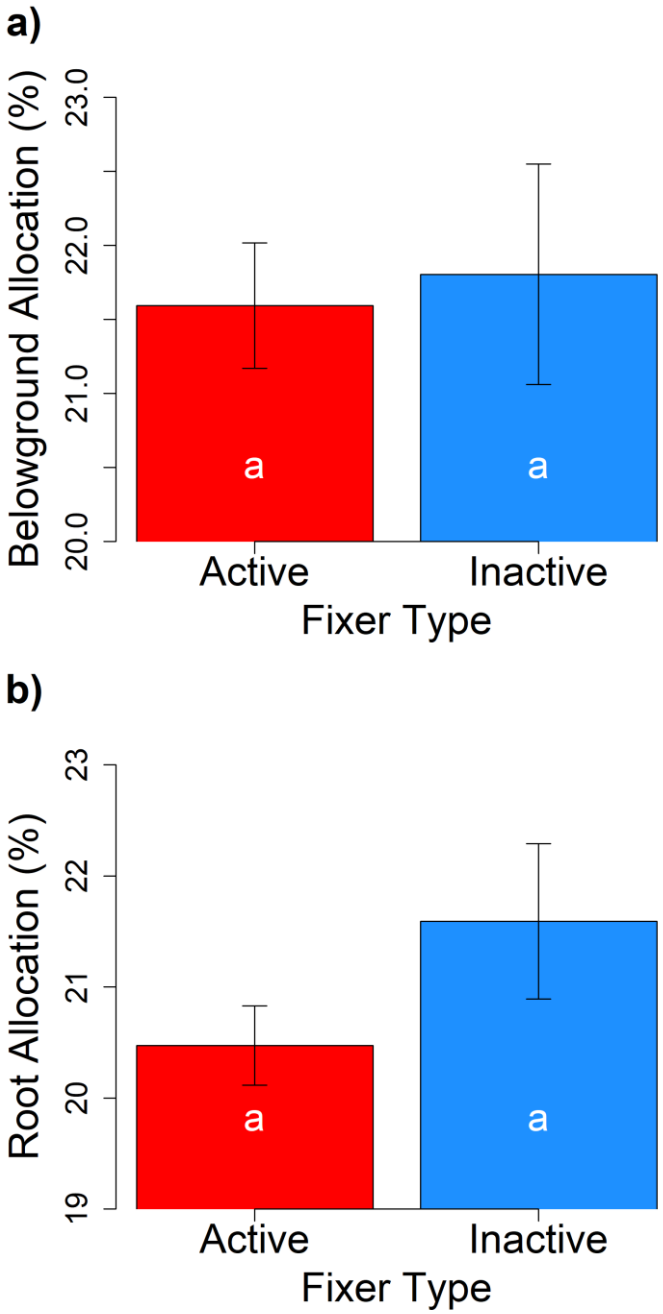

Figure S9. The percent of total biomass that active (red) and inactive (blue) N fixers allocate to **a)** all belowground tissue and **b)** root tissue. For each fixer type, all environmental and competition treatments are pooled. Letters and error bars are as in Figure 9 of the main text.

APPENDIX 4: SUPPLEMENTARY INFORMATION FOR CHAPTER 4

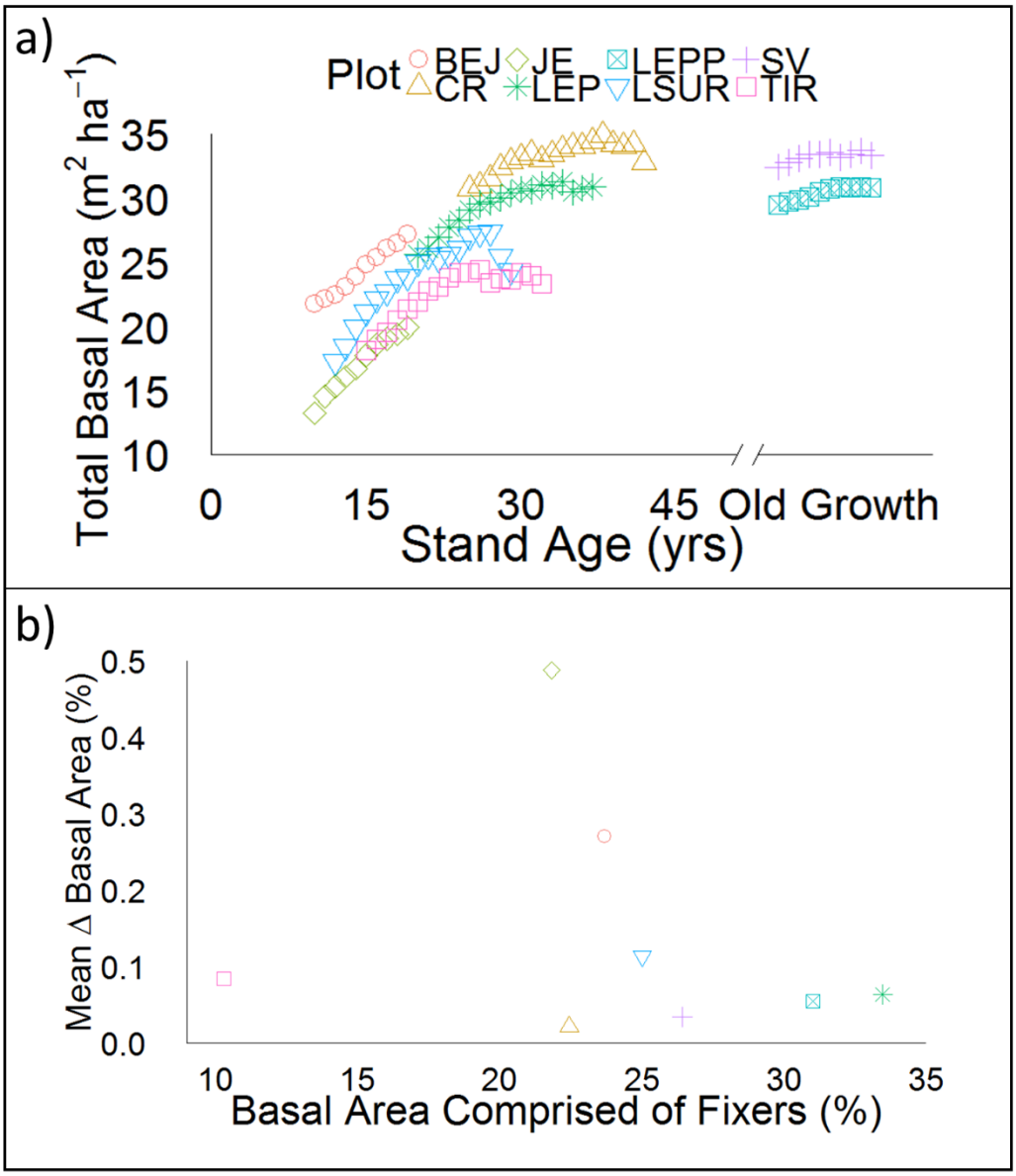

Figure S1. a) Summed basal area of each plot in each census year. b) The proportional change in the total basal area of a plot (change in basal area divided by the total basal area for each plot in each census period) averaged across the entire study duration for each plot plotted against the mean proportion of the plot's basal area comprised of N fixers.

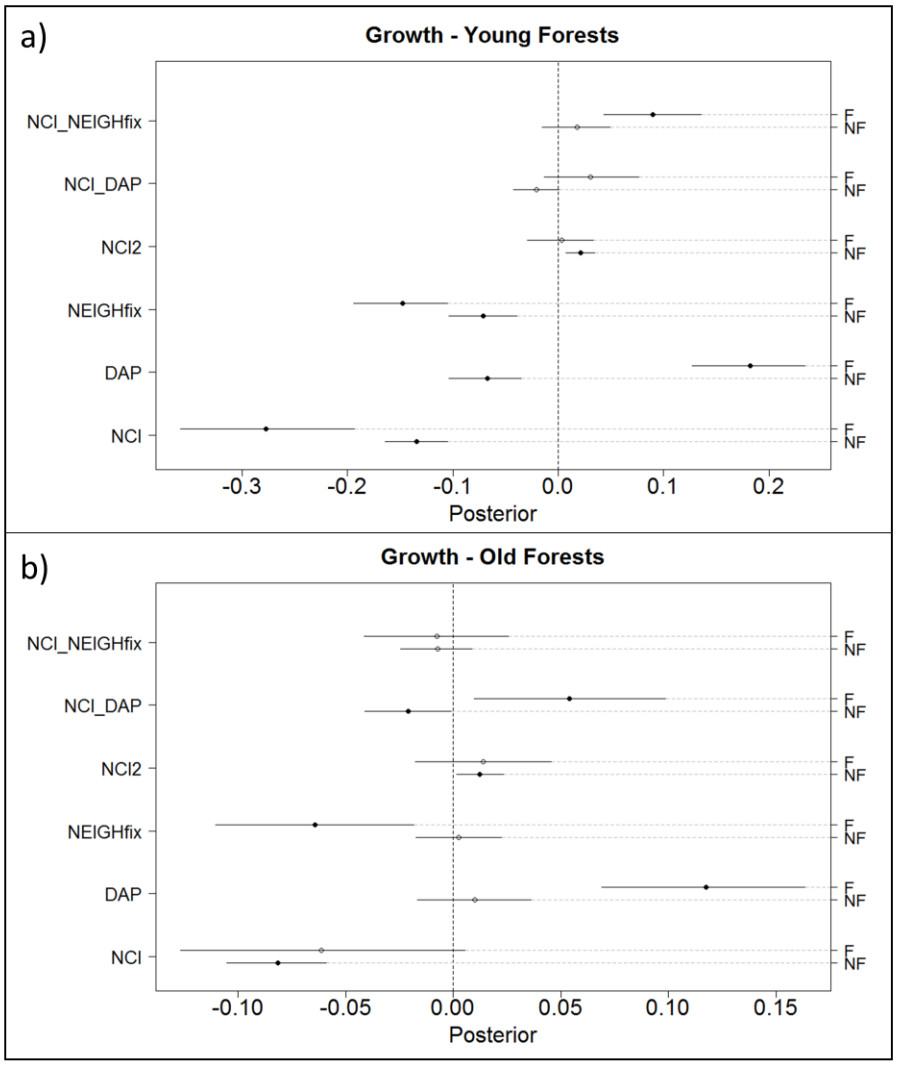

Figure S2. Parameter estimate plot for the effect of each model covariate (left axis) on the relative growth rate of N fixers and non-fixers (right axis) in forests a) ≤ 25 yrs, and b) > 25 yrs since disturbance. Covariates from bottom to top are NCI, DBH, the proportion of NCI comprised of N fixers (NEIGHfix), NCI^2, NCI x DBH, and NCI x the proportion of NCI comprised of N fixers. Dots represent the parameter estimate for each covariate with the 95% credible interval (CI) represented by solid lines on either side of the dot. Solid dots represent covariates for which the 95% CI does not overlap 0 (which we interpret as statistical significance), and open circles represent those covariates for which the 95% CI does overlap 0.

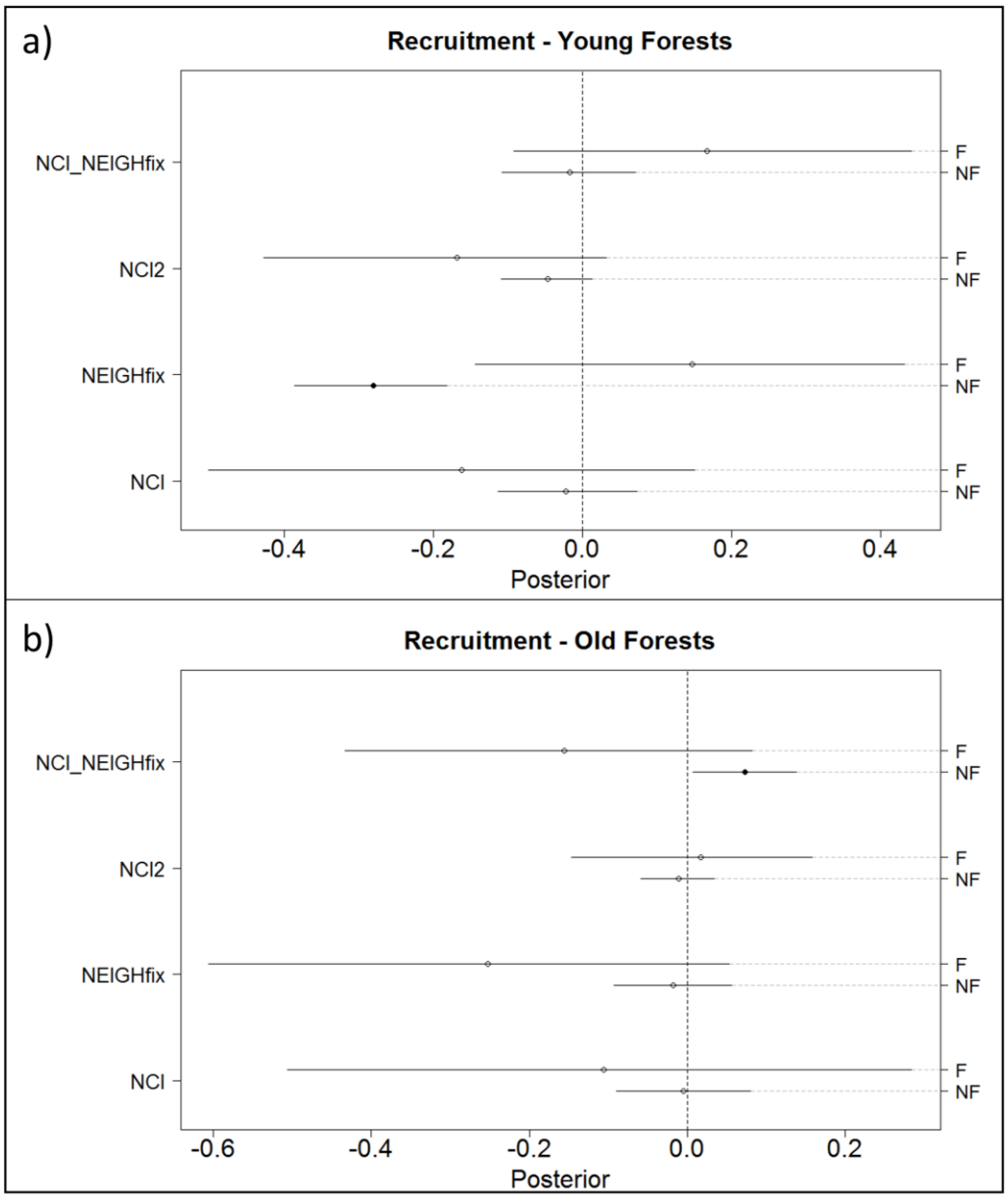

Figure S3. Parameter estimate plot for the effect of each model covariate (left axis) on the recruitment of N fixers and non-fixers (right axis) in forests a) ≤ 25 yrs, and b) > 25 yrs since disturbance. All covariates and symbols correspond to the description above in the caption for Figure S2.

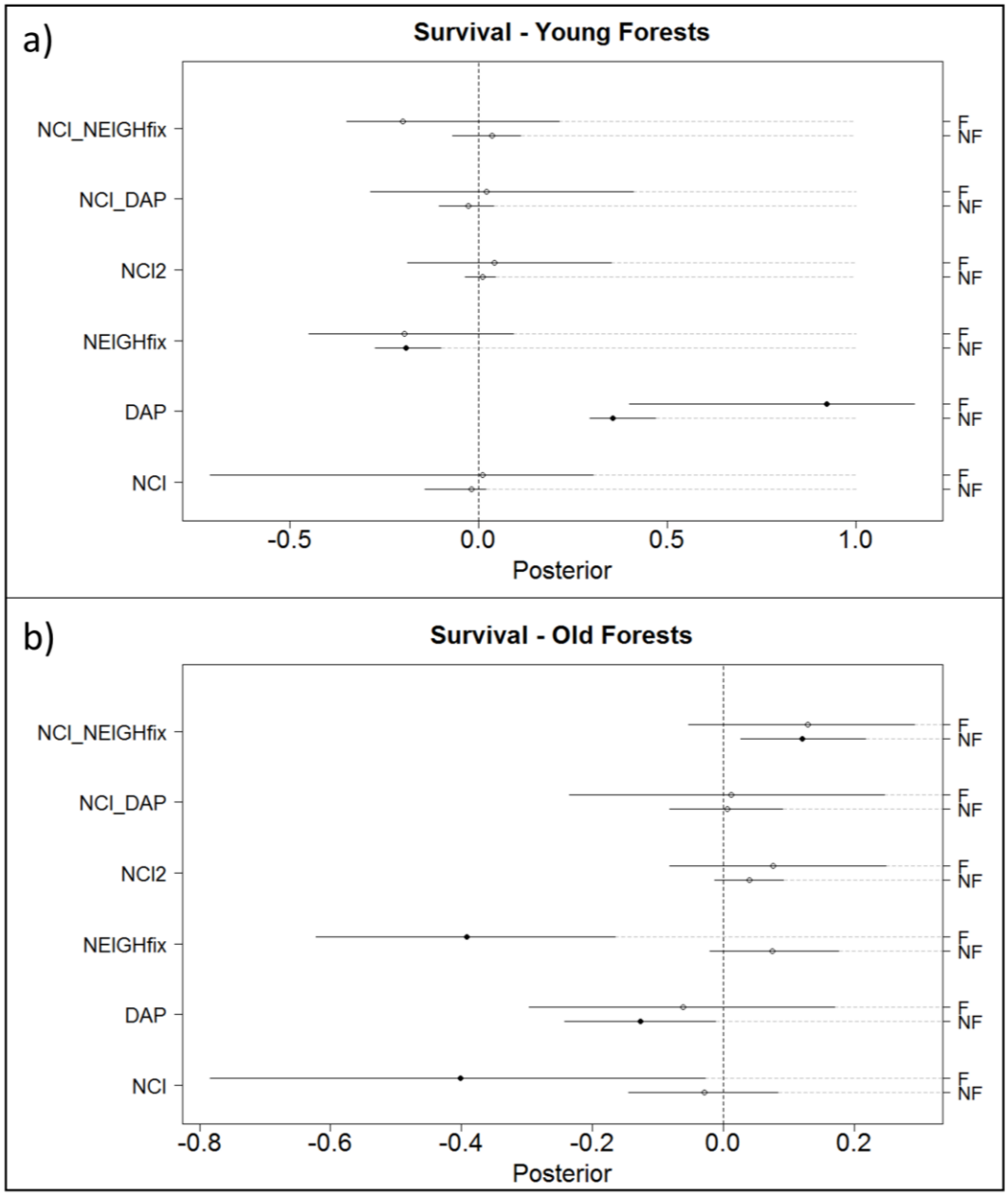

Figure S4. Parameter estimate plot for the effect of each model covariate (left axis) on the survival of N fixers and non-fixers (right axis) in forests a) ≤ 25 yrs, and b) > 25 yrs since disturbance. All covariates and symbols correspond to the description above in the caption for Figure S2.

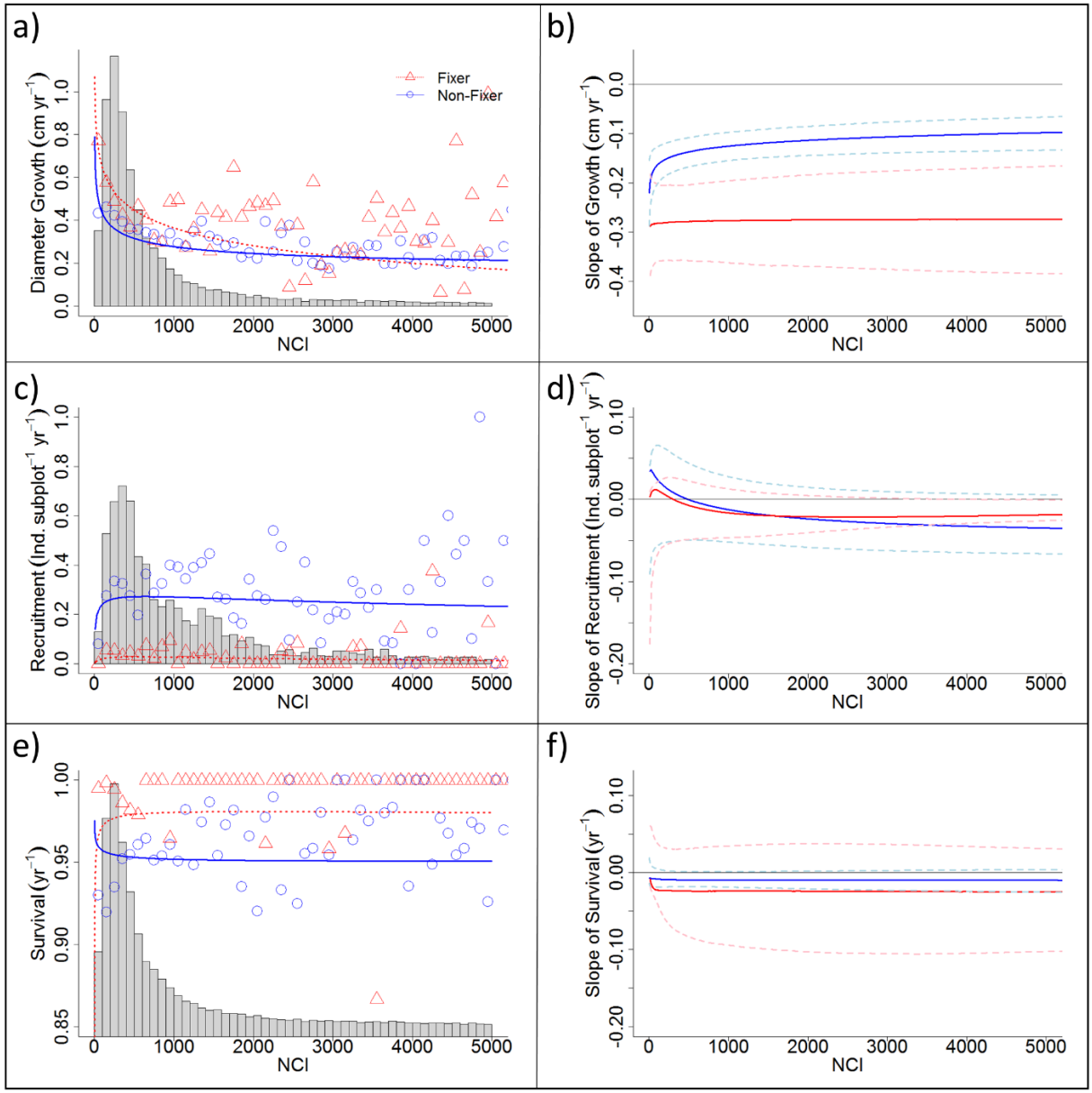

Figure S5. Effects of NCI on N fixers and non-fixers in young (≤ 25 yr) forests. Growth (a), recruitment (c), and survival (e) of N fixers (red) and non-fixers (blue) are plotted as a function of crowding (NCI). Each symbol represents an average of trees binned across 50 NCI units. Curves represent model fit means as a function of NCI, for an average DBH and proportion of NCI coming from N fixers. Histograms represent the relative data density in each proportion bin. Median slopes are shown for growth (b), recruitment (d), and survival (f) from posterior distributions of our individual-scale models. Dashed lines show 95% credible intervals (CI's) around the median. Where 95% CI's do not overlap 0 indicates that negative or positive effects of NCI are significant. Where 95% CI's for N fixers and non-fixers do not overlap each other indicates that NCI has significantly different effects on N fixers and non-fixers.

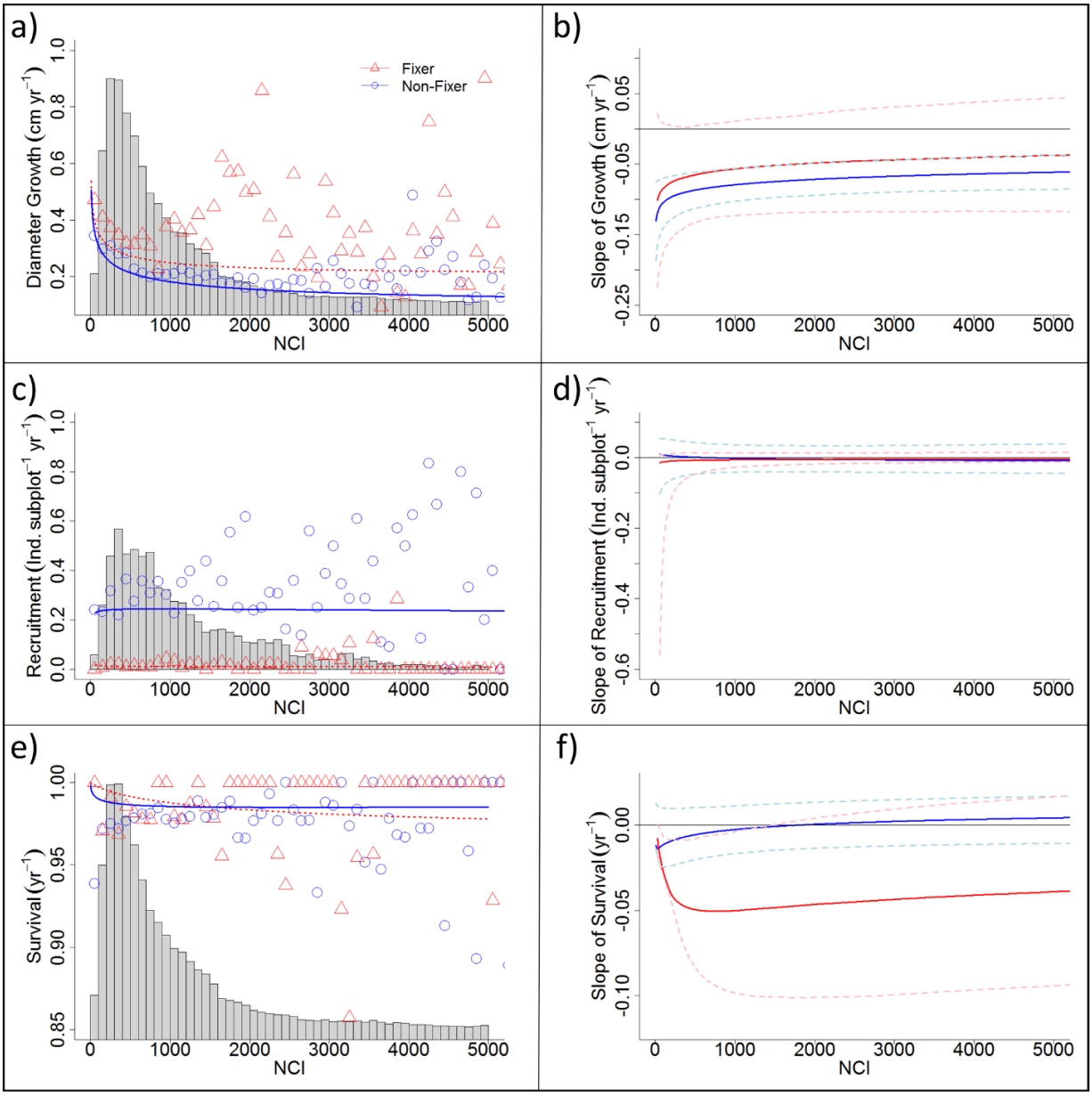

Figure S6. Effects of NCI on N fixers and non-fixers in old (> 25 yr) forests. Growth (a), recruitment (c), and survival (e) of N fixers (red) and non-fixers (blue) are plotted as a function of crowding (NCI). Each symbol represents an average of trees binned across 50 NCI units. Curves represent model fit means as a function of NCI, for an average DBH and proportion of NCI coming from N fixers. Histograms represent the relative data density in each proportion bin. Median slopes are shown for growth (b), recruitment (d), and survival (f) from posterior distributions of our individual-scale models. Colors and symbols are as in Fig S5.

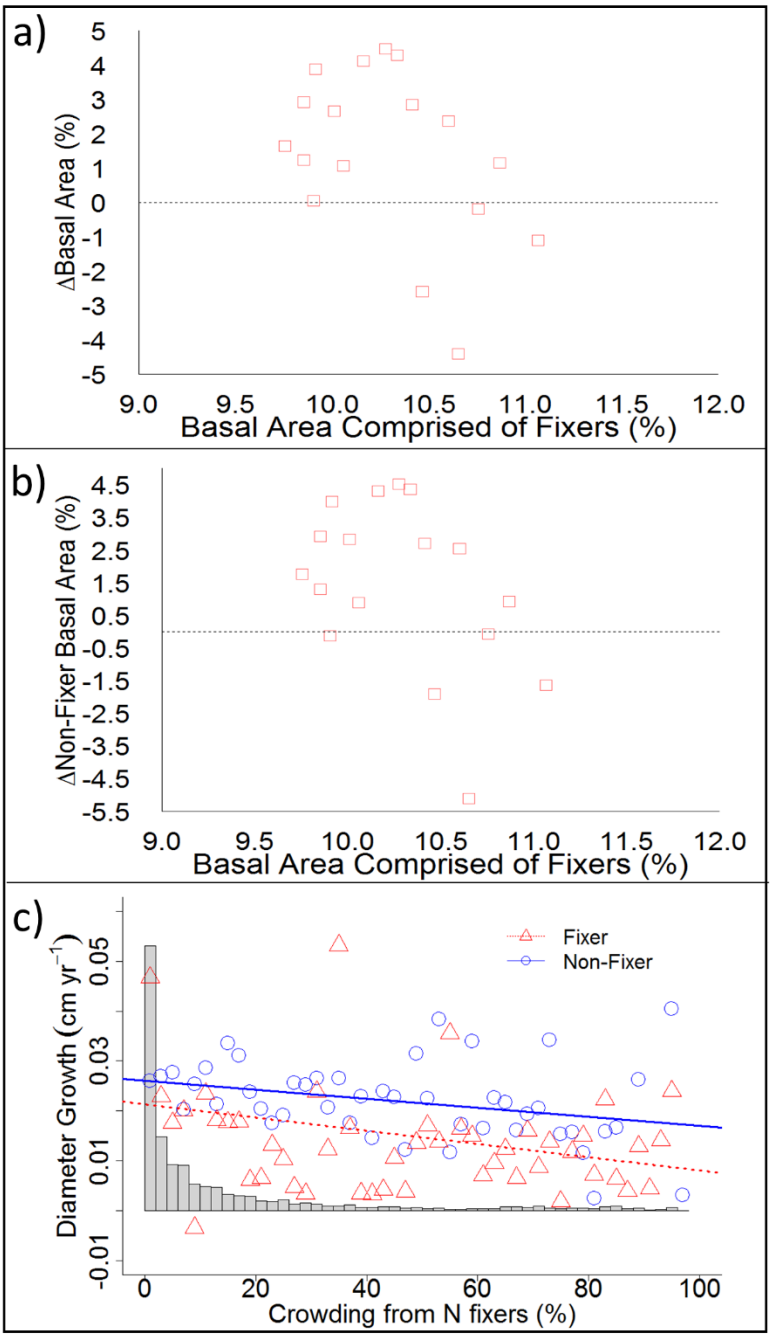

Figure S7. The effect of N fixers on plot- and individual-level growth in study plot TIR, which does not contain *Pentaclethra macroloba*, the dominant N fixer in the other 7 plots. At the plot level, the prevalence of N fixers was marginally negatively correlated with the change in basal area of a) all trees ($P = 0.08$), and b) non-fixers ($P = 0.06$). C) Effect of crowding by N fixers on the growth of individual N fixers (red; $P < 0.001$) and non-fixers (blue; $P < 0.001$). Lines represent linear regression models, and all colors and symbols for c) are as in Fig S5.

Table S1. Table of model coefficient values for growth model of assessing the impact of neighbor crowding (NCI), the proportion of crowding due to N fixers (neigh_fix), DBH, and the interactions between these variables on the growth of individual N fixers and non-fixers. Values are the parameter estimate (50%) and lower (2.5%) and upper (97.5) bounds of the credible interval in the model output for each covariate's effect on the growth of individuals based on their fixation status. Values are presented for the separate models run for young (≤ 25 years stand age) and old (> 25 years stand age) forests. These values correspond to those presented in Figure S2.

Growth in Young Forests				
Model Covariate	**Fixation Status**	**2.50%**	**50%**	**97.50%**
NCI	Non-Fixer	-0.16418094	-0.134102662	-0.104257413
DBH	Non-Fixer	-0.103423634	-0.067419913	-0.034675755
neigh_fix	Non-Fixer	-0.103728397	-0.071454147	-0.038667516
NCI^2	Non-Fixer	0.007321601	0.021485471	0.035561224
NCI x DBH	Non-Fixer	-0.042379625	-0.020651502	0.001210065
NCI x neigh_fix	Non-Fixer	-0.015345086	0.017714527	0.050194316
NCI	Fixer	-0.358381355	-0.277450844	-0.192622521
DBH	Fixer	0.127240105	0.182198306	0.234983854
neigh_fix	Fixer	-0.194316016	-0.147636904	-0.10453367
NCI^2	Fixer	-0.02908105	0.003046833	0.034010012
NCI x DBH	Fixer	-0.013363898	0.030953798	0.077401146
NCI x neigh_fix	Fixer	0.043517734	0.089533507	0.136421931
Growth in Old Forests				
Model Covariate	**Fixation Status**	**2.50%**	**50%**	**97.50%**
NCI	Non-Fixer	-0.105249342	-0.081489878	-0.058621957
DBH	Non-Fixer	-0.016836474	0.009990375	0.03638741
neigh_fix	Non-Fixer	-0.01727689	0.002397728	0.022621499
NCI^2	Non-Fixer	0.001435007	0.012393082	0.023654503
NCI x DBH	Non-Fixer	-0.041167616	-0.021043018	-0.000755745
NCI x neigh_fix	Non-Fixer	-0.024536377	-0.007380389	0.009079975
NCI	Fixer	-0.126736741	-0.061206613	0.005860932
DBH	Fixer	0.069044509	0.117456514	0.163885657
neigh_fix	Fixer	-0.110517166	-0.064197328	-0.017969619
NCI^2	Fixer	-0.017591095	0.014016779	0.045857013
NCI x DBH	Fixer	0.00967944	0.05404792	0.098911931
NCI x neigh_fix	Fixer	-0.041376023	-0.007438615	0.025897038

Table S2. Table of model coefficient values for recruitment model of assessing the impact of neighbor crowding (NCI), the proportion of crowding due to N fixers (neigh_fix), and the interactions between these variables on the frequency of individual N-fixer and non-fixer recruitment into individual 10 x 10 m subplots. Values are the parameter estimate (50%) and lower (2.5%) and upper (97.5) bounds of the credible interval in the model output for each covariate's effect on the frequency of N-fixer and non-fixer recruits. Values are presented for the separate models run for young (≤ 25 years stand age) and old (> 25 years stand age) forests. These values correspond to those presented in Figure S3.

Recruitment in Young Forests				
Model Covariate	**Fixation Status**	**2.50%**	**50%**	**97.50%**
NCI	Non-Fixer	-0.113898176	-0.0224169	0.07398544
neigh_fix	Non-Fixer	-0.386787044	-0.280389413	-0.181315198
NCI^2	Non-Fixer	-0.109266161	-0.046608219	0.013765278
NCI x neigh_fix	Non-Fixer	-0.108672516	-0.017124927	0.071095037
NCI	Fixer	-0.501886647	-0.162055515	0.151130145
neigh_fix	Fixer	-0.144741257	0.146970515	0.433011194
NCI^2	Fixer	-0.427513366	-0.168821451	0.032282261
NCI x neigh_fix	Fixer	-0.092806729	0.167381842	0.442299601
Recruitment in Old Forests				
Model Covariate	**Fixation Status**	**2.50%**	**50%**	**97.50%**
NCI	Non-Fixer	-0.089887787	-0.004677652	0.080639129
neigh_fix	Non-Fixer	-0.092932231	-0.018160485	0.056816558
NCI^2	Non-Fixer	-0.059063451	-0.010470275	0.034575821
NCI x neigh_fix	Non-Fixer	0.007322807	0.07277068	0.139009277
NCI	Fixer	-0.506362899	-0.105380147	0.284810064
neigh_fix	Fixer	-0.605860659	-0.252632135	0.054128547
NCI^2	Fixer	-0.146281631	0.016602165	0.158914944
NCI x neigh_fix	Fixer	-0.433279658	-0.156137697	0.082861559

Table S3. Table of model coefficient values for survival model of assessing the impact of neighbor crowding (NCI), the proportion of crowding due to N fixers (neigh_fix), DBH, and the interactions between these variables on the survival of individual N fixers and non-fixers. Values are the parameter estimate (50%) and lower (2.5%) and upper (97.5) bounds of the credible interval in the model output for each covariate's effect on the survival of individuals based on their fixation status. Values are presented for the separate models run for young (≤ 25 years stand age) and old (> 25 years stand age) forests. These values correspond to those presented in Figure S4.

Survival in Young Forests				
Model Covariate	**Fixation Status**	**2.50%**	**50%**	**97.50%**
NCI	Non-Fixer	-0.020836856	0.019010394	0.141736029
DBH	Non-Fixer	-0.470285359	-0.35583688	-0.29499912
neigh_fix	Non-Fixer	0.09977168	0.192149015	0.274575392
NCI^2	Non-Fixer	-0.045635487	-0.009900515	0.035112159
NCI x DBH	Non-Fixer	-0.041118099	0.027606086	0.104739243
NCI x neigh_fix	Non-Fixer	-0.111492709	-0.034132167	0.069400179
NCI	Fixer	-0.302547946	-0.010808257	0.71128891
DBH	Fixer	-1.154464216	-0.922759952	-0.399401099
neigh_fix	Fixer	-0.091861221	0.197977736	0.449237138
NCI^2	Fixer	-0.351842072	-0.041930587	0.188479978
NCI x DBH	Fixer	-0.409102606	-0.021330851	0.286060579
NCI x neigh_fix	Fixer	-0.211824753	0.200588751	0.349449829
Survival in Old Forests				
Model Covariate	**Fixation Status**	**2.50%**	**50%**	**97.50%**
NCI	Non-Fixer	-0.084042625	0.029387412	0.144510804
DBH	Non-Fixer	0.011358366	0.126916717	0.243061532
neigh_fix	Non-Fixer	-0.176862724	-0.073848598	0.021254437
NCI^2	Non-Fixer	-0.092670035	-0.03939129	0.01366022
NCI x DBH	Non-Fixer	-0.091697314	-0.005506539	0.08217381
NCI x neigh_fix	Non-Fixer	-0.217975717	-0.120630146	-0.025872088
NCI	Fixer	0.027934381	0.401842926	0.783572587
DBH	Fixer	-0.169199369	0.062252245	0.296572807
neigh_fix	Fixer	0.164908907	0.392357934	0.622249847
NCI^2	Fixer	-0.248014146	-0.075279998	0.082372637
NCI x DBH	Fixer	-0.24534621	-0.012076941	0.234946439
NCI x neigh_fix	Fixer	-0.291619738	-0.128485222	0.053620839

Table S4. Species represented in our dataset. Each of the 366 species and its putative fixation status is listed in order of the frequency of stems represented in our full dataset. The relative abundance (percent of stems) of each species for each plot is presented as the average over the census period for that plot.

Species	Fixer Status	Frequency	CR Relative Abundance	LSUR Relative Abundance	BEJ Relative Abundance	TIR Relative Abundance	JE Relative Abundance	LEPP Relative Abundance	SV Relative Abundance
Pentaclethra macroloba	Fixer	14024	11.49	18.76	24.61	0.00	14.73	5.75	6.49
Miconia affinis	Non-Fixer	7495	0.08	18.88	14.53	5.16	10.67	0.22	0.00
Casearia arborea	Non-Fixer	6897	8.13	7.24	2.67	2.76	2.93	1.04	0.51
Socratea exorrhiza	Non-Fixer	4338	1.32	3.64	1.42	0.08	0.16	1.99	0.34
Goethalsia meiantha	Non-Fixer	4134	1.09	10.34	0.48	0.25	0.61	0.73	0.00
Euterpe precatoria var. longevaginata	Non-Fixer	4099	8.24	5.82	0.15	0.01	0.08	4.41	4.03
Anaxagorea crassipetala	Non-Fixer	3932	15.76	0.22	0.00	0.00	0.00	0.11	0.00
Virola sebifera	Non-Fixer	3414	2.27	4.89	1.07	1.94	4.06	1.47	0.45
Vochysia ferruginea	Non-Fixer	3316	1.45	1.06	3.52	10.08	4.05	0.31	0.45
Laetia procera	Non-Fixer	3110	6.46	0.36	0.68	0.40	0.29	0.45	0.26
Iriartea deltoidea	Non-Fixer	2806	0.63	1.03	0.10	0.00	0.00	4.79	3.50
Dendropanax arboreus	Non-Fixer	2787	2.05	1.03	1.48	5.52	2.16	2.24	2.40
Simarouba amara	Non-Fixer	2702	0.31	1.23	4.02	5.84	6.00	0.62	0.13
Warszewiczia coccinea	Non-Fixer	2701	5.49	0.06	2.17	1.41	0.09	1.57	0.90
Miconia elata	Non-Fixer	2692	0.00	0.65	12.33	2.38	8.05	0.17	0.04
Cordia bicolor	Non-Fixer	2023	2.16	0.03	0.20	2.12	0.97	0.00	0.00
Piper colonense	Non-Fixer	1910	4.16	2.29	0.20	1.89	0.20	0.02	0.25

Species	Fixer Status	Frequency	CR Relative Abundance	LSUR Relative Abundance	BEJ Relative Abundance	TIR Relative Abundance	JE Relative Abundance	LEPP Relative Abundance	SV Relative Abundance
Inga cocleensis	Fixer	1775	0.07	0.09	0.40	8.68	0.38	0.00	0.09
Xylopia sericophylla	Non-Fixer	1561	2.67	2.48	1.82	0.11	1.75	0.10	0.09
Welfia regia	Non-Fixer	1503	0.41	0.00	0.00	0.00	0.09	5.19	7.71
Miconia prasina	Non-Fixer	1331	0.00	0.00	7.67	0.00	5.26	0.00	0.00
Cespedesia spathulata	Non-Fixer	1225	0.49	0.21	1.16	3.25	1.33	0.48	0.76
Miconia multispicata	Non-Fixer	1144	0.32	0.15	0.04	4.02	0.11	0.22	0.39
Hampea appendiculata	Non-Fixer	919	0.18	0.70	0.20	1.42	4.02	0.00	0.00
Guatteria amplifolia	Non-Fixer	874	0.18	2.10	0.16	0.89	0.52	0.33	0.62
Hernandia didymantha	Non-Fixer	825	0.37	0.33	0.15	1.50	0.41	0.00	0.17
Cryosophila warscewiczii	Non-Fixer	812	0.00	0.00	0.00	0.00	0.00	4.20	0.00
Annona papilionella	Non-Fixer	799	1.09	1.24	0.40	0.40	1.82	0.00	0.00
Protium confusum	Non-Fixer	781	0.18	0.01	0.00	2.23	0.08	1.07	1.60
Protium ravenii	Non-Fixer	754	0.31	0.16	0.02	0.03	0.00	0.87	4.15
Handroanthus chrysanthus	Non-Fixer	752	0.16	0.00	1.57	1.56	2.44	0.00	0.00
Virola koschnyi	Non-Fixer	737	0.24	0.69	1.44	0.70	1.40	0.61	0.23
Ryania speciosa	Non-Fixer	736	0.00	0.00	0.46	0.00	0.18	4.19	0.00
Capparis pittieri	Non-Fixer	679	1.06	0.34	0.00	0.00	0.00	2.61	0.09
Guatteria aeruginosa	Non-Fixer	670	0.51	1.04	0.09	0.99	0.05	0.43	0.10
Apeiba membranacea	Non-Fixer	667	0.75	0.03	0.00	1.26	0.10	0.10	0.09
Faramea parvibractea	Non-Fixer	656	0.00	0.00	0.00	0.00	0.00	1.80	4.14
Jacaranda copaia	Non-Fixer	608	0.00	2.71	0.17	0.16	0.26	0.00	0.00
Inga pezizifera	Fixer	581	0.36	0.09	0.14	0.17	0.08	0.21	0.00
Brosimum lactescens	Non-Fixer	558	0.19	0.15	0.10	0.00	0.18	2.18	1.67
Cupania glabra	Non-Fixer	557	0.13	0.00	0.01	1.99	0.04	0.00	1.24
Inga alba	Fixer	554	0.44	0.00	0.00	0.09	0.09	0.24	0.64

Species	Fixer Status	Frequency	CR Relative Abundance	LSUR Relative Abundance	BEJ Relative Abundance	TIR Relative Abundance	JE Relative Abundance	LEPP Relative Abundance	SV Relative Abundance
Vochysia guatemalensis	Non-Fixer	552	0.00	0.00	0.00	2.83	0.15	0.00	0.00
Ocotea leucoxylon	Non-Fixer	545	0.54	0.83	0.00	0.12	0.03	0.48	0.30
Casearia commersoniana	Non-Fixer	544	0.36	0.00	0.00	2.07	0.00	0.10	0.17
Pourouma bicolor	Non-Fixer	540	0.88	0.00	0.24	0.00	0.06	0.87	0.70
Inga thibaudiana	Fixer	533	0.04	0.44	0.12	0.42	0.47	0.10	0.00
Protium pittieri	Non-Fixer	525	0.37	0.41	0.00	0.01	0.00	2.57	0.27
Minquartia guianensis	Non-Fixer	516	0.80	0.06	0.36	0.30	0.10	0.86	0.96
Byrsonima crassifolia	Non-Fixer	458	0.40	0.12	0.10	0.00	0.00	0.10	0.43
Pausandra trianae	Non-Fixer	428	0.00	0.00	0.00	0.00	0.00	0.00	3.67
Psychotria elata	Non-Fixer	419	0.00	0.18	1.03	0.03	1.40	0.00	0.16
Psychotria panamensis	Non-Fixer	415	0.52	0.59	0.00	0.01	0.00	0.30	0.00
Tetragastris panamensis	Non-Fixer	415	0.34	0.00	0.20	0.30	0.00	0.10	2.06
Miconia punctata	Non-Fixer	409	0.08	0.00	0.68	0.00	0.44	0.00	2.36
Alibertia atlantica	Non-Fixer	404	0.08	0.00	0.00	0.04	0.00	0.60	2.75
Carapa nicaraguensis	Non-Fixer	388	0.08	0.00	1.21	0.00	0.72	0.83	0.79
Quararibea ochrocalyx	Non-Fixer	387	0.00	0.00	0.00	0.00	0.00	2.70	1.08
Alchorneopsis floribunda	Non-Fixer	368	0.16	1.05	0.19	0.04	0.56	0.20	0.00
Protium panamense	Non-Fixer	366	0.54	0.08	0.00	0.43	0.00	0.91	0.17
Guarea guidonia	Non-Fixer	350	0.22	0.09	0.00	0.05	0.00	2.09	0.45
Stryphnodendron microstachyum	Fixer	343	0.03	0.87	0.00	0.01	0.00	0.00	0.00
Zanthoxylum panamense	Non-Fixer	342	0.07	0.00	1.44	0.47	0.74	0.00	0.00
Croton smithianus	Non-Fixer	341	0.00	0.00	0.57	0.43	1.21	0.00	0.61
Pterocarpus rohrii	Fixer	341	0.14	0.00	0.00	0.02	0.00	0.21	0.09
Alchornea latifolia	Non-Fixer	336	0.23	0.00	0.00	1.44	0.01	0.00	0.07

Species	Fixer Status	Frequency	CR Relative Abundance	LSUR Relative Abundance	BEJ Relative Abundance	TIR Relative Abundance	JE Relative Abundance	LEPP Relative Abundance	SV Relative Abundance
Brosimum guianensis	Non-Fixer	332	0.15	0.00	0.10	0.14	0.09	0.60	1.13
Tapirira guianensis	Non-Fixer	332	0.22	0.00	0.00	0.00	0.00	0.75	1.38
Cordia alliodora	Non-Fixer	321	0.00	0.00	0.90	0.00	2.14	0.00	0.00
Rauvolfia purpurascens	Non-Fixer	319	0.07	0.00	0.00	0.38	0.00	0.41	0.04
Euterpe oleracea	Non-Fixer	301	0.00	0.00	0.63	1.05	0.35	0.00	0.00
Vitex cooperi	Non-Fixer	301	0.16	0.00	0.10	0.89	0.00	0.21	0.00
Vismia baccifera	Non-Fixer	297	0.00	0.04	0.04	0.79	1.27	0.00	0.00
Conceveiba pleiostemona	Non-Fixer	283	0.86	0.06	0.00	0.00	0.00	0.00	0.00
Zanthoxylum ekmanii	Non-Fixer	275	1.21	0.00	0.00	0.00	0.00	0.00	0.00
Erythroxylum macrophyllum	Non-Fixer	262	0.09	0.11	0.00	1.12	0.00	0.00	0.00
Ocotea laetevirens	Non-Fixer	259	0.10	0.00	0.00	0.02	0.00	0.80	0.35
Inga acuminata	Fixer	254	0.00	0.00	0.00	1.05	0.00	0.01	0.00
Ocotea cernua	Non-Fixer	249	0.00	0.12	0.00	0.60	0.00	0.00	0.00
Inga leiocalycina	Fixer	244	0.49	0.01	0.00	0.10	0.06	0.00	0.00
Licaria sarapiquensis	Non-Fixer	230	0.04	0.00	0.10	0.50	0.00	0.35	0.61
Vismia macrophylla	Non-Fixer	222	0.00	0.17	0.10	0.72	0.40	0.00	0.00
Prestoea decurrens	Non-Fixer	217	0.59	0.02	0.00	0.00	0.00	0.56	0.21
Byrsonima arthropoda	Non-Fixer	216	0.00	0.00	0.06	0.00	1.94	0.00	0.00
Cecropia insignis	Non-Fixer	212	0.07	0.42	0.00	0.04	0.09	0.00	0.02
Clethra costaricensis	Non-Fixer	207	0.24	0.00	0.00	0.00	0.18	0.00	0.09
Pouteria calistophylla	Non-Fixer	206	0.07	0.00	0.00	0.03	0.00	1.00	0.75
Vismia billbergiana	Non-Fixer	206	0.05	0.00	0.01	0.04	1.73	0.00	0.00
Calophyllum brasiliense	Non-Fixer	205	0.00	0.00	0.00	0.09	0.13	0.29	1.24
Pourouma minor	Non-Fixer	205	0.49	0.09	0.00	0.03	0.00	0.66	0.06
Guarea bullata	Non-Fixer	196	0.00	0.05	0.00	0.04	0.00	1.39	0.35

Species	Fixer Status	Frequency	CR Relative Abundance	LSUR Relative Abundance	BEJ Relative Abundance	TIR Relative Abundance	JE Relative Abundance	LEPP Relative Abundance	SV Relative Abundance
Naucleopsis naga	Non-Fixer	194	0.08	0.00	0.00	0.00	0.00	0.92	0.75
Neea laetevirens	Non-Fixer	194	0.08	0.00	0.10	0.77	0.09	0.00	0.09
Cupania pseudostipularis	Non-Fixer	189	0.00	0.55	0.00	0.00	0.00	0.31	0.00
Guarea rhopalocarpa	Non-Fixer	189	0.13	0.10	0.00	0.45	0.00	0.44	0.11
Inga umbellifera	Fixer	187	0.08	0.00	0.00	0.03	0.00	0.00	0.17
Colubrina spinosa	Non-Fixer	182	0.11	0.00	0.00	0.16	0.00	0.31	0.40
Rhodostemonodaphne kunthiana	Non-Fixer	180	0.00	0.26	0.06	0.18	0.52	0.00	0.00
Hirtella racemosa	Non-Fixer	175	0.00	0.00	0.00	0.00	0.00	0.00	1.50
Swartzia ochnea	Fixer	173	0.00	0.00	0.00	0.05	0.00	1.50	0.00
Neea popenoei	Non-Fixer	172	0.16	0.00	0.00	0.66	0.00	0.00	0.09
Siparuna cuspidata	Non-Fixer	163	0.30	0.00	0.00	0.11	0.00	0.00	0.52
Casearia sylvestris	Non-Fixer	158	0.00	0.00	0.00	0.78	0.00	0.00	0.09
Aspidosperma desmanthum	Non-Fixer	157	0.08	0.00	0.10	0.00	0.00	0.00	1.11
Ormosia velutina	Fixer	153	0.00	0.00	0.00	0.65	0.00	0.00	0.26
Ocotea macropoda	Non-Fixer	150	0.18	0.00	0.02	0.24	0.31	0.29	0.00
Pseudolmedia spuria	Non-Fixer	150	0.08	0.00	0.00	0.34	0.00	0.10	0.38
Ferdinandusa panamensis	Non-Fixer	149	0.00	0.00	0.00	0.00	0.00	1.54	0.00
Lacunaria panamensis	Non-Fixer	149	0.03	0.00	0.00	0.08	0.00	0.18	0.85
Miconia stevensiana	Non-Fixer	149	0.00	0.00	0.00	0.02	0.06	0.54	0.75
Lacmellea panamensis	Non-Fixer	146	0.08	0.00	0.01	0.25	0.00	0.10	0.21
Psychotria luxurians	Non-Fixer	146	0.00	0.01	0.15	0.40	0.13	0.11	0.00
Cordia dwyeri	Non-Fixer	142	0.00	0.00	0.00	0.00	0.00	0.41	0.42
Ampelocera macrocarpa	Non-Fixer	141	0.00	0.00	0.00	0.05	0.00	0.10	1.05

Species	Fixer Status	Frequency	CR Relative Abundance	LSUR Relative Abundance	BEJ Relative Abundance	TIR Relative Abundance	JE Relative Abundance	LEPP Relative Abundance	SV Relative Abundance
Ilex skutchii	Non-Fixer	141	0.13	0.18	0.00	0.31	0.00	0.00	0.00
Rinorea deflexiflora	Non-Fixer	141	0.00	0.00	0.00	0.01	0.00	0.00	0.72
Trichilia septentrionalis	Non-Fixer	141	0.00	0.08	0.02	0.00	0.03	1.00	0.21
Hieronyma alchorneoides	Non-Fixer	139	0.13	0.01	0.00	0.41	0.00	0.00	0.26
Coccoloba tuerckheimii	Non-Fixer	137	0.00	0.00	0.00	0.72	0.00	0.00	0.00
Faramea multiflora	Non-Fixer	137	0.00	0.00	0.00	0.00	0.00	1.01	0.33
Compsoneura mexicana	Non-Fixer	135	0.08	0.00	0.00	0.00	0.00	0.31	0.75
Pouteria durlandii	Non-Fixer	130	0.00	0.00	0.00	0.00	0.00	0.93	0.34
Pera arborea	Non-Fixer	128	0.00	0.00	0.50	0.00	0.72	0.00	0.00
Pouteria sp1	Non-Fixer	128	0.04	0.00	0.10	0.00	0.00	0.21	0.76
Annona amazonica	Non-Fixer	124	0.05	0.24	0.00	0.35	0.00	0.00	0.00
Maranthes panamensis	Non-Fixer	124	0.08	0.00	0.00	0.19	0.00	0.21	0.43
Inga sertulifera	Fixer	121	0.00	0.00	0.00	0.32	0.00	0.10	0.27
Dussia macroprophyllata	Fixer	119	0.08	0.00	0.00	0.10	0.00	0.00	0.15
Ocotea hartshorniana	Non-Fixer	119	0.19	0.19	0.00	0.03	0.00	0.25	0.00
Posoqueria maxima	Non-Fixer	119	0.00	0.00	0.00	0.00	0.00	0.62	0.51
Balizia elegans	Fixer	118	0.00	0.00	0.40	0.00	0.00	0.21	0.26
Unonopsis pittieri	Non-Fixer	116	0.00	0.00	0.00	0.02	0.00	0.41	0.62
Quararibea bracteolosa	Non-Fixer	115	0.07	0.00	0.00	0.00	0.00	0.30	0.45
Bactris gasipaes	Non-Fixer	112	0.00	0.00	0.31	0.00	0.75	0.00	0.00
Inga spectabilis	Fixer	109	0.00	0.00	0.00	0.00	1.01	0.00	0.00
Hirtella media	Non-Fixer	107	0.00	0.00	0.12	0.04	0.12	0.21	0.46

Species	Fixer Status	Frequency	CR Relative Abundance	LSUR Relative Abundance	BEJ Relative Abundance	TIR Relative Abundance	JE Relative Abundance	LEPP Relative Abundance	SV Relative Abundance
Nectandra umbrosa	Non-Fixer	105	0.00	0.00	0.18	0.10	0.05	0.00	0.54
Licaria misantlae	Non-Fixer	104	0.00	0.00	0.00	0.36	0.00	0.20	0.15
Talisia nervosa	Non-Fixer	104	0.00	0.27	0.00	0.02	0.00	0.00	0.26
Chrysophyllum colombianum	Non-Fixer	103	0.00	0.00	0.10	0.00	0.00	0.13	0.69
Persea americana	Non-Fixer	103	0.00	0.00	0.00	0.00	0.00	0.75	0.26
Beilschmiedia sp.A	Non-Fixer	102	0.08	0.08	0.00	0.00	0.00	0.12	0.19
Inga venusta	Fixer	102	0.00	0.00	0.00	0.00	0.00	0.52	0.29
Ocotea insularis	Non-Fixer	102	0.05	0.41	0.00	0.00	0.00	0.10	0.00
Richeria dressleri	Non-Fixer	102	0.00	0.00	0.00	0.00	0.00	0.50	0.09
Sacoglottis trichogyna	Non-Fixer	102	0.16	0.00	0.00	0.14	0.00	0.31	0.09
Nephelium mutabile	Non-Fixer	98	0.00	0.00	0.40	0.00	0.54	0.00	0.00
Lozania pittieri	Non-Fixer	97	0.12	0.00	0.06	0.12	0.00	0.21	0.17
Marila pluricostata	Non-Fixer	97	0.07	0.00	0.00	0.11	0.00	0.00	0.52
Ossaea brenesii	Non-Fixer	95	0.00	0.00	0.00	0.50	0.00	0.00	0.00
Loreya mespiloides	Non-Fixer	94	0.00	0.00	0.00	0.00	0.87	0.00	0.00
Callicarpa acuminata	Non-Fixer	93	0.33	0.00	0.10	0.00	0.06	0.00	0.00
Cinnamomum chavarrianum	Non-Fixer	92	0.21	0.00	0.00	0.00	0.00	0.09	0.00
Meliosma donnellsmithii	Non-Fixer	92	0.00	0.00	0.00	0.28	0.07	0.10	0.17
Terminalia amazonia	Non-Fixer	91	0.08	0.00	0.00	0.28	0.00	0.00	0.17
Eugenia hammelii	Non-Fixer	90	0.00	0.00	0.00	0.00	0.00	0.00	0.77
Phyllanthus skutchii	Non-Fixer	90	0.24	0.19	0.00	0.00	0.00	0.00	0.00
Qualea polychroma	Non-Fixer	88	0.00	0.00	0.10	0.00	0.00	0.00	0.67
Andira inermis	Fixer	86	0.00	0.05	0.20	0.19	0.00	0.21	0.00
Ardisia fimbrillifera	Non-Fixer	84	0.14	0.00	0.00	0.00	0.00	0.17	0.00
Maquira guianensis	Non-Fixer	83	0.00	0.03	0.00	0.02	0.00	0.29	0.15

Species	Fixer Status	Frequency	CR Relative Abundance	LSUR Relative Abundance	BEJ Relative Abundance	TIR Relative Abundance	JE Relative Abundance	LEPP Relative Abundance	SV Relative Abundance
Cecropia obtusifolia	Non-Fixer	82	0.00	0.00	0.15	0.01	0.61	0.00	0.00
Hieronyma oblonga	Non-Fixer	82	0.08	0.00	0.00	0.00	0.00	0.00	0.09
Virola multiflora	Non-Fixer	81	0.04	0.00	0.00	0.00	0.01	0.00	0.62
Zygia gigantifoliola	Fixer	80	0.00	0.00	0.00	0.28	0.00	0.24	0.00
Vouarana anomala	Non-Fixer	78	0.16	0.00	0.00	0.00	0.00	0.00	0.09
Chrysophyllum venezuelanense	Non-Fixer	77	0.08	0.00	0.00	0.26	0.00	0.10	0.00
Senna papillosa	Non-Fixer	75	0.00	0.11	0.00	0.13	0.26	0.00	0.00
Abarema adenophora	Fixer	74	0.24	0.00	0.00	0.00	0.00	0.00	0.17
Eugenia sp	Non-Fixer	71	0.00	0.00	0.00	0.00	0.00	0.00	0.17
Coussarea hondensis	Non-Fixer	70	0.00	0.04	0.00	0.00	0.00	0.28	0.00
Dystovomita paniculata	Non-Fixer	70	0.00	0.00	0.00	0.00	0.00	0.31	0.34
Ocotea mollifolia	Non-Fixer	70	0.17	0.00	0.00	0.00	0.00	0.00	0.00
Psidium guajava	Non-Fixer	70	0.00	0.00	0.10	0.04	0.49	0.00	0.00
Licania sp. A	Non-Fixer	69	0.00	0.00	0.00	0.00	0.00	0.51	0.17
Mabea occidentalis	Non-Fixer	69	0.00	0.00	0.00	0.00	0.00	0.00	0.15
Psychotria calidicola	Non-Fixer	69	0.00	0.00	0.00	0.00	0.00	0.71	0.00
Sorocea pubivena	Non-Fixer	69	0.00	0.00	0.08	0.13	0.00	0.00	0.00
Pouteria campechiana	Non-Fixer	67	0.00	0.00	0.04	0.07	0.00	0.31	0.17
Dipteryx panamensis	Non-Fixer	66	0.00	0.00	0.10	0.00	0.33	0.00	0.17
Perebea hispidula	Non-Fixer	66	0.00	0.00	0.00	0.04	0.00	0.01	0.50
Pouteria torta	Non-Fixer	65	0.08	0.00	0.00	0.00	0.00	0.21	0.17
Hirtella lemsii	Non-Fixer	64	0.16	0.00	0.00	0.00	0.00	0.21	0.00
Swartzia nicaraguensis	Fixer	64	0.16	0.00	0.00	0.09	0.00	0.10	0.00
Quiina macrophylla	Non-Fixer	63	0.04	0.00	0.00	0.08	0.00	0.18	0.17
Ocotea sp1	Non-Fixer	58	0.00	0.00	0.00	0.00	0.00	0.08	0.43
Pouteria reticulata	Non-Fixer	58	0.08	0.00	0.00	0.00	0.00	0.10	0.26

Species	Fixer Status	Frequency	CR Relative Abundance	LSUR Relative Abundance	BEJ Relative Abundance	TIR Relative Abundance	JE Relative Abundance	LEPP Relative Abundance	SV Relative Abundance
Psychotria cooperi	Non-Fixer	58	0.00	0.00	0.00	0.00	0.54	0.00	0.00
Syzygium jambos	Non-Fixer	58	0.00	0.00	0.58	0.00	0.00	0.00	0.00
Inga chocoensis	Fixer	57	0.24	0.00	0.00	0.02	0.00	0.00	0.00
Hippotis panamensis	Non-Fixer	56	0.10	0.00	0.00	0.00	0.00	0.00	0.28
Lecythis ampla	Non-Fixer	56	0.00	0.00	0.00	0.09	0.00	0.00	0.17
Lacistema aggregatum	Non-Fixer	55	0.00	0.00	0.00	0.00	0.00	0.10	0.00
Hymenolobium mesoamericanum	Fixer	54	0.00	0.00	0.00	0.09	0.00	0.10	0.00
Ocotea pentagona	Non-Fixer	54	0.08	0.00	0.00	0.00	0.00	0.00	0.31
Hedyosmum scaberrimum	Non-Fixer	52	0.07	0.04	0.00	0.02	0.10	0.13	0.00
Chrysophyllum hirsutum	Non-Fixer	51	0.22	0.00	0.00	0.00	0.00	0.00	0.00
Croton schiedeanus	Non-Fixer	51	0.07	0.00	0.00	0.00	0.00	0.06	0.26
Guatteria recurvisepala	Non-Fixer	51	0.00	0.00	0.30	0.05	0.10	0.00	0.00
Talauma gloriensis	Non-Fixer	51	0.00	0.00	0.10	0.00	0.06	0.00	0.30
Humiriastrum diguense	Non-Fixer	50	0.00	0.00	0.00	0.00	0.00	0.00	0.43
Xylosma chlorantha	Non-Fixer	50	0.00	0.00	0.10	0.00	0.09	0.10	0.17
Chrysochlamys silvicola	Non-Fixer	49	0.07	0.00	0.00	0.00	0.00	0.00	0.28
Ocotea floribunda	Non-Fixer	49	0.00	0.00	0.00	0.26	0.00	0.00	0.00
Astrocaryum confertum	Non-Fixer	48	0.08	0.00	0.00	0.02	0.08	0.03	0.00
Cedrela odorata	Non-Fixer	48	0.00	0.13	0.10	0.03	0.06	0.00	0.00
Casearia coronata	Non-Fixer	47	0.01	0.23	0.00	0.00	0.00	0.00	0.00
Heisteria concinna	Non-Fixer	47	0.00	0.02	0.00	0.02	0.00	0.41	0.00
Jacaratia dolichaula	Non-Fixer	47	0.00	0.14	0.00	0.00	0.00	0.10	0.00
Mollinedia costaricensis	Non-Fixer	46	0.16	0.00	0.00	0.00	0.00	0.00	0.09
Pholidostachys pulchra	Non-Fixer	46	0.00	0.00	0.00	0.00	0.00	0.48	0.00
Swartzia costaricensis	Fixer	46	0.00	0.00	0.00	0.00	0.00	0.48	0.00

Species	Fixer Status	Frequency	CR Relative Abundance	LSUR Relative Abundance	BEJ Relative Abundance	TIR Relative Abundance	JE Relative Abundance	LEPP Relative Abundance	SV Relative Abundance
Myrcia splendens	Non-Fixer	43	0.00	0.00	0.00	0.03	0.00	0.18	0.00
Gmelina arborea	Non-Fixer	42	0.00	0.00	0.00	0.22	0.00	0.00	0.00
Pachira aquatica	Non-Fixer	42	0.00	0.00	0.00	0.00	0.00	0.00	0.00
Tachigali costaricensis	Fixer	41	0.00	0.06	0.05	0.00	0.04	0.00	0.18
Annona subnubila	Non-Fixer	40	0.00	0.00	0.00	0.00	0.00	0.21	0.17
Couepia polyandra	Non-Fixer	40	0.00	0.00	0.00	0.00	0.00	0.21	0.17
Mabea klugii	Non-Fixer	40	0.00	0.00	0.00	0.00	0.00	0.00	0.34
Vantanea occidentalis	Non-Fixer	40	0.00	0.00	0.20	0.00	0.00	0.00	0.17
Garcinia intermedia	Non-Fixer	37	0.00	0.00	0.00	0.00	0.00	0.10	0.23
Bunchosia macrophylla	Non-Fixer	36	0.08	0.09	0.00	0.00	0.00	0.00	0.00
Psychotria chagrensis	Non-Fixer	36	0.00	0.00	0.00	0.19	0.00	0.00	0.00
Trophis involucrata	Non-Fixer	35	0.00	0.00	0.00	0.00	0.00	0.27	0.08
Faramea glandulosa	Non-Fixer	34	0.00	0.00	0.00	0.00	0.00	0.35	0.00
Sapium glandulosum	Non-Fixer	34	0.07	0.00	0.00	0.09	0.00	0.00	0.00
Cestrum racemosum	Non-Fixer	33	0.02	0.05	0.00	0.09	0.00	0.00	0.00
Inga oerstediana	Fixer	33	0.00	0.00	0.20	0.07	0.00	0.00	0.00
Inga sapindoides	Fixer	33	0.00	0.08	0.00	0.04	0.00	0.00	0.00
Conostegia montana	Non-Fixer	32	0.00	0.00	0.00	0.09	0.00	0.06	0.08
Sclerolobium costaricense	Fixer	32	0.00	0.17	0.00	0.00	0.00	0.00	0.00
Symphonia globulifera	Non-Fixer	32	0.00	0.00	0.00	0.00	0.00	0.26	0.00
Unonopsis hammelii	Non-Fixer	32	0.05	0.00	0.00	0.00	0.00	0.11	0.09
Graffenrieda galeottii	Non-Fixer	31	0.08	0.00	0.00	0.07	0.00	0.00	0.00
Pouteria bracteata	Non-Fixer	30	0.00	0.00	0.00	0.00	0.00	0.00	0.26
Sloanea guianensis	Non-Fixer	30	0.00	0.00	0.00	0.00	0.00	0.00	0.26
Allophylus psilospermus	Non-Fixer	29	0.00	0.00	0.00	0.15	0.00	0.00	0.00
Eschweilera longirachis	Non-Fixer	29	0.00	0.00	0.00	0.00	0.00	0.30	0.00

Species	Fixer Status	Frequency	CR Relative Abundance	LSUR Relative Abundance	BEJ Relative Abundance	TIR Relative Abundance	JE Relative Abundance	LEPP Relative Abundance	SV Relative Abundance
Ardisia standleyana	Non-Fixer	28	0.00	0.00	0.00	0.15	0.00	0.00	0.00
Neea amplifolia	Non-Fixer	28	0.00	0.00	0.00	0.09	0.00	0.10	0.00
Parathesis trichogyne	Non-Fixer	28	0.08	0.00	0.00	0.00	0.00	0.10	0.00
Persea laevifolia	Non-Fixer	28	0.00	0.00	0.00	0.00	0.00	0.00	0.24
Sterculia recordiana	Non-Fixer	28	0.00	0.00	0.00	0.09	0.00	0.00	0.09
Lonchocarpus latisiliquus	Fixer	27	0.00	0.00	0.00	0.00	0.00	0.28	0.00
Neea delicatula	Non-Fixer	27	0.00	0.00	0.00	0.00	0.00	0.28	0.00
Unonopsis sp	Non-Fixer	27	0.00	0.00	0.00	0.00	0.00	0.00	0.17
Clusia croatii	Non-Fixer	25	0.00	0.00	0.00	0.00	0.23	0.00	0.00
Cordia porcata	Non-Fixer	24	0.00	0.00	0.00	0.00	0.00	0.25	0.00
Ficus colubrinae	Non-Fixer	24	0.00	0.00	0.00	0.13	0.00	0.00	0.00
Palicourea guianensis	Non-Fixer	24	0.00	0.00	0.00	0.00	0.22	0.00	0.00
Eugenia sp1	Non-Fixer	23	0.00	0.00	0.00	0.00	0.00	0.00	0.09
Miconia appendiculata	Non-Fixer	23	0.00	0.00	0.00	0.00	0.21	0.00	0.00
Syzygium malaccensis	Non-Fixer	23	0.00	0.00	0.23	0.00	0.00	0.00	0.00
Ceiba pentandra	Non-Fixer	21	0.06	0.00	0.00	0.00	0.00	0.00	0.06
Licaria sp	Non-Fixer	21	0.01	0.00	0.00	0.03	0.00	0.00	0.09
Alchornea costaricensis	Non-Fixer	20	0.00	0.00	0.00	0.00	0.18	0.00	0.00
Aniba venezuelana	Non-Fixer	20	0.00	0.00	0.00	0.00	0.00	0.00	0.17
Cocos nucifera	Non-Fixer	20	0.00	0.00	0.00	0.00	0.18	0.00	0.00
Coussarea psychotrioides	Non-Fixer	20	0.00	0.00	0.00	0.00	0.00	0.10	0.09
Eschweilera collinsii	Non-Fixer	20	0.00	0.00	0.00	0.00	0.00	0.00	0.17
Eugenia glandulosopunctata	Non-Fixer	20	0.00	0.00	0.00	0.00	0.00	0.21	0.00
Guarea ciliata	Non-Fixer	20	0.00	0.00	0.00	0.00	0.00	0.21	0.00

Species	Fixer Status	Frequency	CR Relative Abundance	LSUR Relative Abundance	BEJ Relative Abundance	TIR Relative Abundance	JE Relative Abundance	LEPP Relative Abundance	SV Relative Abundance
Inga marginata	Fixer	20	0.00	0.00	0.00	0.11	0.00	0.00	0.00
Ossaea macrophylla	Non-Fixer	20	0.00	0.00	0.00	0.04	0.00	0.12	0.00
Pouteria glomerata	Non-Fixer	20	0.00	0.00	0.00	0.00	0.00	0.21	0.00
Ruptiliocarpon caracolito	Non-Fixer	20	0.00	0.00	0.00	0.00	0.00	0.00	0.17
Xylopia bocatorena	Non-Fixer	20	0.00	0.00	0.00	0.00	0.00	0.00	0.17
Dussia sp. A	Fixer	19	0.00	0.00	0.00	0.05	0.00	0.10	0.00
Inga ruiziana	Fixer	19	0.00	0.00	0.00	0.00	0.00	0.00	0.00
Nectandra reticulata	Non-Fixer	19	0.00	0.00	0.00	0.00	0.18	0.00	0.00
Calatola costaricensis	Non-Fixer	18	0.08	0.00	0.00	0.00	0.00	0.00	0.00
Casearia tacanensis	Non-Fixer	18	0.08	0.00	0.00	0.00	0.00	0.00	0.00
Chimarrhis parviflora	Non-Fixer	18	0.08	0.00	0.00	0.00	0.00	0.00	0.00
Chrysophyllum brenesii	Non-Fixer	18	0.08	0.00	0.00	0.00	0.00	0.00	0.00
Cinnamomum sp1	Non-Fixer	18	0.08	0.00	0.00	0.00	0.00	0.00	0.00
Cordia correae	Non-Fixer	18	0.08	0.00	0.00	0.00	0.00	0.00	0.00
Freziera grisebachii	Non-Fixer	18	0.00	0.00	0.00	0.09	0.00	0.00	0.00
Guarea chiricana	Non-Fixer	18	0.00	0.09	0.00	0.00	0.00	0.00	0.00
Henrietella tuberculosa	Non-Fixer	18	0.00	0.00	0.00	0.00	0.00	0.19	0.00
Herrania purpurea	Non-Fixer	18	0.00	0.00	0.00	0.00	0.00	0.00	0.00
Maquira costaricana	Non-Fixer	18	0.00	0.00	0.00	0.00	0.00	0.00	0.00
Nectandra belizensis	Non-Fixer	18	0.08	0.00	0.00	0.00	0.00	0.00	0.00
Ormosia subsimplex	Fixer	18	0.00	0.00	0.00	0.09	0.00	0.00	0.00
Piper auritifolium	Non-Fixer	18	0.00	0.00	0.00	0.00	0.00	0.07	0.00
Symplocos striata	Non-Fixer	18	0.08	0.00	0.00	0.00	0.00	0.00	0.00
Vochysia allenii	Non-Fixer	18	0.08	0.00	0.00	0.00	0.00	0.00	0.00
Vernonia patens	Non-Fixer	17	0.00	0.00	0.00	0.00	0.16	0.00	0.00
Conostegia lasiopoda	Non-Fixer	16	0.03	0.00	0.00	0.00	0.00	0.10	0.00

Species	Fixer Status	Frequency	CR Relative Abundance	LSUR Relative Abundance	BEJ Relative Abundance	TIR Relative Abundance	JE Relative Abundance	LEPP Relative Abundance	SV Relative Abundance
Hirtella triandra	Non-Fixer	16	0.07	0.00	0.00	0.00	0.00	0.00	0.00
Miconia trinervia	Non-Fixer	16	0.05	0.00	0.00	0.02	0.00	0.00	0.00
Nectandra membranacea	Non-Fixer	16	0.00	0.00	0.00	0.08	0.00	0.00	0.00
Protium glabrum	Non-Fixer	16	0.00	0.00	0.00	0.08	0.00	0.00	0.00
Stephanopodium costaricense	Non-Fixer	16	0.00	0.00	0.00	0.00	0.00	0.00	0.14
Coussarea nigrescens	Non-Fixer	15	0.03	0.00	0.00	0.00	0.00	0.08	0.00
Ficus tonduzii	Non-Fixer	15	0.04	0.00	0.00	0.00	0.00	0.00	0.00
Miconia dorsiloba	Non-Fixer	15	0.01	0.00	0.00	0.00	0.00	0.00	0.00
Ocotea dendrodaphne	Non-Fixer	15	0.03	0.00	0.00	0.00	0.00	0.00	0.08
Chrysochlamys nicaraguensis	Non-Fixer	14	0.00	0.00	0.00	0.04	0.00	0.03	0.03
Miconia ligulata	Non-Fixer	14	0.02	0.00	0.00	0.03	0.00	0.02	0.02
Inga tonduzii	Fixer	13	0.00	0.00	0.00	0.00	0.12	0.00	0.00
Simira maxonii	Non-Fixer	12	0.05	0.00	0.00	0.00	0.00	0.00	0.00
Citrus sinensis	Non-Fixer	11	0.00	0.00	0.00	0.00	0.10	0.00	0.00
Psychotria suerrensis	Non-Fixer	11	0.00	0.00	0.00	0.00	0.00	0.00	0.00
Tabernaemontana amygdalifolia	Non-Fixer	11	0.00	0.00	0.00	0.00	0.00	0.11	0.00
Ardisia sp	Non-Fixer	10	0.00	0.00	0.00	0.00	0.00	0.10	0.00
Bactris gracilior	Non-Fixer	10	0.00	0.00	0.00	0.00	0.00	0.00	0.09
Bactris sp	Non-Fixer	10	0.00	0.00	0.00	0.00	0.00	0.00	0.09
Castilla elastica	Non-Fixer	10	0.00	0.00	0.10	0.00	0.00	0.00	0.00
Chione venosa	Non-Fixer	10	0.00	0.00	0.00	0.00	0.00	0.00	0.09
Clusia uvitana	Non-Fixer	10	0.00	0.00	0.10	0.00	0.00	0.00	0.00
Coussarea impetiolaris	Non-Fixer	10	0.00	0.00	0.00	0.00	0.00	0.00	0.09

Species	Fixer Status	Frequency	CR Relative Abundance	LSUR Relative Abundance	BEJ Relative Abundance	TIR Relative Abundance	JE Relative Abundance	LEPP Relative Abundance	SV Relative Abundance
Cymbopetalum costaricense	Non-Fixer	10	0.00	0.00	0.00	0.00	0.00	0.00	0.09
Drypetes standleyi	Non-Fixer	10	0.00	0.00	0.00	0.00	0.00	0.00	0.09
Elaeoluma glabrescens	Non-Fixer	10	0.00	0.00	0.10	0.00	0.00	0.00	0.00
Garcinia sp1	Non-Fixer	10	0.00	0.00	0.00	0.00	0.00	0.00	0.09
Genipa americana	Non-Fixer	10	0.00	0.00	0.00	0.00	0.09	0.00	0.00
Geonoma interrupta	Non-Fixer	10	0.00	0.00	0.10	0.00	0.00	0.00	0.00
Guarea grandiflora	Non-Fixer	10	0.00	0.00	0.00	0.00	0.00	0.10	0.00
Guarea pilosa	Non-Fixer	10	0.00	0.00	0.00	0.00	0.00	0.10	0.00
Licania hypoleuca	Non-Fixer	10	0.00	0.00	0.00	0.00	0.00	0.10	0.00
Licania kallunkiae	Non-Fixer	10	0.00	0.00	0.00	0.00	0.00	0.00	0.09
Maytenus guyanensis	Non-Fixer	10	0.00	0.00	0.00	0.00	0.00	0.00	0.09
Miconia bubalina	Non-Fixer	10	0.00	0.00	0.00	0.05	0.00	0.00	0.00
Miconia sparrei	Non-Fixer	10	0.00	0.00	0.00	0.00	0.00	0.07	0.03
Mouriri gleasoniana	Non-Fixer	10	0.00	0.00	0.00	0.00	0.00	0.00	0.09
Myrcia aliena	Non-Fixer	10	0.00	0.00	0.00	0.00	0.00	0.00	0.09
Ocotea bijuga	Non-Fixer	10	0.00	0.00	0.00	0.00	0.00	0.10	0.00
Persea silvatica	Non-Fixer	10	0.00	0.00	0.00	0.00	0.00	0.10	0.00
Posoqueria latifolia	Non-Fixer	10	0.00	0.00	0.00	0.00	0.00	0.00	0.00
Randia mira	Non-Fixer	10	0.00	0.00	0.00	0.00	0.00	0.00	0.09
Spachea correae	Non-Fixer	10	0.00	0.00	0.00	0.00	0.00	0.00	0.09
Spondias mombin	Non-Fixer	10	0.00	0.00	0.00	0.00	0.00	0.00	0.09
Tabernaemontana arborea	Non-Fixer	10	0.00	0.00	0.00	0.00	0.00	0.10	0.00

Species	Fixer Status	Frequency	CR Relative Abundance	LSUR Relative Abundance	BEJ Relative Abundance	TIR Relative Abundance	JE Relative Abundance	LEPP Relative Abundance	SV Relative Abundance
Tetrorchidium gorgonae	Non-Fixer	10	0.00	0.00	0.00	0.00	0.00	0.00	0.09
Theobroma simiarum	Non-Fixer	10	0.00	0.00	0.00	0.00	0.00	0.00	0.09
Zanthoxylum sp	Non-Fixer	10	0.00	0.00	0.00	0.00	0.00	0.00	0.09
Luehea seemannii	Non-Fixer	9	0.00	0.00	0.00	0.05	0.00	0.00	0.00
Ouratea valerioi	Non-Fixer	9	0.00	0.00	0.00	0.00	0.00	0.00	0.08
Pradosia atroviolacea	Non-Fixer	9	0.00	0.00	0.00	0.05	0.00	0.00	0.00
Tetrorchidium euryphyllum	Non-Fixer	9	0.00	0.00	0.00	0.00	0.00	0.00	0.00
Neea urophylla	Non-Fixer	8	0.00	0.00	0.00	0.00	0.00	0.08	0.00
Hirtella sp	Non-Fixer	7	0.00	0.00	0.00	0.00	0.00	0.00	0.06
Mangifera indica	Non-Fixer	7	0.00	0.00	0.07	0.00	0.00	0.00	0.00
Miconia minutiflora	Non-Fixer	7	0.00	0.00	0.07	0.00	0.00	0.00	0.00
Psychotria poeppigiana	Non-Fixer	7	0.00	0.00	0.00	0.00	0.05	0.00	0.00
Quararibea parvifolia	Non-Fixer	7	0.00	0.00	0.00	0.00	0.00	0.00	0.06
Theobroma mammosum	Non-Fixer	7	0.00	0.00	0.00	0.00	0.00	0.07	0.00
Cestrum microcalyx	Non-Fixer	6	0.01	0.02	0.00	0.00	0.00	0.00	0.00
Clusia flava	Non-Fixer	6	0.00	0.00	0.00	0.00	0.06	0.00	0.00
Ficus insipida	Non-Fixer	6	0.00	0.00	0.06	0.00	0.00	0.00	0.00
Inga densiflora	Fixer	6	0.00	0.00	0.00	0.00	0.00	0.00	0.00
Siparuna pauciflora	Non-Fixer	6	0.03	0.00	0.00	0.00	0.00	0.00	0.00
Inga edulis	Fixer	5	0.00	0.00	0.00	0.00	0.05	0.00	0.00
Miconia nervosa	Non-Fixer	5	0.00	0.00	0.00	0.03	0.00	0.00	0.00
Crescentia cujete	Non-Fixer	4	0.00	0.00	0.04	0.00	0.00	0.00	0.00
Trophis racemosa	Non-Fixer	4	0.00	0.00	0.00	0.00	0.00	0.00	0.00
Eschweilera costaricensis	Non-Fixer	3	0.01	0.00	0.00	0.00	0.00	0.00	0.00

Species	Fixer Status	Frequency	CR Relative Abundance	LSUR Relative Abundance	BEJ Relative Abundance	TIR Relative Abundance	JE Relative Abundance	LEPP Relative Abundance	SV Relative Abundance
Macrolobium costaricense	Non-Fixer	3	0.00	0.00	0.00	0.00	0.00	0.00	0.00
Ocotea atirrensis	Non-Fixer	3	0.00	0.00	0.00	0.00	0.00	0.00	0.03
Persea sp	Non-Fixer	3	0.00	0.00	0.00	0.00	0.00	0.00	0.03
Peschiera arborea	Non-Fixer	3	0.00	0.00	0.00	0.00	0.00	0.03	0.00
Psychotria sp1	Non-Fixer	3	0.01	0.00	0.00	0.00	0.00	0.00	0.00
Spondias radlkoferi	Non-Fixer	3	0.01	0.00	0.00	0.00	0.00	0.00	0.00
Zygia longifolia	Fixer	3	0.01	0.00	0.00	0.00	0.00	0.00	0.00
Cassipourea elliptica	Non-Fixer	2	0.00	0.00	0.00	0.00	0.00	0.00	0.02
Solanum novo-granatense	Non-Fixer	2	0.00	0.01	0.00	0.00	0.00	0.00	0.00

This page intentionally left blank